

https://dspace.org/

Molecular mechanisms of inflammation-induced cardiac dysfunction in a rat model of rheumatoid arthritis

Manilall, Ashmeetha

2022
https://hdl.handle.net/10539/35662

Downloaded from a DSpace repository. https://dspace.org/

Molecular mechanisms of inflammation-induced cardiac dysfunction in a rat model of rheumatoid arthritis

Ashmeetha Manilall
0504496W

A thesis submitted to the Faculty of Health Sciences, University of the Witwatersrand, in fulfilment of the requirements for the degree of Doctor of Philosophy

Johannesburg, South Africa
2022

DECLARATION

I, Ashmeetha Manilall, declare that this thesis is my own, except to the extent indicated in the contribution and acknowledgments sections. It is being submitted for the degree of Doctor of Philosophy in the School of Physiology, Faculty of Health Sciences, University of the Witwatersrand, Johannesburg. The work contained in this thesis has not been submitted for any degree or examination in this or any other University.



.....

Ashmeetha Manilall

Signed on 1st day of August, 2022.

ABSTRACT

Heart failure with a preserved ejection fraction (HFpEF) accounts more than 50% of all heart failure cases. In comorbid conditions associated with HFpEF such as obesity, hypertension and diabetes mellitus, chronic systemic inflammation has been proposed as the underlying causal mechanism of cardiac dysfunction. However, confounding factors associated with these comorbid conditions preclude the understanding of the independent contribution of inflammation to the molecular mechanisms underlying the different phenotypes of HFpEF. This thesis comprises a series of animal and cell culture studies designed to advance our understanding of the impact of systemic inflammation on the cellular pathways involved in the development of HFpEF.

Left ventricular (LV) diastolic dysfunction is the primary abnormality associated with HFpEF. Both passive LV stiffness and active processes contribute to LV diastolic dysfunction. Cardiac fibrosis contributes to passive LV stiffness. Independent of confounding factors, the role of inflammation in cardiac fibrosis and its contribution to LV diastolic dysfunction remain uncertain. In the first study, using a model of collagen induced arthritis (CIA), I determined the role of systemic inflammation, and the effects of inhibiting circulating tumour necrosis factor alpha (TNF-α) with etanercept, on the mRNA expression of genes associated with myocardial fibrosis and markers of LV geometry and function measured by echocardiography in 70 Sprague-Dawley rats. I showed that after inoculating rats with collagen, inflammation caused an increase in the LV relative gene expression of pro-fibrotic genes including collagen I (*Col1*, $p < 0.0001$), lysyl oxidase (*LOX*, $p = 0.002$), and transforming growth factor β (*TGFβ*, $p = 0.03$) compared to control rats, consistent with the increased relative wall thickness, a marker of LV concentric remodelling. I also showed that the relative gene expression of matrix metalloproteinase 2 (*MMP2*), which degrades extracellular matrix components and contributes to collagen turnover, was increased after exposing rats to inflammation compared to controls ($p = 0.04$). Inhibiting circulating TNF-α prevented the inflammation-induced increased expression of pro-fibrotic genes, collagen turnover genes and development of LV concentric remodelling. Despite preventing the increased profibrotic gene expression and concentric remodelling, inhibiting circulating TNF-α did not prevent the inflammation-induced LV diastolic dysfunction. These data suggest that inflammation-induced fibrosis and dysregulated LV extracellular matrix remodelling contributes to LV concentric remodelling, and this process is mediated by TNF-α. However, inflammation-induced LV diastolic dysfunction is likely independent of myocardial fibrosis.

Besides changes in the extracellular matrix composition, changes in the cardiomyocyte spring protein, titin, also contribute to LV passive stiffness and LV diastolic dysfunction. Therefore, in the second study I assessed the role of inflammation and inhibiting circulating TNF-α, on the genes regulating the molecular

pathways involved in titin phosphorylation in 73 Sprague-Dawley rats exposed to CIA and to TNF-α inhibition. LV relative mRNA expression of vascular cell adhesion molecule 1 (*VCAM1*, $p = 0.007$), pentraxin 3 (*PTX3*, $p < 0.0001$), and inducible nitric oxide synthase (*iNOS*, $p = 0.0003$) were increased in CIA rats compared to controls, indicating local microvascular inflammation and immune cell activation in response to collagen inoculation. In turn, the relative LV gene expression of *sGCα2* and *sGCβ2* were decreased, suggesting downregulation of the nitric oxide-regulated soluble guanylate cyclase-cyclic guanosine monophosphate (NO-sGC-cGMP) signalling pathway, implicated in titin phosphorylation. Inhibiting circulating TNF-α prevented collagen-induced changes in *VCAM1*, *iNOS, sGCα2* and *sGCβ2* expression. Collagen inoculation increased the LV relative gene expression of *PP5*, which codes for the protein that dephosphorylates the N2B stretch element of titin, making it less compliant. Like the echocardiographic measures of LV diastolic dysfunction, inflammation-induced increased *PP5* expression was not prevented by inhibition of TNF-α. These results suggest that inflammation-induced LV diastolic dysfunction may be mediated by increased PP5 expression and increased dephosphorylation of the N2B stretch element of titin that is independent of TNF-α signalling, rather than by titin phosphorylation via the TNF-α-induced downregulation of NO-sGC-cGMP signalling.

Active processes within the cardiomyocyte contribute to the development of LV diastolic dysfunction. Recent evidence suggests subclinical systolic dysfunction in HFpEF, even when ejection fraction is normal. The impact of inflammation on active processes that may contribute to LV diastolic and early-stage systolic dysfunction is uncertain. In the third study, in 68 Sprague-Dawley rats exposed to CIA and subsequent TNF-α inhibition, and in a human adult cardiomyocyte cell line (AC16) exposed to TNF-α, I assessed the role of TNF-α on the expression of genes associated with the active cellular processes, including calcium homeostasis, oxidative stress, apoptosis and myosin heavy chain isoforms, that may be implicated in the active processes of impaired LV diastolic and systolic function. Inflammation did not alter the LV mRNA expression of *SERCA2a* or *S100A1*, genes involved in calcium handling in rats. In AC16 cells exposed to TNF-α, mRNA expression of SERCA2a was not altered. These results suggest that systemic inflammation and TNF-α does not impair calcium reuptake in LV diastolic dysfunction. In the CIA model, consistent with the preserved ejection fraction, systemic inflammation and inhibiting TNF-α did not alter the expression of markers of mitochondrial oxidative stress (*SOD2*) or apoptosis (*BAX/Bcl2*). In AC16 cells exposed to TNF-α, there was a small increase in expression of markers of apoptosis (*BAX/Bcl2*), however there was a substantial increase in the expression of *SOD2*, the superoxide dismutase that inactivates reactive oxygen species, which likely explains the minimal increase in apoptosis. Taken together, these results indicate that the energy-dependent active process is not compromised in the early stages of inflammation-induced cardiac dysfunction. Systemic inflammation impaired systolic function, as

myocardial deformation (global longitudinal strain) and motion (global longitudinal velocity) were impaired in the CIA rats. Consistent with this finding, systemic inflammation resulted in a shift in the expression patterns of myosin heavy chain (MyHC) genes from fast-twitch to slow-twitch, as the ratio of *Myh6/Myh7* was decreased in the CIA rats, which may account for the impaired myocardial systolic function. Inhibiting circulating TNF-α prevented the inflammation-induced impairments in LV systolic function and the MyHC isoform shift. These results suggest that inflammation-induced systolic functional changes result from MyHC isoform shifts, which may be, at least in part, mediated by TNF-α.

In addition to TNF-α, the inflammatory cytokine, interleukin 6 (IL-6), has also been implicated in inflammation-induced cardiac dysfunction. In the fourth study, in 68 Sprague-Dawley rats exposed to CIA, I investigated the role of IL-6, by using the IL-6 receptor blocker tocilizumab, on expression of genes implicated in the passive and active processes involved in LV diastolic and systolic dysfunction. Blocking circulating IL-6 did not prevent any of the inflammation-induced increases in LV relative mRNA expressions of pro-fibrotic genes, the genes involved in titin regulation, or the genes involved in the active mechanisms of myocardial relaxation or contraction. These findings are consistent with the echocardiographic results that showed blocking IL-6 did not prevent the inflammation induced increases in concentric remodelling (relative wall thickness), impaired relaxation (e') or increased filling pressures (E/e') or impaired myocardial deformation and motion. However, the inflammation induced increase in the LV mRNA expression of *LOX*, which codes for the enzyme that cross-links collagen, was partially offset in the IL-6 blocker rats, which may have contributed to the partial reduction in LV stiffness (e'/a'). Taken together, the effect of IL-6 receptor blockers on inflammation-induced changes in cellular mechanisms underlying LV diastolic and systolic dysfunction remain inconclusive, likely, in part, because of the complex signalling of IL-6 and the immunogenic effects of using a human monoclonal antibody.

In conclusion, the findings reported in this thesis advance our understanding of several molecular mechanisms whereby inflammation induces LV diastolic and systolic dysfunction. Evidence is provided that circulating TNF-α is implicated in the development of LV fibrosis and the resultant concentric remodelling, but that LV concentric remodelling is not the main catalyst for the development of LV diastolic dysfunction. This thesis further showed that inflammation may induce hypophosphorylation of titin that contributes to LV diastolic dysfunction, likely via increased expression of PP5 and not primarily via TNF-α mediated nitric oxide-mediated cGMP signalling. This thesis also provides evidence that diastolic calcium reuptake and the energy-dependent active process of diastolic relaxation is not compromised in the early stages of inflammation-induced LV diastolic dysfunction and that these processes do not contribute to early-stage systolic dysfunction. Lastly this thesis provides evidence that TNF-α contributes to early-stage systolic dysfunction in HFpEF, by disrupting myocardial contractile properties.

PUBLICATIONS AND PRESENTATIONS ARISING FROM THIS RESEARCH

Publications

Manilall, A., L. Mokotedi, S. Gunter, R. Le Roux, S. Fourie, C. A. Flanagan and A. M. E. Millen (2021). "Inflammation-induced left ventricular fibrosis is partially mediated by tumour necrosis factor-α." Physiological Reports 9(21).

Manilall, A., L. Mokotedi, S. Gunter, R. Le Roux, S. Fourie, C. A. Flanagan and A. M. E. Millen (2022). "Protein phosphatase 5 mediates inflammation-induced left ventricular dysfunction in collagen-induced arthritis." *(Submitted to BMC Cardiovascular Disorders, under review).*

Oral presentations

Manilall, A., L. Mokotedi, S. Gunter, R. Le Roux, S. Fourie, C. A. Flanagan and A. M. E. Millen. "Inflammation-induced left ventricular fibrosis is partially mediated by tumour necrosis factor-α." Faculty of Health Sciences Research Day, Johannesburg, South Africa, September 2020.

Manilall, A., L. Mokotedi, S. Gunter, R. Le Roux, S. Fourie, C. A. Flanagan and A. M. E. Millen. "Protein phosphatase 5 mediates inflammation-induced left ventricular dysfunction in collagen-induced arthritis." African Association of Physiological Sciences / Physiology Society of Southern Africa (PSSA) Virtual Conference, September 2021.

STATEMENT OF CONTRIBUTION TO THIS RESEARCH

As part of the declaration of this thesis, I acknowledge contributions by various individuals. This thesis forms part of a larger study investigating the role of inflammation in the development of cardiovascular diseases using a rat model of collagen induced arthritis. As part of a team of researchers including Ms Regina Le Roux, Ms Serena Fourie, Dr Lebogang Mokotedi and Prof Aletta Millen, we conducted the animal study. Of the 110 animals included in the larger study, 92 were included in a manuscript published in 2022 where we reported the animal characteristics, the characterization of the animal model and a portion of the echocardiography variables (Le Roux et al. 2022). For the larger study, the WITS animal ethics committee recommended that we reduce harm to laboratory animals by maximizing the questions addressed and measures made for the number of rats used. Therefore, in this thesis 89 rats were used, for the molecular analyses that partially overlap with the 92 rats from the previous publication. In the current thesis I describe the molecular mechanisms of inflammation-induced changes in cardiac geometry and function. To put these molecular analyses into context, I provide the animal characteristics, serum levels of inflammatory markers and a small selection of echocardiographic measures for a partially overlapping group of animals. As part of my contribution to the larger study and publication, I participated in all rat termination procedures and was personally responsible for collection of blood samples, collection and storage of serum aliquots, weighing and storing of tissue samples and provided editorial input to the manuscript (Le Roux et al 2022). I was solely responsible for the establishment, optimization and execution of all protocols for RNA extraction, cDNA synthesis and gene expression PCR assays that were performed. The cell culture study was designed by myself with the guidance of my supervisors, Prof Aletta Millen and Dr Colleen Flanagan, and I was solely responsible for all experimental procedures and data collection. I performed all data analysis, interpreted the data and wrote the manuscripts for this thesis with the help of my supervisors. All the co-authors on the individual manuscripts contributed to data interpretation, critical revisions and provided expert opinions.

ACKNOWLEDGMENTS

This research would not have been possible without the people mentioned above, whom I'd like to thank for all their support and guidance with special mention of my supervisors; Prof Aletta Millen and Dr Colleen Flanagan. They went above and beyond what is a reasonable expectation to help me meet my submission deadline and for this, I cannot thank them enough.

I am extremely grateful to the National Research Foundation and the University of the Witwatersrand for the funding that supported this research project. I would like to thank Ms Monica Gomes for performing the ELISA assays and the staff of the WITS Research Animal Facility for their assistance with the animal model.

I would like to thank my family (especially Nivz, Mom, Fats, Mo, Boo), my friends (Kishen, Serena and Ashika) for all their encouragement, and my husband (Shayur) for the inspiration to undertake this degree.

TABLE OF CONTENTS

Declaration ii
Abstract iii
Publications and presentations arising from this research vi
Statement of contribution to this research vii
Acknowledgments viii
Table of contents ix
List of figures xiii
List of tables xv
Abbreviations xvi
Preface xxi
Chapter 1: Introduction 1
1.1 Introduction 2
1.2 Heart failure 3
1.3 Characteristics of LV diastolic dysfunction 5
1.4 Phenotypes of LV diastolic dysfunction 6
1.4.1 Cellular mechanisms that cause LV diastolic dysfunction by increasing passive stiffness 7
1.4.2 Cellular mechanisms that cause DD by disrupting active relaxation 8
1.5 Systolic function in HFpEF 9
1.6 Systemic signals associated with the development of LV diastolic dysfunction 11
1.6.1 The role of inflammation in extracellular matrix remodelling and fibrosis 12
1.6.2 The role of inflammation in titin compliance 13
1.6.3 The role of inflammation in calcium homeostasis 14
1.6.4 The role of inflammation in systolic dysfunction 15
1.7 Therapeutic interventions for the management of LV diastolic and systolic dysfunction in HFpEF 16
1.8 Problem statement 17
1.9 Study aims 18
Chapter 2: Materials and methods 19
2.1 Experimental design and animal treatment 20
2.2 Echocardiography 21
2.3 Circulating inflammatory markers 24
2.4 Cell culture and treatment of adult cardiomyocyte cell line (AC16) 24

2.5 Preparation of cDNA for comparative gene expression using real time PCR 24
2.6 Comparative gene expression RT-PCR 24
2.7 Reference gene selection 25
2.8 Data analysis 28
Chapter 3: Inflammation-induced left ventricular fibrosis is partially mediated by TNF-α 29
3.1 Abstract 30
3.2 Introduction 31
3.3 Results 32
3.3.1 Effect of collagen inoculation and anti-TNF-α treatment on body mass, blood pressure and circulating inflammatory markers 32
3.3.2 Effect of collagen inoculation and anti-TNF-α treatment on tissue inflammatory markers 32
3.3.3 Effect of collagen inoculation on LV geometry and LV relaxation 34
3.3.4 Effect of collagen inoculation and anti-TNF-α treatment on extracellular matrix gene expression 34
3.3.5 Effect of collagen inoculation and anti-TNF-α treatment on markers of collagen turnover 38
3.4 Discussion 43
Chapter 4: Protein phosphatase 5 mediates inflammation-induced left ventricular dysfunction in collagen-induced arthritis 47
4.1 Abstract 48
4.2 Introduction 49
4.3 Results 50
4.3.1 Body mass, blood pressure, markers of inflammation and diastolic function measures 50
4.3.2 Effect of collagen inoculation and anti-TNF-α treatment on expression of genes involved in microvascular inflammation and immune cell activation 50
4.3.3 Effect of collagen inoculation and anti-TNF-α treatment on expression of genes involved in the NO signalling pathway 52
4.3.4 Effect of collagen inoculation and anti-TNF-α treatment on expression of protein phosphatase gene 52
4.4 Discussion 55
Chapter 5: The role of TNF-α in active processes of inflammation-induced LV diastolic and systolic dysfunction 59
5.1 Abstract 60
5.2 Introduction 61
5.3 Results 63
5.3.1 Body mass, blood pressure, markers of inflammation and diastolic function measures 63
5.3.2 Inflammatory cytokine expression in LV tissue and AC16 cells 63

5.3.3 Expression of genes that regulate (diastolic) calcium sequestration 63
5.3.4 Effect of collagen inoculation and anti-TNF-α treatment on expression of genes involved in apoptosis 66
5.3.5 Effect of collagen inoculation and anti-TNF-α treatment on expression of a gene involved in mitochondrial function 66
5.3.6 Effect of collagen inoculation and anti-TNF-α treatment on markers of LV systolic function 69
5.3.7 Effect of collagen inoculation and anti-TNF-α treatment on expression of genes involved in cardiac contractility 69
5.4 Discussion 72
Chapter 6: The role of interleukin-6 in passive and active processes of inflammation-induced lv diastolic and systolic dysfunction 77
6.1 Abstract 78
6.2 Introduction 79
6.3 Results 80
6.3.1 The effect of IL-6 blocker treatment on body mass, blood pressure and, circulating and LV tissue expression of inflammatory markers 80
6.3.2 The effect of IL-6 blocker treatment on LV geometry, diastolic and systolic function 81
6.3.3 The effect of IL-6 blocker treatment on extracellular matrix gene expression 84
6.3.4 The effect of IL-6 blocker treatment on expression of genes involved in microvascular inflammation, immune cell infiltration and NO-signalling pathways 84
6.3.5 The effect of IL-6 blocker treatment on gene expression of markers of calcium handling, oxidative stress and apoptosis 87
6.3.6 The effect of IL-6 blocker treatment on myocardial contractility genes 87
6.4 Discussion 91
Chapter 7: Summary and conclusion 95
7.1 Summary 96
7.2 Inflammation-induced LV fibrosis is partially mediated by TNF-α 96
7.3 The role of TNF-α in signalling pathways of titin phosphorylation 96
7.4 The role of TNF-α in active processes of inflammation-induced LV diastolic and systolic dysfunction 97
7.5 The role of IL-6 in passive and active processes of inflammation-induced LV diastolic and systolic dysfunction 98
7.6 Limitations and future recommendations 101
7.7 Conclusion 101
Chapter 8: References 101
Chapter 9: Appendices 122

9.1 Appendix A: Animal ethical clearance certificate 123
9.2 Appendix B: Modification/Extension clearance for animal study 124
9.3 Appendix C: Ethical waiver 127
9.4 Appendix D: Copy of publication of data in larger animal study 128

LIST OF FIGURES

Figure 2.1. Representation of echocardiographic measures. 23

Figure 2.2. Comprehensive stability ranking of reference genes by RefFinder. 27

Figure 3.1. Echocardiographic measures of LV geometry and diastolic dysfunction. 35

Figure 3.2. LV expression of extracellular matrix expression genes. 36

Figure 3.3. *LOX* and *COL1* markers of extracellular matrix gene expression. 37

Figure 3.4. Regression analysis of relative wall thickness with *Col1, LOX, TGFβ, CD68, αSMA* and *Myh7* in left ventricular tissues of all rat groups 39

Figure 3.5. LV expression of matrix metalloproteinase genes 41

Figure 4.1. LV expression of microvascular inflammation and immune cell activation genes. 51

Figure 4.2. LV expression of sGC subunit genes. 53

Figure 4.3. LV expression of protein phosphatase genes 54

Figure 5.1. Expression of inflammatory cytokine genes in LV tissue and a cardiomyocyte cell line. 64

Figure 5.2. Expression of calcium handling genes in LV tissue and a cardiomyocyte cell line. 65

Figure 5.3. Expression of apoptotic genes in LV tissue and a cardiomyocyte cell line. 67

Figure 5.4. Expression of *SOD2* in LV tissue and a cardiomyocyte cell line. 68

Figure 5.5. Echocardiographic measures of LV systolic function. 70

Figure 5.6. LV expression of contractility genes. 71

Figure 6.1. LV expression of extracellular matrix genes. 85

Figure 6.2. LV expression of microvascular inflammation, immune cell activation and sGC subunit genes. 86

Figure 6.3. LV expression of protein phosphatase genes 88

Figure 6.4. LV expression of calcium handling, mitochondrial dysfunction and apoptotic genes. 89

Figure 6.5. LV expression of myocardial contractility genes. 90

Figure 6.5. Schematic depicting the effects of systemic inflammation and inhibition of circulating TNF-α on molecular markers of left ventricular diastolic and systolic dysfunction..... 100

LIST OF TABLES

Table 2.1. Description of candidate reference genes 27

Table 3.1. Body mass, blood pressure, and circulating and tissue inflammatory markers in control, CIA, and anti-TNF-α groups..... 33

Table 3.2. Association between expression of matrix metalloproteinases and pro-inflammatory and pro-fibrotic genes..... 42

Table 6.1. Body mass, blood pressure and circulating and tissue inflammatory markers in control, CIA and IL-6 blocker groups..... 82

Table 6.2. Echocardiographic measures of left ventricular myocardial remodelling, diastolic function and systolic function in control, CIA and IL-6 blocker rats. 83

ABBREVIATIONS

α	alpha
β	beta
γ	gamma
αSMA	alpha smooth muscle actin
a'	mitral annular tissue lengthening during late diastole
AC16	human cardiomyocyte cell line 16
ACTB	β-actin
ANOVA	analysis of variance
ATP	adenosine triphosphate
BAX	Bcl-2-associated X protein
Bcl-2	B-cell lymphoma 2
Ca^{2+}	calcium
cDNA	complementary deoxyribonucleic acid
CD68	cluster of differentiation 68
cGMP	cyclic guanosine monophosphate
CIA	collagen-induced arthritis
CI	confidence interval
cm	centimetre
cm/s	centimetre per second
CO_2	carbon dioxide
COL1	collagen type 1

CRP	C-reactive protein
Ct	cycle threshold
DBP	diastolic blood pressure
D	diastole
DMEM	Dulbecco’s Modified Eagle Medium
DNA	deoxyribonucleic acid
E	mitral inflow velocity during early diastole
e'	mitral annular tissue lengthening during early diastole
e’/a’	ratio of early to late mitral annulus flow velocity
E/e’	index of left ventricular filling pressures
EF	ejection fraction
ELISA	enzyme-linked immunosorbent assay
FBS	foetal bovine serum
FSmid	midwall fractional shortening
g	gram
GAPDH	glyceraldehyde 3-phosphate dehydrogenase
GMP	guanosine monophosphate
h	hour
HFpEF	heart failure with a preserved ejection fraction
HFmrEF	heart failure with a mildly reduced ejection fraction
HFrEF	heart failure with a reduced ejection fraction
HPRT1	hypoxanthine phosphoribosyltransferase 1

ICAM1	intercellular adhesion molecule 1
IL-6	interleukin-6
IL-6R	interleukin-6 receptor
iNOS	inducible nitric oxide synthase
IQR	interquartile range
IVST_D	intraventricular septal wall thickness during diastole
IVST_S	intraventricular septal wall thickness during systole
kg	kilogram
LOX	lysyl-oxidase
LV	left ventricular
LVEDD	left ventricular end-diastolic internal diameter
LVESD	left ventricular end systolic internal diameter
M	molar
min	minutes
mg	milligram
ml	millilitre
mRNA	messenger ribonucleic acid
MyHC	myosin heavy chain
Myh6	myosin heavy chain 6
Myh7	myosin heavy chain 7
Na^+	sodium
NO	nitric oxide

PCR	polymerase chain reaction
PKG	protein kinase G
PP	protein phosphatase
PTX3	pentraxin 3
PWT_D	posterior wall thickness during diastole
PWT_S	posterior wall thickness during systole
r	correlation coefficient
RNA	ribonucleic acid
ROS	reactive oxygen species
Rpl32	60S ribosomal protein L32
RT	real time
RWT	relative wall thickness
RyR2	ryanodine receptor 2
S	systole
S100A1	S100 calcium-binding protein A1
SD	standard deviation
SEM	standard error of the mean
SERCA	sarcoplasmic reticulum ATPase pump
sIL-6R	soluble interleukin-6 receptor
SR	sarcoplasmic reticulum
STE	speckle tracking echocardiography
TBP	TATA-box binding protein

TGFβ	transforming growth factor beta
TDI	Tissue Doppler imaging
sGC	soluble guanylate cyclase
TNF-α	tumour necrosis factor alpha
VCAM1	vascular cell adhesion molecule 1

PREFACE

The management of heart failure with a preserved ejection fraction (HFpEF) is suboptimal, largely because of its complex pathophysiology. This limited understanding of HFpEF can be ascribed to its wide range of aetiologies and heterogeneous presentation. Systemic inflammation has recently been suggested as an underlying cause in the development of HFpEF. Yet, treatment approaches aimed at reducing inflammation failed to provide the desired clinical outcomes. Some of the reasons for these failures include treatments not targeting phenotypic variations and biological heterogeneity of HFpEF. Furthermore, certain failed trials where more than 80% of participants were obese or overweight suggested that comorbid intervention before HFpEF ensues may have been beneficial. Therefore, this thesis was prompted by a need to address the lack of understanding of the molecular mechanisms underlying inflammation-induced cardiac dysfunction in HFpEF, independent of comorbid conditions.

Diastolic abnormalities are believed to be the main feature of HFpEF. Both passive LV stiffness and active processes contribute to LV diastolic dysfunction. Myocardial fibrosis and adverse extracellular matrix remodelling contributes to passive LV stiffness. Independent of confounding factors, the role of inflammation in myocardial fibrosis and its contribution to LV diastolic dysfunction remain uncertain. Therefore, I investigated the role of systemic inflammation and the effects of inhibiting circulating tumour necrosis factor alpha (TNF-α) with etanercept, on pro-fibrotic genes and genes involved in extracellular matrix remodelling in the development of myocardial fibrosis in a rat model of collagen-induced arthritis (CIA).

Second, changes in cardiomyocyte spring protein, titin, which are believed to be initiated as a result of microvascular endothelial dysfunction, also contribute to LV passive stiffness. The phosphorylation status of titin isoforms contributes to cardiomyocyte compliance and is regulated by several intracellular pathways. Although dysregulated nitric oxide signalling which disrupts the soluble guanylate cyclase-cyclic guanosine monophosphate (NO-sGC-cGMP) signalling pathway, has been implicated in aberrant titin phosphorylation in a model of metabolic disorder-induced systemic inflammation, whether this signalling pathways is impacted in a model of systemic inflammation independent of the confounding factors is uncertain. Therefore, I investigated the role of inflammation and inhibiting circulating TNF-α, on genes involved in microvascular inflammation and titin phosphorylation in a rat model of CIA.

Third, aside from passive processes, active processes in cardiomyocytes may result in impaired relaxation which contributes to LV diastolic dysfunction. Furthermore, although ejection fraction is preserved in HFpEF, evidence suggests that these patients do have subclinical systolic dysfunction. The mechanisms of subclinical systolic dysfunction in HFpEF are limited and indirect. Therefore, I investigated the effects of

inflammation and inhibiting circulating TNF-α on the expression of genes involved in several active energy dependent cellular processes that may impact LV systolic and diastolic function in the CIA rat model. To further delineate the role of TNF-α in these processes, I investigated the genes involved in active relaxation processes in a human adult cardiomyocyte cell line (AC16) exposed to TNF-α.

Lastly, the inflammatory cytokine, interleukin 6 (IL-6), has also been implicated in the development of HFpEF. Some suggest that IL-6 is instrumental in adverse myocardial remodelling. However, these results are not supported by all studies, and indeed some suggest IL-6 has a protective effect in the heart. Furthermore, the role of IL-6 on passive cardiomyocyte stiffness and the active processes involved in LV diastolic and systolic dysfunction is unknown. Hence, in the fourth study in the CIA rat model, I investigated the effects of blocking circulating IL-6, using the IL-6 receptor blocker tocilizumab, on echocardiographic markers and expression of genes implicated in several passive and active processes involved in LV diastolic and systolic dysfunction.

This thesis was compiled as a series of semi-independent chapters. In the first chapter, the thesis begins with a literature review that summarises the current knowledge and where I highlight the reasons for conducting the various experiments in this thesis. This is followed by a description of the research methods in chapter 2. Thereafter, each research question is presented in a separate chapter, each with its own abstract, introduction, results and discussion sections (chapters 3 to 6). Chapter 7 summarizes the main findings and highlights its relevance. Chapter 8 details the references cited in this thesis and the final chapter (9), provides the list of appendices.

CHAPTER 1: INTRODUCTION

1.1 Introduction

Cardiovascular disease is the number one cause of death globally (WHO 2021). In low- to middle-income countries, such as South Africa, the prevalence and contribution of cardiovascular disease to deaths are increasing (Yuyun et al. 2020). Cardiovascular disease is a group of disorders of the cardiovascular system including coronary heart disease and rheumatic heart disease that often result in varying degrees of heart failure (WHO 2021). It is well established that traditional risk factors including old age, hypertension, diabetes mellitus, smoking and dyslipidaemia play a significant role in the development of cardiovascular disease (Petrie et al. 2018). Although chronic low-grade inflammation that accompanies comorbidities such as hypertension, obesity and diabetes mellitus has long been proposed as a risk factor for heart failure (Ross and Glomset 1976; Libby 2002), recently Paulus and Tschöpe proposed that the inflammation-induced molecular mechanisms, which ultimately lead to altered vascular and cardiac function, may be the driving factor in the development of HFpEF (Paulus and Tschöpe 2013). Furthermore, evidence suggests that disorders associated with chronic high-grade inflammation, such as rheumatoid arthritis and lupus erythematosus, markedly exacerbate the risk for cardiovascular events (Avina-Zubieta et al. 2012).

Inflammation has particularly been implicated in the development of heart failure with a preserved ejection fraction (HFpEF). HFpEF has been described as the "single largest unmet need in cardiovascular medicine" and accounts for at least half of all cases of heart failure (Hamdani et al. 2021). Left ventricular (LV) diastolic dysfunction is a subclinical measure that often progresses to HFpEF (Wan et al. 2014). However, the pathophysiology of LV diastolic dysfunction is poorly understood (Lewis et al. 2017). Although there is some evidence to support the role of chronic inflammation in the pathogenesis of LV diastolic dysfunction, the exact mechanisms that mediate this role are uncertain. Moreover, the confounding effects of comorbid conditions limits understanding of the independent role of inflammation in the development of LV diastolic dysfunction (Paulus and Tschöpe 2013). Furthermore, although diastolic abnormalities are believed to be the main pathophysiological feature of HFpEF, clinical evidence also points to subclinical systolic dysfunction. However, the understanding of the mechanisms underlying subclinical systolic dysfunction in HFpEF is limited.

The limited effective treatment strategies currently available for the management of HFpEF, underscore the need for a better understanding of the pathophysiology of this condition. Considering the strong association between inflammatory markers and HFpEF and LV diastolic dysfunction in cross-sectional clinical studies, the suggestion to explore anti-inflammatory drugs as potential therapeutic targets for HFpEF is warranted (Upadhya, Haykowsky, and Kitzman 2018). Nevertheless, the use of anti-inflammatory drugs in the management of HFpEF has shown contradictory outcomes. Moreover, even in

those studies where anti-inflammatory drugs were associated with improved cardiac function, the mechanisms for these associations are unclear (Reina-Couto et al. 2021).

Taken together, it has been proposed that systemic inflammation plays a central role in the pathophysiology of LV diastolic dysfunction and HFpEF (Paulus and Tschöpe 2013). However, the independent effect of inflammation on the different molecular pathways implicated in LV diastolic dysfunction is currently under investigation. Furthermore, subclinical systolic dysfunction may be present in HFpEF, however, the mechanisms are poorly understood. Lastly, as there are currently no effective treatment strategies for HFpEF (Upadhya, Haykowsky, and Kitzman 2018), a better understanding of the exact role of inflammation and the applicability of anti-inflammatory treatment in LV diastolic and systolic dysfunction is warranted.

In the present thesis, I conducted a series of studies designed to advance our understanding of the impact of inflammation on the molecular pathways underlying the development of LV diastolic and systolic dysfunction, independent of comorbid conditions. I also explored the role of blocking circulating cytokines to further aid our understanding of the roles of specific cytokines within the signalling pathways that contribute to LV dysfunction. In the present chapter, I will highlight the different types of heart failure, and then focus on the role of LV diastolic dysfunction in the development of heart failure. Subsequently, I will discuss the pathophysiology and different phenotypes of LV diastolic dysfunction, as well as how systolic function is affected in the development of LV diastolic dysfunction. Thereafter, I will highlight what is currently known about the role of inflammation in the molecular pathways underlying the development of LV diastolic dysfunction and systolic dysfunction. In so doing, in the present chapter, I will highlight areas where there is a lack of evidence and where the studies conducted in the present thesis may contribute to the existing knowledge.

1.2 Heart failure

Congestive heart failure is a complex clinical syndrome defined as an inability of the heart to meet the systemic demands of circulation (Malik et al. 2022). Heart failure symptoms or signs result from either functional or structural cardiac abnormalities that lead to impaired ventricular filling or ejection of blood into the systemic circulation (Bozkurt et al. 2021; Malik et al. 2022). Estimates of the incidence of heart failure globally are unreliable, and largely reflect the epidemiology from high-income countries. Nevertheless, the estimated prevalence of heart failure world-wide ranges between 37 million and 64 million cases, which amounts to 1-3% of the adult population (Malik et al. 2022; Ziaeian and Fonarow 2016). In high-income countries, heart failure contributes to a significant proportion of cardiovascular mortality, and it amounts to more than 20 billion dollars in healthcare expenditure in the United States alone

(Ziaeian and Fonarow 2016). Although the evidence of heart failure prevalence in low- to middle-income countries is scarcer, it is well recognized that due to the epidemiological transition, there is a rapid shift from communicable to non-communicable diseases as the leading cause of death (Agbor et al. 2018). In sub-Saharan Africa, it has been predicted that non-communicable diseases, to which heart failure is a substantial contributor, will surpass HIV/AIDS as the biggest cause of death in the next decade (Keates et al. 2017; Mensah et al. 2015).

In high-income countries, the primary driver for the heart failure burden is the ageing population. Indeed, more than 50% of patients hospitalized with heart failure in high-income countries are over the age of 75 years (Ziaeian and Fonarow 2016). In contrast, in low- to middle-income countries, heart failure is mainly a disease of the middle-aged adult, with the mean age of admission for heart failure ranging between 50 and 70 years, hence affecting mostly economically active individuals (Agbor et al. 2018; Agbor et al. 2020). Heart failure is further a major public health concern because it is associated with recurrent hospitalization, high morbidity and mortality, poor quality of life and loss of economic productivity (Agbor et al. 2020).

Besides age, several risk factors, genetic factors and systemic diseases have been identified as causes of either structural or functional myocardial abnormalities that lead to heart failure. Altogether 17 primary aetiologies contribute to heart failure (Hawkins et al. 2009). Most of all heart failure cases can be attributed to four underlying causes namely, ischaemic heart disease, chronic obstructive pulmonary disease, hypertensive heart disease, and rheumatic heart disease (Ziaeian and Fonarow 2016). Historically, most heart failure cases were associated with ischaemic causes due to coronary artery disease and myocardial infarctions, which are disproportionately reported in high-income countries (Malik et al. 2022; Ziaeian and Fonarow 2016). In contrast, in low-income and middle-income countries especially in Africa, hypertensive heart disease, cardiomyopathy, myocarditis and rheumatic heart disease are the primary catalysts of heart failure (Agbor et al. 2020; Ziaeian and Fonarow 2016).

Heart failure is diagnosed based on the signs and symptoms of the patient and on the presence of structural and functional cardiac changes. High resolution ultrasound imaging of the heart (echocardiography) is routinely used in the identification of cardiac structural and functional changes. Until recently, the primary cardiac functional change used to indicate the onset of heart failure was a reduced LV ejection fraction (LVEF), a measure of LV systolic chamber function. It is now well established that heart failure can exist even if LVEF is normal (Bozkurt et al. 2021). Hence, heart failure is classified into three subtypes based on the LVEF, which include heart failure with reduced ejection fraction (HFrEF, LVEF <40%), heart failure with mildly reduced ejection fraction (HFmrEF, LVEF 40 – 49%) and heart failure with preserved ejection fraction (HFpEF, LVEF ≥50%) (Bozkurt et al. 2021). HFrEF accounts for only about half of all hospital

admissions for heart failure. Between 44% and 72% of all cases of heart failure admission patients have normal systolic chamber function (LVEF) (Hogg et al. 2004; Simmonds et al. 2020). Despite a normal LVEF, the prognostic outcomes in these patients are as poor as heart failure with systolic chamber dysfunction. Moreover, current treatment strategies for managing HFpEF are largely unsuccessful (Lewis et al. 2017). Hence, the need to improve our understanding of the pathophysiology of HFpEF has been highlighted as a critical need in cardiovascular medicine. In this regard, the fundamental pathophysiological abnormality associated with the development of HFpEF is impaired LV diastolic function (Mohammed et al. 2012; Shah et al. 2014; Wan et al. Chen 2014; Westermann et al. 2008). Impaired LV diastolic function represents a subclinical cardiac alteration identified via echocardiographic assessment that is consistently associated with the development of HFpEF and adverse cardiovascular outcomes (Aurigemma et al. 2001; Wan et al. 2014). Impaired LV diastolic function leads to increases in filling pressures in the ventricle and ultimately to the clinical and pathological features of heart failure, which include exercise intolerance, pulmonary congestion and right-sided heart failure. Despite the identification of LV diastolic dysfunction as a predisposing condition to HFpEF, it has a broad range of aetiologies and has a heterogeneous structural and functional presentation (Lewis et al 2017). Therefore, in the next section I will briefly highlight the pathophysiology of LV diastolic dysfunction and the current approaches to quantify LV diastolic dysfunction.

1.3 Characteristics of LV diastolic dysfunction

During diastole, the ventricles relax to allow adequate LV filling with blood for the subsequent ejection phase. Both active and passive processes contribute to adequate myocardial relaxation (Borlaug and Kass 2006). Active processes require adenosine triphosphate (ATP) to facilitate the removal of calcium (Ca^{2+}) from the cytosol to allow for the dissociation of cross-bridges (Biesiadecki et al. 2014). Passive processes contribute to diastolic relaxation by means of adequate compliance to allow the ventricle to recoil (Biesiadecki et al. 2014). LV diastolic dysfunction arises when structural or functional LV abnormalities prevent myocardial relaxation leading to inadequate LV filling during diastole (Kapila and Mahajan 2009). The hallmarks of LV diastolic dysfunction are elevated LV end diastolic and left atrial pressures (Chinnaiyan et al. 2007; Lewis et al. 2017).

Structural and functional cardiac changes in LV diastolic dysfunction are routinely diagnosed by echocardiography. In this regard, structural changes in the heart are determined by changes in cardiac geometry and LV mass. Using two-dimensional M-mode imaging the diameter of the interventricular septum wall and posterior wall, as well as the internal diameter, are measured to allow for calculation of the relative wall thickness (RWT) and LV mass. RWT describes the relationship between LV wall thickness

and chamber diameter (Lang et al. 2015). The RWT and LV mass are used to assess either concentric or eccentric remodelling patterns of the left ventricle. LV concentric remodelling is a subtle and early change in cardiac geometry associated with LV diastolic dysfunction (Cuspidi et al. 2002). Besides LV hypertrophy, left atrial dilatation is another frequently measured marker of LV diastolic dysfunction. Using echocardiography, left atrial diameter and volume is measured and used as an indicator of LV pressures. Nevertheless, substantial morphological heterogeneity has been reported in LV diastolic dysfunction and hence not all patients present with concentric remodelling patterns, increased LV mass or left atrial dilatation (Lewis et al. 2017).

In addition to structural remodelling, echocardiography allows for the assessment of several functional diastolic measures. Briefly, mitral inflow velocity during early (E) and late (A) diastole using pulsed wave Doppler allows visualization of the phases of ventricular filling. In LV diastolic dysfunction, altered pressures in the ventricle and atrium alter the filling patterns of the ventricle. Therefore, changes in the E/A ratio may indicate impaired LV relaxation (Redfield et al. 2003). However, pulsed wave Doppler is rate and pressure dependent and is therefore not used in isolation as a measure of LV diastolic function. Tissue Doppler imagining (TDI) is used to measure tissue lengthening at the mitral annulus during early (e') and late (a') diastole (Nagueh et al. 2008; Park and Marwick 2011). As it is less rate and pressure dependent, a reduced e' is considered one of the earliest markers of impaired LV relaxation. In addition, the ratio of e'/a' is deemed a marker of LV stiffness. Furthermore, as the E wave is dependent on relaxation alone, the ratio of E/e' is considered an index of LV filling pressures (Sharifov et al. 2016). Indeed, these echocardiographic measures of impaired relaxation (E/A and e'), LV stiffness (e'/a') and increased filling pressures (E/e') are reported in patients with LV diastolic dysfunction (Smiseth 2017) and are associated with the development of heart failure and adverse cardiovascular outcomes (Aurigemma et al. 2001; Redfield et al. 2003). Although reasonable consensus has been reached regarding its definition, LV diastolic dysfunction represents a broad cohort of patients with a wide range of comorbid conditions. Hence, the underlying disease mechanisms of LV diastolic dysfunction are heterogeneous and can be classified into different biological phenotypes. In the section below I will discuss the different phenotypes of LV diastolic dysfunction to identify potential cellular processes and mechanisms involved in the development of LV diastolic dysfunction.

1.4 Phenotypes of LV diastolic dysfunction

The lack of understanding the pathophysiology of LV diastolic dysfunction is attributed to the diversity in the cellular processes which may contribute to its development. In this regard, several cellular mechanisms involved in either active or passive processes of myocardial relaxation (Borlaug and Kass 2006), contribute

to impaired relaxation and increased myocardial stiffness that may ultimately lead to the development of LV diastolic dysfunction. In this section, I will briefly highlight the changes in passive and active processes of diastole that may contribute to impaired diastolic function.

1.4.1 Cellular mechanisms that cause LV diastolic dysfunction by increasing passive stiffness

1.4.1.1 Extracellular matrix remodelling and fibrosis

Chamber stiffness, which represents ventricular passive elasticity, influences LV filling during diastole. One component that contributes to passive elasticity is the composition of the extracellular matrix. Adverse remodelling of the extracellular matrix contributes to increased LV stiffness and LV diastolic dysfunction (Borlaug and Kass 2006). The extracellular matrix consists mainly of a linked network of collagen and elastin fibres, which provides the structural integrity to the myocardium. Although many subtypes of collagen exist, the main isoforms found in the myocardial extracellular matrix are collagen I and III (Kular et al. 2014). Increased collagen I, the stiffer isotype, is believed to be the main pro-fibrotic extracellular matrix component of the diseased myocardium and is characteristic of myocardial fibrosis (Husse et al. 2007; Lopez et al. 2012). Increases in collagen volume also result in concentric remodelling of the LV. Myocardial fibrosis and concentric LV remodelling are associated with increased LV stiffness and impaired LV relaxation (El Hajj et al. 2017; Gonzalez-Santamaria et al. 2016; Páramo 2017) and predict the development of heart failure (Krum et al. 2011). Collagen is degraded by matrix metalloproteinases (MMPs), to ensure continuous turnover of the collagen network. Altered MMP expression and activity result in dysregulated collagen turnover that contributes to myocardial fibrosis and stiffness (Lopez et al. 2012; Rodriguez et al. 2008; Skioldebrand et al. 2017). In addition to the collagen volume and turnover, cross-linking between collagen fibres also contributes to LV stiffness and LV diastolic dysfunction (Lopez et al. 2012). Cross linking of collagen occurs when covalent bonds form via lysine oxidation, which is catalysed by lysyl oxidase (LOX) (Nagueh 2021). Thus, it is well accepted that extracellular matrix remodelling, and LV fibrosis contribute to impaired myocardial relaxation and passive filling, ultimately contributing to LV diastolic dysfunction. Nevertheless, recent evidence has shown that LV diastolic dysfunction can develop independently of concentric remodelling (Lewinter and Meyer 2013; Lewis et al. 2017). Therefore, factors predisposing the development of LV fibrosis and concentric remodelling and their roles in LV diastolic dysfunction remain a topic if interest. A further factor that confounds understanding of the role of extracellular matrix remodelling in LV diastolic dysfunction is that extracellular matrix remodelling is not the only cellular mechanism involved in passive LV stiffness.

1.4.1.2 Titin compliance in the regulation of myocyte stiffness

Myocyte stiffness also contributes to LV relaxation. Titin compliance contributes to the passive elasticity of the ventricles and facilitates LV relaxation and filling during diastole. Titin is the giant cytoskeletal protein that is responsible for the elastic recoil of the myocardial sarcomere during diastole. Titin compliance and its spring-like capacity is regulated by post-transcriptional and post-translational modifications (Lewinter and Granzier 2014). Differential splicing results in two different isoforms, namely the N2B, which is the shorter and stiffer isoform, and the N2BA isoform, which is the longer and more compliant isoform. Although they co-exist within the sarcomere, an increased N2B:N2BA ratio has been associated with reduced compliance of the cardiomyocyte (Lewis et al. 2017). In addition, the phosphorylation state of these titin isoforms also contributes to its compliance (Zile et al. 2015). The N2B element of titin is phosphorylated to minimize resting tension (Sorop et al. 2018). Hypophosphorylation of the N2B element of titin has been associated with impaired LV relaxation and LV diastolic dysfunction (Zile et al. 2015). Although the contribution of titin hypophosphorylation to passive LV stiffness has received considerable attention in recent years, the molecular pathways leading to titin hypophosphorylation remain uncertain.

1.4.2 Cellular mechanisms that cause DD by disrupting active relaxation

1.4.2.1 Mitochondrial function

Under normal physiological functioning the heart muscle has a high demand on mitochondrial function for energy in the form of ATP, which fuels cardiomyocyte active contraction and relaxation (Marelli-Berg and Aksentijevic 2019). During diastole, ATP facilitates relaxation by allowing the actin and myosin cross-bridges to dissociate. Most of the ATP in myocardium is produced from mitochondrial oxidative phosphorylation (Rech et al. 2018). In HFpEF, cardiac energetic deficiencies contribute to impaired myocardial function (Phan et al. 2009) and altered energy reserve equilibrium has been associated with LV diastolic dysfunction (Heinonen et al. 2020). Changes in coronary vasculature and LV hypertrophy, which increase the oxygen diffusion distance, may reduce the oxygen supply to the cardiomyocyte. Moreover, with the increased resting tension associated with LV diastolic dysfunction, myocardial oxygen demand is increased, which further exacerbates dysregulation in oxygen and energy supply-and-demand, making the cardiomyocyte prone to hypoxia. Furthermore, production of myocardial reactive oxygen species (ROS) in HFpEF damages mitochondria, thereby contributing to deficiencies in ATP production (Hiebert et al. 2019). Therefore, reduced availability of ATP may contribute to LV diastolic dysfunction.

1.4.2.2 Calcium homeostasis

Altered Ca^{2+} homeostasis has been implicated as the main process of impaired active cardiomyocyte relaxation in LV diastolic dysfunction (Pironti et al. 2018). During both systole and diastole, intracellular Ca^{2+} concentration is regulated by several Ca^{2+}-handling proteins and ion channels (Sutanto et al. 2020). During systole, electric signals at the sarcolemma cause Ca^{2+} to move from the extracellular space into the cardiomyocytes through voltage-gated channels. This process induces Ca^{2+} release from the sarcoplasmic reticulum (SR) through the ryanodine receptor 2 (RyR2), thereby causing an increase in cytoplasmic Ca^{2+} concentrations, which drives actin-myosin cross-bridge formation and hence facilitates myocardial contraction. During diastole, myocardial relaxation is facilitated when Ca^{2+} is removed from the cytosol via several Ca^{2+} channels. In diastolic dysfunction, abnormal function of the Ca^{2+} ion channels responsible for Ca^{2+} homeostasis (Adeniran et al. 2015; Park and Oh 2013), results in increased cytosolic Ca^{2+} concentration, which leads to a persistent cross-bridge formation that increases resting diastolic tension and impairs myocardial relaxation (Lewis et al. 2017). Several Ca^{2+} ion channels and cellular mechanisms have been identified that contribute to the increased cytosolic Ca^{2+} concentrations during diastole. These include reduced expression and activity of sarcoplasmic/endoplasmic reticulum Ca^{2+}ATPase 2a (SERCA2a), which moves Ca^{2+} from the sarcoplasm through reuptake into the sarcoplasmic reticulum (SR) (Lipskaia et al. 2010; Park and Oh 2013); decreased sarcolemmal Ca^{2+} efflux due to abnormalities in the sodium-calcium exchanger and persistent leaking of Ca^{2+} from the SR via the RyR2 ryanodine receptor during diastole (Lewis et al 2017). However, whether these changes in Ca^{2+} channels are a cause, or a consequence of LV diastolic dysfunction is currently uncertain.

1.5 Systolic function in HFpEF

As indicated in the definition, in patients with HFpEF systolic function, as measured by systolic chamber pump function, is usually preserved and the condition is characterised by diastolic abnormalities (as discussed in the sections above). LVEF is the most common index of systolic function and is a measure of systolic chamber function (Borlaug et al., 2009). Systolic chamber function is largely preserved in LV diastolic dysfunction, because of the concentrically remodelled left ventricle (Pavlopoulos et al. 2008). However, other measures of systolic function can identify impairments in systolic myocardial function long before changes in systolic chamber pump function are detected. Midwall fractional shortening (FSmid), which measures the degree of systolic shortening in midwall fibres, together with TDI measures of shortening in the septal or lateral wall of the LV can be used to identify deformities of myocardial systolic function in concentrically remodelled hearts (Lang et al. 2015). Indeed, decreases in these more sensitive measures of systolic myocardial function have been reported in HFpEF (Yip 2002; Yu et al. 2002).

Nevertheless, both TDI-determined systolic function and midwall fractional shortening are angle dependent and are often preserved in patients with LV diastolic dysfunction, into the advanced stages of heart failure (Stokke et al. 2017). However, two-dimensional speckle tracking echocardiography (STE) has been advocated as an angle-independent measure of systolic function and hence a more sensitive index of myocardial systolic performance (Mor-Avi et al. 2011). STE affords a more comprehensive assessment of global and regional myocardial deformation and motion in different planes (Augustine et al. 2013; Leitman et al. 2004). Myocardial deformation has been shown in patients with HFpEF (Wang et al. 2007).

Although clinical data denote the presence of abnormal LV systolic myocardial function in HFpEF, currently the cellular mechanisms underlying these observations are limited and indirect (Nagueh 2021). In hypertrophic cardiomyopathy, interstitial fibrosis has been implicated in impaired regional systolic dysfunction, as it may interfere with force generation and transmission, which ultimately results in decreased heart wall motion or hypokinesis (Maragiannis et al. 2018). In this regard, myocardial fibrosis has been associated with changes in expression patterns of different myosin heavy chain isoforms (Pandya, Kim, and Smithies 2006). In cardiomyocytes, myosin forms cross-bridges with actin and the cross-bridge activity is the basis for muscle contraction. Each myosin molecule is composed of four light chains and two heavy chains. Different myosin isoforms are associated with specific contractile properties (England and Loughna 2013). The α-isoform of mammalian cardiac myosin heavy chain (α-MyHC) is regarded as the 'fast-twitch' isoform associated with higher ATPase activity compared with the β-isoform of mammalian cardiac myosin heavy chain (β-MyHC), which is considered the 'slow-twitch' isoform (Stuart et al. 2016). Although increased β-MyHC expression is traditionally considered a marker of hypertrophy, evidence suggests it is increasingly expressed in areas of fibrosis (Pandya, Kim, and Smithies 2006; Pandya and Smithies 2011). Moreover, due to their differential ATPase activities, cardiac MyHC isoform expression patterns influence myocardial energetics and contractile properties (Nakao et al. 1997). Indeed, in both human and rat failing hearts, β-MyHC is predominantly expressed, whereas healthy hearts have greater expression of α-MyHC (Nakao et al. 1997; Warren et al. 2003; Miyata et al. 2000). Furthermore, changes in MyHC isoform expression have been associated with impaired systolic function in HFpEF (Nakao et al. 1997). Moreover, in hypertrophic cardiomyopathy mutations in the myosin heavy chain genes are associated with altered myocardial contractility and relaxation (Anderson et al. 2018). However, changes in MyHC isoform expression and contractile efficiency associated with fibrosis have not been shown in HFpEF. In addition to the speculation that fibrosis may cause changes in MyHC isoform expression patterns, fibrosis and altered collagen volume have also been associated with myocyte slippage in dilated cardiomyopathy (Kong, Christia, and Frangogiannis 2014). In contrast, others have shown that even in

patients with advanced cardiomyopathy there is no association between fibrosis and systolic dysfunction (Cordero-Reyes et al. 2014).

Besides fibrosis, altered Ca^{2+} homeostasis has been suggested to contribute to systolic dysfunction in HFpEF (Eisner et al. 2020). Changes in Ca^{2+} handling and ion channel regulation are some of the hallmark features of systolic chamber dysfunction associated with HFrEF (Ge et al. 2019). Changes in Ca^{2+} homeostasis in HFrEF contribute to malignant arrhythmias and ultimately to cardiomyocyte apoptosis (Ge et al. 2019; Simmonds et al. 2020). There is a currently paucity of data to assess whether intracellular Ca^{2+} levels and changes in Ca^{2+} ion channels contribute to systolic dysfunction in HFpEF or not (Eisner et al. 2020). Another major contributor to systolic dysfunction in HFrEF is myocardial mitochondrial dysfunction. In this regard, defects in mitochondrial function are strongly implicated in contractile dysfunction as it results in abnormal Ca^{2+} handling, increased ROS production and apoptosis (Brown et al. 2017; Ge et al. 2019). Although impaired mitochondrial function has been implicated in LV diastolic dysfunction, whether it contributes to systolic dysfunction in HFpEF is unknown.

Taken together, LVEF is maintained in patients with LV diastolic dysfunction, likely as a result of the compensatory concentric hypertrophy. However, changes in more sensitive measures of myocardial systolic function have been reported in patients with LV diastolic dysfunction. Currently there is no direct evidence to explain whether the cellular mechanisms associated with LV diastolic dysfunction also contribute to subclinical systolic dysfunction. Considering that systolic dysfunction in HFpEF patients portends a worse clinical outcome, a greater understanding of the pathophysiological mechanisms of systolic dysfunction in HFpEF is necessary.

1.6 Systemic signals associated with the development of LV diastolic dysfunction

It is well established that several traditional risk factors including advanced age, hypertension and diabetes mellitus are strongly associated with the development of LV diastolic dysfunction (Agbor et al. 2020; Ziaeian and Fonarow 2016). The pathophysiological mechanisms underlying the associations between these comorbid conditions and LV diastolic dysfunction have been the subject of research interest for several years. Although the pathophysiological mechanisms remain contentious, it has been proposed that these comorbid conditions induce a state of chronic systemic inflammation that is one of the underlying causal mechanisms for the development of LV diastolic dysfunction and HFpEF (Paulus and Tschöpe 2013). In the general population, inflammatory cytokines are strongly related to LV diastolic dysfunction and HFpEF (Deswal et al. 2001; Torre-Amione et al. 1996). Moreover, in patients with chronic systemic inflammation induced by auto-immune diseases such as rheumatoid arthritis and lupus erythematosus, the risk for developing HFpEF is doubled compared to the general population (Packer 2020). Indeed, in cross-sectional

studies in rheumatoid arthritis patients, increased concentrations of circulating inflammatory markers are independently associated with increased prevalence of LV diastolic dysfunction (Aslam et al. 2013; Crowson et al. 2013; GonzalezJuanatey 2004). Also, in a rodent model of systemic inflammation, we recently showed strong associations between circulating inflammatory markers and impaired LV diastolic dysfunction (Mokotedi et al. 2020).

It has been suggested that inflammation may play a role in the various phenotypes of LV diastolic dysfunction (Van Linthout and Tschöpe 2017). In a model of comorbidity-induced inflammation, it was reported that inflammation affects several cellular processes involved in the development of LV diastolic dysfunction (Franssen et al. 2016). However, the confounding factors in comorbid conditions make it difficult to delineate the independent effects of inflammation on the cellular mechanisms underlying LV diastolic dysfunction. In this section, I will briefly highlight the current evidence that inflammation impacts cellular mechanisms underlying the different phenotypes of LV diastolic dysfunction.

1.6.1 The role of inflammation in extracellular matrix remodelling and fibrosis

Inflammation impacts several processes linked to extracellular matrix remodelling and the development of myocardial fibrosis. Increased expression of pro-inflammatory cytokines upregulates the cardiac expression of transforming growth factor β (TGFβ) (Villar et al. 2009; Westermann and Heymans 2014), which in turn activates cardiac fibroblasts that transdifferentiate into collagen-producing myofibroblasts. Fibroblasts are also known to produce LOX enzymes, which catalyse collagen cross-linking. Collagen that is cross-linked becomes resistant to degradation. Therefore, this inflammation-induced increase in myocardial collagen deposition and cross-linking is associated with stiffening of the myocardial extracellular matrix and pathological changes in LV geometry (Kuwahara et al. 2002; Villar et al. 2009) (Kuwahara et al. 2002; Villar et al. 2009). Cardiac macrophages have been identified as sources of profibrotic cytokines, TGFβ1 and interleukin-10 in a mouse model of hypertension and advanced age (Hulsmans et al. 2018). Although macrophages are pro-inflammatory cells that are resident in both normal and diseased cardiac tissues (Heidt et al. 2014; Hulsmans et al. 2018), evidence of their contribution to extracellular matrix remodelling that leads to LV diastolic dysfunction and HFpEF in chronic inflammatory conditions, independent of comorbidities is lacking.

Inflammation also impacts collagen turnover, which may contribute to adverse extracellular matrix remodelling. Some studies suggest that in the process of fibrosis, collagen deposition exceeds collagen degradation (Samak et al. 2016; Strassheim et al. 2019). This imbalance between collagen deposition and degradation leads to dysregulated collagen turnover, which contributes to myocardial stiffness (Goldsmith, Bradshaw, and Spinale 2013; Gonzalez-Santamaria et al. 2016; McKleroy, Lee, and Atabai 2013). In

contrast, *in vivo* studies using animal models have shown that inflammatory cytokines, such as TNF-α, induce the cardiac-specific production of matrix metalloproteinases (MMPs), which catalyse collagen degradation (Liu, Sun, and Sader 2006). ROS, which are regulated by inflammatory cytokines, have also been implicated in the increased production of MMPs. Although the main function of MMPs is degradation of extracellular matrix components, upregulated MMP expression stimulates the disordered production of collagen-I fibres (Li et al. 2000). Hence, upregulation of MMPs contributes to fibrosis and adverse extracellular matrix remodelling (Li et al. 2000; Liu, Sun, and Sader 2006). Although it has been suggested that low-grade inflammation induced by comorbidities is associated with some of the mechanisms involved in myocardial fibrosis and extracellular matrix remodelling (Paulus and Tschöpe 2013), the independent effect of inflammation on these processes and whether they contribute to LV diastolic dysfunction is uncertain.

1.6.2 The role of inflammation in titin compliance

In a paradigm proposed by Paulus & Tschöpe (2013), it was suggested that comorbidity-induced systemic inflammation is one of the main catalysts of passive myocyte stiffness. It was postulated that increased circulating levels of pro-inflammatory cytokines, such as TNF-α and interleukin-6 (IL-6), lead to microvascular endothelial inflammation measured by the increased expression of endothelial activation markers such as vascular cell adhesion molecule 1 (VCAM1), intracellular adhesion molecule 1 (ICAM1) and E-selectin. In turn, these adhesion molecules stimulate the production of ROS, which impacts the production of nitric oxide (NO) and hence decreases NO bioavailability (Paulus and Tschöpe 2013). Under normal physiological functioning, NO has a central role in the cyclic guanosine monophosphate (cGMP) pathway as the primary activator of soluble guanylate cyclase (sGC). When NO binds to and activates sGC, cGMP production is upregulated, promoting activation of protein kinase G (PKG) signalling. PKG phosphorylates titin, thereby ensuring the elastic recoil that is needed for cardiomyocyte compliance and effective myocardial relaxation. Decreased bioavailability of NO, dysregulates the NO-cGMP signalling pathway, which leads to the hypophosphorylation of the titin N2B isoform, which has been implicated in the development of LV diastolic dysfunction (Lewinter and Granzier 2014). Subsequent animal models of comorbidity-induced inflammation have indeed supported this paradigm (Franssen and Gonzalez Miqueo 2016). Nevertheless, PKG is not the only regulator of titin function (Zile et al 2015). Indeed, several other protein kinases and phosphatases regulate titin phosphorylation (Franssen and Gonzalez Miqueo 2016; Krysiak et al. 2018; Zile et al. 2015). The impact of inflammation on the other regulators of titin phosphorylation, particularly phosphatases, is uncertain. Moreover, in comorbid conditions such as diabetes mellitus and hypertension, the effects of insulin and pressure overload, respectively, may stimulate cellular

signals that affect titin phosphorylation (Krysiak et al. 2018). Hence the independent effect of inflammation on the regulation of titin phosphorylation warrants investigation.

1.6.3 The role of inflammation in calcium homeostasis

Changes in intracellular Ca^{2+} concentrations are one of the primary mechanisms of active relaxation of the myocardium during diastole, as discussed above in section 1.4.2. However, the impact of inflammation on the cellular processes involved in Ca^{2+} homeostasis is controversial. As the activity of SERCA2a is central to maintaining cellular Ca^{2+} transients, several studies have focused on the effects of inflammation on SERCA2a expression and activity. Pro-inflammatory cytokines, such as TNF-α and interleukin 1β (IL-1β), have been shown to downregulate the mRNA and protein expression of the SERCA2a (Hedayat et al. 2010; McTiernan et al. 1997). It has been implied that the decreased expression of SERCA2a would decrease Ca^{2+} re-uptake into the SR during diastole and hence impair myocardial relaxation (Fredersdorf et al. 2012). In contrast, others have shown that inflammation does not affect the expression of SERCA2a (Pironti et al. 2018) and that its expression contributes little to the regulation of diastolic Ca^{2+} transient in models of inflammation (Wagner, Maier, and Bers 2015). Instead, it has been proposed that inflammation-induced increased Ca^{2+} leakage from the SR via the RyR2 receptor, coupled with decreased plasmalemmal Ca^{2+} ATPase and impaired Na^{+}/Ca^{2+} exchange, two major sources of Ca2+ efflux, may contribute more strongly to cardiac dysfunctions (Wagner, Maier, and Bers 2015). Aside from the expression of SERCA2a, some studies have reported that inflammation impacts the expression and phosphorylation of phospholamban, the Ca^{2+}-handling protein that regulates the activity of SERCA2a (Combes et al. 2002). In contrast, others have shown no change in cardiomyocyte phospholamban expression when exposed to pathological concentrations of TNF-α (McTiernan et al. 1997).

Considering the large demand on mitochondrial ATP production for the maintenance of Ca^{2+} homeostasis, it is important to consider the impact of inflammation on myocardial mitochondrial function. In HFrEF; resulting from conditions of ischemia, infection or toxicity, dysfunctional mitochondria produce pathological concentrations of ROS, which stimulate autophagy, apoptosis and necrosis, resulting in progressive cardiomyocyte loss (Hare 2001). Although basal concentrations of ROS are part of normal cellular functioning, pathologically increased levels of ROS create a cytotoxic environment that ultimately results in cell death (Peoples et al. 2019). Although the paradigm proposed by Paulus & Tschöpe (2013) (as discussed in section 1.6.2) suggested increased ROS production as a catalyst of endothelial dysfunction in comorbidity-induced inflammation and HFpEF, whether systemic inflammation directly impacts mitochondrial function, is currently uncertain.

Taken together, inflammatory cytokines may alter the cellular mechanisms involved in extracellular matrix remodelling, passive myocyte stiffness and active processes involved in LV relaxation. The resultant effects are increased myocardial stiffness, impaired relaxation and impaired LV filling that underlie the pathogenesis of LV diastolic dysfunction. However, the majority of the evidence to support the effect of inflammation on these cellular processes has been derived from cell culture models or animal models of comorbidity-induced inflammation. Therefore, currently the evidence that systemic inflammation in the absence of confounding comorbidity impacts these cellular processes in an *in vivo* model independent of comorbid conditions is lacking. *Hence, in this thesis, I aimed to determine the independent effects of inflammation on the active and passive cellular mechanisms involved in LV diastolic dysfunction in an animal model of systemic inflammation, independent of comorbidities, where LV diastolic function was impaired.*

1.6.4 The role of inflammation in systolic dysfunction

Although LV diastolic dysfunction is considered the predominant pathophysiology in HFpEF, several studies have shown that myocardial systolic function may also be impaired (as discussed in section 1.5). Considering the central role of inflammation in cellular mechanisms underlying the development of diastolic dysfunction, how is systolic function impacted by inflammation? Cross-sectional studies in the general population and in patients with auto-immune diseases have shown that circulating inflammatory markers are associated with TDI indices of systolic dysfunction, as well as with myocardial deformation and impaired motion (Lo Gullo et al. 2018). Moreover, we have recently shown that circulating inflammatory markers are strongly associated with impaired STE-derived measures of systolic function in an animal model of systemic inflammation in the absence of reduced ejection fraction (Mokotedi et al. 2020; Rudominer et al. 2009).

Regarding the mechanisms of inflammation-induced systolic dysfunction, in HFrEF, inflammation is associated with cardiomyocyte damage and loss by apoptosis (Simmonds et al. 2020). Inflammation is produced in the cardiomyocytes following a predisposing event such as ischaemia, toxicity or infection. This local inflammation has been associated with impaired Ca^{2+} homeostasis and mitochondrial dysfunction, which promote myocardial cell death (Ge et al. 2019). In contrast to HFpEF, it has been proposed that systemic inflammation drives the development of cardiac dysfunction due to an immune–inflammatory activation in the heart that is strongly associated with the progression of LV diastolic dysfunction (Glezeva and Baugh 2014; Paulus and Tschöpe 2013). However, the mechanisms of systemic inflammation-induced systolic dysfunction are uncertain. Moreover, although several mechanisms of systolic dysfunction in HFpEF have been proposed; including aberrant Ca^{2+} handling, mitochondrial

dysfunction and fibrosis-induced changes in contractile protein properties and myocyte slippage (as discussed in section 1.5), there is currently no direct evidence that these mechanisms contribute to systolic dysfunction in HFpEF and secondly, whether inflammation directly impacts these mechanisms (Nagueh 2021). *Therefore, in the current thesis, in an animal model of systemic inflammation-induced LV diastolic dysfunction that is independent of comorbidities, I aimed to investigate the cellular processes that contribute to altered myocardial systolic function as indexed by STE measurements.*

1.7 Therapeutic interventions for the management of LV diastolic and systolic dysfunction in HFpEF

Over the past decade, significant advances have been made in the management and treatment of HFrEF (Shah et al. 2014). However, therapies shown to benefit patient outcomes in HFrEF have consistently shown unsatisfactory results in HFpEF (Shah et al. 2014). The failure of these therapies in large outcome-based clinical trials may be a result of the heterogeneity of the phenotypes of HFpEF and the different systemic and myocardial signalling in HFpEF compared to HFrEF (Lewis et al. 2017; Paulus and Tschöpe 2013; Shah et al. 2014). Even controlling the underlying predisposing factors, mainly hypertension, using a variety of therapeutic interventions has proven unsuccessful in the treatment of HFpEF (Glezeva and Baugh 2014; Paulus and van Ballegoij 2010). Considering systemic inflammation as a possible underlying cause for the development of LV diastolic function (Paulus and Tschöpe 2013), it has become increasingly recognised that treating chronic inflammation may be a more suitable strategy for treating HFpEF (Glezeva and Baugh 2014; Paulus and Tschöpe 2013). Despite the recognised role of inflammation in the mechanisms of LV diastolic dysfunction, therapeutic strategies aimed at improving inflammation or endothelial dysfunction using broad-spectrum anti-inflammatory or immune-modulatory approaches, such as anti-TNF-α therapy, or antioxidant therapy have not been effective (Gong et al. 2007; Heymans et al. 2009; Massie et al. 2008; Redfield et al. 2013). Nevertheless, most of these therapeutics were used in patients with HFrEF. Moreover, in patients with auto-immune diseases characterised by chronic systemic inflammation, biologic disease modifying anti-inflammatory treatments that target specific inflammatory cytokines have shown significant improvements in disease progression (Kim et al. 2015). However, the use of these targeted anti-inflammatory treatments in managing HFpEF has been controversial. Some evidence suggests that anti-inflammatory treatment improves LV diastolic function in patients with rheumatoid arthritis (Omair et al. 2017). However, not all studies support these results (Baniaamam et al. 2018). Nevertheless, in animal models, targeting inflammation has shown promising results in managing specific pathways underlying LV diastolic dysfunction development (Gu et al. 2010; Heymans et al. 2005; Westermann et al. 2011). Taken together, the inefficient treatment strategies and poor outcomes for patients with HFpEF may be ascribed to the limited understanding of the pathophysiological mechanisms associated

with the development of LV diastolic dysfunction, as well as the "one-size fits-all" approach (Lewis et al. 2017). Based on the experimental data that show a benefit of anti-inflammatory treatment on mechanisms of LV diastolic dysfunction, the precise identification of the inflammatory pathways that contribute to the pathogenesis of the different phenotypes of LV diastolic dysfunction should be identified to develop specific immune-modulating agents that could be used in managing HFpEF. *Hence, in the current thesis I aimed to elucidate the role of different inflammatory modulators in the molecular pathways involved in an animal model of inflammation-induced LV diastolic and systolic dysfunction, by blocking specific circulating inflammatory cytokines. To further delineate the role of TNF-α on the molecular pathways involved in the development of LV diastolic and systolic function, I investigated the effect of exposing a human cardiomyocyte cell line (AC16 cells) to TNF-α.*

1.8 Problem statement

The present thesis was designed to address uncertainties regarding the molecular mechanisms of systemic inflammation-induced LV diastolic and systolic dysfunction. It has been proposed that chronic systemic inflammation may be the underlying causal mechanism for the development of LV dysfunction associated with HFpEF in patients with comorbid conditions such as diabetes mellitus and hypertension. However, the impact of systemic inflammation on the molecular mechanisms of LV diastolic dysfunction is confounded by factors such as insulin-resistance and hypertension. Patients with chronic systemic inflammation due to auto-immune diseases also have increased prevalence of LV diastolic dysfunction and HFpEF. Moreover, some patients with HFpEF also exhibit impaired systolic myocardial function and the molecular mechanisms of inflammation-induced systolic dysfunction in HFpEF are poorly understood. Despite inflammation being implicated in the development of LV diastolic dysfunction, the use of anti-inflammatory drugs in the management of these patients has shown contradictory outcomes, possibly owing to the limited understanding of the roles of specific cytokines in the pathophysiology of HFpEF. Considering the diverse aetiologies and heterogeneous presentation of LV diastolic dysfunction, a better understanding of the role of inflammation in the pathophysiological mechanisms underlying LV diastolic and systolic dysfunction is needed. Although human subjects are most desirable to understand the exact biology, human studies are largely cross-sectional with numerous confounders that limit the inference of cause and effect. The collagen-induced arthritis (CIA) rat provides a model of systemic inflammation that is independent of the confounding factors associated with comorbid diseases. It can be used to directly assess the effects of specific circulating proinflammatory cytokines on the molecular pathways in LV tissue that mediate development of the diastolic and systolic dysfunctions that lead to HFpEF.

1.9 Study aims

The aims of the present thesis were therefore, to use a rat model of collagen-induced arthritis to determine the contributions of systemic inflammation, circulating TNF-α and circulating IL-6 to the molecular mechanisms involved in LV diastolic and systolic dysfunction by investigating the effects of:

1. collagen-induced inflammation and inhibition of TNF-α on the development of fibrosis.
2. collagen-induced inflammation and inhibition of TNF-α on the pathways that regulate titin phosphorylation.
3. collagen-induced inflammation and inhibition of TNF-α on the active, energy dependent processes involved in LV relaxation and contraction and the effect of TNF-α on AC16 cardiomyocyte expression of genes important for these processes.
4. collagen-induced inflammation and blockade of IL-6 on the development of fibrosis, the regulation of titin phosphorylation and the active processes of LV relaxation and contraction.

CHAPTER 2: MATERIALS AND METHODS

2.1 Experimental design and animal treatment

Experimental procedures were approved by the Animal Ethics Screening Committee of the University of the Witwatersrand (AESC numbers: 2017/03/21C and 2019/02/10C). Procedures were performed in compliance with the Guide for the Care and Use of Laboratory Animals and reported in accordance with the ARRIVE guidelines. Three-month-old Sprague-Dawley rats were obtained from the Wits Research Animal Facility. Rats were randomly assigned into the control or experimental group using an online random number generator. Rats in the control group (n = 28, males n = 16; females n = 13) received a subcutaneous injection of saline (0.2ml), at the base of the tail. To induce systemic inflammation, rats in the experimental group were injected subcutaneously, at the base of the tail, with bovine type II collagen (2mg/ml in 0.05M acetic acid; Chondrex catalogue #20021, Redmond, WA, USA) emulsified in incomplete Freund's adjuvant (1:1 volume, 0.2ml; Chondrex catalogue #7002, Redmond, WA, USA). A booster injection (0.1ml) was given seven and twenty-one days after the first immunization. Rats in the experimental group were further randomized into the collagen induced arthritis (CIA) group (n = 29, males n = 14; females n = 15), the TNF-α inhibitor group (anti-TNF-α, n = 16, males n = 8; females n = 8) and the IL-6 blocker group (n = 16, males n = 8, females n = 8). Following the onset of joint inflammation, the rats in the anti-TNF-α group received etanercept (10mg/kg), a TNF-α inhibitor, by intraperitoneal injection every three days for six weeks. The IL-6 blocker group received tocilizumab (8mg/kg), an IL-6 receptor blocker, by intraperitoneal injection once a week for 6 weeks. All rats inoculated with collagen also received 1-4 mg/kg Tramazec daily, for pain relief.

Body weight and disease severity of all rats were measured weekly. To confirm development of joint inflammation, rat hind paws were scored using a 0-4 grading scale (Winter et al. 1962). Hind paws were scored as follows, a score of '0' reflected absence of swelling or focal redness of the paws; a score of '1' reflected slight swelling with/without focal redness, a score of '2' reflected mild-to-moderate paw oedema, a score of '3' reflected the presence of pronounced oedema with limited use of the joint and a score of '4' reflected the presence of excessive oedema with deformation and joint rigidity. The cumulative score for the hind paws of each rat (maximum score of 8) was used to represent the overall severity of inflammation. As the paw score is a subjective quantification of inflammation, the hind paw diameter at the metatarsal and ankle joint were also measured by digital calliper. Paw scores and paw thickness at the ankle joint and metatarsal joint were measured both prior to induction of inflammation and every second week thereafter for the duration of the study.

Tail cuff blood pressure was measured using non-invasive blood pressure amplifiers (Biopac Systems, Santa Barbara, CA, USA). To measure the tail-cuff blood pressure, rats were placed in restraints with

adjustable restriction panels. Prior to commencement of recording blood pressure measurements, rats were habituated to restraints for two weeks. The tail of the rat was placed on heating pad for 10 minutes prior to measuring the blood pressure. Measurements were performed at midday and measured every two weeks. An average of three measurements were taken.

For this study, 89 rats that are part of a larger study in which echocardiography was performed (Le Roux et al. 2022), were used for assessment of LV mRNA expression of genes involved in the passive and active processes of LV diastolic and systolic dysfunction.

2.2 Echocardiography

Following six weeks of drug treatments, rats were anaesthetized by intramuscular injections of ketamine (100 $mg.kg^{-1}$) and xylazine (5 $mg.kg^{-1}$) and echocardiography was performed by a single experienced operator who was not blinded to the experimental groups, using an ultrasound (Acuson SC 2000, Siemens Medical Solutions, USA, Inc.). Intra-observer studies were conducted on 20 echocardiographic exams. Pearson's correlations for repeat measures for LV end diastolic diameter, septal wall thickness, posterior wall thickness, E, A, and e' ranged between 0.82 and 0.94 (all $p < 0.001$). The respective coefficients of variation ranged between 1.4% and 4.7% for all the aforementioned measures and there were no differences in the repeat measures on paired t-tests (all $p > 0.2$).

Using a high resolution (paediatric) ultrasound probe (10MHz) the parasternal long axis view of the LV was obtained. Using two-dimensional M-mode imaging, the left ventricular end diastolic diameter (LVEDD) and left ventricular end systolic diameter (LVESD), the interventricular septal thickness (IVST) and posterior wall thickness (PWT) were measured in systole (S) and diastole (D) according to the American Society of Echocardiography convention (Figure 2.1a) (Lang et al. 2015). LV end diastolic volume (LVEDV) and LV end systolic volume (LVESV) were calculated using the Teicholz formula (Teichholz et al. 1976). As a measure of systolic chamber pump function, LV ejection fraction (LVEF) was calculated as (LVEDV-LVESV)/LVEDV x 100 (Teichholz et al. 1976). Midwall fractional shortening (FSmid), as a marker of myocardial systolic function was calculated as [(LVEDD + PWT_D/2 + IVST_/2) - (LVESD + H_S/2)]/[LVEDD + PWT_D/2 + IVST_D/2)] x 100, where H represents the combined septal and posterior was thickness (de Simone et al., 1994). As a marker of concentric remodelling and LV fibrosis (Travers et al. 2016), LV relative wall thickness (RWT) was calculated as (IVST in diastole + PWT in diastole)/LVEDD) (Ganau et al. 1992).

Diastolic function was measured using pulsed wave Doppler and Tissue Doppler Imaging. Mitral inflow velocity was measured in the apical four chamber view during early (E) and late diastole (A), with the

cursor placed at the mitral valve leaflet tips (Figure 2.1b). Tissue Doppler Imagining was used to measure tissue lengthening at the mitral annulus of the lateral wall during early (e') and late (a') periods of diastole (Figure 2.1c). A decreased e' measurement is considered one of the earliest markers of impaired LV relaxation, and hence was used a marker of impaired relaxation in this thesis. As mitral inflow velocity (E) is dependent on both ventricular relaxation and left atrial force, while e' is considered an index of relaxation, the E/e' was calculated as an index of left ventricular filling pressures. The lateral wall e'/a' ratio was calculated as an index of LV stiffness (Sharifov et al. 2016).

Using STE, B-mode images were obtained to determine myocardial deformation (longitudinal strain and strain rate) and myocardial motion (longitudinal velocity and displacement) in the apical four chamber view, as a more sensitive measures of LV systolic function. B-mode video loops for analysis were selected based on the video quality and whether the endocardial and epicardial boarders were well defined. For minimization of beat-to-beat variability, five consecutive cardiac cycles were used for all measures. Automatic border detection software (Siemens Medical Solutions, USA, Inc.) was used to trace the endocardial and epicardial borders with manual adjustments to ensure optimal tracking in a frame-by-frame manner. Global longitudinal peak systolic strain, strain rate, displacements and velocities were calculated as the average of the six anatomical segments over three consecutive cardiac cycles (Weytjens et al. 2006) (Figure 2.1d).

Following echocardiography, rats were terminated by thoracotomy, a blood sample was obtained after which the hearts were removed. The hearts were weighed using an analytical balance (Precisa Gravimetrics AG, Lucerne, Switzerland). The ventricles were dissected and weighed. The left ventricles were stored (-80˚C) in RNAlater® (Ambion, Sigma Aldrich, Germany).

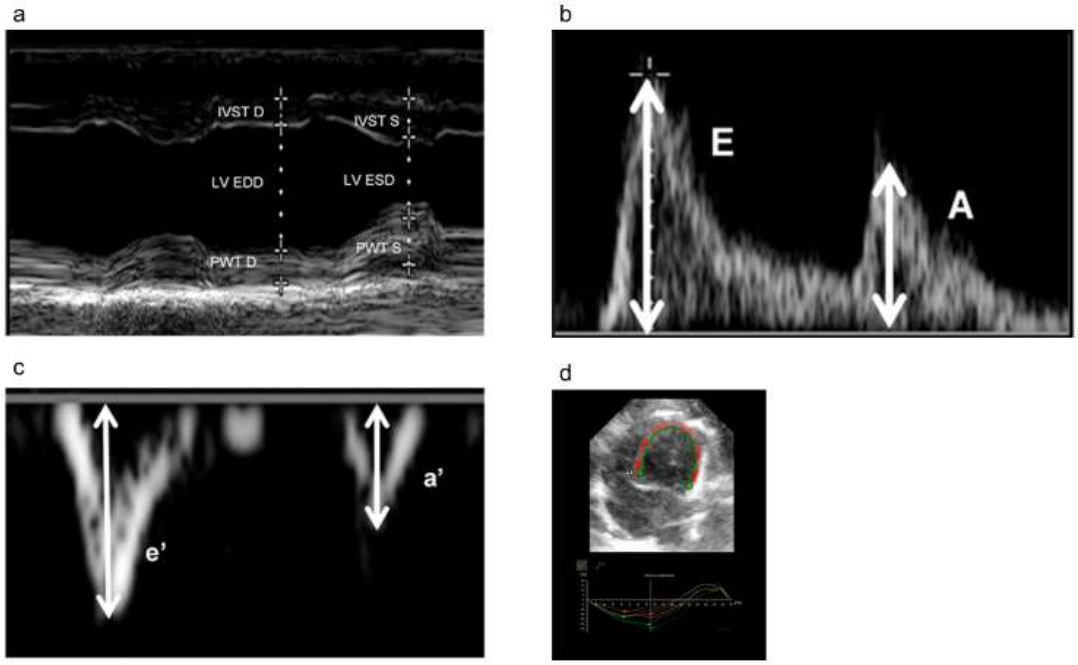

Figure 2.1. Representation of echocardiographic measures. Images showing M Mode measurement of left ventricular dimensions (a), pulse waved Doppler obtained from the mitral valve leaflet tips (b) the rate of tissue relaxation at the mitral annulus using tissue Doppler imaging (c), and speckle tracking analysis of left ventricle (d).

2.3 Circulating inflammatory markers

Whole blood samples were collected into sterile vacutainer tubes with clot activators present for collection of serum. Vacutainers were incubated on ice for 30 minutes prior to centrifugation at 5000rpm for 10 minutes (Universal 320, Hettich, Germany). Serum was collected, aliquots were made and stored at -80°C for further analysis. TNF-α, IL-6 and C-reactive protein (CRP) concentrations in serum were measured in duplicate by sandwich enzyme-linked immunosorbent assay (ELISA, Elabscience Biotechnology, USA).

2.4 Cell culture and treatment of adult cardiomyocyte cell line (AC16)

An immortalised adult human ventricular cardiomyocyte cell line, AC16 (Catalogue number 9Q019D; Sigma Aldrich, St. Louis, MO), was used as an *in vitro* model of inflammation to assess the direct effect of TNF-α on cardiomyocytes in the absence of other myocardial cell types. AC16 cells were maintained in HyClone Dulbecco's Modified Eagle Medium (DMEM) + Ham's F-12 (GE Healthcare, Chicago, IL), supplemented with 10% foetal bovine serum (FBS, Gibco; Thermo Fisher Scientific) and incubated at 37°C with 5% CO_2.

The cells were seeded into 12-well plates using serum-free + Ham's F-12 supplemented with 5% Penicillin-Streptomycin and allowed to reach ~85% confluence. Cells were then incubated with or without TNF-α (10µg/ml; Sigma Aldrich, St. Louis, MO) for 5 minutes (min), 8 hours (h) or 24 h with 4 wells per treatment and each experiment was performed three times.

2.5 Preparation of cDNA for comparative gene expression using real time PCR

Rat LV samples were homogenized by sonication and total RNA was extracted using an illustra™ Mini Spin RNA extraction kit (GE Healthcare, Buckinghamshire, UK). For cell culture experiments, cells were lysed, and total RNA was extracted using an illustra™ Mini Spin RNA extraction kit (GE Healthcare, Buckinghamshire, UK), according to the manufacturer's instructions. The resulting RNA (2µl) was used to reverse-transcribe messenger RNA to produce cDNA using SuperScript™ IV VILO™ cDNA synthesis master mix (18µl, Thermo Fisher Scientific, Life Technologies, Carlsbad, USA).

2.6 Comparative gene expression RT-PCR

Comparative gene expression RT-PCR was performed in duplex reactions on duplicated plates using a StepOne Plus thermocycler (Thermo Fisher Scientific, Life Technologies, Carlsbad, USA) with cDNA (~2µg), pre-designed TaqMan® probe mixes for the selected reference gene (0.25µl,), pre-designed TaqMan® probe mixes for each gene of interest (0.5µl, TaqMan® gene expression assay) and TaqMan® advanced PCR master mix (5µl) in a final volume of 10µl. Cycling conditions consisted of an initial hold

at 50°C for 2 minutes, a hot start hold at 95°C for 10 minutes, followed by 40 cycles at 95°C for 15 seconds and 60°C for 1 minute. When results for individual rats were outside the detection range of the PCR assay in duplicate plates, these data points were excluded from the analysis. The fold-change in relative expression was then calculated as $2^{-\Delta\Delta Ct}$, using the delta-delta Ct method (Livak and Schmittgen 2001).

For the assessment of extracellular matrix remodelling and fibrosis, comparative gene expression of the following genes was assessed using TaqMan® probes: *Col1* which codes for collagen I protein (Rn01463848_m1), *TGFβ* (Rn99999016_m1), *LOX* which codes for lysyl oxidase protein (Rn01491829_m1), *TNF-α* (Rn00562055_m1), *IL-6* (Rn01410330_m1), α smooth muscle actin (*αSMA,* Rn01759928_g1), *CD68* (Rn01495634_g1), *MMP2* (Rn01538170_m1) and *MMP9* (Rn00579162_m1).

For the assessment of the pathways involved in titin phosphorylation, comparative gene expression of the following genes was assessed using TaqMan® probes: *VCAM1* (Rn00563627_m1), *PTX3* which codes for pentraxin-3 protein (Rn01769850_m1), *iNOS* (Rn00561646_m1), *PP1γ*, which codes for protein phosphatase 1 (Rn04339209_m1), *PP5*, which codes for protein phosphatase 5 (Rn00669044_g1), *sGCα2* (Rn00675050_m1) and *sGCβ2* (Rn01636981_m1), which code for the sGC alpha 2 and sGC beta 2 subunits respectively.

To assess the contribution of active, energy dependent mechanisms of LV relaxation comparative gene expression of the following genes was assessed in LV tissues using TaqMan® probes: *Myh6* which codes for α-MyHC (Rn00568304_m1), *Myh7* which codes for β-MyHC (Rn00568328_m1), *iNOS* (Rn00561646_m1), *SOD2* which codes for superoxide dismutase 2 (Rn00690588_g1), *SERCA2a* which codes for SERCA protein (Rn00568762_m1), *BAX* which codes for Bcl-2-associated X-protein (Rn01480161_g1) and *Bcl-2* which codes for B-cell lymphoma 2 protein (ID: Rn99999125_m1).

To further delineate the role of TNF-α in the active processes underlying LV diastolic and systolic function comparative gene expression of the following genes was assessed in AC16 cells using TaqMan® probes: *TNF-α* (Hs00174128_m1), *IL-6* (Hs00174131_m1), *SERCA2a* (Hs00544877_m1), *SOD2* (Hs00167309_m1), *Bcl-2* (Hs04986394_s1) and *BAX* (Hs00180269_m1) in duplex reactions with *GAPDH* (0.25µl) in duplicated plates.

2.7 Reference gene selection

The strategy for selecting the most suitable reference gene usually involves analysis of a panel of reference genes relative to a target gene for either a subset or all of the test samples, where the expression of the target gene is correlated with the degree of the intervention outcome (Cabiati et al. 2012). Several software programmes are available for testing the reliability of a reference gene, including BestKeeper (Pfaffl MW

2004), geNorm (Vandesompele J 2002) and NormFinder (Andersen CL 2004). While each software tool employs a unique algorithm, all are based on estimating the variance in cycle threshold (Ct) values of each reference gene across the different treatment groups or tissue types being investigated (St-Pierre, Grégoire, and Vaillancourt 2017).

All RT-PCR sample reactions were performed in duplicate using pre-designed TaqMan® primer/probe mixes (TaqMan® gene expression assay; Applied Biosystems) and TaqMan® advanced PCR master mix (Applied Biosystems) on a StepOne Plus Real-Time PCR System (Thermo Fisher Scientific). No cDNA template was added to the negative controls. Four endogenous reference genes, *HPRT1* (TaqMan® assay ID: Rn01527838_g1), *Rpl32* (TaqMan® assay ID: Rn00820748_g1), *Tbp* (TaqMan® assay ID: Rn01455646_m1) and *ACTB* (TaqMan® assay ID: Rn00667869_m1), as described in table 2.1, were tested using samples of cDNA from all study groups (n=5 per group, n=20 total). IL-6 (TaqMan® assay ID: Rn01410330_m1) was used as the target gene in duplex reactions (final volume = 10μL) for each reference gene.

Cycling conditions consisted of an initial hold at 50°C for 2 minutes, a hot start hold at 95°C for 10 minutes, followed by 40 cycles at 95°C for 15 seconds and 60°C for 1 minute. The fold-change in relative expression was then calculated as $2^{-\Delta\Delta Ct}$ (Livak and Schmittgen 2001). For BestKeeper analysis, Ct values were used to calculate the geometric and arithmetic means as well as standard deviation and coefficient of variance. The reference genes were subsequently ranked from most stable to least stable based on these outcomes (Pfaffl MW 2004). For NormFinder analysis, Ct values were used to calculate the geometric means of all reference genes and similarly ranked in terms of reliability (Andersen CL 2004). The data were then analysed using RefFinder, which uses a single data input to compute multiple algorithms equivalent to the most popular stability testing programs available including the delta Ct method, BestKeeper, Normfinder and geNorm to assign a value to each gene and subsequently calculate the geometric mean of the assigned values for an overall ranking of the potential reference genes tested (Panina et al. 2018).

ACTB was excluded from the stability analysis altogether because it yielded numerous failed PCR reactions, which is consistent with an unstable reference gene. All analyses identified *Hprt1* as the most suitable reference gene in LV heart tissue of the four animal groups in this study (Figure 2.2) and it was used as the endogenous reference gene for all RT-PCR analyses of the animal model. *GAPDH* (Hs99999905_m1, Thermo Fisher Scientific, Life Technologies, Carlsbad, USA) was selected using RefFinder software (as described above) as the most suitable reference gene for the cell culture experiments when compared with *Hprt1* and *Tbp*.

Table 2.1. Description of candidate reference genes

Reference Gene	Full Gene Name	Gene Function
Hprt1	Hypoxanthine guanine phosphoribosyl-transferase 1	Transferase has a central role in the generation of purine nucleotides (Molina et al. 2018)
Tbp	TATA-box binding protein	Transcription factor involved in the initiation of eukaryotic mRNA synthesis (Cabiati et al. 2012)
Rpl32	60S ribosomal protein L32	Component of the large subunit of ribosomal protein L32
ACTB	β-actin	Component of cytoskeletal structures (Cabiati et al. 2012)

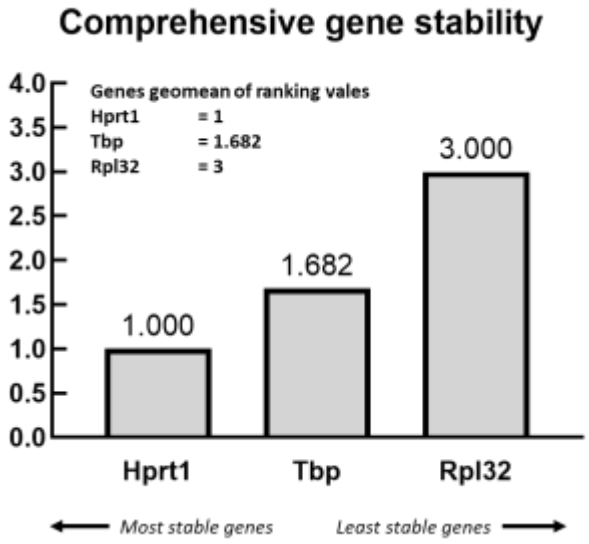

Figure 2.2. Comprehensive stability ranking of reference genes by RefFinder. All software analyses show that *Hprt1* is the best-fit reference gene when compared with geomean stability rankings of *Tbp* and *Rpl32*.

2.8 Data analysis

Statistical analyses were performed using SAS software, version 9.4 (SAS Institute Inc., USA). Normally distributed variables are expressed as mean ± standard error of the mean (SEM) and non-normally distributed variables are expressed as median (interquartile range, IQR). Differences in normally distributed variables between the groups were determined by two-way analysis of variance (ANOVA) with group and sex as the main effects, followed by Tukey *post-hoc* tests. For non-normally distributed variables group differences were determined by Kruskal-Wallis tests. As there were no differences in the molecular markers between males and females, results were combined. Associations were determined using Pearson's correlations. To determine the independent contribution of molecular markers to LV remodelling, linear regression analysis was performed. Non-normally distributed variables were log transformed prior to inclusion in regression analysis. In the AC16 cells, differences between the cells not exposed to TNF-α (control) and those exposed to TNF-α (+TNF-α) were determined by two-way ANOVA with group and time as the main effects, followed by Tukey *post-hoc* tests. Results were considered statistically significant if $p \leq 0.05$.

CHAPTER 3: INFLAMMATION-INDUCED LEFT VENTRICULAR FIBROSIS IS PARTIALLY MEDIATED BY TUMOUR NECROSIS FACTOR-ALPHA

The data in this chapter forms part of a publication in Physiological Reports

Manilall, A., Mokotedi, L., Gunter, S., Le Roux, R., Fourie, S., Flanagan, C.A., & Millen, A. M. E. (2021). Inflammation-induced left ventricular fibrosis is partially mediated by tumour necrosis factor-α. *Physiological Reports*, 9, e15062.

3.1 Abstract

Objective: To determine the mechanisms of inflammation-induced LV remodelling and effects of blocking circulating TNF-α in a model of systemic inflammation.

Method: Seventy Sprague-Dawley rats were divided into three groups: the control group, the CIA group, and the anti-TNF-α group. Inflammation was induced in the CIA and anti- TNF-α groups. Following the onset of arthritis, the anti-TNF-α group received the TNF-α inhibitor, etanercept, for six weeks. LV geometry and function were assessed with echocardiography. Circulating inflammatory markers were measured by ELISA and LV gene expression was assessed by comparative TaqMan® polymerase chain reaction.

Results: The LV relative gene expression of pro-fibrotic genes, transforming growth factor β (*TGFβ*) ($p = 0.03$), collagen I (*Col1*) ($p < 0.0001$), and lysyl-oxidase (*LOX*) ($p = 0.002$), was increased in the CIA group compared with controls, consistent with increased relative wall thickness ($p = 0.0009$). *Col1* and *LOX* expression in the anti-TNF-α group were similar to controls (both, $p > 0.05$) and tended to be lower compared to the CIA group ($p = 0.06$ and $p = 0.08$, respectively), and may, in part, contribute to the decreased relative wall thickness in the anti-TNF-α group compared to the CIA group ($p = 0.03$). In the CIA group, the relative gene expression of matrix metalloproteinase 2 (*MMP2*) was increased compared to control ($p = 0.04$) and anti-TNF-α ($p < 0.0001$) groups, respectively.

Conclusion: Chronic systemic inflammation induces fibrosis and dysregulated LV extracellular matrix remodelling by increasing local cardiac pro-fibrotic gene expression, which is partially mediated by TNF-α. Inflammation-induced LV diastolic dysfunction is likely independent of myocardial fibrosis.

3.2 Introduction

LV diastolic dysfunction is a pre-clinical condition that often progresses to HFpEF (Wan et al. 2014). Although low-grade systemic inflammation is believed to be a causal mechanism underlying LV diastolic dysfunction development in patients with comorbid conditions such as diabetes mellitus, obesity and hypertension; other factors in these conditions confound understanding of the contribution of inflammation to development of LV diastolic dysfunction (Van Linthout and Tschöpe 2017). Patients with autoimmune conditions characterized by chronic systemic inflammation, have increased risk for developing LV diastolic dysfunction (Aslam et al. 2013). Indeed, models of systemic inflammation provide useful information about the mechanisms whereby inflammation contributes to development of diastolic dysfunction (Glezeva and Baugh 2014).

Myocardial fibrosis contributes to concentric remodelling of the LV, which is characteristic of diastolic dysfunction. Myocardial fibrosis is characterized by extracellular matrix changes and hypertrophic growth of cardiomyocytes (Baum and Duffy 2011). Several factors, including increased collagen volume, collagen cross-linking, and disruption of collagen turnover contribute to formation of a stiffened extracellular matrix (El Hajj et al. 2017). Inflammation modulates the mechanisms of extracellular matrix remodelling and may thus contribute to the development of diastolic dysfunction (Goldsmith, Bradshaw, and Spinale 2013; Gu et al. 2015). Increased expression of pro-inflammatory cytokines has been associated with accelerated collagen formation (Porter and Turner 2009), increased collagen cross-linking (Suthahar et al. 2017) and altered collagen degradation, which ultimately lead to dysregulation of collagen turnover and LV fibrosis (Li et al. 2000). Although low-grade inflammation induced by comorbidities has been associated with these mechanisms of myocardial fibrosis and remodelling (Paulus and Tschöpe 2013), the effect of inflammation on these mechanisms of the LV remodelling and diastolic dysfunction, in the absence of confounding comorbidities is uncertain.

Anti-inflammatory drug treatment in auto-immune conditions characterized by systemic inflammation is known to reduce disease progression. The effects of these drugs on myocardial remodelling and diastolic dysfunction have been contradictory (Kosmas et al. 2019). Some have shown that blocking circulating inflammatory cytokines positively impacts the cellular mechanisms implicated in myocardial remodelling (Kleveland et al. 2016; Li et al. 2017), while others have failed to show positive outcomes (Hartman et al. 2016). Nevertheless, the beneficial effects were shown in systems that did not involve chronic inflammation (Kleveland et al. 2016; Li et al. 2017). We have recently shown that systemic inflammation induced concentric remodelling, diastolic dysfunction (Le Roux et al. 2022; Mokotedi et al. 2020) and increased collagen area fraction (Mokotedi et al. 2020) in the CIA rat model (Mokotedi et al. 2020). The aim of the

current study was to assess the molecular mechanisms of inflammation-induced cardiac fibrosis in LV diastolic dysfunction and to use the TNF-α inhibitor, etanercept, to assess the role of circulating TNF-α in development of fibrosis.

3.3 Results

3.3.1 Effect of collagen inoculation and anti-TNF-α treatment on body mass, blood pressure and circulating inflammatory markers

The full characterisation of the animal model is reported elsewhere (Le Roux et al. 2022). Briefly, for the partially overlapping group of animals included in this thesis, the body mass was lower in the anti-TNF-α ($p = 0.03$) and the CIA rats ($p = 0.002$) compared to controls (Table 3.1). Blood pressure was similar between groups (Table 3.1). The paw scores were increased in both the CIA and anti-TNF-α groups compared to controls (both $p < 0.05$). The thickness of the ankle joint and tarsometatarsal joints were increased in the CIA group compared to controls (both $p < 0.05$). The joint thickness of both joints in the anti-TNF-α group were not different from controls (both $p > 0.05$), and the tarsometatarsal joint thickness was lower in the anti-TNF-α group compared to the CIA group ($p = 0.01$). Circulating inflammatory marker concentrations were higher in both groups of rats inoculated with collagen compared to the control group ($p < 0.0001$, Table 3.1). Circulating CRP concentrations were lower in the anti-TNF-α group compared to the CIA group ($p = 0.04$).

3.3.2 Effect of collagen inoculation and anti-TNF-α treatment on tissue inflammatory markers

Collagen inoculation did not affect LV relative mRNA expression of *TNF-α* (Table 3.1). The LV relative mRNA expression of *IL-6* was higher in the CIA group ($p = 0.001$) than in controls (Table 3.1). Relative mRNA expression of *IL-6* was similar in the anti-TNF-α and control rats ($p = 0.06$). Compared to the control rats, the relative mRNA expression of *CD68*, a marker of monocytes and macrophages present in the LV tissue, was higher in the CIA rats ($p = 0.03$), but not in the anti-TNF-α rats ($p = 0.92$).

Table 3.1. Body mass, blood pressure and circulating and tissue inflammatory markers in control, CIA, and anti-TNF-α groups

	Control	CIA	anti-TNF-α
n	28	29	16
Female n (%)	13 (46)	15 (52)	8 (50)
Body mass (g)	460 ± 9	426 ± 9*	405 ± 12*
SBP (mm Hg)	128 ± 2	130 ± 2	131 ± 2
DBP (mm Hg)	87 ± 2	88 ± 1	86 ± 2
Paw score	0	4 (3 – 6)****	3.5 (2 – 5)****
Ankle joint thickness (mm)	8.6 ± 0.1	9.17 ± 0.1**	8.6 ± 0.2
Tarsometatarsal joint thickness (mm)	5.0 ± 0.1	5.5 ± 0.1**	5.0 ± 0.1†
Circulating inflammatory marker concentrations			
TNF-α (pg/ml)	93.9 ± 7.1	155.8 ± 3.9*	145.6 ± 2.9*
IL-6 (pg/ml)	16.4 ± 2.1	29.9 ± 2.0*	27.8 ± 2.6*
CRP (ng/ml)	0.10 ± 0.04	0.56 ± 0.04*	0.43 ± 0.05*†
Tissue inflammatory marker expressions (mRNA)			
TNF-α	1.02 (0.71 - 1.27)	1.03 (0.85 - 1.28)	1.14 (1.04 - 1.47)
IL-6	0.85 (0.65 - 0.93)	1.54 (0.88 - 2.22)*	1.04 (0.86 - 1.28)
CD68	0.92 ±0.06	1.14 ±0.06*	0.96 ±0.07

Data are expressed as means ± SEM or median (IQR). CIA, collagen-induced arthritis, anti-TNF-α, collagen-inoculated and treated with tumour necrosis factor alpha inhibitor, SBP, systolic blood pressure, DBP, diastolic blood pressure, TNF-α, tumour necrosis factor alpha, IL-6, interleukin 6, CRP, C-reactive protein. * $p < 0.05$ versus control; *** $p < 0.001$ versus control , **** $p < 0.0001$ versus control † $p < 0.05$ versus CIA.

3.3.3 Effect of collagen inoculation on LV geometry and LV relaxation

The LV RWT was higher in the CIA group than in the control group ($p = 0.0009$, Figure 3.1a), showing that collagen inoculation induced concentric remodelling. The RWT in the anti-TNF-α-treated rats was lower than in the CIA rats ($p = 0.03$) and was not different from controls ($p = 0.77$, Figure 3.1a). Myocardial diastolic function was significantly impaired in the CIA and anti-TNF-α groups. LV relaxation, as indexed by a decreased e', was impaired in both the CIA ($p < 0.0001$) and anti-TNF-α ($p < 0.0001$) groups compared to the control group (Figure 3.1b). LV lateral wall e'/a' ratio was decreased in the CIA group ($p = 0.04$) and the anti-TNF-α group ($p = 0.0001$) compared to the control group (Figure 3.1c), indicating increased LV stiffness in both groups inoculated with collagen. Similarly, the E/'e ratio was significantly increased in the CIA ($p = 0.0005$) and anti-TNF-α ($p = 0.0008$) groups compared to the control group, suggesting an increased filling pressure in the groups inoculated with collagen (Figure 3.1d). Including body mass as a potential confounder in the analysis did not materially alter the results.

3.3.4 Effect of collagen inoculation and anti-TNF-α treatment on extracellular matrix gene expression

The relative mRNA expression of *TGFβ*, which codes for the protein that stimulates fibrosis in LV tissue, was higher in CIA ($p = 0.03$) and anti-TNF-α ($p = 0.03$) rats compared to control rats (Figure 3.2a). Treatment with etanercept did not impact the increase in relative mRNA expression of *TGFβ* that was induced by collagen inoculation ($p = 0.92$; Figure 3.2a). Since TGFβ is primarily produced by monocytes in the resolution phase of inflammation (Netea et al. 2017), I assessed the association between the expression of *TGFβ* and expression of the monocyte marker, *CD68*. The relative mRNA expression of *TGFβ* was not associated with *CD68* expression (r (95%CI) = -0.004 (-0.27 - 0.28), $p = 0.98$).

The relative mRNA expression of *Col1*, which codes for the extracellular matrix protein collagen 1, was higher in the CIA group ($p < 0.0001$), but not in the anti-TNF-α ($p = 0.07$) rats compared to the control rats (Figure 3.2b). The expression of *Col1* was lower in the anti-TNF-α rats than in the CIA rats but did not reach statistical significance ($p = 0.06$). Consistent with the function of TGFβ in stimulating expression of collagen (Mollmann et al. 2010), *Col1* expression was correlated with *TGFβ* expression in all groups ($p = 0.005$; Figure 3.4a) and in the control and CIA rats ($p = 0.02$; Figure 3.4c). Since monocytes are the major source of *TGFβ*, I assessed the association between *Col1* expression and *CD68* expression. LV *Col1* expression was not associated with *CD68* expression in all groups ($p = 0.79$, Figure 3.4b) or in the control and inflammation groups ($p = 0.52$; Figure 3.4d), consistent with no association of *TGFβ* expression with *CD68* expression.

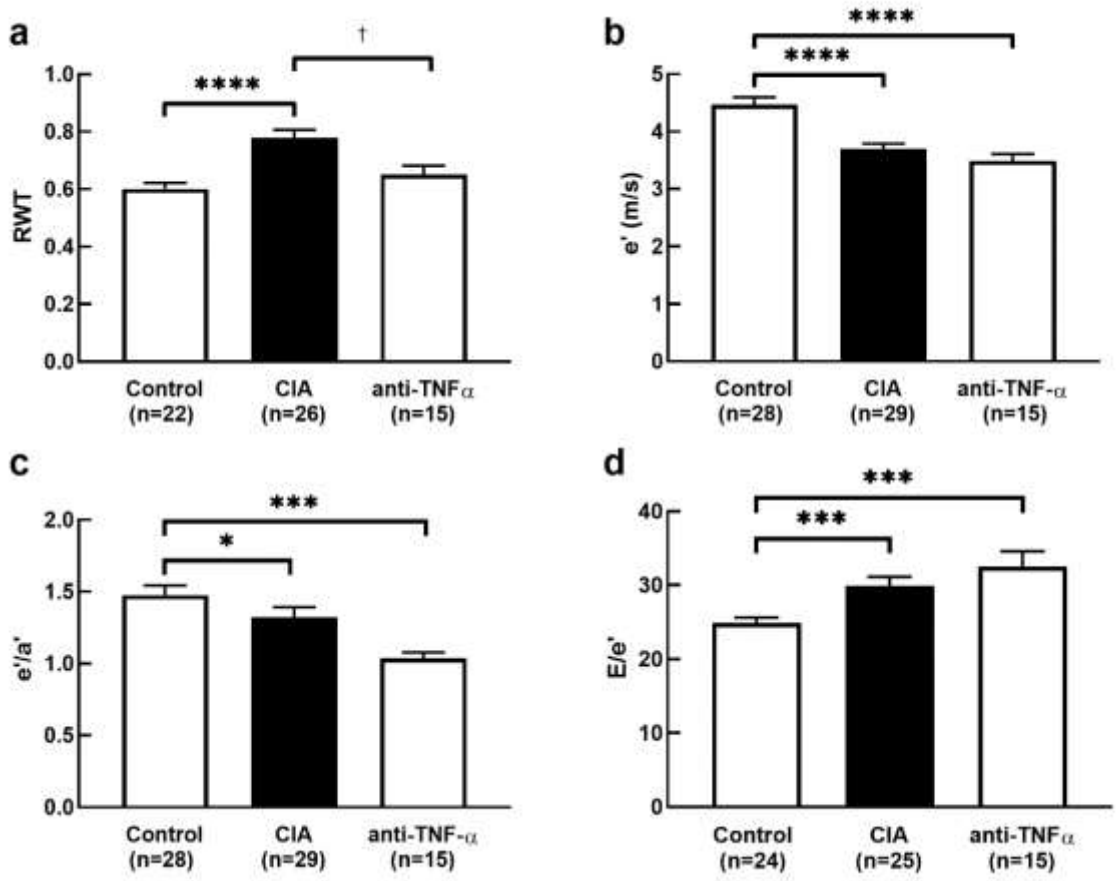

Figure 3.1. Echocardiographic measures of LV geometry and LV diastolic function. Echocardiographic measures of relative wall thickness (RWT) (a), e' (b), e'/a' (c) and E/'e (d) of control, CIA and anti-TNF-α rats. Data presented as means ± SEM; * $p < 0.05$ versus control; *** $p < 0.001$ versus control; ****$p < 0.0001$ versus control; $^{\dagger}p < 0.05$ versus CIA.

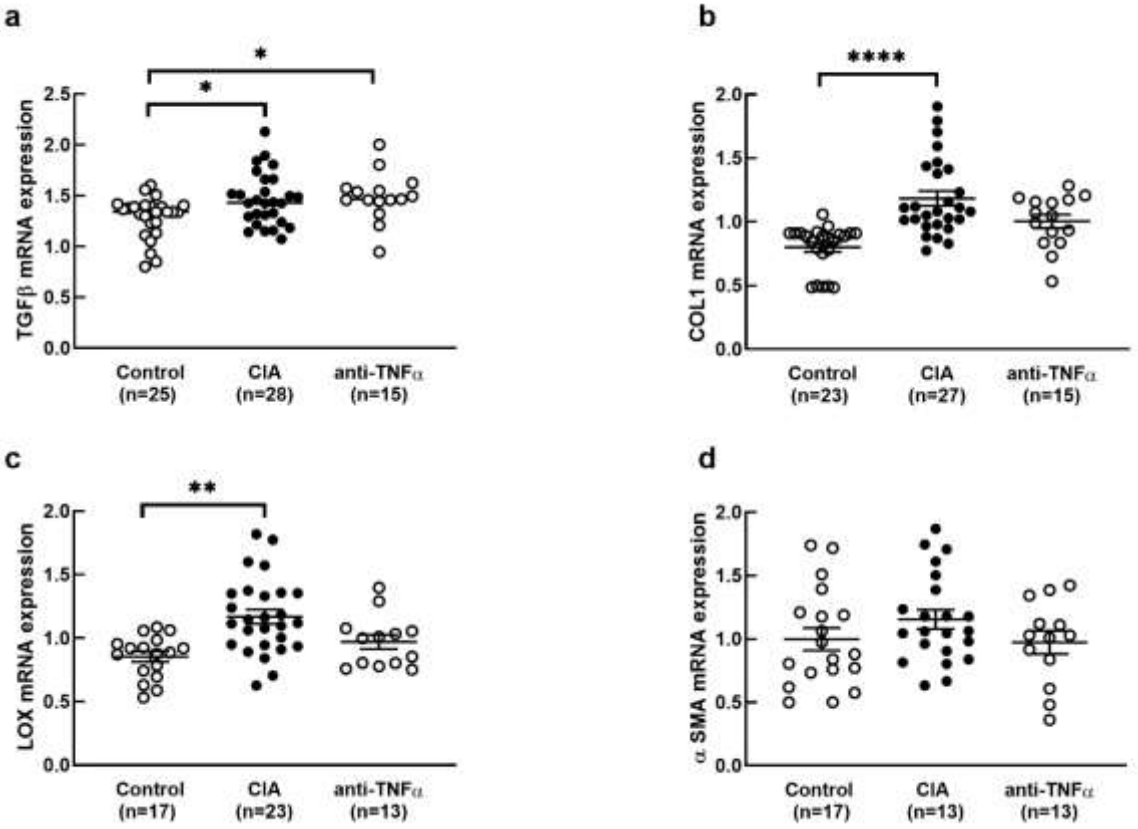

Figure 3.2. LV expression of extracellular matrix genes. Rats were inoculated with collagen (CIA) and treated with a TNF-α inhibitor (anti-TNF-α) before measurement of relative mRNA expression of *TGFβ* (a), *Col1* (b), *LOX* (c) and *αSMA* (d). Results are expressed in arbitrary units normalized for the expression of the endogenous reference gene, *HPRT1*, using the ΔΔCt method. Data presented as means ± SEM; * $p < 0.05$ versus control; ** $p < 0.01$ vs control; ****$p < 0.0001$ versus control.

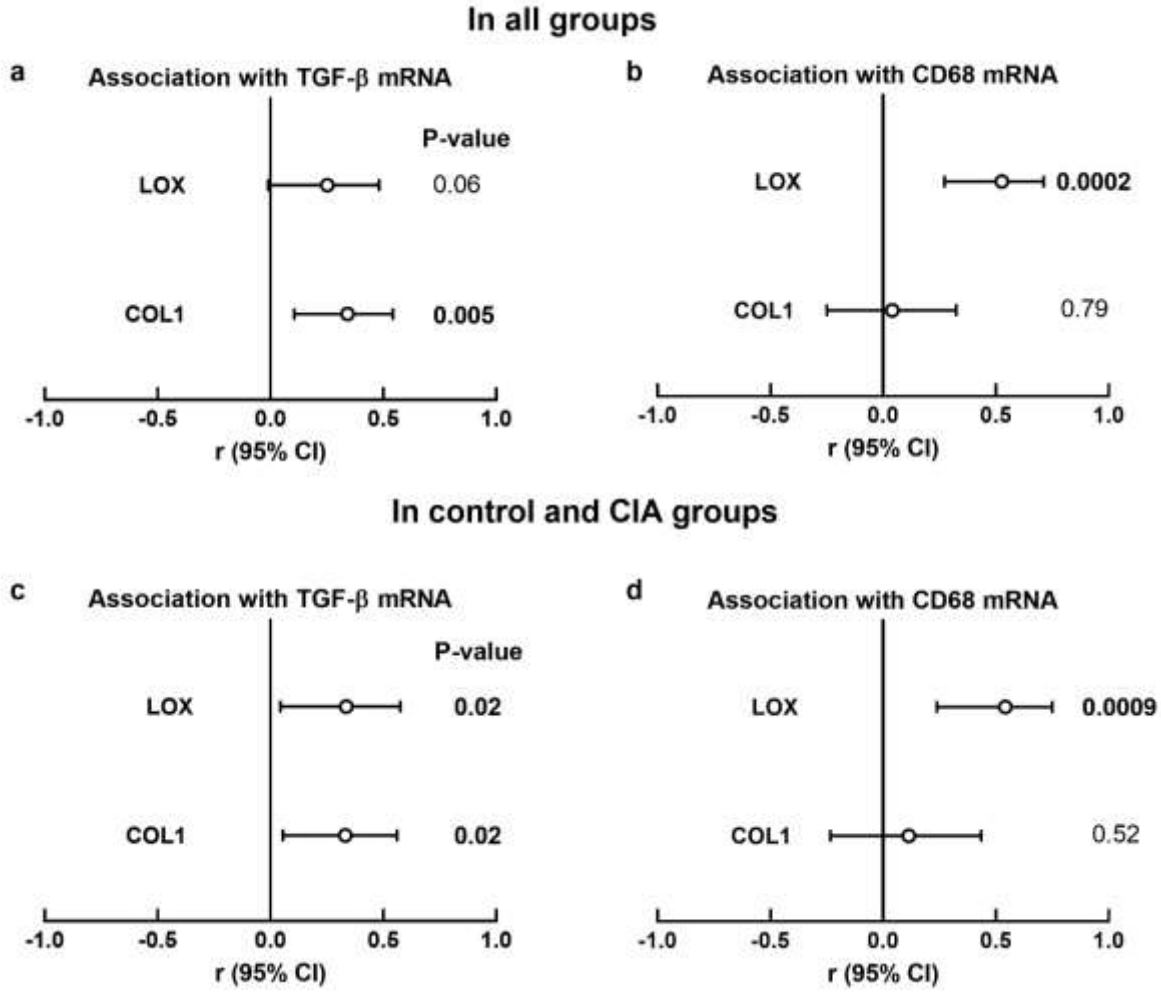

Figure 3.3. *LOX* and *COL1* markers of extracellular matrix gene expression. Pearson's correlations of *TGFβ* and *CD68* with *Col1* and *LOX* in all groups (a, b) and control vs CIA groups only (c, d). Open circles represent correlation coefficients and error bars represent 95% CI.

Compared to the control rats, relative mRNA expression of *LOX*, which codes for the enzyme that catalyses collagen cross-linking, was higher in the CIA rats (p = 0.002), but not in the anti-TNF-α rats (p = 0.26, Figure 3.2c). The expression of *LOX* was lower in the anti-TNF-α group than in the CIA group but did not reach statistical significance (p = 0.08). This suggests that blocking circulating TNF-α reduces inflammation-induced upregulation of *LOX* expression. Since *LOX* is expressed in fibroblasts that are regulated by *TGFβ*, which is produced by monocytes, I assessed the association between *LOX* expression and the expression of *CD68* and *TGFβ.* The relative mRNA expression of *LOX* was associated with *CD68,* in all groups (p = 0.0002; Figure 3.3b) and in the control and CIA groups only (p = 0.0009; Figure 3.3d). The relative mRNA expression of *LOX* was associated with the relative mRNA expression of *TGFβ* in the control and CIA groups (p = 0.02; Figure 3.3c), but not when all groups were included in the analysis (p = 177 0.06, Figure 3.3a). There were no differences between the groups in the LV relative mRNA expression of *αSMA* (Figure 3.2d). The mean ± SEM LV relative expression of *Myh7* was higher in the CIA rats (1.25 ± 0.05) compared to the control rats (0.97 ± 0.05; p = 0.0005), showing collagen inoculation induced LV hypertrophy. Expression of *Myh7* was lower in the anti-TNF-α group (0.91 ± 0.06) compared to the CIA group (p = 0.0002) and was not different from controls (p = 0.74). When determining the independent contribution of pro-fibrotic and hypertrophy gene expression markers to RWT, only *Col1* was associated with an increased RWT (std β (95%CI) = 0.62 (0.22-1.02), p = 0.003; Figure 3.4).

3.3.5 Effect of collagen inoculation and anti-TNF-α treatment on markers of collagen turnover

The LV relative mRNA expression of *MMP2*, which codes for a protein that degrades ECM components and contributes to collagen turnover, was higher in the CIA group than in the control group (p = 0.04, Figure 3.5a). LV relative mRNA expression of *MMP2* in the anti-TNF-α group tended to be lower than the CIA group (p = 0.07) and was similar to the control group (p = 0.99). Since matrix metalloproteinases play an important role in regulating collagen turnover, and inflammation resulted in increased collagen production, it is not clear whether matrix metalloproteinase expression is likely to be stimulated by systemic inflammation or by local fibrosis. Therefore, I assessed the association between *MMP2* expression and circulating inflammatory proteins and local LV expression of cytokines and pro-fibrotic genes. LV relative mRNA expression of *MMP2* was not associated with circulating IL-6 (r (95% CI), 0.10 (-0.16-0.35); p = 0.45), TNF-α (r (95% CI), 0.10 (-0.16-0.34); p = 0.46) or CRP (r (95% CI), 0.07 (-0.19-0.32); p = 0.61) concentrations (Table 3.2). *MMP2* expression was associated with local LV expression of *IL-6* (r (95% CI), 0.42 (0.15-0.62); p = 0.002), *TGFβ* (r (95% CI), 0.48 (0.27-0.64); p < 0.0001) and *Col1* (r (95% CI), 0.49 (0.28-0.66); p < 0.0001) (Table 3.2).

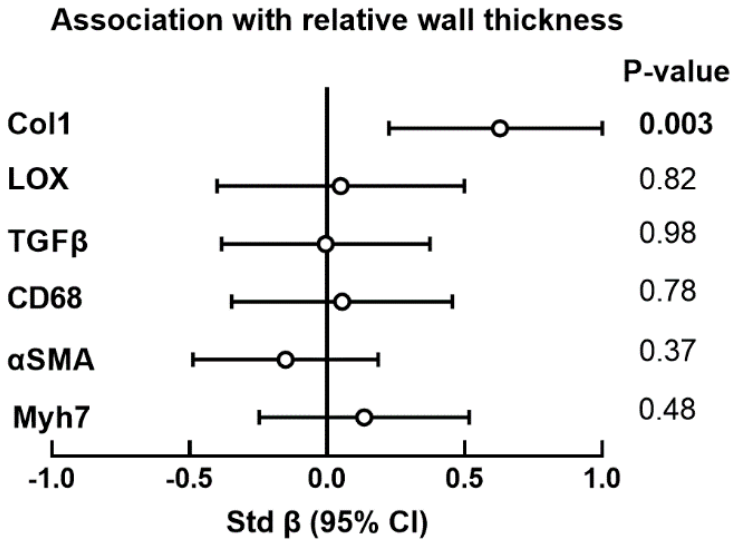

Figure 3.4. Regression analysis of relative wall thickness with *Col1*, *LOX*, *TGFβ*, *CD68*, *αSMA* and *Myh7* in left ventricular tissues of all rat groups. Open circles represent standardized beta coefficients and error bars represent 95% CI.

The LV relative mRNA expression of *MMP9*, was significantly lower in the anti-TNF-α group compared to the control ($p = 0.001$) and CIA ($p < 0.0001$) groups (Figure 3.5b), showing that blocking circulating TNFα decreases LV expression of *MMP9*. I also assessed the correlation of *MMP9* expression with circulating inflammatory proteins and local LV expression of cytokines and pro-fibrotic genes. Local LV relative mRNA expression of *MMP9* was only associated with *LOX* (r (95% CI), 0.34 (0.06-0.56); $p = 0.02$) (Table 3.2). Since matrix metalloproteinases increase extracellular matrix turnover, altered expression would be expected to affect myocardial stiffness. This is consistent with impaired LV relaxation (Figure 3.1b), increased LV stiffness (Figure 3.1c) and increased LV filling pressures (Figure 3.1d).

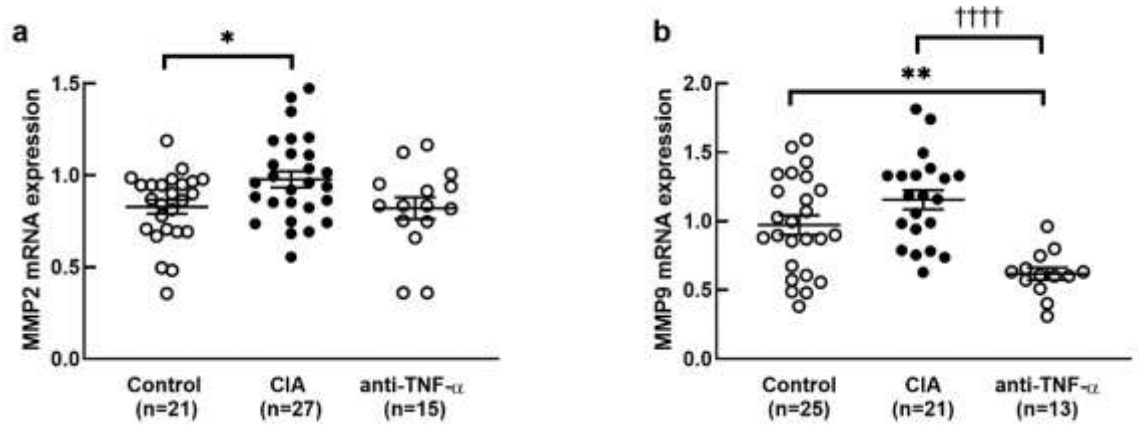

Figure 3.5. LV expression of matrix metalloproteinase genes. Rats were inoculated with collagen (CIA) and treated with a TNF-α inhibitor (anti-TNF-α) before measurement of relative mRNA expression of MMP2 (a) and MMP9 (b) in left ventricular tissues of control, CIA and anti-TNF-α rats. Relative mRNA expression results are expressed in arbitrary units normalized for the expression of the endogenous reference gene, HPRT1, using the ΔΔCt method. Data are from duplicate real time PCR experiments. Data presented as means ± SEM; * $p < 0.05$ versus control; ** $p < 0.01$ versus control; ††††$p < 0.0001$ versus CIA

Table 3.2. Association between expression of matrix metalloproteinases and pro-inflammatory and pro-fibrotic genes

	MMP2 versus				***MMP9 versus***			
	All groups (n = 77)		**Control and CIA (n = 62)**		**All groups (n = 77)**		**Control and CIA (n = 62)**	
	r(95%CI)	**p**	**r (95%CI)**	**p**	**r (95%CI)**	**p**	**r (95%CI)**	**p**
Circulating inflammatory proteins								
CRP	0.07 (-0.19-0.32)	0.61	0.17 (-0.13-0.44)	0.25	0.22 (-0.07-0.47)	0.13	0.34 (0.03-0.60)	**0.03**
IL-6	0.10 (-0.16-0.35)	0.45	0.22 (-0.09-0.48)	0.15	0.13 (-0.15-0.40)	0.35	0.27 (-0.06-0.54)	0.10
TNF-α	0.10 (-0.16-0.34)	0.46	0.25 (-0.05-0.50)	0.09	0.09 (-0.20-0.36)	0.55	0.25 (-0.08-0.53)	0.14
Tissue inflammation genes								
IL-6	0.36 (0.09-0.59)	**0.009**	0.35 (0.04-0.60)	**0.03**	0.24 (-0.10-0.53)	0.16	0.19 (-0.11-0.46)	0.21
TNF-α	-0.13(-0.38-0.13)	0.32	-0.04 (0.34-0.26)	0.80	0.08 (-0.20-0.36)	0.57	0.29 (-0.04-0.56)	0.08
Tissue fibrosis genes								
LOX	0.21 (-0.06-0.44)	0.13	0.22 (0.08-0.49)	0.15	0.34 (0.06-0.56)	**0.02**	0.44 (0.14-0.67)	**0.005**
Col1	0.49 (0.28-0.66)	< **0.0001**	0.47 (0.22-0.66)	**0.001**	-0.15 (-0.41-0.12)	0.27	-0.16 (-0.45-0.16)	0.33
Genes expressed by inflammatory cells								
TGFβ	0.44 (0.22-0.62)	< **0.0001**	0.45 (0.20-0.64)	**0.001**	-0.13 (-0.38-0.14)	0.34	-0.06 (-0.35-0.24)	0.70
CD68	0.02 (-0.27-0.30)	0.91	-0.03 (0.36-0.30)	0.84	0.20 (-0.11-0.47)	0.19	0.23 (-0.13-0.53)	0.21

Data are presented as r (95%CI). MMP2, matrix metalloproteinase 2; MMP9, matrix metalloproteinase 9; CIA, collagen-induced inflammation, CRP, C-reactive protein, IL-6, interleukin 6; TNF-α, tumour necrosis factor α; LOX, lysyl oxidase; Col1, collagen I; TGFβ, transforming growth factor β, CD68. significance indicated in bold.

3.4 Discussion

This study used a CIA model of systemic inflammation to investigate the molecular mechanisms of inflammation-induced diastolic dysfunction, focusing on LV fibrosis and extracellular matrix remodelling. I showed that the systemic inflammation resulted in local LV tissue inflammation, as evidenced by increased LV expression of *IL-6* and inflammatory leukocyte infiltration, which were inhibited when circulating TNF-α was blocked. LV expression of *TGFβ* was increased in animals inoculated with collagen. Consistent with increased *TGFβ* expression, systemic inflammation resulted in increased LV expression of the collagen gene, *Col1*, and the lysyl oxidase enzyme gene, *LOX*. These results suggest that circulating TNF-α contributes to local LV inflammation, which increases collagen production and cross-linking, that may result in fibrosis. Thus, blocking circulating TNF-α prevents adverse LV remodelling by decreasing local LV inflammation. Systemic inflammation resulted in increased expression of matrix metalloproteinases, suggesting dysregulation of extracellular matrix turnover. Blocking TNF-α prevented the upregulation of matrix metalloproteinase expression. Despite the reduced collagen formation and collagen turnover in the anti-TNF-α group, blocking circulating TNF-α had no effect on echocardiographic measures of LV relaxation or LV stiffness, suggesting that additional factors that are not regulated by TNF-α contribute to LV diastolic dysfunction.

Circulating cytokines such as TNF-α drive inflammation in a receptor-mediated manner and exert pleiotropic effects on a number of different cell types (Paulus and Tschöpe 2013). These cells, in turn, produce acute phase proteins, such as CRP, vascular adhesion molecules, matrix metalloproteinases and growth factors (Ma and Xu 2013; Paulus and Tschöpe 2013; Pironti et al. 2018). Etanercept is a fusion protein that inhibits the action of TNF-α by mimicking the soluble form of the TNF-α receptor, which binds to TNF-α in circulation and blunts its effects (Ma and Xu 2013). In the current study, local expression of *IL-6* in the LV was increased in the CIA group. This suggests that local *IL-6* expression was upregulated in response to the increased circulating cytokines induced by collagen inoculation. Similarly, a previous study in mice with post-ischemic heart failure showed increased levels of circulating cytokines that were associated with the upregulation of genes that encode chemokine and cytokine receptors in cardiac tissues (Lachtermacher et al. 2010). The downregulation of cardiac *IL-6* expression when TNF-α was blocked suggests that increased circulating TNF-α increases local expression of IL-6. There was no increase in local expression of *TNF-α* in any of the groups. *TNF-α* expression is a part of both normal and diseased physiology in the heart (Schumacher and Naga Prasad 2018). Transcription of *TNF-α* mRNA is regulated in response to complex signalling systems (Azzawi and Haselton 1999). Although elevated circulating TNF-α is considered a biomarker for cardiovascular disease, specific cardiomyocyte expression of *TNF-α* has been associated with more progressive forms of heart failure including systolic dysfunction, whereby

the relative gene dosage is proportional to disease severity (Francis 1999; Kubota et al. 2001; Lachtermacher et al. 2010). The unchanged *TNF-α* mRNA expression in this model may be explained by the effects of the intervention on the severity of cardiac dysfunction. Indeed, we and others have previously reported early-stage diastolic dysfunction or mild cardiovascular disease without systolic impairments in similar models (Le Roux et al. 2022; Mokotedi et al. 2020; Sanghera et al. 2019).

In the present study, the increased relative mRNA expression of *CD68* in the CIA group suggests macrophage infiltration of the heart tissues (Franssen et al. 2016). Although the fibroblast-stimulating growth factor, TGFβ, is broadly anti-inflammatory, it is primarily produced by macrophages (Netea et al. 2017). Thus, the increased expression of *CD68* is consistent with increased expression of *TGFβ* and *IL-6* in CIA rats, as macrophages are a source of both TGFβ and IL-6 (Hulsmans et al. 2018; Witasp et al. 2013). Although it did not reach significance, blocking circulating TNF-α tended to lower *CD68* mRNA expression in the anti-TNF-α group compared with the CIA group. This suggests that circulating TNF-α may contribute to macrophage infiltration of the heart. Supporting this, blocking soluble TNF-α has been reported to suppress activation of macrophages in retinal inflammation (Robertson et al. 2003). Consistent with increased relative mRNA expression of *CD68* in the CIA group, I showed increased local expression of *TGFβ* mRNA in this group. Increased expression of pro-inflammatory cytokines upregulates the expression of TGFβ in the heart, which in turn activates cardiac fibroblasts (Villar et al. 2009). Activated cardiac fibroblasts trans-differentiate into collagen-producing myofibroblasts, which express alpha smooth muscle actin as they mature (Lacalzada et al. 2011). Despite the upregulation of *TGFβ* mRNA in the CIA group, I did not show any differences in the mRNA expression of *αSMA*. αSMA is upregulated in response to myocardial injury during trans differentiation to myofibroblasts, but expression decreases after 21 days (Fu et al. 2018). Therefore, the unchanged *αSMA* expression in the current study may be explained by the relatively modest levels of inflammation and the time lapse between inoculation and termination. Therefore, the rate of transition to myofibroblasts may not have been high enough. Consistent with the role of TGFβ signalling in collagen production and cross-linking, I showed increased expression of *Col1* and *LOX* in the CIA group and significant associations of the mRNA expression of T*GFβ* with both *Col1*and *LOX* (Goldsmith, Bradshaw, and Spinale 2013; Páramo 2017). Although, increased deposition of collagen I and collagen III in pro-fibrotic tissues is associated with a less compliant cardiac extracellular matrix, collagen I is more fibrillar and dense in composition compared to the weaker and less mature collagen III (Husse et al. 2007; Querejeta et al. 2004). I also showed increased expression of *Myh7*, which codes for the β-myosin heavy chain, a well-known marker of cardiac hypertrophy (Marian 2021) that has also been localized to areas of fibrosis in the heart (Pandya, Kim, and Smithies 2006). However, I showed that only expression of *Col1* was associated with increased RWT. This suggests that fibrosis, rather than hypertrophy, may have

contributed to the increased concentric remodelling of the LV (Le Roux et al. 2022). Despite the increased expression of *TGFβ* in the anti-TNF-α group, blocking circulating TNF-α may have partially offset the inflammation-induced increase in the mRNA expression of *Col1* and *LOX*. This suggests that TNF-α regulation of collagen deposition and cross-linking of extracellular matrix components may be independent of the effects of *TGFβ.*

Besides the structural changes of LV geometry and evidence of fibrosis, circulating inflammatory markers impact LV extracellular matrix remodelling by altering the expression of matrix metalloproteinases (Baum and Duffy 2011). In the current study, the local relative mRNA expression of *MMP2* was increased and the expression of *MMP9* tended to be elevated in the CIA group compared to controls. The associations between the mRNA expression of *MMP2* and *IL-6, TGFβ* and *Col1* suggest that *MMP2* is upregulated in response to tissue inflammation and collagen deposition, rather than to an increase in circulating inflammatory markers. This is consistent with previous studies that have shown that tissue inflammation and increased collagen deposition in the extracellular matrix is accompanied by increased expression of *MMP2* and *MMP9* (Li et al. 2000; Sivasubramanian et al. 2001). The main function of matrix metalloproteinases is the degradation of extracellular matrix components, particularly collagen, to promote extracellular matrix turnover (Liu, Sun, and Sader 2006). Yet, paradoxically, increased matrix metalloproteinase expression is associated with increased, rather than decreased deposition of fibrotic tissue (Li et al. 2000). This is because products of matrix metalloproteinase activity are known to stimulate collagen-1 synthesis (Li et al. 2000). Consequently, disordered deposition of collagen-1 disrupts extracellular matrix structure causing fibrosis and LV stiffness (Li et al. 2000). This is consistent with our demonstration that *MMP2* expression is associated with *Col1* expression. Tissue inhibitors of metalloproteinases (TIMPs) inhibit the activity of matrix metalloproteinases (Li et al. 2000). It has been suggested that an increased ratio of matrix metalloproteinases to TIMPs favours fibrosis and LV stiffness (Sivasubramanian et al. 2001). Thus, the increased expression of matrix metalloproteinases that I have shown is likely to override the effects of TIMPs. Taken together, the increased collagen deposition, increased collagen cross-linking, and increased matrix metalloproteinase expression may have contributed to impaired LV relaxation and increased LV stiffness in the CIA group in the current study.

A recent study has shown that myocardial infarction caused alterations to elastin, which is another major component of the extracellular matrix that contributes to compliance (Yu et al. 2017). The contribution of elastin to passive stiffness in systemic inflammation requires further investigation. Other molecular pathways independent of extracellular matrix compliance, including cardiomyocyte titin compliance and Ca^{2+} handling may contribute to the LV diastolic dysfunction in this study (Lewinter and Granzier 2014; Lipskaia et al. 2010). This study has some limitations. The inclusion of male and female rats may have

reduced statistical power. Pharmacokinetic properties of the anti-inflammatory drug, which was designed for humans, may have immunogenic effects in rats (Filler et al. 2007). Because etanercept is used to treat rheumatoid arthritis, rather than heart failure, it is possible that it has poor bio-distribution into cardiac tissues and may not block locally produced TNF-α (Mann et al. 2008). Although diastolic function was measured using echocardiography in the current study, including measures of LV performance assessed by pressure volume loop analysis may have improved the interpretation of the results. Furthermore, performing echocardiography under anaesthesia may have impacted echocardiography measures. Lastly, although the presence of inflammatory cells in the heart was supported by mRNA expression of *CD68* and *IL6*, this was not confirmed by histological analysis.

CHAPTER 4: PROTEIN PHOSPHATASE 5 MEDIATES INFLAMMATION-INDUCED LEFT VENTRICULAR DYSFUNCTION IN COLLAGEN-INDUCED ARTHRITIS

The data in this chapter forms part of a publication submitted to BMC Cardiovascular Disorders

Manilall, A., Mokotedi, L., Gunter, S., Le Roux, R., Fourie, S., Flanagan, C.A., & Millen, A. M. E. (2022). Increased protein phosphatase 5 expression in inflammation-induced left ventricular dysfunction in collagen-induced arthritis in rats *(Under review)*.

4.1 Abstract

Objective: To determine the independent effects of inflammation on expression of genes that regulate titin phosphorylation in the CIA model of LV diastolic dysfunction. The TNF-α inhibitor, etanercept, was used to dissect the role of this pro-inflammatory cytokine in the pathways that regulate titin phosphorylation.

Method: The effects of collagen-induced inflammation and subsequent TNF-α inhibition on mRNA expression of genes involved in regulating titin phosphorylation were investigated in 70 Sprague-Dawley rats. LV diastolic function was assessed with echocardiography. Circulating inflammatory markers were quantified by ELISA and relative LV gene expression was assessed by Taqman® polymerase chain reaction.

Results: Collagen inoculation increased LV relative mRNA expression of vascular cell adhesion molecule 1 (*VCAM1*), pentraxin 3 (*PTX3*), and inducible nitric oxide synthase (*iNOS*) compared to controls, indicating local microvascular inflammation. Collagen inoculation decreased soluble guanylate cyclase alpha-2 (*sGCα2*) and soluble guanylate cyclase beta-2 (*sGCβ2*) expression, suggesting downregulation of nitric oxide-soluble guanylate cyclase-cyclic guanosine monophosphate (NO-sGC-cGMP) signalling. Inhibiting TNF-α prevented collagen-induced changes in *VCAM1*, *iNOS*, *sGCα2* and *sGCβ2* expression. Collagen inoculation increased protein phosphatase 5 (*PP5*) expression. Like LV diastolic dysfunction, increased *PP5* expression was not prevented by TNF-α inhibition.

Conclusion: Inflammation-induced LV diastolic dysfunction may be mediated by a TNF-α-independent increase in *PP5* expression and dephosphorylation of the N2-Bus stretch element of titin, rather than by TNF-α-induced downregulation of NO-sGC-cGMP pathway-dependent titin phosphorylation. The steady rise in number of patients with inflammation-induced diastolic dysfunction, coupled with low success rates of current therapies warrants a better understanding of the systemic signals and molecular pathways responsible for decreased titin phosphorylation in development of LV diastolic dysfunction. The therapeutic potential of inhibiting PP5 upregulation in LV diastolic dysfunction requires investigation.

4.2 Introduction

HFpEF accounts for approximately 50% of heart failure cases (Simmonds et al. 2020). Chronic systemic inflammation associated with comorbid conditions such as obesity and diabetes mellitus has been implicated in the development of LV diastolic dysfunction, the condition that frequently precedes HFpEF (Franssen et al. 2016; Paulus and Tschöpe 2013; Van Linthout and Tschöpe 2017; Wan et al. 2014). It has been proposed that inflammation contributes to LV diastolic dysfunction by disrupting phosphorylation of the giant spring protein, titin (Franssen and Gonzalez Miqueo 2016). Decreased titin phosphorylation increases sarcomere tension contributing to deceased cardiomyocyte compliance and hence increases passive cardiomyocyte stiffness, impairing myocardial relaxation (Franssen and Gonzalez Miqueo 2016; Gerassimou et al. 2007; Kang, Kang, and Shin 2013; Luiking, Engelen, and Deutz 2010).

Chronic systemic inflammation increases circulating concentrations of pro-inflammatory proteins that are thought to disrupt myocardial signalling and cardiomyocyte function by upregulating cardiac microvascular endothelial cell expression of cell adhesion proteins (Franssen et al. 2016; Paulus and Tschöpe 2013). These adhesion molecules enhance trans-endothelial movement of leukocytes and stimulate production ROS (Kong et al. 2018), which disrupt NO signalling (Franssen et al. 2016). NO released from endothelial cells enters cardiomyocytes, activating sGC to produce cGMP, which activates protein kinase G (PKG) (Mitrovic et al. 2011). Activated PKG phosphorylates multiple sites within the N2B spring element (N2B) of titin (Hamdani et al. 2017; Salcan et al. 2020). Phosphorylation of the N2B by PKG and other kinases decreases titin-based passive tension within cardiomyocytes (Koser et al. 2019). Thus, decreased NO availability has been proposed to result in hypophosphorylation of titin, which contributes to increased myocardial stiffness (Paulus and Tschöpe 2013).

Titin function is also regulated by protein phosphatase enzymes, which dephosphorylate the N2B, increasing sarcomere tension. Protein phosphatases PP1 and PP2A have been implicated in inflammation-induced dephosphorylation of titin in obese rats with HFpEF (Franssen et al. 2016). However, these phosphatases are stimulated by metabolic signals (Kleveland et al. 2016), hence their contribution to regulating titin phosphorylation independent of metabolic signals is uncertain.

PP 5 specifically dephosphorylates the titin N2B. Increased expression of PP5 increased dephosphorylation of the titin N2B *in vitro* and *in vivo* and increased cardiomyocyte passive tension (Krysiak et al. 2018). It was suggested that "pathological triggers" may activate PP5 in heart disease (Krysiak et al. 2018). Although the proximal intracellular signalling molecules that activate PP5 have been reported (Krysiak et al. 2018; Neumann et al. 2021), it is unknown whether systemic inflammation affects PP5 activity or expression.

It has been suggested that inflammation associated with comorbid conditions such as hypertension, obesity and diabetes mellitus, causes LV diastolic dysfunction and HFpEF (Paulus and Tschöpe 2013). However, the effects of insulin, pressure and volume overload in these comorbidities confound understanding of the inflammation-induced effects on the protein kinase pathways that mediate phosphorylation of titin and the protein phosphatases that dephosphorylate titin (Rastogi et al. 2003). Nevertheless, patients with systemic inflammatory conditions, such as rheumatoid arthritis, are at increased risk of developing LV diastolic dysfunction and HFpEF, independent of comorbid diseases (Ahlers et al. 2020; Kim et al. 2017). Although inflammation has been directly linked to the development of LV diastolic dysfunction in patients with rheumatoid arthritis (Liang et al. 2010), the effects of TNF-α inhibitors on LV diastolic dysfunction and HFpEF have been contradictory (Baniaamam et al. 2018). Therefore, this study used the CIA rat model to determine the independent effects of inflammation on expression of genes that regulate titin phosphorylation and development of LV diastolic dysfunction. I also used the TNF-α inhibitor, etanercept, to dissect the role of this pro-inflammatory cytokine in the pathways that regulate titin phosphorylation.

4.3 Results

4.3.1 Body mass, blood pressure, markers of inflammation and diastolic function measures

The characterization of the animal model and echocardiographic measures are reported in Table 3.1 and Figure 3.1 (Chapter 3).

4.3.2 Effect of collagen inoculation and anti-TNF-α treatment on expression of genes involved in microvascular inflammation and immune cell activation

The mean ± SEM relative LV mRNA expression of *VCAM1*, a marker of endothelial activation, was significantly increased in the CIA group (1.55 ± 0.08; $p = 0.007$), but not in the anti-TNF-α group (1.18 ± 0.11; $p = 0.98$) compared to the control group (1.16 ± 0.09, Figure 4.1a). The relative mRNA expression of *VCAM1* was significantly lower in the anti-TNF-α group compared to the CIA group ($p = 0.03$, Figure 4.1a). The relative LV mRNA expression of *PTX3*, a marker of local inflammation, (median (IQR)) was significantly higher in the CIA (2.40 (1.74-4.06); $p < 0.0001$) and the anti-TNF-α (1.71 (1.48-2.00); $p = 0.001$) groups compared to the control group (1.18 (0.43-1.3, Figure 4.1b). The relative mRNA expression of *PTX3* in the anti-TNF-α group was significantly lower than in the CIA group ($p = 0.05$, Figure 4.1b). The relative mRNA expression of *iNOS*, a marker of infiltrating leukocytes, was significantly increased in

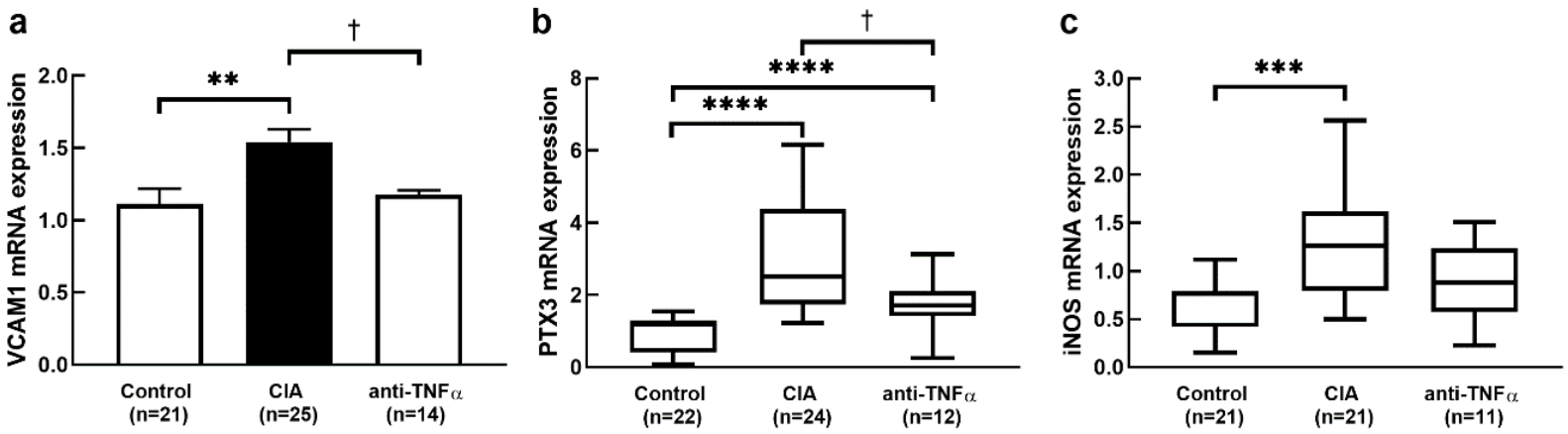

Figure 4.1. LV expression of microvascular inflammation and immune cell activation genes. Rats were inoculated with collagen (CIA) and treated with a TNF-α inhibitor (anti-TNF-α) before measurement of relative mRNA expression of *VCAM1* (a), *PTX3* (b) and *iNOS* (c) in left ventricular tissues of control, CIA and anti-TNF-α rats. Relative mRNA expression results are expressed in arbitrary units normalized for the expression of the endogenous reference gene, *HPRT1*, using the ΔΔCt method. Data are from duplicate real time PCR experiments. Data presented as means ± SEM for *VCAM1* and median and interquartile range for *PTX3* and *iNOS*; ** $p < 0.01$ vs control, *** $p < 0.001$ vs control, **** $p < 0.0001$ vs control, $^{\dagger}p < 0.05$ vs CIA.

the CIA group (median (IQR); 1.26 (0.80 - 1.62); p = 0.0003) compared to the control group (0.76 (0.43 - 0.78), but not in the anti-TNF-α group (0.88 (0.58-1.23); p = 0.10) (Figure 4.1c).

4.3.3 Effect of collagen inoculation and anti-TNF-α treatment on expression of genes involved in the NO signalling pathway

The mean ± SEM relative mRNA expression of *sGCα2* (Figure 4.2a) and *sGCβ2* (Figure 4.2b), the isoforms that code for the sGC enzyme that initiates NO-stimulated cGMP signalling, were significantly decreased in the CIA group (*sGCα2*: 1.10 ± 0.06; *sGCβ2*: 453.3 ± 44.8) compared to control group (*sGCα2*: 1.37 ± 0.06, p = 0.02, *sGCβ2*: 641.8 ± 43.3, p = 0.01). The relative mRNA expression of *sGCα2* and *sGCβ2* in the anti-TNF-α rats (1.32 ± 0.09; p = 0.13, 674.9 ± 62.4, p = 0.90, respectively) were similar to controls. The relative mRNA expression of *sGCβ2* was significantly increased in the anti-TNF-α group compared to the CIA group (p = 0.02).

4.3.4 Effect of collagen inoculation and anti-TNF-α treatment on expression of protein phosphatase gene

The mean ± SEM relative mRNA expression of *PP1γ*, the protein phosphatase previously implicated in titin phosphorylation, was not different between the three groups (p > 0.05, Figure 4.3a). The relative mRNA expression of the protein phosphatase *PP5* was significantly higher in both groups of rats inoculated with collagen (CIA, 1.61 ± 0.09, p = 0.008; anti-TNF-α, 1.59 ± 0.11, p = 0.04), compared to the control group (1.24 ± 0.09, Figure 4.3b) and was not different between the CIA and anti-TNF-α groups (p > 0.05).

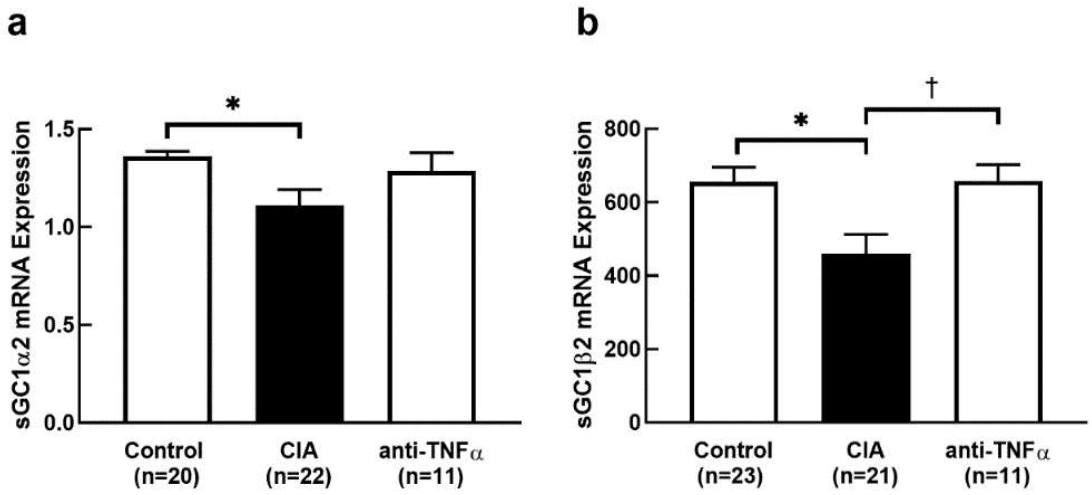

Figure 4.2. LV expression of sGC subunit genes. Rats were inoculated with collagen (CIA) and treated with a TNF-α inhibitor (anti-TNF-α) before measurement of relative mRNA expression of *sGCα2* (a) and *sGCβ2* (b) in left ventricular tissues of control CIA, and anti-TNF-α. Relative mRNA expression results are expressed in arbitrary units normalized for the expression of the endogenous reference gene, *HPRT1*, using the ΔΔCt method. Data are from duplicate real time PCR experiments. Data presented as means ± SEM; * $p < 0.05$ vs control, $^{\dagger}p < 0.05$ vs CIA.

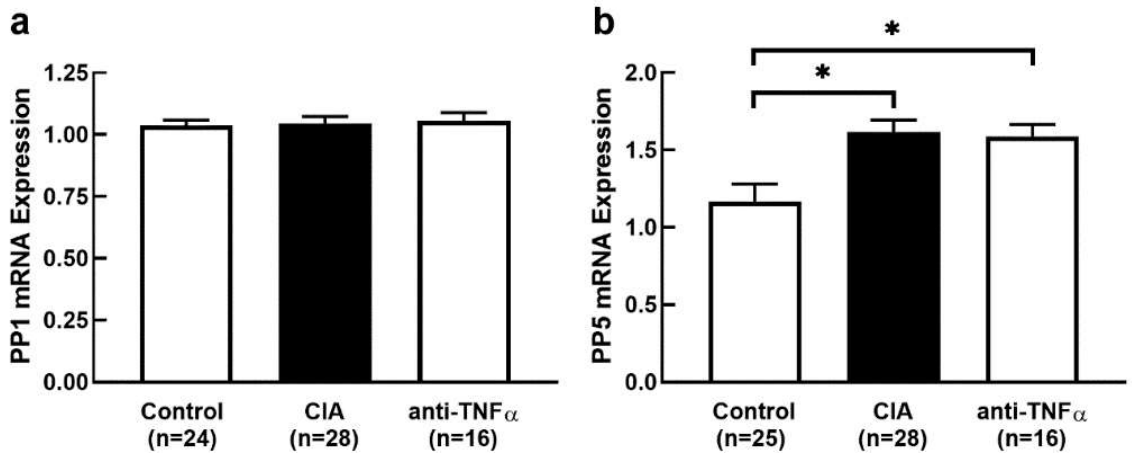

Figure 4.3. Expression of protein phosphatase genes. Rats were inoculated with collagen (CIA) and treated with a TNF-α inhibitor (anti-TNF-α) before measurement of relative mRNA expression of *PP1γ* (a) and *PP5* (b) in left ventricular tissues of control, CIA and anti-TNF-α. Relative mRNA expression results are expressed in arbitrary units normalized for the expression of the endogenous reference gene, *HPRT1,* using the ΔΔCt method. Data are from duplicate real time PCR experiments. Data presented as means ± SEM; * $p < 0.05$ vs control.

4.4 Discussion

This study investigated the effects of chronic systemic inflammation, in the absence of metabolic confounders, on expression of genes involved in LV microvascular endothelial activation, NO-sGC-cGMP signalling and titin dephosphorylation, implicated in LV diastolic dysfunction. I showed that collagen inoculation increased LV expression of *VCAM1*, suggesting endothelial activation. Furthermore, I showed increased LV expression of *PTX3* and *iNOS* indicating increased local tissue inflammation and leukocyte invasion. Supporting the role of decreased NO-dependent signalling in development of LV diastolic dysfunction, collagen inoculation decreased the expression *sGCα2* and *sGCβ2*, which code for isoforms of the sGC enzyme that initiates NO-stimulated cGMP signalling. The increased expression of *VCAM1*, *PTX3* and *iNOS*, together with decreased expression of sCG were prevented by treatment with a TNF-α inhibitor. Taken together, these results show that increased circulating TNF-α stimulates vascular inflammation, increases LV tissue inflammation and disrupts NO-sGC-cGMP signalling, which may modulate cardiomyocyte elasticity likely by phosphorylating the titin N2B. However, the collagen-induced LV diastolic dysfunction is not reversed by blocking circulating TNF-α (Chapter 3), suggesting that TNF-α and hence, decreased NO-sGC-cGMP signalling is likely not the primary mechanism of inflammation-induced LV diastolic dysfunction. Collagen inoculation had no effect on expression of *PP1γ*, but it significantly increased expression of *PP5*, a major catalyst of titin dephosphorylation (Krysiak et al. 2018). Like the inflammation-induced LV diastolic dysfunction, the inflammation-induced upregulation of *PP5* expression was not reversed by inhibiting circulating TNF-α. These results show that increased expression of *PP5*, may increase cardiomyocyte stiffness by decreasing the net phosphorylation level of the N2B stretch element of titin, which may partially mediate chronic systemic inflammation-induced LV diastolic dysfunction.

A recent paradigm suggested that in response to increased circulating inflammatory cytokines, microvascular inflammation drives altered myocardial signalling that ultimately results in hypophosphorylation of the titin N2B and consequently decreased myocyte compliance (Paulus and Tschöpe 2013). The paradigm was supported by an obese diabetic rat model of metabolic risk-associated systemic inflammation, which showed evidence of microvascular inflammation and disruption of NO signalling (Franssen et al. 2016). Our model of collagen-induced systemic inflammation, which is independent of metabolic confounders, showed upregulated LV mRNA expression of *VCAM1*. VCAM1 is a glycoprotein that is expressed predominantly on the surfaces of endothelial cells and is activated by pro-inflammatory cytokines (Kong et al. 2018; Szmitko et al. 2003). Microvascular inflammation resulting from increased expression of cell adhesion molecules, including VCAM1, promotes leukocyte transmigration (Brenes-Castro et al. 2018; Shiraki et al. 2016) and enhances ROS production that are characteristic of an

oxidative stress environment (Akhigbe and Ajayi 2021; Cerutti and Ridley 2017; Totoson et al. 2016). Supporting this, we previously showed that collagen inoculation increased CD68 expression in LV tissues, showing infiltration of leukocytes (Chapter 3). In the present study, *PTX3* and *iNOS* expression was increased in CIA rats, further indicating leukocyte infiltration in the heart tissues and hence local inflammation. PTX3 is an acute-phase protein that is structurally similar to CRP (Ristagno et al. 2019), and is produced by inflammatory cells, such as monocytes and neutrophils, but it is also produced locally by vascular endothelial cells at the sites of inflammation (Witasp et al. 2013). Leukocytes that express iNOS are known for their production of ROS, which disrupt NO bioavailability by facilitating dissociation of endothelial NOS dimers (Wang et al. 2014; Witasp et al. 2013) and by reacting with NO to produce peroxynitrite (Gunnett et al. 2005). Thus, microvascular inflammation causes the transmigration of immune cells that increase local production of ROS, which interfere with NO–sGC signalling by reducing NO bioavailability (Ghosh, Wang, and McNeill 2004).

NO diffuses into cardiomyocytes, where it activates sGC to produce cGMP, which activates PKG, one of the kinases that decrease sarcomere tension by phosphorylating the titin N2B region. Whereas decreased local NO concentrations would result in decreased NO-sGC-cGMP signalling, it has been reported that ROS also decrease the responsiveness of the NO-sGC-cGMP system to exogenous NO donors, suggesting that decreased activity or expression of sGC may further decrease cGMP signalling (Gerassimou et al. 2007). ROS have been shown to disrupt cGMP production by oxidizing the haem required for NO to bind to sGC and by decreasing protein and mRNA expression of sGC subunits (Gerassimou et al. 2007; Mitrovic et al. 2011; Rogers et al. 2014). We have shown that systemic inflammation decreased mRNA expression of both the *sGCα2* and *sGCβ2* genes. This suggests that the decreased *sGCα2* and *sGCβ2* expression induced by collagen inoculation is likely mediated by increased ROS production and that the decreased expression will result in decreased NO-sGC-cGMP signalling (Peters et al. 2004).

In the current study, blocking circulating TNF-α prevented the inflammation-induced upregulation of *VCAM1, PTX3* and *iNOS* and therefore arguably inhibited pathological ROS production. Furthermore, blocking TNF-α also prevented the inflammation-induced downregulation of mRNA expression of *sGC* genes. Taken together, our results suggest that increased circulating TNF-α increases LV microvascular endothelial activation, which increases ROS production by endothelial cells and via immune cell transmigration. The resultant increased ROS decrease sGC expression and likely also decrease its activity (Gerassimou et al. 2007; Rogers et al. 2014). This will result in decreased cGMP signalling and hence decreased PKG phosphorylation of the titin N2B region. However, despite the impact of TNF-α blockers on microvascular inflammation and NO-dependent cGMP signalling, we have shown that LV diastolic dysfunction induced by collagen inoculation was not reversed by blocking circulating TNF-α (Le Roux et

al. 2022). This indicates that TNF-α and, decreased cGMP-stimulated phosphorylation of titin, may not be the primary mechanisms of LV diastolic dysfunction induced by systemic inflammation. In this regard, it is important to consider that kinases other than NO-dependent PKG phosphorylate the N2B region of titin (Lewis et al. 2017) and that the net phosphorylation state of titin is also regulated by the phosphatases that dephosphorylate the residues phosphorylated by the kinases, increasing titin stiffness (Herwig et al. 2020). Like protein kinases, protein phosphatases are also regulated by systemic and intracellular signalling pathways (Golden, Swingle, and Honkanen 2008).

Phosphorylation and dephosphorylation of titin are part of normal cardiomyocyte contraction. Increased expression of protein phosphatases causes decreased net phosphorylation of cardiac proteins (Ferreira et al. 2019). It has been suggested that increased expression of protein phosphatases PP1 and PP2A may contribute to the hypophosphorylation of titin, characteristic of LV diastolic dysfunction (Franssen et al. 2016). In the present study, we showed that the relative mRNA expression of *PP1γ*, which codes for a major eukaryotic protein serine/threonine phosphatase that regulates a variety of cellular functions (Ferreira et al. 2019; Kiss, Erdődi, and Lontay 2019; Weber et al. 2015), was not altered in response to systemic inflammation or TNF-α inhibitor treatment. This is in contrast to a previous study that reported increased PP1 protein expression in rats that developed diastolic dysfunction in a model of obesity-associated inflammation (Franssen et al. 2016). Considering the well-known impact of metabolic signals on the regulation of PP1 expression (Kiss, Erdődi, and Lontay 2019; Petersen and Shulman 2018), the increased PP1 expression in the prior study may be explained by the metabolic dysfunction likely to result from obesity (Franssen et al. 2016). Therefore, the unchanged expression of *PP1γ* in our model of systemic inflammation independent of metabolic dysfunction suggests that PP1 expression may not be directly regulated by chronic systemic inflammation.

The N2B region of titin was recently found to also be dephosphorylated by PP5 (Krysiak et al. 2018). PP5 is ubiquitously expressed in eukaryotic cells and its activity is enhanced by ROS (Golden, Swingle, and Honkanen 2008; Krysiak et al. 2018). PP5 expression was shown to be increased in tissue from end-stage failing human hearts and from dogs with LV diastolic dysfunction (Krysiak et al. 2018). However, the stimulus for the increased PP5 expression in diastolic dysfunction and heart failure was not explored. In the current study we showed that systemic inflammation, independent of metabolic dysfunction, increased relative mRNA expression of *PP5* in collagen-inoculated rats with LV diastolic dysfunction. Our results suggest that systemic inflammation-induced LV diastolic dysfunction may, at least in part, be mediated by increased *PP5* expression and hence dephosphorylation of titin. However, other phosphoprotein phosphatases such as PP2C (Gergs et al. 2019) and PP2A (Franssen et al. 2016), that were not measured, may also be involved in titin phosphorylation. Furthermore, molecular pathways independent of titin

compliance including myocardial fibrosis and Ca^{2+} handling may contribute to LV diastolic dysfunction in this study (Le Roux et al. 2022; Lewis et al. 2017).

Importantly, in contrast to the NO-sGC-cGMP pathway, the inflammation-induced upregulation of *PP5* expression was not reversed by blocking circulating TNF-α. This suggests that the local *PP5* expression may be regulated by a circulating inflammatory signal other than TNF-α. Although PP5 expression is known to be regulated by several intracellular signals (Krysiak et al. 2018; Neumann et al. 2021), the extracellular signals that stimulate these pathways to PP5 expression and activity require further investigation. Since both the upregulation of *PP5* expression and the accompanying LV diastolic dysfunction are not mediated by TNF-α, our results suggest that diastolic dysfunction may, at least in part, result from increased expression of *PP5*, which increases cardiomyocyte stiffness by decreasing the net phosphorylation level of the N2B stretch element of titin, whereas disruption of the NO-sGC-cGMP pathway is likely less important.

This study has some limitations. The inclusion of both male and female rats may have reduced statistical power. The use of mRNA expression may not reflect protein expression and function, hence direct measures of NO, ROS and titin phosphorylation may have strengthened the interpretations of this study. Although etanercept has been successfully used in previous animal models (Totoson et al. 2016), it is a human fusion protein, which may elicit an immunogenic response in rats. In summary, our results show that systemic inflammation induced by collagen inoculation, contributes to microvascular endothelial inflammation and reduced *sGC* subunit expression, possibly disrupting the NO-sGC-cGMP signalling pathway that increases titin phosphorylation. Our findings suggest that pathological downregulation of NO-sGC-cGMP signalling may not be the primary signal for hypophosphorylation of the titin N2B in HFpEF (Paulus and Tschöpe 2013), since blocking circulating TNF-α prevented the inflammation-induced effects on NO-sGC-cGMP signalling but had no effect on LV diastolic dysfunction. Like LV diastolic dysfunction, the inflammation-induced increase in *PP5* expression was not prevented by inhibiting circulating TNF-α. Therefore, our results suggest that the activity of PP5 is likely a mediator of inflammation-induced LV stiffness and that inflammatory signals other than TNF-α regulate *PP5* expression. Future studies should explore the systemic inflammatory signals responsible for increased PP5 expression. Furthermore, although etanercept treatment is useful for decreasing inflammatory symptoms in patients with rheumatoid arthritis, it may not modulate cardiac expression of PP5 and its effects on the development of HFpEF. The therapeutic potential of inhibiting PP5 in the management of LV diastolic dysfunction warrant investigation.

CHAPTER 5: THE ROLE OF TUMOUR NECROSIS FACTOR APLHA IN ACTIVE PROCESSES OF INFLAMMATION-INDUCED LV DIASTOLIC AND SYSTOLIC DYSFUNCTION

The data in this chapter forms part of a manuscript that is in preparation for submission to the Journal of Cardiovascular Pharmacology.

Manilall, A., Mokotedi, L., Gunter, S., Le Roux, R., Fourie, S., Flanagan, C.A., & Millen, A. M. E. (2022). *(Manuscript in preparation).*

5.1 Abstract

Objective: To determine the effect of inflammation and inhibiting circulating TNF-α, on the mRNA expression of genes involved in Ca^{2+} handling, apoptosis, mitochondrial function and myosin heavy chain (MyHC) isoforms that may be involved in the development of LV diastolic dysfunction and myocardial systolic dysfunction in the CIA model.

Methods: To elucidate the role of TNF-α in the active processes involved in LV diastolic and systolic dysfunction, inflammation was induced with a collagen-induced arthritis protocol with subsequent TNF-α inhibition in 68 Sprague-Dawley rats. To further elucidate the role of TNF-α in these processes, adult cardiomyocytes (AC16 cells) were exposed to TNF-α. In rats, LV function was assessed with pulsed wave Doppler, Tissue Doppler and speckle tracking echocardiography. Circulating inflammatory markers were quantified by ELISA. In rats and cell culture experiments, LV mRNA expression was assessed by Taqman® polymerase chain reaction relative to specified housekeeping genes.

Results: Collagen inoculation and inhibiting circulating TNF-α did not affect relative mRNA expression of *SERCA2a* and *S100A1* in rat LV tissues (all $p > 0.05$). Exposing AC16 cells to TNF-α also did not increase *SERCA2a* mRNA expression ($p > 0.05$), suggesting that neither systemic inflammation nor TNF-α disrupt Ca^{2+} reuptake in LV diastolic dysfunction. Collagen inoculation and TNF-α did not affect *BAX, Bcl-2 or SOD2* mRNA expression in LV tissue. In AC16 cells, TNF-α caused a slight decreased *BAX* expression at 24 hours ($p = 0.046$) and induced a small increase in the *BAX/Bcl-2* ratio, only after 24 hours ($p = 0.046$), suggesting that mitochondrial function is likely intact. This may be explained by TNF-α induced upregulation of *SOD2* at 8h and 24h (both $p < 0.0001$) in the AC16 cells. *SOD2* is the gene that codes for superoxide dismutase that inactivates ROS and hence prevents ROS-induced apoptosis. However, exposure to inflammation results in the MyHC isoform shift from fast-twitch to slow-twitch, as the expression of *Myh6* ($p = 0.03$) decreased while *Myh7* expression ($p = 0.0002$) increased in the CIA group compared to controls. Inhibiting circulating TNF-α prevented the inflammation induced change in *Myh6* and *Myh7* expression. Consistent with contractile gene changes, inflammation impaired LV global longitudinal strain ($p = 0.03$) and velocity ($p = 0.04$) in CIA rats compared to controls, that was offset by inhibiting circulating TNF-α.

Conclusion: Inflammation and TNF-α is unlikely to affect Ca^{2+} reuptake or energy dependent active processes, and that these processes may not contribute to the development of LV diastolic or systolic dysfunction in models of systemic inflammation. TNF-α mediates inflammation-induced impairment in early systolic dysfunction, which may be ascribed to a change in myosin heavy chain contractile properties.

5.2 Introduction

Increasing evidence supports a role for inflammation in the pathogenesis of cardiovascular diseases (Martinez & White, 2018). In particular, the role of inflammation in the development of HFpEF has received considerable attention (Paulus and Tschöpe 2013; Van Linthout and Tschöpe 2017). Considering the poor treatment outcomes of patients with HFpEF, using therapeutic options aimed at reducing heart failure symptoms (Pitt et al 2014), and the use of anti-inflammatory treatments in the management of HFpEF have been suggested (Glezeva and Baugh 2014). Although some studies using anti-inflammatory treatments in managing impaired cardiac function in patients with HFpEF have shown improved patient outcomes, this is not replicated by all studies (Baniaamam et al. 2018). Therefore, a clearer understanding of the mechanisms whereby inflammation contributes to HFpEF is required for optimal pharmacological treatments.

The pathogenesis of HFpEF is complex as several phenotypes have been identified (Lewis et al 2017). HFpEF is believed to be mainly due to diastolic abnormalities (Nagueh 2021). Indeed, LV diastolic dysfunction is the subclinical measure that precedes HFpEF development (Wan et al. 2014). Diastolic function depends on both active and passive processes (Lewis et al. 2017). The active process requires mitochondrial ATP production for the detachment of actin-myosin cross bridges and removal of Ca^{2+} from the cytoplasm into the SR by SERCA2a (Biesiadecki et al. 2014). Decreased availability of energy for SERCA2a function due to mitochondrial dysfunction or reduced SERCA2a expression or activity impairs the ability of the SR to sequester Ca^{2+}. The residual cytoplasmic Ca^{2+} increases diastolic tension and impairs cardiomyocyte relaxation (Adeniran et al. 2015; Biesiadecki et al. 2014; Lewis et al. 2017; Pironti et al. 2018). Inflammatory cytokines have been shown to impair processes involved in intracellular Ca^{2+} transport, including the expression and activity of SERCA2 and phospholamban, in cultured cells (Combes et al. 2002; McTiernan et al. 1997). Regarding passive processes, ventricular filling during diastole is also influenced by chamber stiffness (Lewis et al 2017). Both adverse extracellular matrix remodelling (Zile et al. 2015) and hypophosphorylation of the giant spring protein, titin, (van Heerebeek and Paulus 2014) contribute to passive myocardial stiffness which affects the ability of the heart to relax during diastole. Using a CIA rat model, I have previously shown, that increased systemic inflammation increased pro-fibrotic gene expression. The changes were prevented by treatment with a TNF-α blocker, showing that TNF-α contributes to LV fibrosis (Chapter 3). I further showed that systemic inflammation likely impaired titin phosphorylation, but that this was not mediated by TNF-α (Chapter 4). To our knowledge the impact of systemic inflammation and TNF-α on active relaxation processes in this model has not been reported.

Although it is thought that HFpEF is mainly due to diastolic abnormalities (Lewis et al. 2017), subclinical myocardial systolic dysfunction has recently been reported in patients with HFpEF, despite a preserved ejection fraction (Brucks et al. 2005; Fukuta and Little 2007; Jasemian et al. 2011; Yip 2002; Yu et al. 2002). In patients with chronic systemic inflammatory conditions, subclinical systolic dysfunction has also been reported (Di Minno et al. 2020; Hamdy 2007; Midtbø et al. 2017; Sitia et al. 2010; Lo Gullo et al. 2018), which were associated with circulating inflammatory markers (Hamdy 2007; Lo Gullo et al. 2018). Indeed, we have also shown associations between inflammatory markers and impaired myocardial systolic function as measured by STE in the CIA rat model (Mokotedi et al. 2020). The cellular processes underlying inflammation-induced impairments in myocardial deformation and motion are currently not known (Nagueh 2021). Although aberrant intracellular Ca^{2+} transport (Hedayat et al. 2010; Jozwiak et al. 2019) mitochondrial dysfunction and changes in the contractile protein properties contribute to HFrEF (Fitzsimons et al. 1998; Jozwiak et al. 2019; Marelli-Berg and Aksentijevic 2019; Nakao et al. 1997; Simmonds et al. 2020), whether these processes contribute to subclinical systolic myocardial dysfunction in HFpEF warrant investigation. Moreover, although TNF-α is one of the main drivers of altered cardiac function (Hedayat et al. 2010; Prabhu 2004; Tsai et al. 2015), the role of circulating TNF-α in the inflammation-induced changes in active relaxation and systolic dysfunction requires elucidation. Therefore, the current study aimed to determine the role of TNF-α in the active processes involved in LV relaxation and myocardial systolic dysfunction using a model of collagen-induced systemic inflammation with- and without- TNF-α blockade, and TNF-α treatment in a cardiomyocyte (AC16) cell line.

5.3 Results

5.3.1 Body mass, blood pressure, markers of inflammation and diastolic function measures

The characterization of the animal model and echocardiographic data are reported in Table 3.1 and Figure 3.1 (Chapter 3).

5.3.2 Inflammatory cytokine expression in LV tissue and AC16 cells

Compared to controls (0.79±0.16), the LV relative mRNA expression of *IL-6* was increased in the CIA rats (1.65 ± 0.13, p = 0.0004), but not in the anti-TNF-α rats (1.15 ± 0.23, p = 0.40, Figure 5.1a), suggesting that TNF-α mediates the inflammation-induced increase in *IL-6* expression. To assess whether TNF-α directly stimulates expression of inflammatory cytokines in cardiomyocytes, AC16 cells were incubated with TNF-α. The AC16 cells showed increased relative mRNA expression of *IL-6* after exposure to TNF-α for 8h (27.99 ± 0.59) and 24h (30.13 ± 4.51), compared to the cells not exposed to TNF-α (8h: 1.72 ± 0.33, 24h: 1.01 ± 0.01, both p < 0.0001, Figure 5.1c).

There were no differences in *TNF-α* relative mRNA expression between any of the rats LV tissues (all p > 0.05, Figure 5.1b). However, in the AC16 cells, the relative mRNA expression of *TNF-α* was increased in the cells exposed to TNF-α after 8h (20.05 ± 2.70) and 24h (16.47 ± 1.37), compared to the control cells (8h: 1.21 ± 0.17, 24h: 1.35 ± 0.59, both p < 0.0001, Figure 5.1d).

5.3.3 Expression of genes that regulate (diastolic) calcium sequestration

The relative mRNA expression of *SERCA2a*, which codes for the transporter responsible for Ca^{2+} reuptake into the SR during diastole in LV tissues, was similar between the LV tissues of all the groups (p > 0.05, Figure 5.2a). The relative mRNA expression of *S100A1*, which codes for the Ca^{2+}-binding protein S100A1 that is considered a regulator of SR function, was not different between any of the groups (p > 0.05, Figure 5.2b). Consistent with the LV tissue results, exposure of the AC16 cells to TNF-α did not affect expression of *SERCA2a* at 8h (p = 0.99) or 24h (p = 0.30) compared to the control cells (Figure 5.2c).

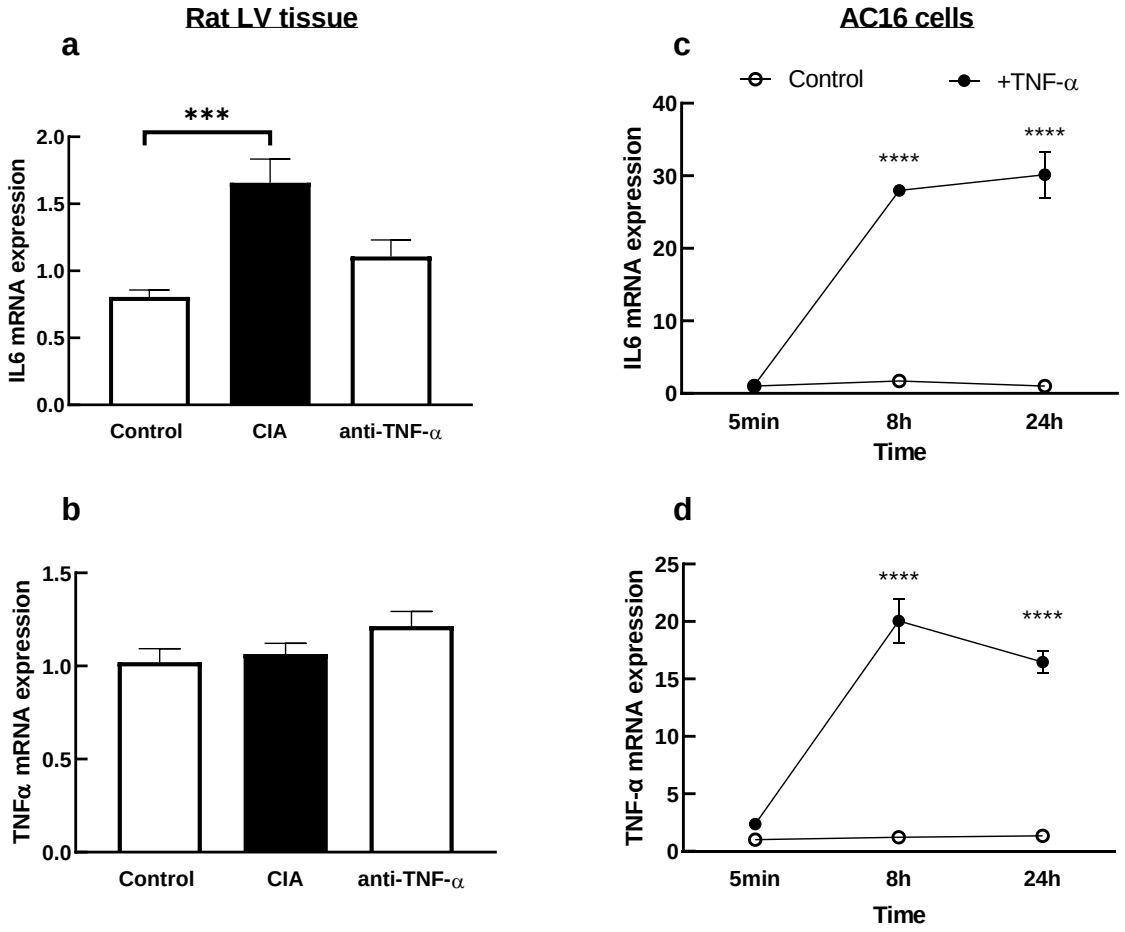

Figure 5.1. Expression of inflammatory cytokine genes in LV tissue and cardiomyocyte (AC16) cells. Rats were inoculated with collagen (CIA) and treated with a TNF-α inhibitor (anti-TNF-α) before measurement of relative mRNA expression of *IL-6* (a) and *TNF-α* (b) in left ventricular tissues of control, CIA, and anti-TNF-α rat groups (left panel). AC16 cardiomyocytes were incubated without or with TNF-α (10 µg/ml) at 5min, 8h and 24h before determination of relative mRNA expression of *IL-6* (c) and *TNF-α* (d) (right panel). Results are presented in arbitrary units normalized for the expression of the endogenous reference gene, *HPRT1* for LV tissues and *GAPDH* for AC16 cells, using the ΔΔCt method. Data presented as means ± SEM. For the AC16 cells, each data point represents the mean ± SEM for three independent experiments performed in quadruplicate. *** $p < 0.001$ versus control, **** $p < 0.0001$ versus control.

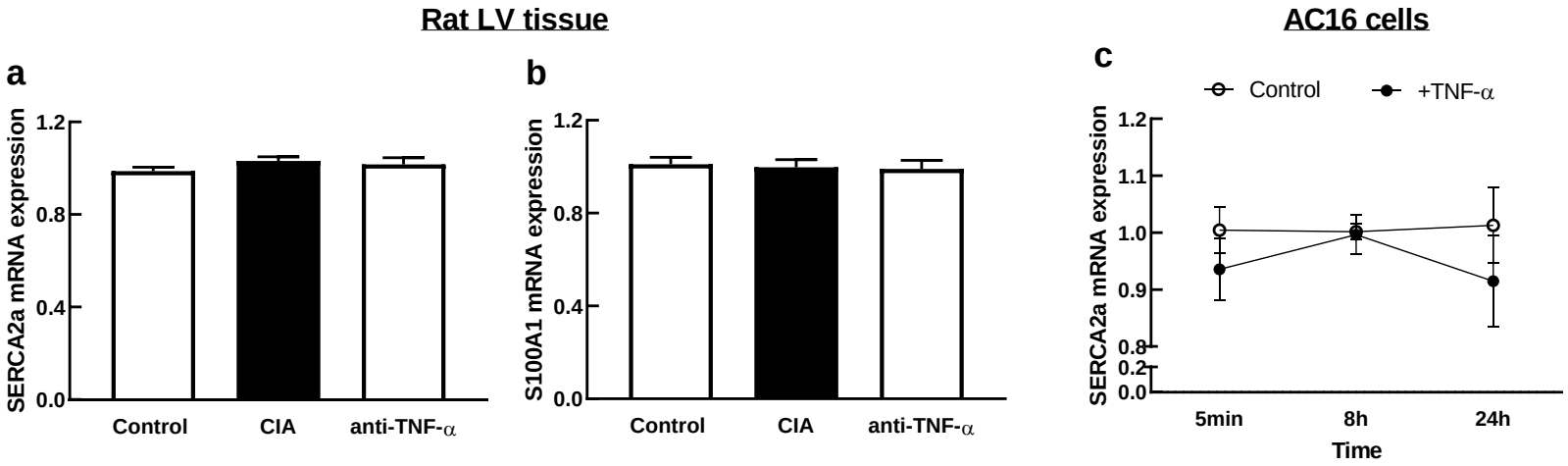

Figure 5.2. Expression of calcium handling genes in LV tissue and a cardiomyocyte cell line. Rats were inoculated with collagen (CIA) and treated with a TNF-α inhibitor (anti-TNF-α) before measurement of relative mRNA expression of *SERCA2a* (a) and *S100A1* (b) in left ventricular tissue of control, CIA, and anti-TNF-α rat groups and expression of *SERCA2a* (c) in AC16 cells exposed to control conditions (0 µg/ml) or to TNF-α (10 µg/ml) at 5min, 8h and 24h. Results are presented in arbitrary units normalized for the expression of the endogenous reference gene, *HPRT1* for LV tissues and *GAPDH* for AC16 cells, using the ΔΔCt method. Data presented as means ± SEM. For the AC16 cells, each data point represents the mean ± SEM for three independent experiments performed in quadruplicate.

5.3.4 Effect of collagen inoculation and anti-TNF-α treatment on expression of genes involved in apoptosis

The relative LV tissue mRNA expression of the pro-apoptotic marker; *BAX* (Figure 5.3a), and the anti-apoptotic marker; *Bcl-2* (Figure 5.3c) were not different between any of the rat groups (all $p > 0.05$). Consistent with these findings, the ratio of *BAX* to *Bcl-2* was also not different between any of the rat groups ($p > 0.05$, Figure 5e).

In the AC16 cells TNF-α caused a small decrease in relative mRNA expression of *BAX* at 24hr (0.82 ± 0.07) compared to control cells (1.00 ± 0.05, $p = 0.046$) but had no significant effect at 8h (Figure 5.3b). The relative mRNA expression of *Bcl-2* was decreased in TNF-α-stimulated cells at 8hr (0.72 ± 0.03) compared to control cells (1.00 ± 0.02, $p = 0.04$), and at 24hr (+TNF-α: 0.66 ± 0.10, control: 1.02 ± 0.12, $p = 0.009$, Figure 5.3d). The ratio of the relative mRNA expression of *BAX/Bcl-2* was similar in TNF-α-stimulated cells (1.20 ± 0.08) and control cells (1.00 ± 0.01, $p = 0.22$) at 8hr but was increased in the TNF-α-stimulated cells at 24hr (1.29 ± 0.12) compared to control cells at 24hr (1.01 ± 0.07, $p = 0.046$, Figure 5.3f), suggesting a slightly pro-apoptotic state in the AC16 cells exposed to TNF-α.

5.3.5 Effect of collagen inoculation and anti-TNF-α treatment on expression of a gene involved in mitochondrial function

The LV relative mRNA expression of *SOD2*, a marker of mitochondrial oxidative stress, was not different in LV tissues of any of the rat groups ($p > 0.05$, Figure 5.4a). In the AC16 cells exposed to TNF-α, *SOD2* mRNA expression was significantly increased in the TNF-α-stimulated cells compared to the cells exposed to control conditions at 8h (control: 1.01 ± 0.08, +TNF-α: 8.27 ± 0.19, $p < 0.0001$) and 24h (control: 1.01 ± 0.02, +TNF-α: 9.11 ± 0.41, $p < 0.0001$, Figure 5.4b).

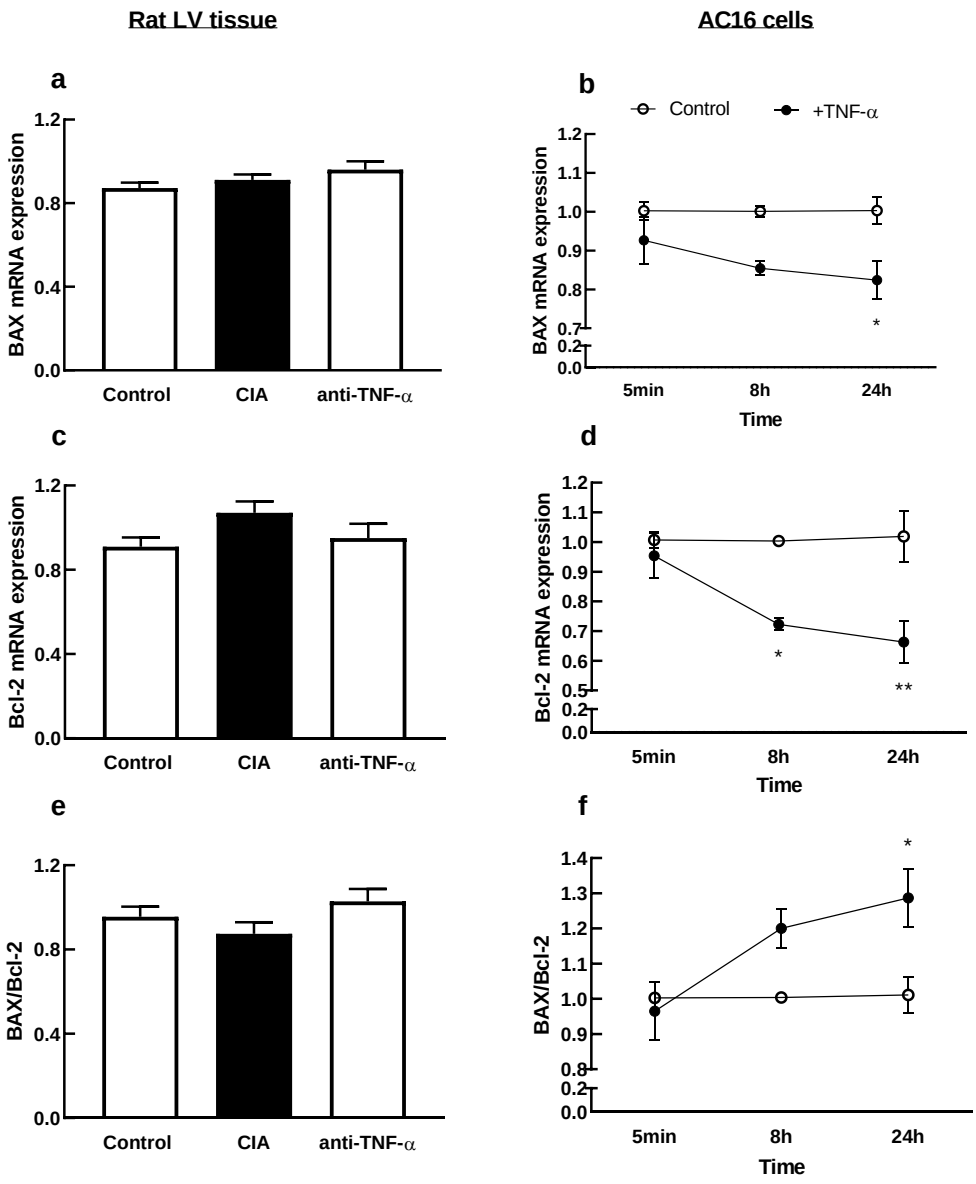

Figure 5.3. Expression of apoptotic genes in LV tissue and a cardiomyocyte cell line. Rats were inoculated with collagen (CIA) and treated with a TNF-α inhibitor (anti-TNF-α) before measurement of relative mRNA expression of *BAX* (a), *Bcl-2* (c) and the ratio of *BAX/Bcl-2* (e) in LV tissues of control, CIA, and anti-TNF-α rat groups (left panel) and *BAX* (d), *Bcl-2* (d) and ratio *BAX/Bcl-2* (f) in AC16 cells exposed to control conditions (0 µg/ml) or to TNF-α (10 µg/ml) at 5min, 8h and 24h (right panel). Results are presented in arbitrary units normalized for the expression of the endogenous reference gene, *HPRT1* for LV tissues and *GAPDH* for AC16 cells, using the ΔΔCt method. Data presented as means ± SEM. For the AC16 cells, each data point represents the mean ± SEM for three independent experiments performed in quadruplicate. * $p < 0.05$ versus control, ** $p < 0.01$ versus control.

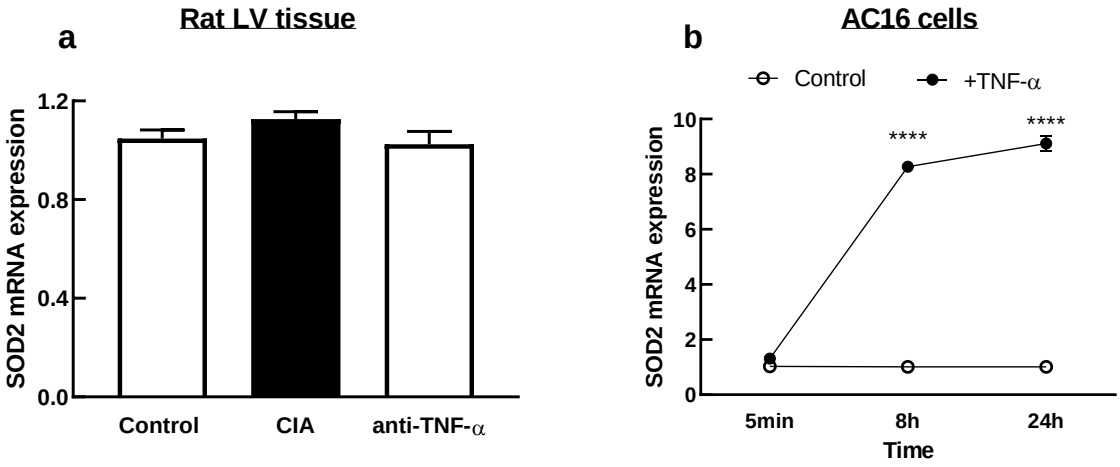

Figure 5.4. Expression of *SOD2* in LV tissue and a cardiomyocyte cell line. Rats were inoculated with collagen (CIA) and treated with a TNF-α inhibitor (anti-TNF-α) before measurement of relative mRNA expression of *SOD2* in LV tissues of control, CIA, and anti-TNF-α rat groups (a) and in AC16 cells (b) exposed to control conditions (0 μg/ml) or to TNF-α (10 μg/ml) at 5min, 8h and 24h. Results are presented in arbitrary units normalized for the expression of the endogenous reference gene, *HPRT1* for LV tissues and *GAPDH* for AC16 cells, using the ΔΔCt method. Data presented as means ± SEM. For the AC16 cells, each data point represents the mean ± SEM for three independent experiments performed in quadruplicate. **** $p < 0.0001$ versus control.

5.3.6 Effect of collagen inoculation and anti-TNF-α treatment on markers of LV systolic function

LV ejection fraction (Figure 5.5a), a measure of LV systolic pump function, and midwall fractional shortening (Figure 5.5b), a measure of myocardial systolic function, were not different between the groups (all $p > 0.05$). The global longitudinal strain, a measure of LV deformation, was impaired in the CIA rats (-16.7 ± 0.76) compared to the control rats (-19.6 ± 0.85, $p = 0.03$, Figure 5.5c). The global longitudinal velocity, a measure of LV motion, was impaired in the CIA rats (0.49 ± 0.03) compared to the control rats (0.59 ± 0.03, $p = 0.04$, Figure 5.5e). The global longitudinal strain and global longitudinal velocity were not different between the control and anti-TNF-α groups (both $p > 0.05$). There were no differences in global longitudinal strain rate (Figure 5.5d) and global longitudinal displacement ($p > 0.05$, Figure 5.5f).

5.3.7 Effect of collagen inoculation and anti-TNF-α treatment on expression of genes involved in cardiac contractility

The relative mRNA expression of *Myh6*, the fast-twitch isoform of myosin, was decreased in CIA rats (0.89±0.04) compared to controls (1.03±0.04, $p = 0.03$) and compared to the anti-TNF-α rats (1.11±0.05; $p = 0.004$, Figure 5.6a). The relative mRNA expression of *Myh7*, the slow-twitch isoform of myosin, was increased in CIA rats (1.25±0.05) compared to controls (0.96±0.05, $p = 0.0002$) and the anti-TNF-α rats (0.91±0.08, $p = 0.0002$, Figure 5b). The ratio of *Myh6/Myh7* mRNA expression was decreased in CIA rats (0.79±0.06) compared to controls (1.13±0.07, $p = 0.002$), and compared to the anti-TNF-α rats (1.24±0.09, $p = 0.0004$, Figure 1c).

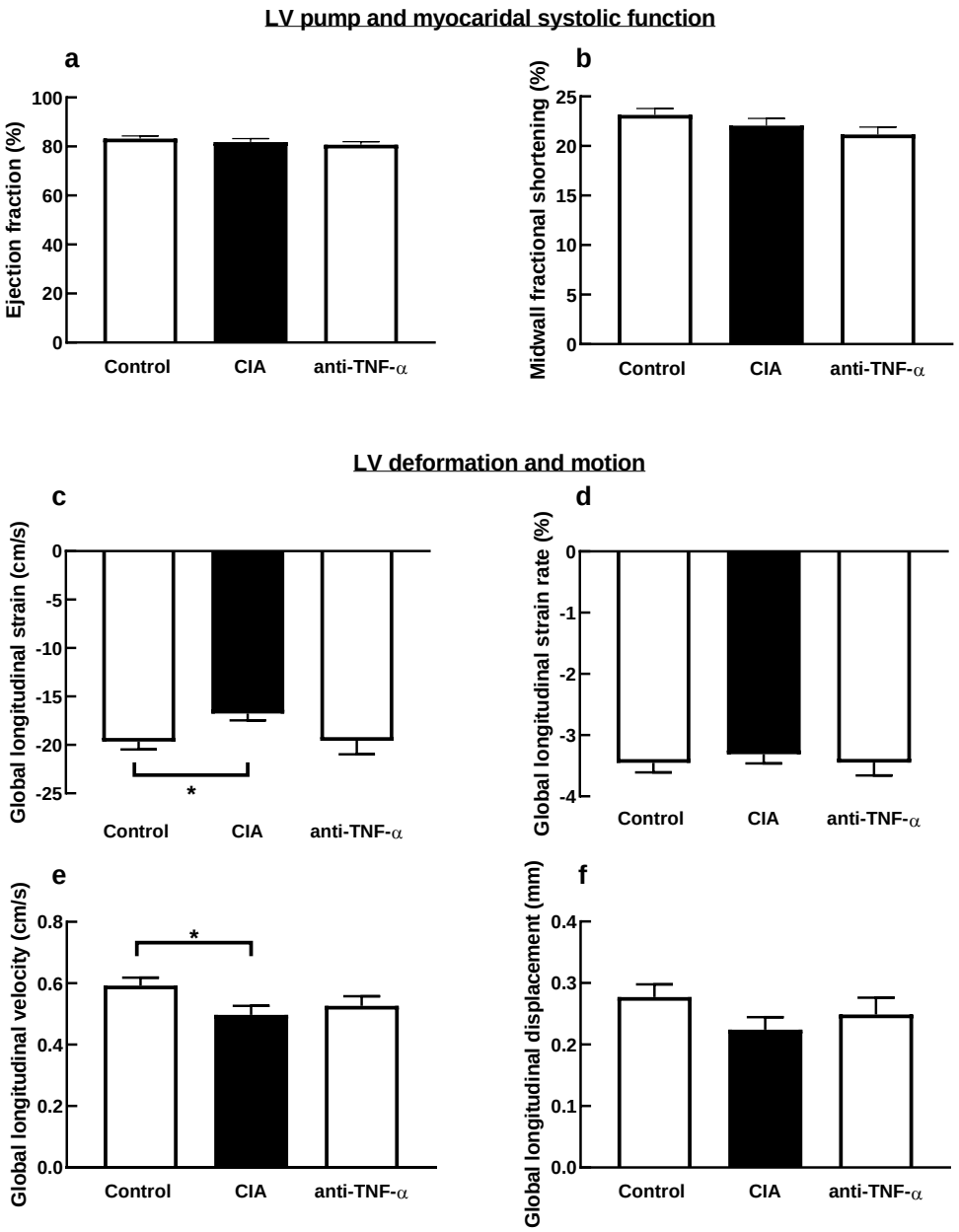

Figure 5.5. Echocardiographic measures of LV systolic function. Rats were inoculated with collagen to induce systemic inflammation (CIA) followed by treatment with a TNF-α inhibitor (anti-TNF-α) prior to STE measures of systolic function. Ejection fraction (a), midwall fractional shortening (b), global longitudinal strain (c), global longitudinal strain rate (d) global longitudinal velocity (e) and global longitudinal displacement (f) were measured in control, CIA, and anti-TNF-α rats. Data presented as means ± SEM. * $p < 0.05$ versus control.

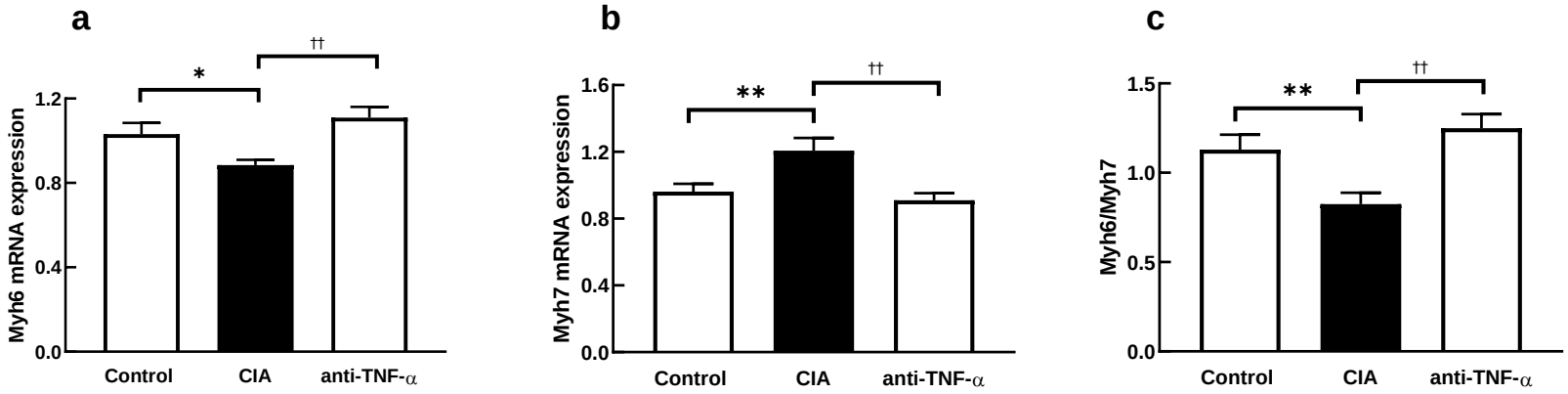

Figure 5.6. LV expression of contractility genes. Rats were inoculated with collagen (CIA) and treated with a TNF-α inhibitor (anti-TNF-α) before measurement of relative mRNA expression of *Myh6* (a), *Myh7* (b), the ratio of *Myh6/Myh7* (c) in left ventricular tissues of control, CIA, and anti-TNF-α rat groups. Relative mRNA expression results are expressed in arbitrary units normalized for the expression of the endogenous reference gene, *HPRT1,* using the ΔΔCt method. Data are from duplicate real time PCR experiments. Data presented as means ± SEM; * $p < 0.05$ versus control, ** $p < 0.01$ versus control, †† $p < 0.01$ versus CIA.

5.4 Discussion

I used a model of collagen-induced systemic inflammation with- and without- TNF-α inhibition, and TNF-α treatment of a cardiomyocyte cell line to investigate the role of TNF-α in the development of inflammation-induced cardiac dysfunction. I show that systemic inflammation and TNF-α inhibition had no effect on the LV mRNA expression of the diastolic Ca^{2+}-regulating genes, *SERCA2a* and *S100A1*, and TNF-α treatment had no effect on *SERCA2a* expression in AC16 cardiomyocytes. This indicates that systemic inflammation and TNF-α may not disrupt diastolic Ca^{2+} reuptake in the early stages of LV diastolic dysfunction. Systemic inflammation and TNF-α inhibition also did not affect expression of the pro- and anti-apoptotic genes, *BAX* and *Bcl-2*, whereas TNF-α stimulated a small decrease in *BAX* expression and a small increase in the *BAX*/*Bcl-2* ratio in AC16 cells, suggesting minimal apoptosis. This minimal apoptosis indicates that mitochondrial function is likely intact and ATP production is not compromised. Taken together these results indicate that the energy-dependent active process of diastolic relaxation is not compromised in the early stages of inflammation-induced LV diastolic dysfunction. Systemic inflammation caused a small TNF-α-dependent increase in LV expression of the mitochondrial oxidative stress marker, *SOD2* that was not statistically significant. However, TNF-α stimulated a robust increase in *SOD2* expression in AC16 cardiomyocytes. Since the SOD2 superoxide dismutase inactivates ROS and prevents ROS-induced apoptosis, the increased *SOD2* expression likely accounts for the minimal increases in the *BAX*/*Bcl-2* ratios. Since we have shown that TNF-α does not mediate LV diastolic dysfunction, we assessed whether TNF-α might contribute to HFpEF development by disrupting systolic function. STE results showed impaired global longitudinal strain and global longitudinal velocity in the CIA rats that were prevented by TNF-α inhibition. This shows that increased systemic concentrations of TNF-α mediate early-stage systolic dysfunction. CIA rats also exhibited decreased mRNA expression of *Myh6* and increased expression of *Myh7*, which resulted in an increased *Myh6/Myh7* ratio that indicates a switch from the fast-twitch to the slow-twitch MyHC isoform that may account for the systolic dysfunction. The changes in *Myh6* and *Myh7* expression were prevented by TNF-α inhibition, showing that the inflammation-induced changes in MyHC isoforms are mediated by circulating TNF-α. These results show that increased systemic TNF-α contributes to HFpEF development by initiating early-stage systolic dysfunction.

During the systolic phase of the cardiac cycle, cytoplasmic Ca^{2+} is increased due to opening of sarcolemma and ER Ca^{2+} channels. This increased cytoplasmic Ca^{2+} induces Ca^{2+} release from the SR through the RyR2 causing a further increase in cytoplasmic Ca^{2+} concentration that drives myocardial contraction. During diastole, myocardial relaxation is initiated when Ca^{2+} is pumped from the cytoplasm into the SR by the ATP-dependent SERCA2a (Lipskaia et al. 2010; Park and Oh 2013). S100A1 is a Ca^{2+}-binding protein that enhances cardiac cycling by regulating both systolic and diastolic Ca^{2+}-handling proteins; including

SERCA2a, RyR2 and cell surface Ca^{2+} channels (Remppis et al. 1996; Rohde et al. 2010; Wright et al. 2009), making it an important regulator of cardiomyocyte contractility (Rohde et al. 2010). S100A1 also regulates mitochondrial ATP production and apoptosis (Duarte-Costa et al. 2014). It has been suggested that decreased expression of SERCA2a, which decreases Ca^{2+} uptake into the SR contributes to the development of LV diastolic dysfunction (Adeniran et al. 2015; Park and Oh 2013). The resulting increased cytoplasmic Ca^{2+} during diastole is thought to cause increased sarcomeric tension, which results in impaired myocardial relaxation (Adeniran et al. 2015; Lewis et al. 2017).

We found no change in the mRNA expression of *SERCA2a* in CIA rats or in TNF-α-stimulated AC16 cardiomyocytes, suggesting that impaired Ca^{2+} reuptake, due to decreased SERCA2a expression, may not be the main contributor to inflammation-induced impaired myocardial diastolic relaxation. This is consistent with the work of Pironti et al (2018) who showed no change in SERCA2a protein expression in mice with collagen antibody-induced arthritis (Pironti et al. 2018). The activity of SERCA2a protein is regulated by phospholamban, which inhibits SERCA2a Ca^{2+} transport in its dephosphorylated state (Combes et al. 2002). Thus, although we have shown no change in *SERCA2a* expression, there may be changes in the regulation of SERCA2a that may alter Ca^{2+} transients independent of a change in its mRNA expression. Nevertheless, it has previously been reported that exposure of cardiomyocytes to TNF-α did not alter phospholamban expression (Mc Tiernan et al 1997) and we have previously shown that expression of protein phosphatase 1, a regulator of phospholamban dephosphorylation (Lompré et al. 2010; MacLennan and Kranias 2003), was unchanged in CIA rats (Chapter 4). It has been reported that acute inflammation (LPS-induced sepsis), decreased SERCA2a expression (Tsai et al. 2015), while another study reported that SERCA2a plays a relatively minor role in Ca^{2+} transients in diastole (Wagner et al 2015). Instead, it was suggested that increased Ca^{2+} leak from the SR via the RyR2 and depressed Na^{+}/Ca^{2+} exchanger and plasmalemmal Ca^{2+} ATPase activities may contribute more to impaired cardiac function (Wagner et al. 2015). In a model of collagen antibody-induced arthritis in mice cardiomyocytes, Ca^{2+} transients were impaired, but no changes in the expression levels of any of the Ca^{2+}-handling proteins were reported (Pironti et al. 2018). Oxidation-dependent modifications of RyR2 channels and other Ca^{2+}-regulating proteins may have compromised Ca^{2+} homeostasis in their model (Pironti et al. 2018).

I also found no change in the expression of *S100A1*, the gene that codes for the Ca^{2+}-binding protein S100A1. Decreased mRNA and protein expression of S100A1 has been reported in experimental heart failure and in human hearts with cardiomyopathy (Pironti et al. 2018; Ritterhoff and Most 2012; Rohde et al. 2010) and were associated with disease severity, progression and mortality (Most et al. 2006). Mice subjected to myocardial infarction showed decreased S100A1 protein levels that were reported to have contributed to contractile dysfunction in these animals (Most et al. 2006). Taken together, the experimental

models in this thesis do not support changes in expression of the *SERCA2a* or *S100A1* Ca^{2+} handling genes in the development of LV diastolic dysfunction.

It is well known that TNF-α directly stimulates the extrinsic apoptosis pathway, which may ultimately lead to impaired myocardial contractility (Simmonds et al. 2020). TNF-α exposure caused apoptosis in primary rat cardiomyocytes (Krown et al. 1996) and overexpression of TNF-α has been linked to a dilated heart associated with systolic dysfunction with evidence of myocyte apoptosis *in vivo* (Bryant et al. 1998). Additionally, increased mitochondrial ROS production (Dubois-Deruy et al. 2020; Peoples et al. 2019) and prolonged elevation of cytoplasmic Ca^{2+} concentrations have been reported to contribute to cell death by the intrinsic, mitochondria-mediated apoptosis pathway (Hajnóczky, Davies, and Madesh 2003; Orrenius, Zhivotovsky, and Nicotera 2003). BAX and Bcl-2 are regulatory proteins of the apoptotic cell death pathway that have opposite functional roles. BAX is pro-apoptotic, Bcl-2 is anti-apoptotic and an increased ratio of BAX to Bcl-2 is associated with apoptosis (Gunnett et al. 2005; Krijnen PAJ 2002; Kubota et al. 2001). I showed no changes in *BAX* or *Bcl-2* LV mRNA expression between any of the rat groups, showing absence of apoptosis that is consistent with numerous reports that myocardial apoptosis is characteristic only of more progressive forms of cardiovascular disease, particularly myocardial infarction and end-stage heart failure (Kim and Kang 2010; Teringova and Tousek 2017). Exposure of AC16 cells to TNF-α, decreased *BAX* expression and moderately increased the *BAX/Bcl-2* expression ratio. This minimal change in pro-apoptotic signalling indicates that apoptosis is unlikely to have disrupted mitochondrial ATP production that would impair active LV relaxation.

Oxidative stress is thought to contribute to inflammation-induced HFpEF. Supporting this, we have previously shown a TNF-α-dependent increase in mRNA expression of *iNOS* in CIA rats (Chapter 4). Excess production of ROS stimulates apoptosis by disrupting mitochondrial integrity, but physiological increases in ROS modulate many cellular signalling pathways, including regulation of cardiomyocyte Ca^{2+} handling (Burgoyne et al. 2012). Elevated ROS levels induce increased expression of ROS-neutralising enzymes, including SOD2, which prevents conversion of superoxide to highly reactive free radicals (Miao and Clair 2009). Therefore, SOD2 is often used as a measure of oxidative stress. However, TNF-α and other cytokines directly increase *SOD2* expression via activation of the NFκB transcription factor (Marelli-Berg and Aksentijevic 2019; Miao and Clair 2009). Therefore, the regulatory mitochondrial anti-oxidant protein SOD2 is often used as a measure of mitochondrial dysfunction and mitochondrial oxidative stress (Burgoyne et al. 2012). I found that collagen-induced upregulation of *SOD2* expression in LV tissues was not significant, indicating minimal changes in mitochondrial ROS production. The increased *iNOS* expression that I previously reported may not produce enough ROS to induce a significant increase in *SOD2* expression.

I showed that TNF-α stimulated increased expression of *SOD2* in AC16 cardiomyocytes. This is likely a direct effect of TNF-α receptor signalling (Miao and Clair 2009). Although it has been suggested that TNF-α also stimulates mitochondrial ROS production in cardiomyocytes (Roberge et al. 2014), it is likely that the TNF-α-stimulated *SOD2* expression protects against ROS-induced apoptosis, as shown by the minimal decrease in *BAX* expression and minimal increase in *BAX*/*Bcl-2* ratio. The absence of a significant increase in *SOD2* expression in the LV tissue of CIA rats, despite increased circulating TNF-α concentrations suggests insufficient TNF-α in the LV tissue, which may result from the absence of increased local *TNF-α* expression. A collagen antibody-induced arthritis (CAIA) mouse model showed upregulation of both *SOD2* and *TNF-α* expression in heart tissue. However, the mice showed impaired LV fractional shortening (Pironti et al. 2018), unlike the present study where ejection fraction and midwall fractional shortening were preserved. This suggests that increased expression of TNF-α in the heart and consequent induction of *SOD2* may be associated with more advanced cardiac dysfunction than is present in the CIA rats of the current study.

It is well-known that increased circulating TNF-α contributes to development of HFpEF, but we have shown that TNF-α blockade does not prevent LV diastolic dysfunction in CIA rats, indicating that the diastolic dysfunction is not mediated by the increased circulating TNF-α (Chapter 3 and 4). Since subclinical systolic dysfunction has recently been reported in patients with HFpEF (Brucks et al. 2005; Fukuta and Little 2007; Kim and Kang 2010; Yip 2002; Yu et al. 2002) and with chronic systemic inflammatory conditions (Di Minno et al. 2020; Fine et al. 2014; Hamdy 2007; Lo Gullo et al. 2018; Sitia et al. 2010), I investigated whether increased circulating TNF-α might regulate systolic function in CIA rats. CIA rats showed early-stage impairment of systolic function, indicated by impaired global longitudinal strain and global longitudinal velocity, despite preserved ejection faction and unchanged fractional shortening. The changes in myocardial deformation (global longitudinal strain) and motion (global longitudinal velocity) were prevented by TNF-α inhibition, which shows that TNF-α is an important contributor to early-stage systolic dysfunction that underlies the development of HFpEF. The preserved ejection faction and unchanged fractional shortening indicate that CIA rats in this study have earlier stage systolic dysfunction than was seen in the collagen antibody-induced arthritis mouse model of Pironti et al. (2018). Nevertheless, in the present study I showed impaired subclinical systolic function measures, including global longitudinal strain and global longitudinal velocity, in the rats exposed to inflammation.

Sarcomeres are composed of myosin and actin filaments that allow for contraction and relaxation of cardiomyocytes (England and Loughna 2013). In mammalian ventricular myocardia, two MyHC isoforms have been identified. In the present study, in the LV tissues of CIA rats I showed decreased expression of *Myh6* that encodes the α-MyHC, which is known as the ‘fast-twitch’ isoform. I also showed increased

expression of *Myh7 that* encodes the β-MyHC, which is known as the 'slow-twitch' isoform, and a decreased *Myh6*/*Myh7* ratio that shows a shift to the slow-twitch isoform, suggesting altered sarcomeric structure. Although changes in the relative expression of these two isoforms are traditionally associated with hypertrophic phenotypes, they are also correlated with the contraction efficiency of the cardiomyocyte and determines systolic function (Fitzsimons et al. 1998). In non-failing hearts, the α-MyHC isoform is predominant. However, it has been shown that numerous pathological stimuli can induce an expressional shift in the MyHC composition of the rodent ventricle from α-MyHC to β-MyHC (Nakao et al. 1997). Similarly, previous studies have shown an altered ratio of α-MyHC to β-MyHC expression upon exposure to inflammatory cytokines (Combes et al. 2002; Pironti et al. 2018). I also showed that inhibiting circulating TNF-α prevented the inflammation-induced MyHC isoform shift, showing that increased circulating TNF-α strongly contributes to the change in MyHC isoform. This result is consistent with the prevention of inflammation-induced changes in global longitudinal strain and velocity when inhibiting circulating TNF-α. Therefore, the TNF-α-dependent changes in the MyHC may account for TNF-α-dependent early-stage impairments of systolic function.

The main limitation of this study is the measurement of mRNA expression, which may not always correlate with protein expression and protein function, such as regulation of Ca^{2+} transients and the production and clearance of ROS, which must be investigated in future studies.

In summary, I have shown that collagen-induced systemic inflammation causes both diastolic and systolic dysfunction. I have also shown that both systemic inflammation and TNF-α have minimal effects on the expression of the genes, *SERCA2a, BAX and Bcl-2,* which are important in the active relaxation component of LV diastolic dysfunction, which may be associated with advanced myocardial dysfunction. Therefore, active processes of myocardial relaxation did not contribute to LV diastolic dysfunction in this study. Furthermore, I have shown that TNF-α inhibition prevented both the inflammation-induced MyHC isoform expressional shift and impaired myocardial deformation and motion. Therefore, early-stage systolic dysfunction in the CIA model likely resulted from the TNF-α mediated changes in MyHC isoform expression and hence increased circulating TNF-α may be an important contributor to the development of HFpEF, by initiating subclinical systolic dysfunction.

CHAPTER 6: THE ROLE OF INTERLEUKIN-6 IN PASSIVE AND ACTIVE PROCESSES OF INFLAMMATION-INDUCED LV DIASTOLIC AND SYSTOLIC DYSFUNCTION

6.1 Abstract

Objective: To delineate the role of IL-6 in the molecular mechanisms responsible for inflammation-induced LV myocardial dysfunction. The IL-6 blocker, tocilizumab, was used to determine the role of this cytokine in the molecular pathways underlying the passive and active processes involved in the development of LV diastolic and systolic dysfunction.

Methods: 73 Sprague-Dawley rats were divided into three groups: the control group, the CIA group and the IL-6 blocker group. Bovine type II collagen emulsified in incomplete Freund's adjuvant was used to induce inflammation in the CIA and IL-6 blocker groups. Following the onset of arthritis, the IL-6 blocker group received an IL-6 receptor blocker, tocilizumab, for six weeks. Circulating inflammatory markers were measured by ELISA and relative LV mRNA gene expressions were assessed by Taqman® polymerase chain reaction. LV diastolic and systolic function were assessed by echocardiography.

Results: Blocking circulating IL-6 did not impact circulating markers of inflammation or LV mRNA expression of inflammatory markers, as there were no differences between any of the circulating or tissue inflammatory markers between the IL-6 blocker group and the CIA group ($p > 0.05$). Blocking circulating IL-6 did not reverse inflammation-induced increases in the LV relative mRNA expressions of genes involved in fibrosis (*TGFβ* and *Col1)*, collagen turnover (*MMP2*) or concentric remodelling (RWT). However, blocking IL-6 prevented the inflammation-induced increase in expression of *LOX*. Blocking circulating IL-6 did not prevent inflammation-induced upregulation of any of the genes involved in titin phosphorylation. Regarding the active processes, similar to the CIA group, there were no changes in the expression of genes involved in Ca^{2+} handling, mitochondrial function or apoptosis in the IL6-blocker group.

Conclusion: The role of IL-6 in molecular mechanisms underlying LV dysfunction are inconclusive.

6.2 Introduction

Although heart failure demonstrates substantial pathophysiological heterogeneity, a growing body of evidence points to the central role of inflammatory cytokines in the pathogenesis of diastolic and systolic dysfunction (Hanna and Frangogiannis 2020). In a recent study that investigated the predictive power of a wide range of biomarkers related to the different phenotypes of HFpEF, inflammatory markers were most strongly related to cases of heart failure that resulted in hospital admissions and death. However, of all the inflammatory biomarkers included in the analysis, only TNF-α and IL-6 were considered among the independent predictors of adverse cardiac outcomes, with IL-6 ranking amongst the top four predictive biomarkers related to cases of heart failure that resulted in hospital admissions and death (Chirinos et al. 2020). Furthermore, in patients with auto-immune diseases such as rheumatoid arthritis, circulating concentrations of IL-6 are independently linked to LV diastolic dysfunction (Liang et al. 2010). Considering its crucial role in disease pathogenesis of conditions associated with inflammation and its involvement in the pathogenesis of heart failure, IL-6 is considered an attractive therapeutic target. However, clinical studies on the effects of blocking circulating IL-6 in cardiac function is scarce. In patients with rheumatoid arthritis without symptoms of myocardial dysfunction, treatment with an IL-6 receptor blocker, tocilizumab, has shown improvements in LV mass, EF, radial strain and expression of N-terminal pro-brain natriuretic peptide (Kobayashi et al. 2014; Kobayashi et al. 2016; Yokoe et al. 2018). Nevertheless, the effects of IL-6 receptor blockers in patients with LV dysfunction or HFpEF are unknown.

IL-6 is a pro-inflammatory cytokine with pleiotropic effects on several processes including cell growth, apoptosis and survival in various organs (Zhao et al. 2016). However, the role of IL-6 in the passive and active cellular processes involved in LV dysfunction is controversial. In this regard, some have proposed that IL-6 is a key regulator of cellular processes involved in cardiac fibrosis and hypertrophy and hence, in extracellular matrix remodelling that may contribute to passive stiffness in the development of LV diastolic dysfunction. However, the role of IL-6 in cardiomyocyte compliance, which is another contributor to LV passive stiffness; and in Ca^{2+} handling, which is the main process involved in active LV relaxation, is uncertain. With regards to the role of IL-6 in fibrosis, Mendelez et al (2010) showed that intraperitoneal infusion of IL-6 in rats for seven days resulted in increased LV stiffness that was ascribed to increases in LV fibrosis and concentric hypertrophy (Meléndez et al. 2010). Others support the role of IL-6 in cardiac fibrosis, as collagen production and hence, the development of myocardial fibrosis was attenuated in IL-6 deficient mice and IL-6 deficient cardiomyocytes (Zhao et al. 2016), but was enhanced in mice where IL-6 was overexpressed (Hirota et al. 1995). In contrast, others showed that IL-6 is not necessary for the development of cardiac hypertrophy or dysfunction in IL-6 deficient mice (Kaminski et al. 2007; Lai et al. 2012). Similarly, in cell culture, direct exposure of cardiac fibroblasts to IL-6 did not result in increased

collagen content (Siwik, Chang, and Colucci 2000). In addition, when blocking plasma IL-6, some have reported that the development of fibrosis was reduced in post-infarct hearts in mice (Kobara et al. 2010) and after viral-induced myocarditis (Savvatis et al. 2014). In contrast, another study showed that blocking plasma IL-6 did not prevent cardiac remodelling and fibrosis (Hartman et al. 2016). These authors further reported that blocking IL-6 may be detrimental as systolic function worsened in the group that received the IL-6 blocker compared to the no-treatment group (Hartman et al 2016). Similarly, others have proposed that IL-6 is necessary for cell-cell interaction in the heart and for myocardial regeneration; whereby the absence of IL-6 may be detrimental to normal cardiac function and cardiac regeneration following injury (Banerjee et al. 2009; Tang et al. 2018). In this regard, the loss of IL-6 function has been linked to increased fibrosis and apoptosis (Banerjee et al. 2009; Tang et al. 2018), which indicates that preventing IL-6-induced myocardial regeneration may impact both LV diastolic and systolic myocardial function. Taken together, although several studies have investigated the effects of IL-6 on extracellular matrix remodelling, there seems to be little consensus on whether it has detrimental or protective roles in cardiac function. This may be accounted for by the differences in experimental models and modes of drug administration that were employed in these investigations.

Besides the controversial role of IL-6 in extracellular matrix remodelling, the understanding of its role in passive cardiomyocyte stiffens; including titin phosphorylation, and in the active processes of LV relaxation is limited. In this regard, one study showed that blocking the IL-6 receptor after viral-induced myocarditis improved titin phosphorylation that resulted in reduced myocyte stiffness (Savvatis et al. 2014). However, these results have not been replicated in models of chronic systemic inflammation. In addition, IL-6 has been associated with the regulation of SERCA2a expression in ventricular myocytes (Gloss et al. 2000; Tanaka et al. 2004; Wu et al. 2011). However, whether this translates to altered myocardial relaxation *in vivo* has not been confirmed. Therefore, the aim of this study was to evaluate the role of IL-6 in molecular processes underlying the development of LV diastolic and systolic dysfunction by blocking its effects, using an IL-6 receptor antagonist, in a rat model of chronic systemic inflammation.

6.3 Results

6.3.1 The effect of IL-6 blocker treatment on body mass, blood pressure and, circulating and LV tissue expression of inflammatory markers

The characterization of the control and CIA rats is reported elsewhere (Le Roux et al. 2022). Briefly, for the partially overlapping subset of animals included in this study, body weight was lower in the IL-6 blocker group compared to the control ($p < 0.001$) and CIA ($p = 0.01$, Table 6.1) groups. There were no differences in systolic or diastolic blood pressure between the groups (all $p > 0.05$). Arthritis scores and the ankle and

tarsometatarsal thickness were increased in the IL-6 blocker group compared to controls (all $p < 0.05$) and no different from the CIA group (all $p > 0.05$). Tocilizumab had no effect on circulating inflammatory marker concentrations as the serum concentrations of TNF-α ($p < 0.0001$), IL-6 ($p = 0.0003$) and CRP ($p < 0.0001$) were significantly increased in the IL-6 blocker group compared to the control group, but were not different to the CIA group (all $p > 0.05$). Blocking circulating IL-6 did not prevent CIA-induced local LV tissue inflammation, as the mRNA expression of *IL-6* and *PTX-3* were greater in the IL-6 blocker group compared to the control group ($p = 0.04$ and $p = 0.006$, respectively) and were not different from the CIA group ($p = 0.92$ and $p = 0.64$, respectively; Table 6.1). The local mRNA expression of *CD68*, a marker of leukocyte and macrophage infiltration, and of *TNF-α*, were not different from the control group ($p = 0.83$ and $p = 0.72$, respectively) or the CIA group ($p = 0.16$ and $p = 0.88$, respectively).

6.3.2 The effect of IL-6 blocker treatment on LV geometry, diastolic and systolic function

Blocking circulating IL-6 had no effect on the inflammation-induced changes in echocardiographic measures of LV geometry, diastolic or systolic function (Table 6.2). In the IL-6 blocker group, similar to the CIA group, the RWT were increased compared to the control group, showing that blocking circulating IL-6 did not inhibit LV concentric remodelling induced by collagen inoculation (Table 6.2). Similar to the CIA group, the LV filling pressures (E/e') were increased, while lateral e', global longitudinal strain and global longitudinal velocity were impaired in the IL-6 blocker group compared to the control group (Table 6.2). This indicates that blocking circulating IL-6 did not prevent the CIA-induced impairments in LV diastolic and systolic function. Although the e'/a', a measure of LV stiffness, was impaired in the IL-6 blocker group compared to the control group, the difference did not reach statistical significance ($p = 0.10$). Like the CIA group, ejection fraction and midwall fractional shortening, markers of systolic function, were not improved in the IL-6 blocker group compared to the control group.

Table 6.1. Body mass, blood pressure and circulating and tissue inflammatory markers in in control, CIA and IL-6 blocker groups

	Control	CIA	IL-6 blocker
n	28	29	16
Female n (%)	12 (43)	16 (55)	8 (50)
Body weight (g)	459.8 ± 9.5	425.5 ± 8.8*	384.1 ± 11.4**†
SBP (mm Hg)	128 ± 2	130 ± 2	129 ± 2
DBP (mm Hg)	87 ± 1	88 ± 1	91 ± 2
Paw score	0	4 (3 – 6)****	4.5 (2 – 7)****
Ankle joint thickness (mm)	8.6 ± 0.1	9.2 ± 0.1**	9.2 ± 0.2*
Tarsometatarsal joint thickness (mm)	5.0 ± 0.1	5.5 ± 0.1**	5.6 ± 0.2*
Circulating inflammatory marker concentrations			
TNF-α (pg/ml)	93.86 ± 7.18	155.77 ± 6.53***	164.08 ± 8.75***
IL-6 (pg/ml)	16.42 ± 2.08	29.89 ± 2.05**	31.29 ± 2.74**
CRP (ng/ml)	0.10 ± 0.04	0.56 ± 0.03***	0.66 ± 0.05***
Tissue inflammatory marker expressions (mRNA)			
TNF-α	1.02 (0.71 – 1.27)	1.04 (0.85 – 1.28)	1.05 (0.92 – 1.31)
IL-6	0.85 (0.65 – 0.93)	1.53 (0.85 – 2.06)**	1.64 (0.76 – 2.03)*
CD68	0.92 ± 0.05	1.12 ± 0.05*	0.97 ± 0.07
PTX-3	1.18 (0.43 – 1.30)	2.40 (1.74 – 4.06)***	2.22 (0.92 – 2.97)**

Data presented as means ± SEM or median (interquartile range). CIA, collagen-induced arthritis, SBP, systolic blood pressure, DBP, diastolic blood pressure, TNF-α, tumour necrosis factor alpha, IL-6, interleukin 6, CRP, C-reactive protein.* $p < 0.05$ versus controls; ** $p < 0.01$ versus controls; *** $p < 0.0001$ versus controls; †$p < 0.05$ versus CIA.

Table 6.2. Echocardiographic measures of left ventricular myocardial remodelling, diastolic function and systolic function in control, CIA and IL-6 blocker rats.

	Control (n = 25)	CIA (n = 27)	IL-6 blocker (n = 16)
Myocardial remodelling			
Relative wall thickness	0.62 ± 0.02	0.73 ± 0.02**	0.71 ± 0.03*
LV diastolic function			
Lateral e' (cm/s)	4.52 ± 0.10	3.61 ± 0.10***	3.62 ± 0.14***
e'/a'	1.45 ± 0.06	1.23 ± 0.06*	1.28 ± 0.08
E/e'	25.12 ± 1.01	31.39 ± 0.98**	29.86 ± 1.27*
LV systolic function			
Ejection fraction (%)	83.0 ± 1.3	82.3 ± 1.3	81.0 ± 1.7
Midwall fractional shortening (%)	22.9 ± 0.7	22.1 ± 0.7	21.9 ± 0.9
Global longitudinal strain (cm/s)	-19.4 ± 0.8	-16.9 ± 0.8*	-16.3 ± 0.9*
Global longitudinal strain rate (%)	-3.43 ± 0.16	-3.33 ± 0.15	-3.06 ± 0.20
Global longitudinal velocity (cm/s)	0.58 ± 0.03	0.49 ± 0.03*	0.47 ± 0.04*
Global longitudinal displacement (mm)	0.28 ± 0.02	0.22 ± 0.02	0.21 ± 0.03

Data presented as means ± SEM. CIA, collagen induced arthritis; IL-6, interleukin-6; BW, body weight; LV, left ventricular; e', peak velocity during early diastole; e'/a', ratio of mitral annular lengthening in early and late diastole; E/e', ratio of early diastolic filling to peak velocity during early diastole; * $p < 0.05$ compared to control; ** $p < 0.01$ compared to control; *** $p < 0.001$ compared to control.

6.3.3 The effect of IL-6 blocker treatment on extracellular matrix gene expression

Treatment with tocilizumab did not offset the inflammation-induced increases in mRNA expression of pro-fibrotic genes. Compared to the control group, the IL-6 blocker group had a significantly greater LV mRNA expression of *TGFβ* ($p = 0.01$, Figure 6.1a) and *Col1* ($p = 0.0004$, Figure 6.1c), which was similar to that of the CIA group ($p > 0.05$ for both). This shows that blocking circulating IL-6 did not prevent the inflammation-induced stimulation of fibrosis, consistent with the increases in RWT (Table 6.2). There were no differences in the LV mRNA expression of *αSMA* between the groups (Figure 6.1b), showing that neither the inflammatory protocol nor tocilizumab treatments resulted in the trans-differentiation of fibroblasts to myofibroblasts. Although the relative mRNA expression of *LOX* in the IL-6 blocker group was increased compared to controls, this increase was not statistically significant ($p = 0.13$). The CIA group showed an upregulation in *LOX* expression compared to controls ($p = 0.0004$, Figure 6.1d), suggesting that blocking circulating IL-6 may have partially offset the inflammation-induced collagen cross-linking. Similar to the CIA group, LV relative mRNA expression of *MMP2* was increased in the IL-6 blocker group compared to the control group ($p = 0.005$, Figure 6.1e), showing that blocking circulating IL-6 did not prevent the inflammation-induced upregulation of collagen turnover. There were no differences in relative mRNA expression of *MMP9* between the groups (all $p > 0.05$, Figure 6.1f).

6.3.4 The effect of IL-6 blocker treatment on expression of genes involved in microvascular inflammation, immune cell infiltration and NO-signalling pathways

The inflammation-induced increased LV relative mRNA expression of *VCAM1* was not impacted by treatment with tocilizumab ($p = 0.02$ versus control, $p = 0.86$ versus CIA, Figure 6.2a), indicating that inflammation-induced microvascular inflammation is not offset by IL-6 blocker treatment. Consistent with the increased *VCAM1* expression, LV relative mRNA expression of *iNOS* was greater in the IL-6 blocker group compared to the control group ($p = 0.001$) and not different from the CIA group ($p = 0.24$, Figure 6.2b). Similar to the CIA group, the LV relative mRNA expression of *sGCα2* and *sGCβ2* were significantly decreased in the IL-6 blocker group compared to control group ($p = 0.02$ and $p = 0.04$, respectively; Figure 6.2c and 6.2d). The relative mRNA expression of *sGCα2* and *sGCβ2* in the IL-6 blocker group were not different from the CIA group ($p = 0.93$ and $p = 0.87$, respectively), showing that blocking circulating IL-6 did not impact the inflammation-induced decreased in expression of the genes that code for subunits of sGC enzyme. These results are consistent with the impaired relaxation (e') and increased filling pressures (E/e') reported in the IL-6 blocker rats (Table 6.2).

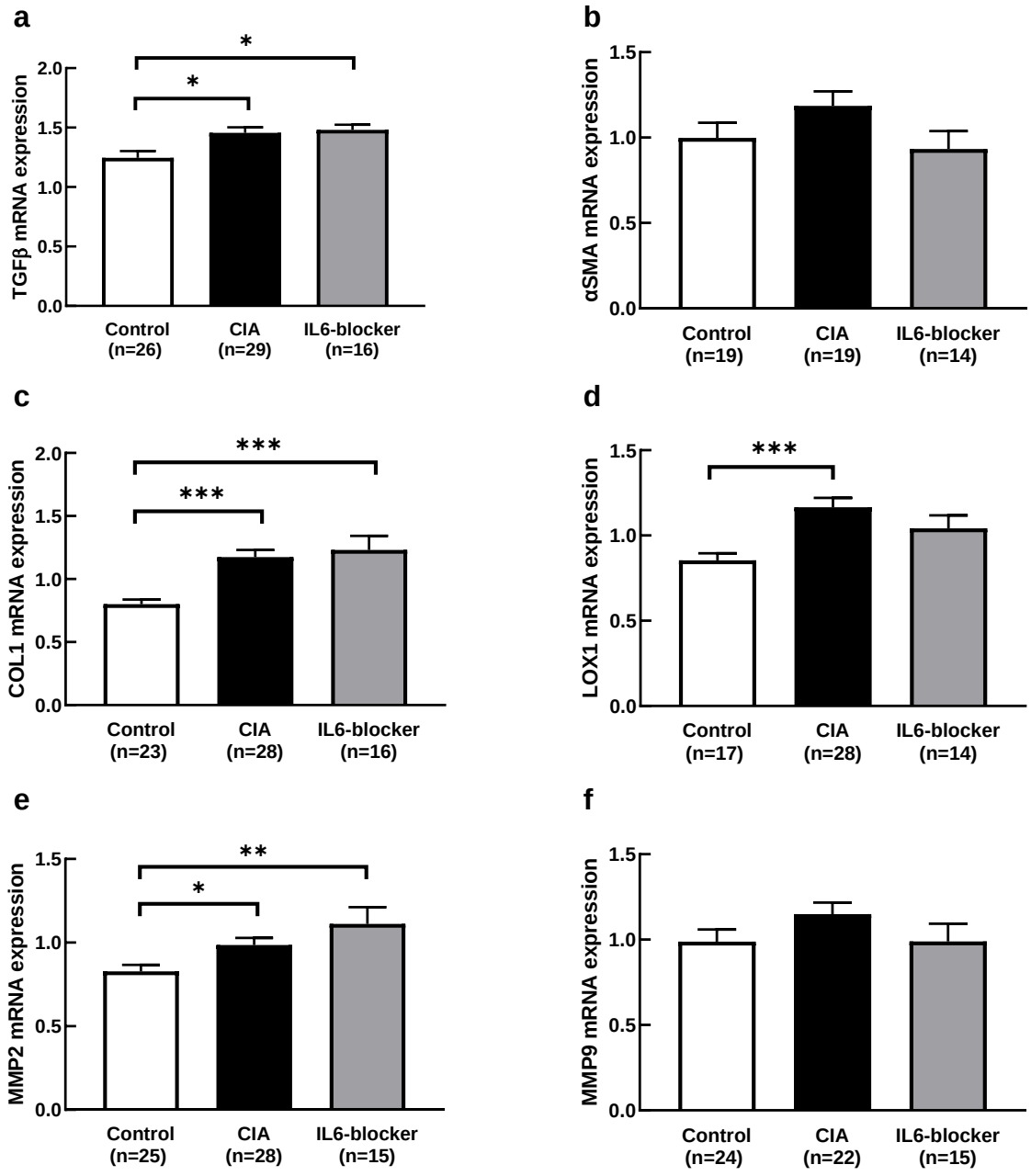

Figure 6.1. LV expression of extracellular matrix genes. Rats were inoculated with collagen (CIA) and treated with an IL-6 blocker before measurement of relative mRNA expression of *TGFβ* (a), *αSMA* (b), *Col1* (c), *LOX* (d), *MMP2* (e) and *MMP9* (f) in left ventricular tissues of control, CIA and IL-6 blocker rats. Relative mRNA expression results are expressed in arbitrary units normalized for the expression of the endogenous reference gene, *HPRT1*, using the ΔΔCt method. Data are from duplicate real-time PCR experiments. Data presented as means ± SEM; * $p < 0.05$ vs control;** $p < 0.01$ vs control; *** $p < 0.001$ versus control.

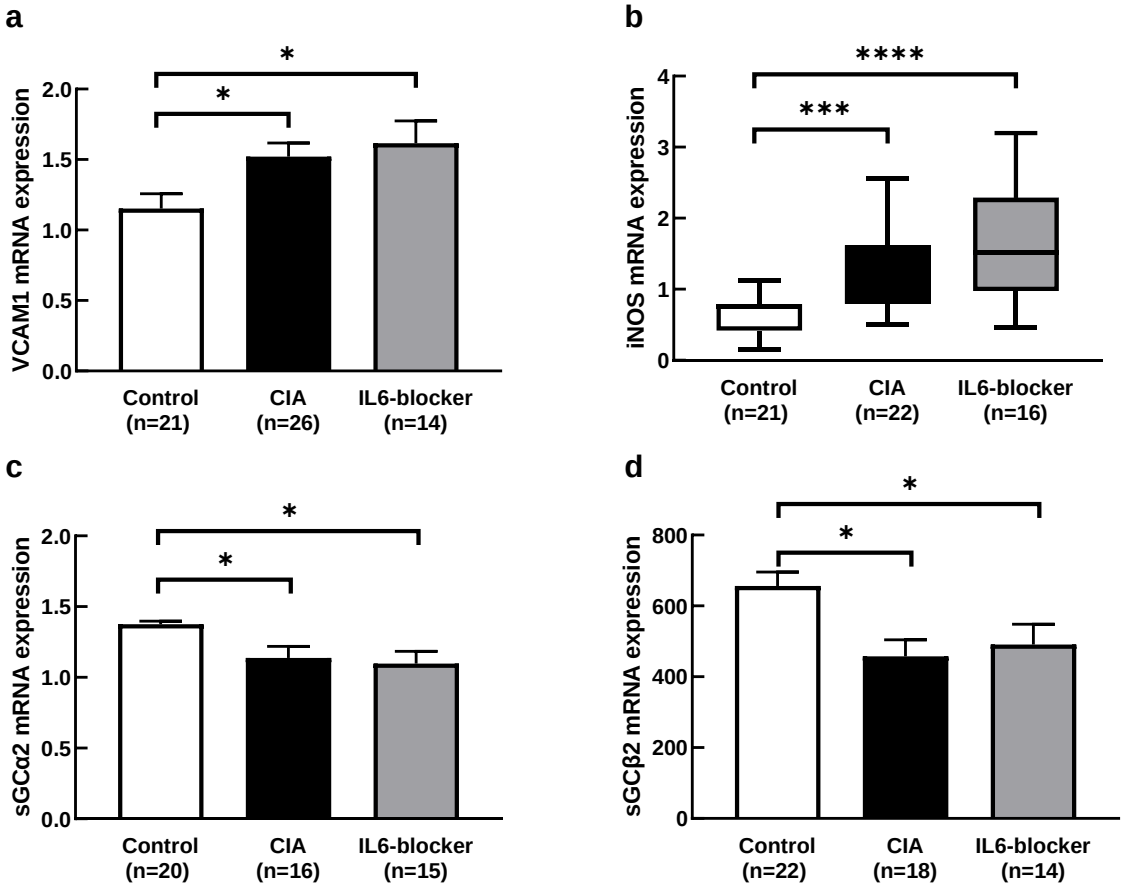

Figure 6.2. LV expression of microvascular inflammation, immune cell activation and sGC subunit genes. Rats were inoculated with collagen (CIA) and treated with an IL-6 blocker before measurement of relative mRNA expression of *VCAM1* (a), *iNOS* (b), *sGCα2* (c) and *sGCβ2* (d) in left ventricular tissues of control, CIA and IL-6 blocker rats. Relative mRNA expression results are expressed in arbitrary units normalized for the expression of the endogenous reference gene, *HPRT1,* using the ΔΔCt method. Data are from duplicate real time PCR experiments. Data presented as means ± SEM for *VCAM1*, *sGCα2* and *sGCβ2* and median and interquartile range for *iNOS*; * $p < 0.05$ vs control; *** $p < 0.001$ vs control.

The LV mRNA expression of *PP1γ*, the protein phosphatase previously implicated in titin phosphorylation, was not different between the three groups ($p > 0.05$; Figure 6.3a). The LV mRNA expression of the protein phosphatase *PP5* was significantly higher in the IL-6 blocker group compared to the control group ($p = 0.02$) but was not different from the CIA groups ($p = 0.98$; Figure 6.3b), suggesting that IL-6 may not be involved in the cellular pathways whereby PP5 contributes to the dephosphorylation of titin.

6.3.5 The effect of IL-6 blocker treatment on gene expression of markers of calcium handling, oxidative stress and apoptosis

The LV mRNA expression of *SERCA2a* and *S100A1* in the IL-6 blocker group were not different from the control ($p = 0.42$ and $p = 0.98$, respectively) or CIA groups ($p = 0.99$ and $p = 0.90$; Figure 6.4a, 6.4b), indicating that neither inflammation nor IL-6 blocker treatment impacted Ca^{2+} handling in LV tissues. The LV mRNA expressions of pro-apoptotic gene; *BAX*, and anti-apoptotic gene; *Bcl-2*, were not different between any of the groups (all $p > 0.05$, Figure 6.4d, 6.4e). Consistent with these findings, the ratio of *BAX* to *Bcl-2* was also not different between the groups (all $p > 0.05$, Figure 6.4f), showing that systemic inflammation and blocking circulating IL-6 did not impact apoptosis in LV tissues. In keeping with these results, the LV mRNA expression of *SOD2*, a marker of mitochondrial oxidative stress, was not different between any of the groups (all $p > 0.05$, Figure 6.4c).

6.3.6 The effect of IL-6 blocker treatment on myocardial contractility genes

The relative mRNA expression of *Myh6*, the gene that codes for the fast-twitch isoform of myosin, was decreased in the IL-6 blocker group compared to the control group ($p = 0.02$) and was not different from the CIA group ($p = 0.87$; Figure 6.5a). The relative mRNA expression of *Myh7*, the gene that codes for the slow-twitch isoform of myosin, was increased in the IL-6 blocker group compared to the control group ($p = 0.002$) and was not different from the CIA group ($p = 0.74$, Figure 6.5b). Consequently, similar to the CIA group, there was a decreased ratio of *Myh6/Myh7* in the IL-6 blocker group compared to the control group ($p = 0.003$; Figure 6.5c). The increased expression of *Myh7* is consistent with the findings of increased pro-fibrotic gene expression in the IL-6 group. Moreover, these findings confirm our previous reports that a switch in myosin isoform expression may contribute to impaired myocardial deformation, as we showed impaired global longitudinal strain and velocity in the IL-6 blocker group (Table 6.2).

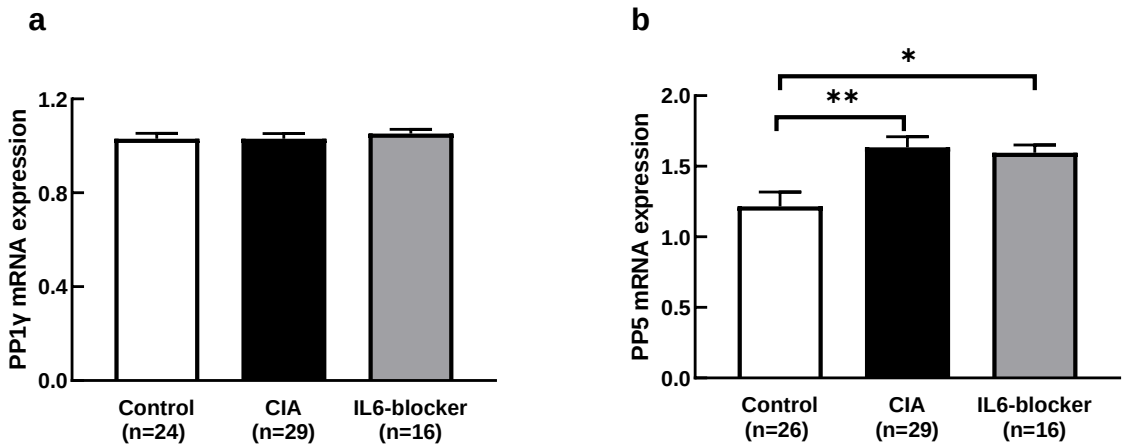

Figure 6.3. LV expression of protein phosphatase genes. Rats were inoculated with collagen (CIA) and treated with an IL-6 blocker before measurement of relative mRNA expression of *PP1γ* (a) and *PP5* (b) in left ventricular tissues of control, CIA and IL-6 blocker rats. Relative mRNA expression results are expressed in arbitrary units normalized for the expression of the endogenous reference gene, *HPRT1,* using the ΔΔCt method. Data are from duplicate real time PCR experiments. Data presented as means ± SEM; * $p < 0.05$ vs control; ** $p < 0.01$ vs control.

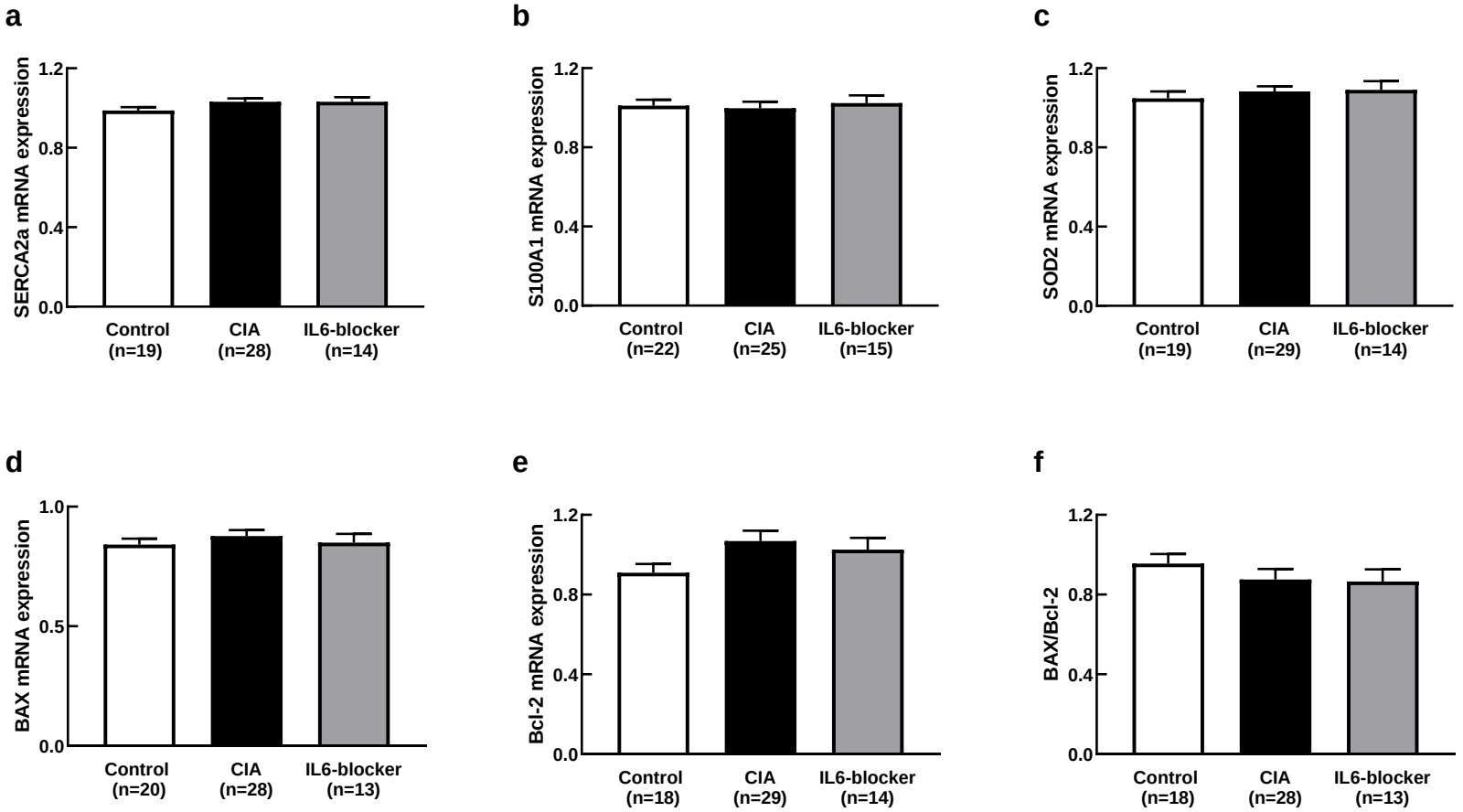

Figure 6.4. LV expression of calcium handling, mitochondrial dysfunction and apoptotic genes. Rats were inoculated with collagen (CIA) and treated with an IL-6 blocker before measurement of relative mRNA expression of *SERCA2a* (a), *S100A1* (b), *SOD2* (c), *BAX* (d), *Bcl-2* (e) and *BAX/Bcl-2* ratio (f) in left ventricular tissues of control, CIA and IL-6 blocker rats. Relative mRNA expression results are expressed in arbitrary units normalized for the expression of the endogenous reference gene, *HPRT1*, using the ΔΔCt method. Data are from duplicate real time PCR experiments. Data presented as means ± SEM.

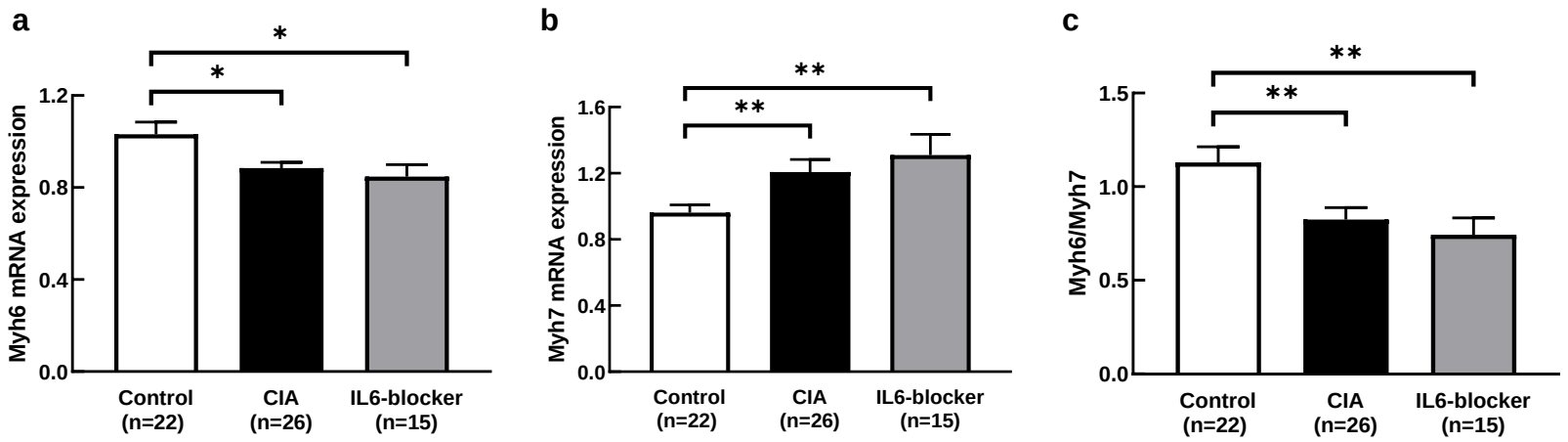

Figure 6.5. LV expression of myocardial contractility genes. Rats were inoculated with collagen (CIA) and treated with an IL-6 blocker before measurement of relative mRNA expression of *Myh6* (a), *Myh7* (b) and *Myh6/Myh7* ratio (c) in left ventricular tissues of control, CIA and IL-6 blocker rats. Relative mRNA expression results are expressed in arbitrary units normalized for the expression of the endogenous reference gene, *HPRT1*, using the ΔΔCt method. Data are from duplicate real time PCR experiments. Data presented as means ± SEM; * $p < 0.05$ vs control; ** $p < 0.01$ vs control.

6.4 Discussion

This study investigated the role of IL-6 in the molecular pathways involved in the development of LV diastolic and systolic dysfunction in a rat model of systemic inflammation. The main findings of this study were that blocking circulating IL-6 with tocilizumab did not impact any of the inflammation-induced increases in circulating or local inflammatory markers or the local expression of genes involved in immune cell infiltration. Blocking circulating IL-6 also did not reverse the inflammation-induced upregulation of pro-fibrotic genes or genes involved in collagen turnover, similar to the CIA rats. However, blocking circulating IL-6 partially offset the inflammation-induced upregulation of *LOX*, a marker of collagen cross-linking. Despite the partial prevention of collagen cross-linking, the increased pro-fibrotic gene expression likely contributed to the increased relative wall thickness and concentric remodelling seen in rats that received the IL-6 blocker, similar to results of the CIA group. In keeping with these findings, IL-6 blockade did not prevent the fibrosis-induced changes in myosin heavy chain isoform gene expression, which may have contributed to the impaired LV systolic function (LV deformation and impaired motion) seen in the IL-6 blocker group. This study also demonstrated that blocking circulating IL-6 did not reverse the inflammation-induced upregulation of the genes involved in titin phosphorylation, which likely contributed to the impaired LV diastolic function in the IL-6 blocker group. Furthermore, similar to the CIA group, the LV mRNA expression of genes involved in apoptosis, Ca^{2+} handling and mitochondrial function were not affected in the IL-6 blocker group, suggesting that these molecular mechanisms are unlikely to contribute to inflammation-induced LV diastolic or systolic dysfunction. Taken together, in a rat model of systemic inflammation-induced LV dysfunction, administering an IL-6 receptor antagonist was largely ineffective in reversing the inflammation-induced changes in passive and active processes underlying the development of LV dysfunction, and hence the role of IL-6 in these processes remains inconclusive.

Several studies have shown that IL-6 is a key stimulus for cardiac fibrosis in various animal and cell culture models (Kaminski et al. 2007; Lai et al. 2012; Siwik, Chang, and Colucci 2000; Zhao et al. 2016). In contrast, our results showed that blocking circulating IL-6 did not prevent the inflammation-induced upregulation of pro-fibrotic genes including *TGFβ, Col1* and *MMP2*. Indeed, others have also shown that IL-6 is not necessary for the development of LV fibrosis (Hartman et al. 2016; Hirota et al. 1995; Meléndez et al. 2010). The increased expression of pro-fibrotic genes in the present study, may have contributed to the increased RWT in the IL-6 blocker group, as we have previously shown (Chapter 3). The increased pro-fibrotic gene expression is further consistent with the increased expression of *Myh7* in the IL-6 blocker group that was similar to that of the CIA group. *Myh7* is the gene that codes for the β-MyHC (England and Loughna 2013), which may have contributed to the impaired LV global longitudinal strain and velocity, which are indicators of early impairments in LV myocardial contractility despite preserved ejection

fraction. Moreover, none of the genes involved in Ca^{2+} handling, apoptosis or oxidative stress were impacted by blocking circulating IL-6. As these genes were also not affected in the CIA group, it remains uncertain whether these processes are in fact a cause or a consequence of LV diastolic or early-stage systolic dysfunction.

In the present study, blocking circulating IL-6 did partially improved the inflammation-induced increase in LV mRNA expression of *LOX*, the gene that codes for lysyl oxidase, an enzyme implicated in collagen cross-linking (El Hajj et al. 2017). Although evidence for a co-regulation between LOX and IL-6 has been shown in pulmonary fibrosis, this has not previously been reported in cardiac tissue and hence, requires further investigation (Nguyen et al. 2021). Nevertheless, increased expression of LOX, and hence, increased collagen cross-linking (Páramo 2017) have been independently linked to increased myocardial stiffness (Gonzalez-Santamaria et al. 2016). Therefore, this partial attenuation of *LOX* expression, may have contributed to the slightly reduced e'/a', an indicator of myocardial stiffness in the IL-6 blocker group (Nishimura and Tajik 1997; Smiseth 2017; Zerbib, Maizel, and Slama 2019). Nevertheless, blocking IL-6 was not sufficient to prevent the inflammation-induced decreases in LV relaxation (lateral e') or increases in filling pressures (E/e'), two other frequently used indicators of LV diastolic dysfunction (Nishimura and Tajik 1997; Smiseth 2017; Zerbib, Maizel, and Slama 2019). Considering we have previously shown (Chapter 3) that fibrosis is unlikely to be the main contributor to LV diastolic dysfunction, the results in this chapter further support a central role for titin phosphorylation in the development of LV diastolic dysfunction. We showed that blocking circulating IL-6 did not prevent the inflammation-induced upregulation of the genes involved in the pathways of titin phosphorylation including *VCAM1, iNOS, sGCα2* or *sGCβ2*, suggesting that tocilizumab did not prevent the inflammation induced NO-cGMP-PKG signalling pathway, previously implicated in titin hypophosphorylation (Franssen and Gonzalez Miqueo 2016). Furthermore, blocking IL-6 also did not prevent the inflammation-induced upregulation of *PP5*, which we have shown may play an important regulatory role in titin phosphorylation (Chapter 3). These results are in contrast to a previous study that showed improved titin phosphorylation when blocking circulating IL-6 in a model of Coxsackie virus B3 (CVB3)-induced myocarditis (Savvatis et al. 2014). However, these authors reported that blocking circulating IL-6 reduced downstream LV tissue immune cell infiltration and activation, as well as reducing the expression of other pro-inflammatory cytokines (Savvatis et al. 2014), which may have disrupted signalling pathways involved in titin phosphorylation. In contrast, in our study, blocking circulating IL-6 did not prevent immune cell infiltration and activation (*IL-6, iNOS* or *CD68* expression).

These largely negative results observed in the IL-6 blocker group may be explained by several reasons. First, IL-6 signalling is rather complex, and several studies have reported that it has both detrimental and

protective effects in the heart, depending on whether IL-6 interacts with the soluble or the membrane-bound forms of its receptor (Hanna and Frangogiannis 2020). In this regard, IL-6 is a member of the gp130 cytokine family that includes several other cytokines that have been implicated in the pathophysiology of cardiovascular diseases, including IL-11, leukaemia inhibitory factor (LIF), and cardiotrophin-1. These cytokines signal via the common signalling receptor subunit gp130 (Hanna and Frangogiannis 2020; Rose-John 2018), accounting for their overlapping biological functions (Garbers et al. 2013). Although the IL-6R was believed to be specific for IL-6, other cytokines belonging to the gp130 cytokine family were also able to bind to the IL-6R and induce signalling (Garbers et al. 2012). Indeed, activation of gp130 signalling, in the absence of IL-6, have been associated with myocardial remodelling (Hirota et al. 1995).

Second, IL-6 is able to signal via different mechanisms. Classic IL-6 signalling involves binding of IL-6 cytokines to its receptors (IL-6Rs) on the cell surface, and the subsequent association of the IL-6/IL-6R complexes with gp130, causes dimerization and initiation of a signalling cascade (Hanna and Frangogiannis 2020; Rose-John 2012, 2018). However, IL-6 is also able to signal in the absence of cell surface IL-6R. Disintegrin and Metalloprotease (ADAM) proteases cleave IL-6Rs from the cell surfaces to generate a soluble form of the IL-6R (sIL-6R). Most soluble receptors in the body act as antagonists as they compete with the membrane-bound receptor for the ligand (Hanna and Frangogiannis 2020). In contrast, the sIL-6R, acts as an agonist on cells that are not stimulated exclusively by IL-6. The sIL-6R binds IL-6 initiating gp130 signalling in cells that do not express IL-6R on their surfaces (Zhang et al. 2020). This mechanism, known as trans-signalling, expands the cellular actions of IL-6. The pro- and anti-inflammatory effects of IL-6 have been linked to the different signalling pathways, where trans-signalling has been implicated in pro-inflammatory signalling, while the classic-signalling mechanism may be responsible for anti-inflammatory signals (Rose-John 2012). In this regard, it has been suggested that the *in vivo* role of IL-6 depends on the stimulation of the different receptors in different experimental inflammatory models (Hanna and Frangogiannis 2020). Although the relative contributions of these IL-6 signalling pathways in heart failure have not been systematically studied, studies have reported that the adverse effects of IL-6 on cardiac remodelling were dependent on the presence of the sIL-6R (Chou et al. 2018; Meléndez et al. 2010).

The use of anti-IL-6 therapeutics is complicated by the classic- versus trans-signalling mechanisms of IL-6 action. Tocilizumab functions by inhibiting IL-6 interactions with both soluble and membrane-bound forms of its cognate receptor, thereby downregulating IL-6-mediated signalling (Abdel-Maged et al. 2018). This means that tocilizumab blocks both classic- and trans-signalling pathways and therefore, blocks both pro- and anti-inflammatory activities of IL-6 (Rose-John 2012). Hence, in the current study, blocking IL-6 with tocilizumab may have impacted both the pro- and anti-inflammatory signalling pathways.

Lastly, tocilizumab used in this study is a human monoclonal antibody and may have caused immunogenic effects in rats. In this regard, over the past four decades, recombinant DNA technology has progressed significantly from using hybridomas through to the chimeric, humanized monoclonal antibodies and finally, to the fully human therapeutic monoclonal antibodies currently available (Sheppard et al. 2017). However, these advances have been engineered for human applications rather than for animal disease models. While further humanization of antibody variable regions has led to a subsequent further decrease in immunogenicity, this has been tested for human tolerance only. Therefore, the application of tocilizumab, in this study, although being less immunogenic in humans (Sheppard et al. 2017), may well be more immunogenic in rats. This is supported by my results, which showed no downstream reductions in CRP concentrations or prevention of immune cell infiltration and activation. Indeed, other experimental models that have shown reduced circulating cytokine levels or cardio-protective effects of IL-6 blockers, used a rat anti-mouse IL-6R monoclonal antibody (Hartman et al. 2016; Kobara et al. 2010; Savvatis et al. 2014). Only one other experimental model of rheumatoid arthritis successfully used a human monoclonal IL-6 antibody in rats. These authors reported reduced serum IL-6 concentrations and reduced inflammation-induced joint damage (Abdel-Maged et al 2018). However, in the prior study, the drug was administered intraplanar, which may further explain the lack of effects in this current study.

This study has further limitations. The inclusion of male and female rats may have reduced statistical power. Because tocilizumab is used in the treatment of rheumatoid arthritis, its bioavailability to cardiac tissues is uncertain and were not tested in the current study. The use of mRNA expression may not reflect protein expression and function, hence direct measures of the intracellular signalling intermediates and end products may have strengthened the interpretations of this study.

In conclusion, anti-IL-6 treatment was not effective in reducing circulating cytokine concentrations and was largely ineffective in ameliorating the inflammation-induced upregulation of genes involved in the cellular pathways associated with LV diastolic dysfunction. The effects of IL-6 receptor blockers on inflammation-induced changes in cellular pathways of cardiac dysfunction remain inconclusive and requires further investigation.

CHAPTER 7: SUMMARY AND CONCLUSION

7.1 Summary

Treatment strategies for HFpEF are suboptimal, largely because of the diverse aetiologies and heterogeneous presentation of the disease. Therefore, a better understanding of the pathophysiological mechanisms underlying HFpEF development is needed. It has recently been proposed that chronic systemic inflammation may be the underlying causal mechanism for the development of HFpEF. Nevertheless, the use of anti-inflammatory drugs in the management of these patients has shown contradictory outcomes, which is likely due to the limited knowledge of the roles of specific cytokines in the pathophysiology of HFpEF. Therefore, in the current thesis, a series of investigations was performed to advance the understanding of the molecular mechanisms of systemic inflammation-induced LV diastolic and systolic dysfunction, and to elucidate the roles of TNF-α and IL-6 in these molecular pathways.

7.2 Inflammation-induced LV fibrosis is partially mediated by TNF-α

HFpEF is mainly characterised by diastolic abnormalities. During diastole, the ventricles relax to allow adequate LV filling with blood for the subsequent ejection phase. Both active and passive processes contribute to adequate myocardial relaxation (Borlaug and Kass 2006). LV diastolic dysfunction, the subclinical condition that often precedes HFpEF, has variable phenotypes that affect either active or passive processes of myocardial relaxation (Borlaug and Kass 2006). Pathological alterations in the molecular mechanisms underlying either the active or passive processes contribute to impaired relaxation and increased myocardial stiffness that may ultimately contribute to LV diastolic dysfunction. Myocardial fibrosis is characterized by changes in the extracellular matrix that contribute to passive myocardial stiffness and concentric remodelling of the LV, which is associated with LV diastolic dysfunction.

In the present thesis, in an effort to understand the role of systemic inflammation, and specifically TNF-α, in extracellular matrix remodelling and its contribution to LV diastolic dysfunction, several molecular markers of cardiac fibrosis and collagen turnover were assessed in a rat model of collagen-induced arthritis, with- or without- inhibition of circulating TNF-α, using etanercept. Systemic inflammation caused local LV tissue inflammation in the form of increased mRNA expression of *IL-6*, which was prevented by inhibiting circulating TNF-α. This result is consistent with the increased mRNA expression of *CD68*, suggesting LV infiltration by macrophages, which produce both IL-6 and TGFβ. TGFβ is known to activate cardiac fibroblasts to produce collagen (Villar et al. 2009). Consistent with this, systemic inflammation increased LV mRNA expression of *TGFβ* and other pro-fibrotic genes, including *Col1* and *LOX*. The increased pro-fibrotic gene expressions likely stimulated the upregulation of *MMP2*, which caused further dysregulation in collagen turnover, thereby contributing to an increase in RWT, a marker of concentric remodelling that is consistent with fibrosis. Although inhibiting circulating TNF-α prevented adverse LV

remodelling (prevented the increase in RWT) by decreasing local LV inflammation (prevented the increased mRNA expression of *IL-6*, *CD68*) and partially preventing the upregulation of pro-fibrotic genes, it did not prevent inflammation-induced LV diastolic dysfunction in the CIA rat model. An important implication of these findings is that myocardial fibrosis is mediated by TNF-α, but that fibrosis may not be the main driver for the development of LV diastolic dysfunction.

7.3 The role of TNF-α in signalling pathways of titin phosphorylation

Although fibrosis and extracellular matrix remodelling are key characteristics of passive stiffness in LV diastolic dysfunction, not all patients with HFpEF have concentric remodelling. Indeed, a recent paradigm suggested that systemic inflammation contributes to passive LV stiffness by affecting the compliance of the cardiomyocyte. In this regard, inflammation causes endothelial dysfunction in the microvasculature that results in the production of ROS, which decreases the bioavailability of NO. In turn, altered NO signalling causes dysregulated intracellular pathways in the myocardium that disrupt phosphorylation of the giant spring protein, titin (Paulus & Tschöpe, 2013). Aberrant titin phosphorylation affects cardiomyocyte compliance, which contributes to decreased passive elasticity of the sarcomere which ultimately impairs LV relaxation and filling during diastole (Lewinter and Granzier 2014).

Therefore, in the second study the effect of inflammation and inhibition of circulating TNF-α on several genes involved in the regulation of titin phosphorylation, were investigated in an animal model of collagen-induced inflammation. Collagen inoculation induced microvascular inflammation as vascular endothelial cell activation was increased, indicated by increased LV mRNA expression of *VCAM1*. The microvascular inflammation resulted in infiltration of leukocytes and local LV tissue inflammation as indicated by the increased LV mRNA expression of *PTX3*, *iNOS* and *CD68*. Leukocytes are sources of ROS, which, like metabolically-induced endothelial dysfunction, limits NO bioavailability and disrupts NO signalling (Franssen et al. 2016). Furthermore, LV mRNA expression of sGC subunit genes was decreased, likely disrupting NO-sGC-cGMP signalling, which phosphorylates titin. Inhibiting TNF-α reversed the inflammation-induced upregulated expression of *VCAM1*, *iNOS*, *CD68* and the decreased expression of sGC subunit genes. This likely resulted in the inhibition of local pathological ROS production and improved NO-sGC-cGMP signalling. More importantly, I showed that inflammation resulted in increased LV mRNA expression of *PP5*, which increases passive cardiomyocyte stiffness by dephosphorylating titin. Increased *PP5* mRNA expression was not reversed by TNF-α inhibition. Since TNF-α inhibition also did not prevent LV diastolic dysfunction, an important implication of these findings is that LV diastolic dysfunction results, at least partially, from the increased LV mRNA expression of *PP5*, which contributes to titin hypophosphorylation. Since the change in sGC subunit expression was prevented by inhibition of

circulating TNF-α, disruption of the NO-sGC-cGMP signalling pathway is likely less important in the development of LV diastolic dysfunction.

7.4 The role of TNF-α in active processes of inflammation-induced LV diastolic and systolic dysfunction

Besides passive LV stiffness, myocardial relaxation also depends on active processes. Thus far, the main active mechanisms proposed to affect active relaxation is the impaired reuptake of Ca^{2+} from the cytosol into the sarcoplasmic reticulum. However, other energy dependent processes, such as mitochondrial ATP synthesis, may also contribute to impaired LV relaxation. Furthermore, subclinical systolic dysfunction has also been reported in patients with HFpEF (Yip 2002; Yu et al. 2002), despite preserved ejection fraction. Inflammation has been implicated in subclinical systolic dysfunction in HFpEF (Lo Gullo et al. 2018), yet the understanding of the mechanisms of inflammation-induced subclinical systolic dysfunction is limited and indirect (Nagueh, 2021).

Therefore, in the third study, the effect of inflammation with- and without- inhibition of circulating TNF-α on several genes involved in cellular processes of active LV myocardial relaxation and contraction, was investigated in our rat model of collagen-induced inflammation. I further elucidated the role of TNF-α in these processes in an adult human cardiomyocyte cell line (AC16). In this investigation, expression of Ca^{2+}-handling genes (*SERCA2a* and *S100A1)* was unchanged and therefore did not contribute to LV diastolic or systolic dysfunction in the CIA model. Further to this, mRNA expression of *SERCA2a,* was also not changed *in vitro*, suggesting that even direct exposure of cardiomyocytes to TNF-α may not disrupt expression of this Ca^{2+} handling gene. Systemic inflammation and TNF-α inhibition did not affect expression of the pro- and anti- apoptotic genes, *BAX* and *Bcl-2* or superoxide dismutase *SOD2*. TNF-α stimulated a small decrease in *BAX* expression and a small increase in the *BAX*/*Bcl-2* ratio in AC16 cells, suggesting a small increase in apoptosis. However, in the AC16 cells, TNF-α stimulated a robust increase in *SOD2* expression, which suggests that ROS were inactivated and hence may explain the only small increase in apoptosis. Nevertheless, these results suggest that in collagen-induced systemic inflammation, mitochondrial function is likely intact and ATP production is not compromised. Hence it is unlikely that disruption of energy dependent processes contributes to diastolic relaxation or contractile dysfunction in the early stages of inflammation-induced LV dysfunction. Despite the preserved ejection fraction in the CIA rats, myocardial deformation and motion were impaired, indicating early-stage systolic dysfunction. This was consistent with the inflammation-induced change in MyHC isoforms from fast-twitch (*myh6,* α-MyHC) to slow-twitch (*myh7,* β-MyHC) expression that is associated with impaired contractile properties of cardiomyocytes (Fitzsimons et al. 1998). Changes in systolic dysfunction and the mRNA expression of

MyHC isoform genes were both offset when circulating TNF-α was inhibited. An important implication of these findings is that inflammation-induced early-stage systolic dysfunction may be due to changes in the MyHC contractile properties, which is mediated by circulating TNF-α. Furthermore, the role of increased circulating TNF-α in development of HFpEF is likely mediated by impaired systolic function.

7.5 The role of IL-6 in passive and active processes of inflammation-induced LV diastolic and systolic dysfunction

Findings from the preceding studies raised the question whether other cytokines may be involved in the cellular processes of active and passive processes of relaxation and systolic dysfunction. Recently IL-6 was ranked among the top four predictive biomarkers related to cases of heart failure that resulted in hospital admissions and death (Chirinos et al. 2020). Furthermore, in patients with inflammatory conditions, circulating IL-6 concentrations are independently linked to LV diastolic dysfunction (Liang et al. 2010). Considering the important role of Il-6 in disease pathogenesis of both inflammatory conditions and heart failure, IL-6 is considered an attractive therapeutic target. However, the understanding of its role in the cellular processes underlying HFpEF is poorly understood.

Therefore, in the fourth study, the role of IL-6 in the molecular processes underlying the development of LV diastolic and systolic dysfunction was investigated in the CIA rat model by blocking its effects, using the IL-6 receptor blocker, tocilizumab. I showed that anti-IL-6 treatment largely failed to ameliorate the inflammation-induced upregulation of genes involved in the cellular pathways associated with LV diastolic and systolic dysfunction. This may have been a result of the complex IL-6 signalling pathways involved in the heart, or the mechanism of drug action and administration in this study. It is possible that protective effects of the human antibody-based drug were overwhelmed by its immunogenic effects in rats. Therefore, the effects of IL-6 receptor blockers on inflammation-induced changes in cellular pathways of cardiac dysfunction remain uncertain.

In summary and as depicted in Figure 7.1, my results suggest that systemic inflammation induces endothelial cell activation, which promotes infiltration of LV tissues by leukocytes causing ROS production and enhancing local tissue inflammation. Leukocytes produce IL-6 and TGFβ, which induce pro-fibrotic signals. Inhibiting circulating TNF-α partially inhibits fibrosis but not development of LV diastolic dysfunction. Local ROS production limits NO bioavailability, which degreases sGC activity. The increased ROS decreased sGC subunit expression, which likely disrupts NO-sGC-cGMP signalling and PKG phosphorylation of titin, which, in turn, may contribute to titin hypophosphorylation and cardiomyocyte stiffness. Although TNF-α inhibition partially prevents disruption of NO-sGC-cGMP signalling pathway,

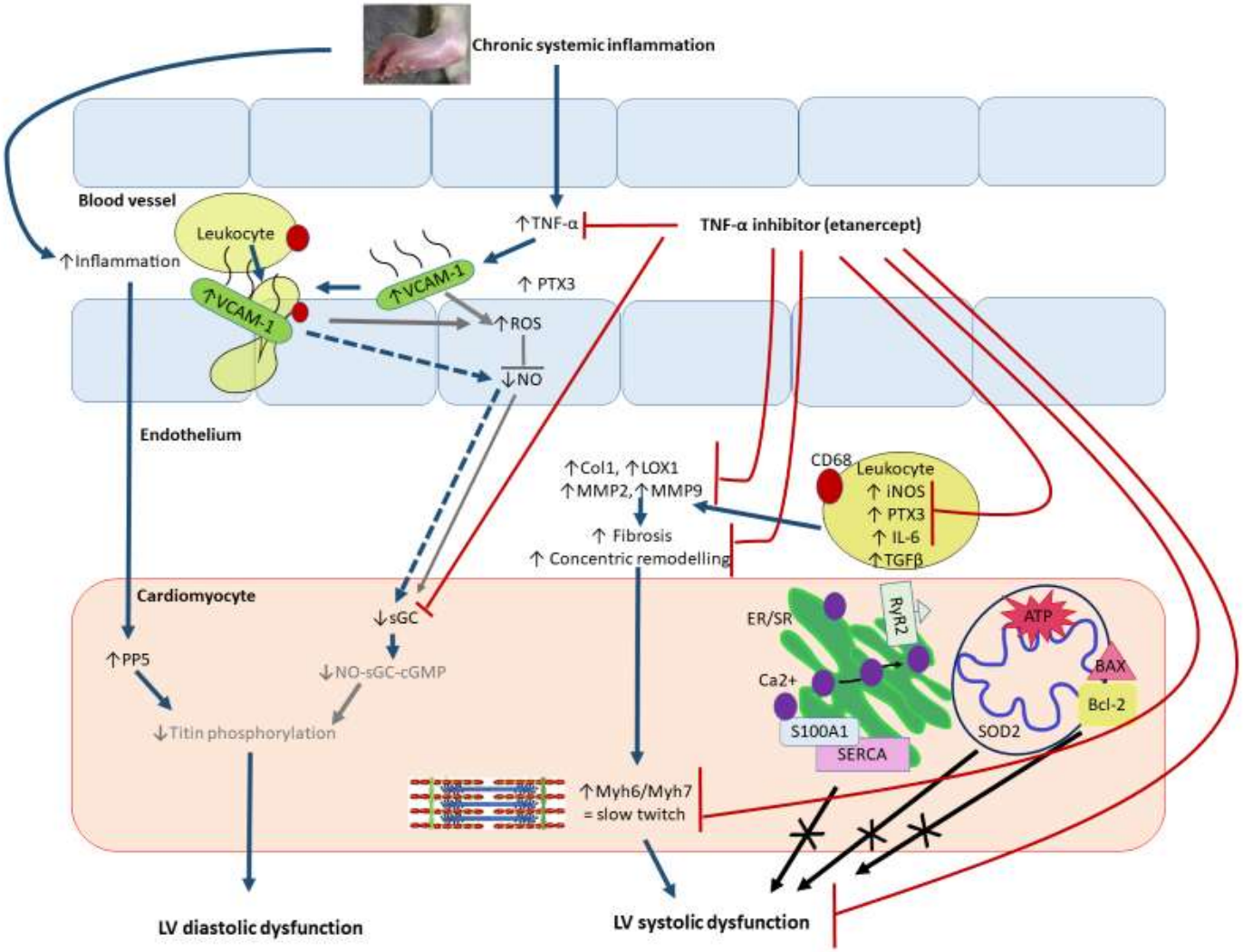

Figure 7.1. Schematic depicting the effects of systemic inflammation and inhibition of circulating TNF-α on molecular markers of left ventricular diastolic and systolic dysfunction.

the inflammation-induced PP5 hypophosphorylation of titin is independent of TNF-α. Active processes of LV relaxation are not impaired by systemic inflammation. However, TNF-α mediates the change in MyHC gene expression that likely impairs myocardial contractility, consistent with measures of systolic dysfunction in the CIA rats.

7.6 Limitations and future recommendations

The specific limitations of each study in this thesis have been addressed at the end of each chapter. However, the following limitations should be noted and addressed in future studies. Firstly, the use of mRNA expression analysis, which may not adequately represent the function of some of the markers that are regulated by post-transcriptional and post-translational mechanisms. Future studies must investigate the protein expression and functions of such markers and correlate the data with the mRNA expression data. Another limitation is that the CIA rats developed a mild form of LV diastolic dysfunction, which may have limited the investigation of the role of active processes in LV relaxation. Future studies should extend the CIA intervention period or consider extending it to the use of other, more severe inflammatory models. Another limitation is the use of tocilizumab as the IL-6 blocker, a humanized monoclonal antibody, which was developed for use in humans (Hashizume et al. 2015). Further to this, because tocilizumab was engineered specifically for treatment of rheumatoid arthritis, a disease of joint inflammation (Hashizume et al. 2015), it may have poor bio-distribution into heart tissues and therefore, not block the effects of local IL-6 expression. Future studies should investigate the confounding effect of comorbid conditions and other potential therapeutic agents, which have shown promise in recent literature. Although the echocardiographic techniques and measures performed in this study are widely accepted and validated, additional techniques including Simpson's biplane and measures of tricuspid regurgitation jet velocity and diastolic strain rate should be considered for future studies.

7.7 Conclusion

In conclusion, the evidence presented in this thesis advances the understanding of the pathophysiological molecular mechanisms and the role of TNF-α in the development of inflammation-induced LV diastolic and systolic dysfunction. Evidence is provided that circulating TNF-α partially mediates the development of LV fibrosis and the resultant concentric remodelling, but that LV concentric remodelling is not the main mechanism for the development of LV diastolic dysfunction. Further evidence is provided to suggest that inflammation may contribute to LV diastolic dysfunction by inducing hypophosphorylation of titin via increased expression of PP5, rather than primarily via TNF-α mediated NO-sGC-cGMP signalling. This thesis also demonstrates that expression of the genes involved in the active process of diastolic relaxation, including Ca2+ removal, mitochondrial dysfunction and apoptosis was not compromised in LV diastolic

dysfunction and that these processes may not contribute to LV diastolic or early-stage systolic dysfunction. Finally, this thesis provides evidence that TNF-α impairs myocardial contractile properties by impacting MyHC isoform expression, thereby contributing to the development of early-stage LV systolic dysfunction.

CHAPTER 8: REFERENCES

Abdel-Maged, A. E., A. M. Gad, A. K. Abdel-Aziz, M. M. Aboulwafa, and S. S. Azab. 2018. 'Comparative study of anti-VEGF Ranibizumab and Interleukin-6 receptor antagonist Tocilizumab in Adjuvant-induced Arthritis', *Toxicology and Applied Pharmacology*, 356: 65-75.

Adeniran, I., D. H. MacIver, J. C. Hancox, and H. Zhang. 2015. 'Abnormal calcium homeostasis in heart failure with preserved ejection fraction is related to both reduced contractile function and incomplete relaxation: an electromechanically detailed biophysical modeling study', *Frontiers in Physiology*, 6: 78.

Agbor, V. N., M. Essouma, N. A. B. Ntusi, U. F. Nyaga, J. J. Bigna, and J. J. Noubiap. 2018. 'Heart failure in sub-Saharan Africa: A contemporaneous systematic review and meta-analysis', *International Journal of Cardiology*, 257: 207-15.

Agbor, V. N., N. A. B., Ntusi, and J. J. Noubiap. 2020. 'An overview of heart failure in low- and middle-income countries', *Cardiovascular Diagnosis and Therapy*, 10: 244-51.

Ahlers, M. J., B. D. Lowery, E. Farber-Eger, T. J. Wang, W. Bradham, M. J. Ormseth, C. P. Chung, C. M. Stein, and D. K. Gupta. 2020. 'Heart failure risk associated with rheumatoid arthritis–related chronic inflammation', *Journal of the American Heart Association*, 9.

Akhigbe, R., and A. Ajayi. 2021. 'The impact of reactive oxygen species in the development of cardiometabolic disorders: A review', *Lipids in Health and Disease*, 20.

Andersen, C. L., Jensen, J. L., and Ørntoft, T. F. 2004. 'Normalization of Real-Time Quantitative Reverse Transcription-PCR data: A model-based variance estimation approach to identify genes suited for normalization, applied to bladder and colon cancer data sets', *Cancer Research*, 64: 5245–50.

Anderson, R. L., D. V. Trivedi, S. S. Sarkar, M. Henze, W. Ma, H. Gong, C. S. Rogers, J. M. Gorham, F. L. Wong, M. M. Morck, J. G. Seidman, K. M. Ruppel, T. C. Irving, R. Cooke, E. M. Green, and J. A. Spudich. 2018. 'Deciphering the super relaxed state of human β-cardiac myosin and the mode of action of mavacamten from myosin molecules to muscle fibers', *Proceedings of National Acaddemy of Science U S A*, 115: E8143-e52.

Aslam, F., S. J. Bandeali, N. A. Khan, and M. Alam. 2013. 'Diastolic dysfunction in rheumatoid arthritis: A meta-analysis and systematic review', *Arthritis Care & Research*, 65: 534-43.

Augustine, D., A. J. Lewandowski, M. Lazdam, A. Rai, J. Francis, S. Myerson, A. Noble, Harald Becher, S. Neubauer, S. E. Petersen, and P. Leeson. 2013. 'Global and regional left ventricular myocardial deformation measures by magnetic resonance feature tracking in healthy volunteers: comparison with tagging and relevance of gender', *Journal of Cardiovascular Magnetic Resonance*, 15: 8.

Aurigemma, G. P., J. S. Gottdiener, L. Shemanski, J. Gardin, and D. Kitzman. 2001. 'Predictive value of systolic and diastolic function for incident congestive heart failure in the elderly: the cardiovascular health study', *Journal of American College of Cardiology*, 37: 1042-8.

Avina-Zubieta, J. A., J. Thomas, M. Sadatsafavi, A. J. Lehman, and D. Lacaille. 2012. 'Risk of incident cardiovascular events in patients with rheumatoid arthritis: a meta-analysis of observational studies', *The Annals of the Rheumatic Diseases*, 71: 1524-9.

Azzawi, M., and P. Haselton. 1999. 'Tumour necrosis factor alpha and the cardiovascular system: its role in cardiac allograft rejection and heart disease', *Cardiovascular Research*, 43: 850-59.

Banerjee, I., J. W Fuseler, A. R. Intwala, and T. A, Baudino. 2009. 'IL-6 loss causes ventricular dysfunction, fibrosis, reduced capillary density, and dramatically alters the cell populations of the developing and adult heart', *American Journal of Physiology-Heart and Circulatory Physiology*, 296: H1694-H704.

Baniaamam, M., W. J. Paulus, A. B. Blanken, and M. T. Nurmohamed. 2018. 'The effect of biological DMARDs on the risk of congestive heart failure in rheumatoid arthritis: a systematic review', *Expert Opinion in Biological Therapeutics*, 18: 585-94.

Baum, J., and H. S. Duffy. 2011. 'Fibroblasts and myofibroblasts: What are we talking about?', *Journal of Cardiovascular Pharmacology*, 57: 376-79.

Biesiadecki, B. J., J. P. Davis, M. T. Ziolo, and P. M. L. Janssen. 2014. 'Tri-modal regulation of cardiac muscle relaxation; intracellular calcium decline, thin filament deactivation, and cross-bridge cycling kinetics', *Biophysiological Reviews*, 6: 273-89.

Borlaug, B. A., and D. A. Kass. 2006. 'Mechanisms of diastolic dysfunction in heart failure', *Trends in Cardiovascular Medicine*, 16: 273-79.

Bozkurt, B., A. J. S. Coats, H. Tsutsui, C. M. Abdelhamid, S. Adamopoulos, N. Albert, S. D. Anker, J. Atherton, M. Böhm, J. Butler, M. H. Drazner, G. Michael Felker, G. Filippatos, M. Fiuzat, G. C. Fonarow, J. E. Gomez-Mesa, P. Heidenreich, T. Imamura, E. A. Jankowska, J. Januzzi, P. Khazanie, K. Kinugawa, C. S. P. Lam, Y. Matsue, M. Metra, T. Ohtani, M. Francesco Piepoli, P. Ponikowski, G. M. C. Rosano, Y. Sakata, P. Seferović, R. C. Starling, J. R. Teerlink, O. Vardeny, K. Yamamoto, C. Yancy, J. Zhang, and S. Zieroth. 2021. 'Universal definition and classification of heart failure: a report of the Heart Failure Society of America, Heart Failure Association of the European Society of Cardiology, Japanese Heart Failure Society and Writing Committee of the Universal Definition of Heart Failure: Endorsed by the Canadian Heart Failure Society, Heart Failure Association of India, Cardiac Society of Australia and New Zealand, and Chinese Heart Failure Association', *European Journal of Heart Failure*, 23: 352-80.

Brenes-Castro, D., E. C. Castillo, E. Vazquez-Garza, G. Torre-Amione, and G. Garcia-Rivas. 2018. 'Temporal frame of immune cell infiltration during heart failure establishment: Lessons from animal models', *International Journal of Molecular Sciences*, 19.

Brown, D. A., J. B. Perry, M. E. Allen, H. N. Sabbah, B. L. Stauffer, S. R. Shaikh, J. G. F. Cleland, W. S. Colucci, J. Butler, A. A. Voors, S. D. Anker, B. Pitt, B. Pieske, G. Filippatos, S. J. Greene, and M. Gheorghiade. 2017. 'Mitochondrial function as a therapeutic target in heart failure', *Nature Reviews Cardiology*, 14: 238-50.

Brucks, S., W. C. Little, T. Chao, D. W. Kitzman, D. Wesley-Farrington, S. Gandhi, and Z. K. Shihabi. 2005. 'Contribution of left ventricular diastolic dysfunction to heart failure regardless of ejection fraction', *American Journal of Cardiology*, 95: 603-6.

Bryant, D., L. Becker, J. Richardson, J. Shelton, F. Franco, R. Peshock, M. Thompson, and B. Giroir. 1998. 'Cardiacfailure in transgenic mice with myocardial expression of tumor necrosis factor-α', *Circulation*, 97: 1375-81.

Burgoyne, J. R, H. Mongue-Din, P. Eaton, and A. M Shah. 2012. 'Redox signaling in cardiac physiology and pathology', *Circulation Research*, 111: 1091-106.

Cabiati, M., S. Raucci, C. Caselli, M. A. Guzzardi, A. D'Amico, T. Prescimone, D. Giannessi, and S. Del Ry. 2012. 'Tissue-specific selection of stable reference genes for real-time PCR normalization in an obese rat model', *Journal of Molecular Endocrinology*, 48: 251-60.

Cerutti, C., and A. J. Ridley. 2017. 'Endothelial cell-cell adhesion and signaling', *Experimental Cell Research*, 358: 31-38.

Chinnaiyan, K. M., D. Alexander, M. Maddens, and P. A. McCullough. 2007. 'Curriculum in cardiology: Integrated diagnosis and management of diastolic heart failure', *American Heart Journal*, 153: 189-200.

Chirinos, J. A., A. Orlenko, L. Zhao, M. D. Basso, M. E. Cvijic, Z. Li, T. E. Spires, M. Yarde, Z. Wang, D. A. Seiffert, S. Prenner, P. Zamani, P. Bhattacharya, A. Kumar, K. B. Margulies, B. D. Car, D. A. Gordon, J. H. Moore, and T. P. Cappola. 2020. 'Multiple plasma biomarkers for risk stratification in patients with heart failure and preserved ejection fraction', *Journal of American College Cardiology*, 75: 1281-95.

Chou, C., C. Hung, C. Liao, L. Wei, C. Chen, C. Shun, W. Wen, C. Wan, X. Wu, and Y. Chang. 2018. 'IL-6 trans-signalling contributes to aldosterone-induced cardiac fibrosis', *Cardiovascular Research*, 114: 690-702.

Combes, A., C. Frye, B. Lemster, S. Brooks, S. Watkins, A. Feldman, and C. McTiernan. 2002. 'Chronic exposure to interleukin 1β induces a delayed and reversible alteration in excitation-contraction coupling of cultured cardiomyocytes', *Pflügers Archiv European Journal of Physiology*, 445: 246-56.

Cordero-Reyes, A. M., K. Youker, J. D. Estep, G. Torre-Amione, and S. F. Nagueh. 2014. 'Molecular and cellular correlates of cardiac function in end-stage DCM: a study using speckle tracking echocardiography', *JACC Cardiovascular Imaging*, 7: 441-52.

Crowson, C. S., K. P. Liao, J. M. Davis, 3rd, D. H. Solomon, E. L. Matteson, K. L. Knutson, M. A. Hlatky, and S. E. Gabriel. 2013. 'Rheumatoid arthritis and cardiovascular disease', *American Heart Journal*, 166: 622-28 e1.

Cuspidi, C., G. Macca, I. Michev, V. Fusi, B. Severgnini, C. Corti, S. Meani, C. Valerio, C. Sala, F. Magrini, and A. Zanchetti. 2002. 'Left ventricular concentric remodelling and extracardiac target organ damage in essential hypertension', *Journal of Human Hypertension*, 16: 385-90.

Deswal, A., N. J. Petersen, A. M. Feldman, J. B. Young, B. G. White, and D. L. Mann. 2001. 'Cytokines and cytokine receptors in advanced heart failure: an analysis of the cytokine database from the Vesnarinone trial (VEST)', *Circulation*, 103: 2055-9.

Di Minno, M. N. D., F. Forte, A. Tufano, A. Buonauro, F. W. Rossi, A. De Paulis, and M. Galderisi. 2020. 'Speckle tracking echocardiography in patients with systemic lupus erythematosus: A meta-analysis', *European Journal of International Medicine*, 73: 16-22.

Duarte-Costa, S., R. Castro-Ferreira, J. S. Neves, and A. F. Leite-Moreira. 2014. 'S100A1: a major player in cardiovascular performance', *Physiological Research*: 669-81.

Dubois-Deruy, E., V. Peugnet, A. Turkieh, and F. Pinet. 2020. 'Oxidative stress in cardiovascular diseases', *Antioxidants*, 9: 864.

Eisner, D. A., J. L. Caldwell, A. W. Trafford, and D. C. Hutchings. 2020. 'The control of diastolic calcium in the heart', *Circulation Research*, 126: 395-412.

El Hajj, E. C., M. C. El Hajj, V. K. Ninh, J. M. Bradley, M. A. Claudino, and J. D. Gardner. 2017. 'Detrimental role of lysyl oxidase in cardiac remodeling', *Journal of Molecular and Cellular Cardiology*, 109: 17-26.

England, J., and S. Loughna. 2013. 'Heavy and light roles: myosin in the morphogenesis of the heart', *Cellular and Molecular Life Sciences*, 70: 1221-39.

Ferreira, M., M. Beullens, M. Bollen, and A. Van Eynde. 2019. 'Functions and therapeutic potential of protein phosphatase 1: Insights from mouse genetics', *Biochimica et Biophysica Acta (BBA) - Molecular Cell Research*, 1866: 16-30.

Filler, S. G., N. V. Solis, J. Guo, G. Doellgast, A. Ruiz-Garcia, and W. J. Pan. 2007. 'Pharmacokinetics of murine p75-Fc fusion protein and MP6-XT22 anti-murine TNF-alpha mAb in mice', *Journal of Investigative Dermatology Symposium Proceedings*, 12: 52-6.

Fine, N. M., C. S. Crowson, G. Lin, J. K. Oh, H. R. Villarraga, and S. E. Gabriel. 2014. 'Evaluation of myocardial function in patients with rheumatoid arthritis using strain imaging by speckle-tracking echocardiography', *The Annals of the Rheumatic Diseases*, 73: 1833-9.

Fitzsimons, D. P., J. R. Patel, and R. L. Moss. 1998. 'Role of myosin heavy chain composition in kinetics of force development and relaxation in rat myocardium', *The Journal of Physiology*, 513: 171-83.

Francis, Gary S. 1999. 'TNF-α and heart failure', *Circulation*, 99: 3213-14.

Franssen, C., and A. G. Miqueo. 2016. 'The role of titin and extracellular matrix remodelling in heart failure with preserved ejection fraction', *Netherlands Heart Journal*, 24: 259-67.

Franssen, C., S. Chen, A. Unger, H. I. Korkmaz, G. W. De Keulenaer, C. Tschöpe, A. F. Leite-Moreira, R. Musters, H. W. M. Niessen, W. A. Linke, W. J. Paulus, and N. Hamdani. 2016. 'Myocardial microvascular inflammatory endothelial activation in heart failure with preserved ejection fraction', *JACC: Heart Failure*, 4: 312-24.

Fredersdorf, S., C. Thumann, W. H. Zimmermann, R. Vetter, T. Graf, A. Luchner, G. A. Riegger, H. Schunkert, T. Eschenhagen, and J. Weil. 2012. 'Increased myocardial SERCA expression in early type 2 diabetes mellitus is insulin dependent: In vivo and in vitro data', *Cardiovascular Diabetology*, 11: 57.

Fu, Xing, H. Khalil, O. Kanisicak, J. G. Boyer, R. J. Vagnozzi, B. D. Maliken, M. A. Sargent, V. Prasad, I. Valiente-Alandi, B. C. Blaxall, and J. D. Molkentin. 2018. 'Specialized fibroblast differentiated states underlie scar formation in the infarcted mouse heart', *Journal of Clinical Investigation*, 128: 2127-43.

Fukuta, H., and W. C. Little. 2007. 'Contribution of systolic and diastolic abnormalities to heart failure with a normal and a reduced ejection fraction', *Progress in Cardiovascular Diseases*, 49: 229-40.

Ganau, A., R. B. Devereux, M. J. Roman, G. De Simone, T. G. Pickering, P.S. Saba, P. Vargiu, I. Simongini, and J. H. Laragh. 1992. 'Patterns of left ventricular hypertrophy and geometric remodeling in essential hypertension', *Journal of the American College of Cardiology*, 19: 1550-58.

Garbers, C., H. M. Hermanns, F. Schaper, G. Müller-Newen, J. Grötzinger, S. Rose-John, and J. Scheller. 2012. 'Plasticity and cross-talk of interleukin 6-type cytokines', *Cytokine Growth Factor Reviews*, 23: 85-97.

Garbers, C., B. Spudy, S. Aparicio-Siegmund, G. H. Waetzig, J. Sommer, C. Hölscher, S. Rose-John, J. Grötzinger, I. Lorenzen, and J. Scheller. 2013. 'An interleukin-6 receptor-dependent molecularswitch mediates signal transduction of the IL-27 cytokine subunit p28 (IL-30) via a gp130 proteinreceptor homodimer', *Journal of Biological Chemistry*, 288: 4346-54.

Ge, Z., A. Li, J. McNamara, C. Dos Remedios, and S. Lal. 2019. 'Pathogenesis and pathophysiology of heart failure with reduced ejection fraction: translation to human studies', *Heart Failure Reviews*, 24: 743-58.

Gerassimou, C., A. Kotanidou, Z. Zhou, D. C. Simoes, C. Roussos, and A. Papapetropoulos. 2007. 'Regulation of the expression of soluble guanylyl cyclase by reactive oxygen species', *British Journal of Pharmacology*, 150: 1084-91.

Gergs, U., T. Jahn, F. Werner, C. Köhler, F. Köpp, C. Großmann, and J. Neumann. 2019. 'Overexpression of protein phosphatase 5 in the mouse heart: Reduced contractility but increased stress tolerance – Two sides of the same coin?', *PLoS ONE*, 14: e0221289.

Ghosh, M., H. Wang, and J. R. McNeill. 2004. 'Role of oxidative stress and nitric oxide in regulation of spontaneous tone in aorta of DOCA-salt hypertensive rats', *British Journal of Pharmacology*, 141: 562-73.

Glezeva, N., and J. A. Baugh. 2014. 'Role of inflammation in the pathogenesis of heart failure with preserved ejection fraction and its potential as a therapeutic target', *Heart Failure Reviews*, 19: 681-94.

Gloss, B., S. Villegas, F. J Villarreal, A. Moriscot, and W. H. Dillmann. 2000. 'Thyroid hormone-induced stimulation of the sarcoplasmic reticulum Ca^{2+} ATPase gene is inhibited by LIF and IL-6', *American Journal of Physiology-Endocrinology and Metabolism*, 278: E738-E43.

Golden, T., M.Swingle, and R. E. Honkanen. 2008. 'The role of serine/threonine protein phosphatase type 5 (PP5) in the regulation of stress-induced signaling networks and cancer', *Cancer and Metastasis Reviews*, 27: 169-78.

Goldsmith, E. C., A. D. Bradshaw, and F. G. Spinale. 2013. 'Cellular mechanisms of tissue fibrosis. 2. Contributory pathways leading to myocardial fibrosis: moving beyond collagen expression', *American Journal of Cellular Physiology*, 304: C393-402.

Gong, K. Z., G. Song, J. P. Spiers, E. J. Kelso, and Z. G. Zhang. 2007. 'Activation of immune and inflammatory systems in chronic heart failure: novel therapeutic approaches', *International Journal of Clinical Practice*, 61: 611-21.

Gonzalez-Santamaria, J., M. Villalba, O. Busnadiego, M. M. Lopez-Olaneta, P. Sandoval, J. Snabel, M. Lopez-Cabrera, J. T. Erler, R. Hanemaaijer, E. Lara-Pezzi, and F. Rodriguez-Pascual. 2016. 'Matrix cross-linking lysyl oxidases are induced in response to myocardial infarction and promote cardiac dysfunction', *Cardiovascular Research*, 109: 67-78.

GonzalezJuanatey, C. 2004. 'Echocardiographic and Doppler findings in long-term treated rheumatoid arthritis patients without clinically evident cardiovascular disease', *Seminars in Arthritis and Rheumatism*, 33: 231-38.

Gu, J., F. Zhao, Y. Wang, J. Gao, X. Wang, J. Xue, and H. Zhou. 2015. 'The molecular mechanism of diastolic heart failure', *Integrative Medicine International*, 2: 143-48.

Gu, ., H. Lee, T. Sorsa, S. R. Simon, and L. M. Golub. 2010. 'Doxycyline inhibits mononuclear cell-mediated connective tissue breakdown', *FEMS Immunology & Medical Microbiology*, 58: 218-25.

Gunnett, C. A., D. D. Lund, A. K. McDowell, F. M. Faraci, and D. D. Heistad. 2005. 'Mechanisms of inducible nitric oxide synthase–mediated vascular dysfunction', *Arteriosclerosis, Thrombosis, and Vascular Biology*, 25: 1617-22.

Hajnóczky, György, Erika Davies, and Muniswamy Madesh. 2003. 'Calcium signaling and apoptosis', *Biochemical and Biophysical Research Communications*, 304: 445-54.

Hamdani, N., S. Costantino, A. Mügge, D. Lebeche, C. Tschöpe, T. Thum, and F. Paneni. 2021. 'Leveraging clinical epigenetics in heart failure with preserved ejection fraction: a call for individualized therapies', *European Heart Journal*, 42: 1940-58.

Hamdani, N., M. Herwig, and W. A. Linke. 2017. 'Tampering with springs: phosphorylation of titin affecting the mechanical function of cardiomyocytes', *Biophysical Reviews*, 9: 225-37.

Hamdy, A. M. 2007. 'Use of strain and tissue velocity imaging for early detection of regional myocardial dysfunction in patients with beta thalassemia', *European Journal of Echocardiography*, 8: 102-9.

Hanna, A., and N. G. Frangogiannis. 2020. 'Inflammatory cytokines and chemokines as therapeutic targets in heart failure', *Cardiovascular Drugs and Therapy*, 34: 849-63.

Hare, J. M. 2001. 'Oxidative stress and apoptosis in heart failure progression', *Circulation Research*, 89: 198-200.

Hartman, M. H. T., I. Vreeswijk-Baudoin, H. E. Groot, K. W. A. Van De Kolk, R. A. De Boer, I. M. Leach, R. Vliegenthart, H.H. W. Sillje, and P. Van Der Harst. 2016. 'Inhibition of Interleukin-6 receptor in a murine model of myocardial ischemia-reperfusion', *PLoS ONE*, 11: e0167195.

Hashizume, M., S. Tan, J. Takano, K. Ohsawa, I. Hasada, A. Hanasaki, I. Ito, M. Mihara, and K. Nishida. 2015. 'Tocilizumab, a humanized anti-IL-6R antibody, as an emerging therapeutic option for rheumatoid arthritis: molecular and cellular mechanistic insights', *International Reviews of Immunology*, 34: 265-79.

Hawkins, N. M., M. C. Petrie, P. S. Jhund, G. W. Chalmers, F. G. Dunn, and J. J. V. McMurray. 2009. 'Heart failure and chronic obstructive pulmonary disease: diagnostic pitfalls and epidemiology', *European Journal of Heart Failure*, 11: 130-39.

Hedayat, M., M. J. Mahmoudi, N. R. Rose, and N. Rezaei. 2010. 'Proinflammatory cytokines in heart failure: double-edged swords', *Heart Failure Reviews*, 15: 543-62.

Heidt, T., G. Courties, P. Dutta, H. B. Sager, M. Sebas, Y. Iwamoto, Y. Sun, N. Da Silva, P. Panizzi, A. M. van der Laan, F. K. Swirski, R. Weissleder, and M. Nahrendorf. 2014. 'Differential contribution of monocytes to heart macrophages in steady-state and after myocardial infarction', *Circulation Research*, 115: 284-95.

Heinonen, I., O. Sorop, B. M. Van Dalen, R. C. I. Wüst, J. Van De Wouw, V. J. De Beer, Y. Octavia, R. W. B. Van Duin, Y. Hoogstrate, L. Blonden, M. Alkio, K. Anttila, A. Stubbs, J. Van Der Velden, D. Merkus, and D. J. Duncker. 2020. 'Cellular, mitochondrial and molecular alterations associate with early left ventricular diastolic dysfunction in a porcine model of diabetic metabolic derangement', *Scientific Reports*, 10.

Herwig, M., D. Kolijn, M. Lódi, S. Hölper, Á. Kovács, Z. Papp, K. Jaquet, P. Haldenwang, C. D. Remedios, P. H. Reusch, A. Mügge, M. Krüger, J. Fielitz, W. A. Linke, and N. Hamdani. 2020. 'Modulation of titin-based stiffness in hypertrophic cardiomyopathy via protein kinase D', *Frontiers in Physiology*, 11.

Heymans, S., E. Hirsch, S. D. Anker, P. Aukrust, J. Balligand, J. W. Cohen-Tervaert, H. Drexler, G. Filippatos, S. B. Felix, L. Gullestad, D.Hilfiker-Kleiner, S. Janssens, R. Latini, G. Neubauer, W. J. Paulus, B. Pieske, P. Ponikowski, B. Schroen, H. Schultheiss, C. Tschöpe, M. Van Bilsen, F. Zannad, J. McMurray, and A. M. Shah. 2009. 'Inflammation as a therapeutic target in heart failure? A scientific statement from the Translational Research Committee of the Heart Failure Association of the European Society of Cardiology', *European Journal of Heart Failure*, 11: 119-29.

Heymans, S., F. Lupu, S. Terclavers, B.Vanwetswinkel, J. Herbert, A. Baker, D. Collen, P. Carmeliet, and L. Moons. 2005. 'Loss or inhibition of UPA or MMP-9 attenuates LV remodeling and dysfunction after acute pressure overload in mice', *The American Journal of Pathology*, 166: 15-25.

Hiebert, J. B., J. Vacek, Z. Shah, F. Rahman, and J. D. Pierce. 2019. 'Use of speckle tracking to assess heart failure with preserved ejection fraction', *Journal of Cardiology*, 74: 397-402.

Hirota, H., K. Yoshida, T. Kishimoto, and T. Taga. 1995. 'Continuous activation of gp130, a signal-transducing receptor component for interleukin 6-related cytokines, causes myocardial hypertrophy in mice', *Proceedings of the National Academy of Sciences*, 92: 4862-66.

Hogg, K., K. Swedberg, and J. McMurray. 2004. 'Heart failure with preserved left ventricular systolic function; epidemiology, clinical characteristics, and prognosis', *Journal of American College Cardiology*, 43: 317-27.

Hulsmans, M., H. B. Sager, J. D. Roh, M. Valero-Munoz, N. E. Houstis, Y. Iwamoto, Y. Sun, R. M. Wilson, G. Wojtkiewicz, B. Tricot, M. T. Osborne, J. Hung, C. Vinegoni, K. Naxerova, D. E. Sosnovik, M.

R. Zile, A. D. Bradshaw, R. Liao, A. Tawakol, R. Weissleder, A. Rosenzweig, F. K. Swirski, F. Sam, and M. Nahrendorf. 2018. 'Cardiac macrophages promote diastolic dysfunction', *Journal of Experimental Medicine*, 215: 423-40.

Husse, B., W. Briest, L. Homagk, G. Isenberg, and M. Gekle. 2007. 'Cyclical mechanical stretch modulates expression of collagen I and collagen III by PKC and tyrosine kinase in cardiac fibroblasts', *American Journal of Physiology-Regulatory, Integrative and Comparative Physiology*, 293: R1898-907.

Jasemian, Y., P. Svendsen, B. Deleuran, and F. Dagnaes-Hansen. 2011. 'Refinement of the collagen induced arthritis model in rats by infrared thermography', *Journal of Advances in Medicine and Medical Research*, 22: 469-77.

Jozwiak, M., A. C. Meli, J. Melka, M. Rienzo, A. d'Anglemont de Tassigny, N. Saint, A. Bizé, L. Sambin, V. Scheuermann, O. Cazorla, L. Hittinger, A. Berdeaux, J. B. Su, B. Bouhemad, A. Lacampagne, and B. Ghaleb. 2019. 'Concomitant systolic and diastolic alterations during chronic hypertension in pig', *Journal of Molecular Cellular Cardiology*, 131: 155-63.

Kaminski, K. A., E. Oledzka, K. Bialobrzewska, M Kozuch, W. J Musial, and M. M Winnicka. 2007. 'The effects of moderate physical exercise on cardiac hypertrophy in interleukin 6 deficient mice', *Advances in Medical Science*, 52: 164-68.

Kang, Y. H., J. S. Kang, and H. M. Shin. 2013. 'Vasodilatory effects of cinnamic acid via the nitric oxide-cGMP-PKG pathway in rat thoracic aorta', *Phytotherapeutic Research*, 27: 205-11.

Kapila, R., and R. P. Mahajan. 2009. 'Diastolic dysfunction', *The Annals of Cardiac Anaesthesia*, 9: 29-33.

Keates, A. K., A. O. Mocumbi, M. Ntsekhe, K. Sliwa, and S. Stewart. 2017. 'Cardiovascular disease in Africa: epidemiological profile and challenges', *Nature Reviews Cardiology*, 14: 273-93.

Kim, C. H, S. G Al-Kindi, B. Jandali, A. D. Askari, M. Zacharias, and G. H. Oliveira. 2017. 'Incidence and risk of heart failure in systemic lupus erythematosus', *Heart*, 103: 227-33.

Kim, G. W., N. R. Lee, R. H. Pi, Y. S. Lim, Y. M. Lee, J. M. Lee, H. S. Jeong, and S. H. Chung. 2015. 'IL-6 inhibitors for treatment of rheumatoid arthritis: past, present, and future', *Archives of Pharmacal Research*, 38: 575-84.

Kim, Nam-Ho, and Peter M. Kang. 2010. 'Apoptosis in cardiovascular diseases: mechanism and clinical implications', *Korean Circulation Journal*, 40: 299.

Kiss, A., F. Erdődi, and B. Lontay. 2019. 'Myosin phosphatase: Unexpected functions of a long-known enzyme', *Biochimica et Biophysica Acta (BBA) - Molecular Cell Research*, 1866: 2-15.

Kleveland, O., G. Kunszt, M. Bratlie, T. Ueland, K. Broch, E. Holte, A. E. Michelsen, B. Bendz, B. H. Amundsen, T. Espevik, S. Aakhus, J. K. Damås, P. Aukrust, R. Wiseth, and L. Gullestad. 2016. 'Effect of a single dose of the interleukin-6 receptor antagonist tocilizumab on inflammation and troponin T release in patients with non-ST-elevation myocardial infarction: a double-blind, randomized, placebo-controlled phase 2 trial', *European Heart Journal*, 37: 2406-13.

Kobara, M., K. Noda, M. Kitamura, A. Okamoto, T. Shiraishi, H. Toba, H. Matsubara, and T. Nakata. 2010. 'Antibody against interleukin-6 receptor attenuates left ventricular remodelling after myocardial infarction in mice', *Cardiovascular Research*, 87: 424-30.

Kobayashi, H., Y. Kobayashi, J. T Giles, K. Yoneyama, Y. Nakajima, and M. Takei. 2014. 'Tocilizumab treatment increases left ventricular ejection fraction and decreases left ventricular mass index in patients with rheumatoid arthritis without cardiac symptoms: assessed using 3.0 tesla cardiac magnetic resonance imaging', *The Journal of Rheumatology*, 41: 1916-21.

Kobayashi, Y., H. Kobayashi, J. T. Giles, M. Hirano, Y. Nakajima, and M. Takei. 2016. 'Association of tocilizumab treatment with changes in measures of regional left ventricular function in rheumatoid arthritis, as assessed by cardiac magnetic resonance imaging', *International Journal of Rheumatic Diseases*, 19: 1169-74.

Kong, D, YR Kim, MR Kim, JH Jang, and S Lee. 2018. 'Emerging Roles of Vascular Cell Adhesion Molecule-1 (VCAM-1) in Immunological Disorders and Cancer', *International Journal of Molecular Sciences*, 19: 1057.

Kong, P., P. Christia, and N. G. Frangogiannis. 2014. 'The pathogenesis of cardiac fibrosis', *Cellular and Molecular Life Sciences*, 71: 549-74.

Koser, F., C. Loescher, and W. A. Linke. 2019. 'Posttranslational modifications of titin from cardiac muscle: how, where, and what for?', *The FEBS Journal*, 286: 2240-60.

Kosmas, C. E., D. Silverio, A. Sourlas, P. D. Montan, E. Guzman, and M. J. Garcia. 2019. 'Anti-inflammatory therapy for cardiovascular disease', *Annual Translational Medicine*, 7: 147.

Krijnen P. A. J., R. Nijmeijer, C. J. L. M. Meijer, C. A. Visser , C. E. Hack & H. W. N. Niessen. 2002. 'Apoptosis in myocardial ischaemia and infarction', *Journal of Clinical Pathology*, 55: 801-11.

Krown, K. A., M. T. Page, C. Nguyen, D. Zechner, V. Gutierrez, K. L. Comstock, C. C. Glembotski, P. J. Quintana, and R. A. Sabbadini. 1996. 'Tumor necrosis factor alpha-induced apoptosis in cardiac myocytes. Involvement of the sphingolipid signaling cascade in cardiac cell death', *Journal of Clinical Investigation*, 98: 2854-65.

Krum, H., M. Elsik, H. G. Schneider, A. Ptaszynska, M. Black, P. E. Carson, M. Komajda, B. M. Massie, R. S. McKelvie, J. J. McMurray, M. R. Zile, and I. S. Anand. 2011. 'Relation of peripheral collagen markers to death and hospitalization in patients with heart failure and preserved ejection fraction: results of the I-PRESERVE collagen substudy', *Circulation Heart Failure*, 4: 561-8.

Krysiak, J., A. Unger, L. Beckendorf, N. Hamdani, M. Von Frieling-Salewsky, M. M. Redfield, C. G. Dos Remedios, F. Sheikh, U. Gergs, P. Boknik, and W. A. Linke. 2018. 'Protein phosphatase 5 regulates titin phosphorylation and function at a sarcomere-associated mechanosensor complex in cardiomyocytes', *Nature Communications*, 9.

Kubota, T., M. Miyagishima, C. S. Frye, S. M. Alber, G. S. Bounoutas, T. Kadokami, S. C. Watkins, Charles F. McTiernan, and Arthur M. Feldman. 2001. 'Overexpression of tumor necrosis factor- α activates both anti- and pro-apoptotic pathways in the myocardium', *Journal of Molecular and Cellular Cardiology*, 33: 1331-44.

Kular, J. K., S. Basu, and R. I. Sharma. 2014. 'The extracellular matrix: Structure, composition, age-related differences, tools for analysis and applications for tissue engineering', *Journal of Tissue Engineering*, 5: 204173141455711.

Kuwahara, F., H. Kai, K. Tokuda, M. Kai, A. Takeshita, K. Egashira, and T. Imaizumi. 2002. 'Transforming growth factor-β function blocking prevents myocardial fibrosis and diastolic dysfunction in pressure-overloaded rats', *Circulation*, 106: 130-35.

Lacalzada, J., A. Duque, A. De La Rosa, A. Barragan, M. Manuela, E. Arroyo, A. Laynez, and I. Laynez. 2011. 'Evaluation of left ventricular diastolic function by echocardiography.' in *InTech*.

Lachtermacher, S., B. L. B. Esporcatte, F. Montalvão, P. C. Costa, D. C. Rodrigues, L. Belem, A. Rabischoffisky, H. C. C. Faria Neto, R. Vasconcellos, S. Iacobas, D. A. Iacobas, H. F. R. Dohmann, D. C. Spray, R. C. S. Goldenberg, and A. C. Campos-De-Carvalho. 2010. 'Cardiac gene expression and systemic cytokine profile are complementary in a murine model of post-ischemic heart failure', *Brazilian Journal of Medical and Biological Research*, 43: 377-89.

Lai, N. C., M. Hua Gao, E. Tang, R. Tang, T. Guo, N. D. Dalton, A. Deng, and T. Tang. 2012. 'Pressure overload-induced cardiac remodeling and dysfunction in the absence of interleukin 6 in mice', *Laboratory Investigation*, 92: 1518-26.

Lang, R. M., L. P. Badano, V. Mor-Avi, J. Afilalo, A. Armstrong, L. Ernande, F. A. Flachskampf, E. Foster, S. A. Goldstein, T. Kuznetsova, P. Lancellotti, D. Muraru, M. H. Picard, E. R. Rietzschel, L. Rudski, K. T. Spencer, W. Tsang, and J. Voigt. 2015. 'Recommendations for cardiac chamber quantification by echocardiography in adults: An update from the American Society of Echocardiography and the European Association of Cardiovascular Imaging', *Journal of the American Society of Echocardiography*, 28: 1-39.e14.

Le Roux, R., L. Mokotedi, S. Fourie, A. Manilall, S. Gunter, and A. M. E. Millen. 2022. 'TNF-α inhibitors reduce inflammation-induced concentric remodelling, but not diastolic dysfunction in collagen-induced arthritis', *Clinical and Experimental Rheumatology*, 40: 24–32.

Leitman, M., P. Lysyansky, S. Sidenko, V. Shir, E. Peleg, M. Binenbaum, E. Kaluski, R. Krakover, and Z. Vered. 2004. 'Two-dimensional strain-a novel software for real-time quantitative echocardiographic assessment of myocardial function', *Journal of American Society for Echocardiography*, 17: 1021-9.

Lewinter, M. M., and H. L. Granzier. 2014. 'Cardiac titin and heart disease', *Journal of Cardiovascular Pharmacology*, 63: 207-12.

Lewinter, M. M., and M. Meyer. 2013. 'Mechanisms of diastolic dysfunction in heart failure with a preserved ejection fraction', *Circulation: Heart Failure*, 6: 1112-15.

Lewis, G. A., E. B. Schelbert, S. G. Williams, C. Cunnington, F. Ahmed, T. A. McDonagh, and C. A. Miller. 2017. 'Biological phenotypes of heart failure with preserved ejection fraction', *Journal of the American College of Cardiology*, 70: 2186-200.

Li, Q., Q. Yu, R. Na, and B. Liu. 2017. 'Etanercept protects rat cardiomyocytes against hypertrophy by regulating inflammatory cytokines secretion and cell apoptosis', *Brazilian Journal of Medical and Biological Research*, 50.

Li, Y., C. F. McTiernan, and A. M. Feldman. 2000. 'Interplay of matrix metalloproteinases, tissue inhibitors of metalloproteinases and their regulators in cardiac matrix remodeling', *Cardiovascular Research*, 46: 214-24.

Liang, K. P., E. Myasoedova, C. S. Crowson, J. M. Davis, V. L. Roger, B. L. Karon, D. D. Borgeson, T. M. Therneau, R. J. Rodeheffer, and S. E. Gabriel. 2010. 'Increased prevalence of diastolic dysfunction in rheumatoid arthritis', *The Annals of the Rheumatic Diseases*, 69: 1665-70.

Libby, P. 2002. 'Inflammation in artherosclerosis', *Nature*, 420: 868-874.

Lipskaia, L., E. R. Chemaly, L. Hadri, A. M. Lompre, and R. J. Hajjar. 2010. 'Sarcoplasmic reticulum Ca(2+) ATPase as a therapeutic target for heart failure', *Expert Opin Biol Ther*, 10: 29-41.

Liu, P., M. Sun, and S. Sader. 2006. 'Matrix metalloproteinases in cardiovascular disease', *Canadian Journal of Cardiology*, 22: 25B-30B.

Livak, K. J., and T. D. Schmittgen. 2001. 'Analysis of relative gene expression data using real-time quantitative PCR and the 2−ΔΔCT Method', *Methods*, 25: 402-08.

Lo Gullo, A., J. Rodríguez-Carrio, C. O. Aragona, G. Dattilo, C. Zito, A. Suárez, S. Loddo, M. Atteritano, A. Saitta, and G. Mandraffino. 2018. 'Subclinical impairment of myocardial and endothelial functionality in very early psoriatic and rheumatoid arthritis patients: Association with vitamin D and inflammation', *Atherosclerosis*, 271: 214-22.

Lompré, A., R. J. Hajjar, S. E. Harding, E. G. Kranias, M. J. Lohse, and A. R. Marks. 2010. 'Ca2+cycling and new therapeutic approaches for heart failure ', *Circulation*, 121: 822-30.

Lopez, B., R. Querejeta, A. Gonzalez, M. Larman, and J. Diez. 2012. 'Collagen cross-linking but not collagen amount associates with elevated filling pressures in hypertensive patients with stage C heart failure: potential role of lysyl oxidase', *Hypertension*, 60: 677-83.

Luiking, Y. C., M. P. Engelen, and N. E. Deutz. 2010. 'Regulation of nitric oxide production in health and disease', *Current Opinion in Clinical Nutrition and Metabolic Care*, 13: 97-104.

Ma, X., and S. Xu. 2013. 'TNF inhibitor therapy for rheumatoid arthritis', *Biomed Rep*, 1: 177-84.

MacLennan, D. H, and E. G Kranias. 2003. 'Phospholamban: a crucial regulator of cardiac contractility', *Nature reviews Molecular cell biology*, 4: 566-77.

Malik, A., D. Brito, S. Vaqar, and L. Chhabra. 2022. 'Congestive Heart Failure.' in *StatPearls* (StatPearls Publishing, Copyright © 2022, StatPearls Publishing LLC.: Treasure Island (FL)).

Mann, D. L., B. Bozkurt, G. Torre-Amione, O. Z. Soran, and N. Sivasubramanian. 2008. 'Effect of the soluble TNF-antagonist etanercept on tumor necrosis factor bioactivity and stability', *Clinical and Translational Science*, 1: 142-5.

Maragiannis, D., P. A. Alvarez, M. G. Ghosn, K. Chin, J. J. Hinojosa, J. M. Buergler, D. J. Shah, and S. F. Nagueh. 2018. 'Left ventricular function in patients with hypertrophic cardiomyopathy and its relation to myocardial fibrosis and exercise tolerance', *The International Journal of Cardiovascular Imaging*, 34: 121-29.

Marelli-Berg, F. M., and D. Aksentijevic. 2019. 'Immunometabolic cross-talk in the inflamed heart', *Cell Stress*, 3: 240-66.

Marian, A. J. 2021. 'Molecular Genetic Basis of Hypertrophic Cardiomyopathy', *Circulation Research*, 128: 1533-53.

Massie, B. M., P. E. Carson, J. J. McMurray, M. Komajda, R. McKelvie, M. R. Zile, S. Anderson, M. Donovan, E. Iverson, C. Staiger, and A. Ptaszynska. 2008. 'Irbesartan in patients with heart failure and preserved ejection fraction', *New England Journal of Medicine*, 359: 2456-67.

McKleroy, W., T. H. Lee, and K. Atabai. 2013. 'Always cleave up your mess: targeting collagen degradation to treat tissue fibrosis', *American Journal of Lung, Cellular and Molecular Physiology*, 304: L709-21.

McTiernan, C. F., B. H. Lemster, C. Frye, S. Brooks, A. Combes, and A. M. Feldman. 1997. 'Interleukin-1 beta inhibits phospholamban gene expression in cultured cardiomyocytes', *Circulation Research*, 81: 493-503.

Meléndez, G. C, J. L. McLarty, S. P. Levick, Y. Du, J. S. Janicki, and G. L. Brower. 2010. 'Interleukin 6 mediates myocardial fibrosis, concentric hypertrophy, and diastolic dysfunction in rats', *Hypertension*, 56: 225-31.

Mensah, G., G. Roth, U. Sampson, A. Moran, V. Feigin, M. Forouzanfar, M. Naghavi, and C. Murray. 2015. 'Mortality from cardiovascular diseases in sub-Saharan Africa, 1990–2013: a systematic analysis of data from the Global Burden of Disease Study 2013: cardiovascular topic', *Cardiovascular Journal Of Africa*, 26: S6-S10.

Miao, Lu, and Daret K St Clair. 2009. 'Regulation of superoxide dismutase genes: implications in disease', *Free Radical Biology and Medicine*, 47: 344-56.

Midtbø, H., A. G. Semb, K. Matre, T. K. Kvien, and E. Gerdts. 2017. 'Disease activity is associated with reduced left ventricular systolic myocardial function in patients with rheumatoid arthritis', *The Annals of Rheumatic Diseases*, 76: 371-76.

Mitrovic, V., A. Jovanovic, and S. Lehinant. 2011. 'Soluble guanylate cyclase modulators in heart failure', *Current Heart Failure Reports*, 8: 38-44.

Miyata, S., W. Minobe, M. R. Bristow, and L. A. Leinwand. 2000. 'Myosin heavy chain isoform expression in the failing and nonfailing human heart', *Circulation Research*, 86: 386-90.

Mohammed, S. F., B. A. Borlaug, V. L. Roger, S. A. Mirzoyev, R. J. Rodeheffer, J. A. Chirinos, and M. M. Redfield. 2012. 'Comorbidity and ventricular and vascular structure and function in heart failure with preserved ejection fraction: a community-based study', *Circulatory Heart Failure*, 5: 710-9.

Mokotedi, L., F. S. Michel, C. Mogane, M. Gomes, A. J. Woodiwiss, G. R. Norton, and A. M. E. Millen. 2020. 'Associations of inflammatory markers with impaired left ventricular diastolic and systolic function in collagen-induced arthritis', *PLoS ONE*, 15: e0230657.

Molina, C. E., E. Jacquet, P. Ponien, C. Muñoz-Guijosa, I. Baczkó, L. S. Maier, P. Donzeau-Gouge, D. Dobrev, R. Fischmeister, and A. Garnier. 2018. 'Identification of optimal reference genes for transcriptomic analyses in normal and diseased human heart', *Cardiovascular Research*, 114: 247-58.

Mollmann, H., H. M. Nef, and C. Troidl. 2010. "Turning the right screw': targeting the interleukin-6 receptor to reduce unfavourable tissue remodelling after myocardial infarction', *Cardiovascular Research*, 87: 395-96.

Mor-Avi, V., R. M. Lang, L. P. Badano, M. Belohlavek, N. M. Cardim, G. Derumeaux, M. Galderisi, T. Marwick, S. F. Nagueh, P. P. Sengupta, R. Sicari, O. A. Smiseth, B. Smulevitz, M. Takeuchi, J. D. Thomas, M. Vannan, J. U. Voigt, and J. L. Zamorano. 2011. 'Current and evolving echocardiographic techniques for the quantitative evaluation of cardiac mechanics: ASE/EAE consensus statement on methodology and indications endorsed by the Japanese Society of Echocardiography', *European Journal of Echocardiography*, 12: 167-205.

Most, P., H. Seifert, E. Gao, H. Funakoshi, M. VöLkers, J. Heierhorst, A. Remppis, S. T. Pleger, B. R. Degeorge, A. D. Eckhart, A. M. Feldman, and W. J. Koch. 2006. 'Cardiac S100A1 protein levels determine contractile performance and propensity toward heart failure after myocardial infarction', *Circulation*, 114: 1258-68.

Nagueh, S. F., C. P. Appleton, T. C. Gillebert, P. N. Marino, J. K. Oh, O. A. Smiseth, A. D. Waggoner, F. A. Flachskampf, P. A. Pellikka, and A. Evangelisa. 2008. 'Recommendations for the evaluation of left ventricular diastolic function by echocardiography', *European Journal of Echocardiography*, 10: 165-93.

Nagueh, S. F. 2021. 'Heart failure with preserved ejection fraction: insights into diagnosis and pathophysiology', *Cardiovascular Research*, 117: 999-1014.

Nakao, K., W. Minobe, R. Roden, M. R. Bristow, and L. A. Leinwand. 1997. 'Myosin heavy chain gene expression in human heart failure', *Journal of Clinical Investigation*, 100: 2362-70.

Netea, M. G., F. Balkwill, M. Chonchol, F. Cominelli, M. Y. Donath, E. J. Giamarellos-Bourboulis, D. Golenbock, M.S. Gresnigt, M. T. Heneka, H. M. Hoffman, R. Hotchkiss, L. A. B. Joosten, D. L. Kastner, M. Korte, E. Latz, P. Libby, T. Mandrup-Poulsen, A. Mantovani, K. H. G. Mills, K. L. Nowak, L. A. O'Neill, P. Pickkers, T. Van Der Poll, P. M. Ridker, J. Schalkwijk, D. A. Schwartz, B. Siegmund, C. J. Steer, H. Tilg, Jos W. M. Van Der Meer, F. L. Van De Veerdonk, and C. A. Dinarello. 2017. 'A guiding map for inflammation', *Nature Immunology*, 18: 826-31.

Neumann, J., Peter B., Uwe K., and U. Gergs. 2021. 'The role of PP5 and PP2C in cardiac health and disease', *Cellular Signalling*, 85: 110035.

Nguyen, X., T. Nishimoto, T. Takihara, L. Mlakar, A. D Bradshaw, and C. Feghali-Bostwick. 2021. 'Lysyl oxidase directly contributes to extracellular matrix production and fibrosis in systemic sclerosis', *American Journal of Physiology-Lung Cellular and Molecular Physiology*, 320: L29-L40.

Nishimura, R. A., and A. J. Tajik. 1997. 'Evaluation of diastolicfilling of left ventricle in health and disease: Doppler echocardiography is the clinician's Rosetta Stone', *Journal of the American College of Cardiology*, 30: 8-18.

Omair, M., R. AlBallaa, E. Alqurtas, and W. Al-Habeeb. 2017. 'Heart failure with preserved ejection fraction in rheumatoid arthritis and the role of interleukin-6 blockade', *International Journal of Clinical Rheumatology*, 12: 005-07.

Orrenius, S., B. Zhivotovsky, and P. Nicotera. 2003. 'Regulation of cell death: the calcium–apoptosis link', *Nature Reviews Molecular cell biology*, 4: 552-65.

Packer, Milton. 2020. 'Link between synovial and myocardial inflammation: Conceptual framework to explain the pathogenesis of heart failure with preserved ejection fraction in patients with systemic rheumatic diseases', *Diabetes*, 18: 20.

Pandya, K., H. S. Kim, and O. Smithies. 2006. 'Fibrosis, not cell size, delineates beta-myosin heavy chain reexpression during cardiac hypertrophy and normal aging in vivo', *Proceedings of the National Academy of Sciences*, 103: 16864-69.

Pandya, Kumar, and Oliver Smithies. 2011. 'β-MyHC and cardiac hypertrophy', *Circulation Research*, 109: 609-10.

Panina, Y., A. Germond, S. Masui, and T. M. Watanabe. 2018. 'Validation of common housekeeping genes as reference for qPCR gene expression analysis during iPS reprogramming process', *Scientific Reports*, 8: 12-18.

Páramo, J.A. 2017. 'New mechanisms of vascular fibrosis: Role of lysyl oxidase', *Clínica e Investigación en Arteriosclerosis (English Edition)*, 29: 166-67.

Park, J., and T. H. Marwick. 2011. 'Use and limitations of E/e' to assess left ventricular filling pressure by echocardiography', *Journal of Cardiovascular Ultrasound*, 19: 169.

Park, J., and J. G. Oh. 2013. 'SERCA2a: a prime target for modulation of cardiac contractility during heart failure', *BMB Reports*, 46: 237-43.

Paulus, W. J., and C. Tschöpe. 2013. 'A novel paradigm for heart failure with preserved ejection fraction: comorbidities drive myocardial dysfunction and remodeling through coronary microvascular endothelial inflammation', *Journal of American College Cardiology*, 62: 263-71.

Paulus, W. J., and J. J. van Ballegoij. 2010. 'Treatment of heart failure with normal ejection fraction: an inconvenient truth!', *Journal of American College Cardiology*, 55: 526-37.

Pavlopoulos, H., J. Grapsa, E. Stefanadi, V. Kamperidis, E. Philippou, D. Dawson, and P. Nihoyannopoulos. 2008. 'The evolution of diastolic dysfunction in the hypertensive disease', *European Journal of Echocardiography*, 9: 772-78.

Peoples, J. N., A. Saraf, N. Ghazal, T. T. Pham, and J. Q. Kwong. 2019. 'Mitochondrial dysfunction and oxidative stress in heart disease', *Experimental & Molecular Medicine*, 51: 1-13.

Peters, H., Y. Wang, T. Loof, S. Martini, S. Kron, S. Krämer, and H. H. Neumayer. 2004. 'Expression and activity of soluble guanylate cyclase in injury and repair of anti-thy1 glomerulonephritis', *Kidney International*, 66: 2224-36.

Petersen, M. C., and G. I. Shulman. 2018. 'Mechanisms of insulin action and insulin resistance', *Physiological Reviews*, 98: 2133-223.

Petrie, J. R., T. J. Guzik, and R. M. Touyz. 2018. 'Diabetes, hypertension, and cardiovascular disease: Clinical insights and vascular mechanisms', *Canadian Journal of Cardiology*, 34: 575-84.

Pfaffl M. W, T. Ales, P. Christian and N. P. Tanja. 2004. 'Determination of stable housekeeping genes, differentially regulated target genes and sample integrity: BestKeeper – Excel-based tool using pair-wise correlations', *Biotechnology Letters*, 26: 509-15.

Phan, T. T., K. Abozguia, G. Nallur Shivu, G. Mahadevan, I. Ahmed, L. Williams, G. Dwivedi, K. Patel, P. Steendijk, H. Ashrafian, A. Henning, and M. Frenneaux. 2009. 'Heart failure with preserved ejection fraction is characterized by dynamic impairment of active relaxation and contraction of the left ventricle on exercise and associated with myocardial energy deficiency', *Journal of American College Cardiology*, 54: 402-9.

Pironti, G., A. Bersellini-Farinotti, N. M. Agalave, K. Sandor, T. Fernandez-Zafra, A. Jurczak, L. H. Lund, C. I. Svensson, and D. C. Andersson. 2018. 'Cardiomyopathy, oxidative stress and impaired contractility in a rheumatoid arthritis mouse model', *Heart*, 104: 2026-34.

Porter, K. E., and N. A. Turner. 2009. 'Cardiac fibroblasts: At the heart of myocardial remodeling', *Pharmacology & Therapeutics*, 123: 255-78.

Prabhu, S. D. 2004. 'Cytokine-induced modulation of cardiac function', *Circulation Research*, 95: 1140-53.

Querejeta, R. B. LóPez, A. GonzáLez, E.SáNchez, M. Larman, J. L. M. Ubago, and J. DíEz. 2004. 'Increased collagen type I synthesis in patients with heart failure of hypertensive origin', *Circulation*, 110: 1263-68.

Rastogi, S., E. Sentex, V. Elimban, N. S. Dhalla, and T. Netticadan. 2003. 'Elevated levels of protein phosphatase 1 and phosphatase 2A may contribute to cardiac dysfunction in diabetes', *Biochimica et Biophysica Acta (BBA) - Molecular Basis of Disease*, 1638: 273-77.

Rech, M., A. B. Aizpurua, V. Van Empel, M. Van Bilsen, and B. Schroen. 2018. 'Pathophysiological understanding of HFpEF: microRNAs as part of the puzzle', *Cardiovascular Research*, 114: 782-93.

Redfield, M. M., H. H. Chen, B. A. Borlaug, M. J. Semigran, K.L. Lee, G. Lewis, M. M. Lewinter, J. L. Rouleau, D. A. Bull, D. L. Mann, A. Deswal, L. W. Stevenson, M. M. Givertz, E. O. Ofili, C. M. O'Connor, G. M. Felker, S. R. Goldsmith, B. A. Bart, S. E. McNulty, J. C. Ibarra, G. Lin, J. K. Oh, M. R. Patel, R. J. Kim, R. P. Tracy, E. J. Velazquez, K. J. Anstrom, A. F. Hernandez, A. M. Mascette and E. Braunwald. 'Effect of Phosphodiesterase-5 inhibition on exercise capacity and clinical status in heart failure with preserved ejection fraction', *Journal of the American Medical Association*, 309: 1268.

Redfield, M. M., S. J. Jacobsen, J. C. Burnett, D. W. Mahoney, K. R. Bailey, and R. J. Rodeheffer. 2003. 'Burden of systolic and diastolic ventricular dysfunction in the community', *Journal of the American Medical Association*, 289: 194.

Reina-Couto, M., P. Pereira-Terra, J. Quelhas-Santos, C. Silva-Pereira, A. Albino-Teixeira, and T. Sousa. 2021. 'Inflammation in human heart failure: Major mediators and therapeutic targets', *Frontiers in Physiology*, 12.

Remppis, A., T. Greten, B. W. Schäfer, P. Hunziker, P. Erne, H. A. Katus, and C.W. Heizmann. 1996. 'Altered expression of the Ca2+-binding protein S100A1 in human cardiomyopathy', *Biochimica et Biophysica Acta (BBA) - Molecular Cell Research*, 1313: 253-57.

Ristagno, G., F. Fumagalli, B. Bottazzi, A. Mantovani, D. Olivari, D. Novelli, and R. Latini. 2019. 'Pentraxin 3 in cardiovascular disease', *Frontiers in Immunology*, 10.

Ritterhoff, J., and P. Most. 2012. 'Targeting S100A1 in heart failure', *Gene Therapy*, 19: 613-21.

Roberge, S., J. Roussel, D. C Andersson, A. C Meli, B. Vidal, F. Blandel, J. T Lanner, J. Le Guennec, A. Katz, and H. Westerblad. 2014. 'TNF-α-mediated caspase-8 activation induces ROS production and TRPM2 activation in adult ventricular myocytes', *Cardiovascular Research*, 103: 90-99.

Robertson, M., J. Liversidge, J. V. Forrester, and A. D. Dick. 2003. 'Neutralizing tumor necrosis factor-α activity suppresses activation of infiltrating macrophages in experimental autoimmune uveoretinitis', *Investigative Opthalmology & Visual Science*, 44: 3034.

Rodriguez, C., J. Martinez-Gonzalez, B. Raposo, J. F. Alcudia, A. Guadall, and L. Badimon. 2008. 'Regulation of lysyl oxidase in vascular cells: lysyl oxidase as a new player in cardiovascular diseases', *Cardiovascular Research*, 79: 7-13.

Rogers, N. M., F. Seeger, E. D. Garcin, D. D. Roberts, and J. S. Isenberg. 2014. 'Regulation of soluble guanylate cyclase by matricellular thrombospondins: implications for blood flow', 5.

Rohde, D., J. Ritterhoff, M. Voelkers, H. A. Katus, T. G. Parker, and P. Most. 2010. 'S100A1: A multifaceted therapeutic target in cardiovascular disease', *Journal of Cardiovascular Translational Research*, 3: 525-37.

Rose-John, S. 2012. 'IL-6 trans-signaling via the soluble IL-6 Receptor: Importance for the pro-inflammatory activities of IL-6', *International Journal of Biological Sciences*, 8: 1237-47.

Rose-John, S. 2018. 'Interleukin-6 family cytokines', *Cold Spring Harbor Perspectives in Biology*, 10: a028415.

Ross, R., and J. A., Glomset. 1976. 'The pathogenesis of atherosclerosis (first of two parts) ', *New England Journal of Medicine*, 295: 369–377.

Rudominer, R. L., M. J. Roman, R. B. Devereux, S. A. Paget, J. E. Schwartz, M. D. Lockshin, M. K. Crow, L. Sammaritano, D. M. Levine, and J. E. Salmon. 2009. 'Independent association of rheumatoid arthritis with increased left ventricular mass but not with reduced ejection fraction', *Arthritis & Rheumatism*, 60: 22-29.

Salcan, S., S. Bongardt, D. M.o Barbosa, I. R. Efimov, T. Rassaf, M. Krüger, and S. Kötter. 2020. 'Elastic titin properties and protein quality control in the aging heart', *Biochimica et Biophysica Acta (BBA) - Molecular Cell Research*, 1867: 118532.

Samak, M., J. Fatullayev, A. Sabashnikov, M. Zeriouh, B. Schmack, M. Farag, A. Popov, Pascal M. Dohmen, Y. Choi, T. Wahlers, and A. Weymann. 2016. 'Cardiac hypertrophy: An introduction to molecular and cellular basis', *Medical Science Monitor Basic Research*, 22: 75-79.

Sanghera, C., L. Man Wong, M. Panahi, A. Sintou, M. Hasham, and S. Sattler. 2019. 'Cardiac phenotype in mouse models of systemic autoimmunity', *Disease Models & Mechanisms*, 12: dmm036947.

Savvatis, K., I. Müller, M. Fröhlich, K. Pappritz, C. Zietsch, N. Hamdani, K. Grote, B. Schieffer, K. Klingel, S. Van Linthout, W. A. Linke, H. Schultheiss, and C. Tschöpe. 2014. 'Interleukin-6 receptor inhibition modulates the immune reaction and restores titin phosphorylation in experimental myocarditis', *Basic Research in Cardiology*, 109.

Schumacher, S. M., and S. V. N. Prasad. 2018. 'Tumor necrosis factor-α in heart failure: an updated review', *Current Cardiology Reports*, 20.

Shah, A. M., B. Claggett, N. K. Sweitzer, S. J. Shah, I. S. Anand, E. O'Meara, A. S. Desai, J. F. Heitner, G. Li, J. Fang, J. Rouleau, M. R. Zile, V. Markov, V. Ryabov, G. Reis, S. F. Assmann, S. M. McKinlay, B. Pitt, M. A. Pfeffer, and S. D. Solomon. 2014. 'Cardiac structure and function and prognosis in heart failure with preserved ejection fraction: findings from the echocardiographic study of the Treatment of Preserved Cardiac Function Heart Failure with an Aldosterone Antagonist (TOPCAT) Trial', *Circulation Heart Failure*, 7: 740-51.

Sharifov, O. F., C. G. Schiros, I. Aban, T. S. Denney, and H. Gupta. 2016. 'Diagnostic accuracy of Tissue Doppler index E/e' for evaluating left ventricular filling pressure and diastolic dysfunction/heart failure with preserved ejection fraction: A systematic review and meta-analysis', *Journal of American Heart Association*, 5.

Sheppard, M., F. Laskou, P. P. Stapleton, S. Hadavi, and B. Dasgupta. 2017. 'Tocilizumab (Actemra)', *Human Vaccines & Immunotherapeutics*, 13: 1972-88.

Shiraki, A., N. Kotooka, H. Komoda, T. Hirase, J. Oyama, and K. Node. 2016. 'Pentraxin-3 regulates the inflammatory activity of macrophages', *Biochemical and Biophysics Reports* 5: 290-95.

Simmonds, S. J., I. Cuijpers, S. Heymans, and E. A. V. Jones. 2020. 'Cellular and molecular differences between HFpEF and HFrEF: A step ahead in an improved pathological understanding', *Cells*, 9: 242.

Sitia, S., L. Tomasoni, F. Atzeni, G. Ambrosio, C. Cordiano, A. Catapano, S. Tramontana, F. Perticone, P. Naccarato, P. Camici, E. Picano, L. Cortigiani, M. Bevilacqua, L. Milazzo, D. Cusi, C. Barlassina, P. Sarzi-Puttini, and M. Turiel. 2010. 'From endothelial dysfunction to atherosclerosis', *Autoimmunity Reviews*, 9: 830-4.

Sivasubramanian, N., M. L. Coker, K. M. Kurrelmeyer, W. R. Maclellan, F. J. Demayo, F. G. Spinale, and D. L. Mann. 2001. 'Left ventricular remodeling in transgenic mice with cardiac restricted overexpression of tumor necrosis factor', *Circulation*, 104: 826-31.

Siwik, D. A, D. Chang, and W. S. Colucci. 2000. 'Interleukin-1β and tumor necrosis factor-α decrease collagen synthesis and increase matrix metalloproteinase activity in cardiac fibroblasts in vitro', *Circulation Research*, 86: 1259-65.

Skioldebrand, E., A. Lundqvist, U. Bjorklund, M. Sandstedt, A. Lindahl, E. Hansson, and L. M. Hulten. 2017. 'Inflammatory activation of human cardiac fibroblasts leads to altered calcium signaling, decreased connexin 43 expression and increased glutamate secretion', *Heliyon*, 3: e00406.

Smiseth, Otto A. 2017. 'Evaluation of left ventricular diastolic function: state of the art after 35 years with Doppler assessment', *Journal of Echocardiography*.

Sorop, O., I. Heinonen, M. Van Kranenburg, J. Van De Wouw, V. J. De Beer, I.T. N. Nguyen, Y. Octavia, R. W. B. Van Duin, K. Stam, R. Van Geuns, P. A. Wielopolski, G. P. Krestin, A. H. Van Den Meiracker, R. Verjans, M. Van Bilsen, A. H. J. Danser, W. J. Paulus, C. Cheng, W. A. Linke, J. A. Joles, M. C. Verhaar, J. Van Der Velden, D. Merkus, and D. J. Duncker. 2018. 'Multiple common comorbidities produce left ventricular diastolic dysfunction associated with coronary microvascular dysfunction, oxidative stress, and myocardial stiffening', *Cardiovascular Research*, 114: 954-64.

St-Pierre, J., J. Grégoire, and C. Vaillancourt. 2017. 'A simple method to assess group difference in RT-qPCR reference gene selection using GeNorm: The case of the placental sex', *Scientific Reports*, 7.

Stokke, T. M., N. E. Hasselberg, M. K. Smedsrud, S. I. Sarvari, K. H. Haugaa, O. A. Smiseth, T. Edvardsen, and E. W. Remme. 2017. 'Geometry as a Confounder When Assessing Ventricular Systolic Function: Comparison Between Ejection Fraction and Strain', *Journal of American College Cardiology*, 70: 942-54.

Strassheim, D. E. C. Dempsey, E. Gerasimovskaya, K. Stenmark, and V. Karoor. 2019. 'Role of inflammatory cell subtypes in heart failure', *Journal of Immunology Research*, 2019: 1-9.

Stuart, C. A., W. L. Stone, M. E. A. Howell, M. F. Brannon, H. K. Hall, A. L. Gibson, and M. H. Stone. 2016. 'Myosin content of individual human muscle fibers isolated by laser capture microdissection', *American Journal of Physiology-Cell Physiology*, 310: C381-C89.

Sutanto, H., A. Lyon, J. Lumens, U. Schotten, D. Dobrev, and J. Heijman. 2020. 'Cardiomyocyte calcium handling in health and disease: Insights from in vitro and in silico studies', *Progress in Biophysics and Molecular Biology*, 157: 54-75.

Suthahar, N., W. C. Meijers, H. H. W. Silljé, and R. A. De Boer. 2017. 'From inflammation to fibrosis—molecular and cellular mechanisms of myocardial tissue remodelling and perspectives on differential treatment opportunities', *Current Heart Failure Reports*, 14: 235-50.

Szmitko, P. E., C. H. Wang, R. D. Weisel, J. R. de Almeida, T. J. Anderson, and S. Verma. 2003. 'New markers of inflammation and endothelial cell activation: Part I', *Circulation*, 108: 1917-23.

Tanaka, T, T Kanda, T Takahashi, S Saegusa, J Moriya, and M Kurabayashi. 2004. 'Interleukin-6-induced reciprocal expression of SERCA and natriuretic peptides mRNA in cultured rat ventricular myocytes', *Journal of international Medical Research*, 32: 57-61.

Tang, Peizhe, Shengjun Ma, Mingfeng Dong, Jiantang Wang, Shoudong Chai, Tao Liu, and Jindong Li. 2018. 'Effect of interleukin-6 on myocardial regeneration in mice after cardiac injury', *Biomedicine & Pharmacotherapy*, 106: 303-08.

Teichholz, L. E., T. Kreulen, M. V. Herman, and R. Gorlin. 1976. 'Problems in echocardiographic volume determinations: echocardiographic-angiographic correlations in the presence of absence of asynergy', *American Journal of Cardiology*, 37: 7-11.

Teringova, E., and P. Tousek. 2017. 'Apoptosis in ischemic heart disease', *Journal of Translational Medicine*, 15.

Torre-Amione, G., S. Kapadia, C. Benedict, H. Oral, J. B. Young, and D. L. Mann. 1996. 'Proinflammatory cytokine levels in patients with depressed left ventricular ejection fraction: a report from the Studies of Left Ventricular Dysfunction (SOLVD)', *Journal of American College Cardiology*, 27: 1201-6.

Totoson, P., K. Maguin-Gaté, M. Nappey, D. Wendling, and C. Demougeot. 2016. 'Endothelial dysfunction in rheumatoid arthritis: Mechanistic insights and correlation with circulating markers of systemic inflammation', *PLoS One*, 11: e0146744.

Travers, J. G., F. A. Kamal, J. Robbins, K. E. Yutzey, and B. C. Blaxall. 2016. 'Cardiac fibrosis: The fibroblast awakens', *Circulation Research*, 118: 1021-40.

Tsai, C. T., C. K. Wu, J. K. Lee, S. N. Chang, Y. M. Kuo, Y. C. Wang, L. P. Lai, F. T. Chiang, J. J. Hwang, and J. L. Lin. 2015. 'TNF-α down-regulates sarcoplasmic reticulum Ca^{2+} ATPase expression and leads to left ventricular diastolic dysfunction through binding of NF-kB to promoter response element', *Cardiovascular Research*, 105: 318-29.

Upadhya, B., M. J. Haykowsky, and D. W. Kitzman. 2018. 'Therapy for heart failure with preserved ejection fraction: current status, unique challenges, and future directions', *Heart Failure Reviews*, 23: 609-29.

van Heerebeek, L, and W. J. Paulus. 2014. 'Impact of comorbidities on myocardial remodeling and dysfunction in heart failure with preserved ejection fraction. *SOJ Pharmacological Sciences*, 1 (2), 20'.

Van Linthout, S., and C. Tschöpe. 2017. 'Inflammation - cause or consequence of heart failure or both?', *Current Heart Failure Reports*, 14: 251-65.

Vandesompele J, De Preter K, Pattyn F, Poppe B, Van Roy N, De Paepe A, Speleman F. 2002. 'Accurate normalization of real-time quantitative RT-PCR data by geometric averaging of multiple internal control genes', *Genome Biology* 3: 0034.1–34.11

Villar, A. V., M. Cobo, M. Llano, C. Montalvo, F. Gonzalez-Vilchez, R. Martin-Duran, M. A. Hurle, and J. F. Nistal. 2009. 'Plasma levels of transforming growth factor-beta1 reflect left ventricular remodeling in aortic stenosis', *PLoS One*, 4: e8476.

Wagner, S., S. Schürmann, S. Hein, J. Schüttler, and O. Friedrich. 2015. 'Septic cardiomyopathy in rat LPS-induced endotoxemia: relative contribution of cellular diastolic Ca^{2+} removal pathways, myofibrillar biomechanics properties and action of the cardiotonic drug levosimendan', *Basic Research in Cardiology*, 110.

Wagner, S., L. S. Maier, and D. M. Bers. 2015. 'Role of sodium and calcium dysregulation in tachyarrhythmias in sudden cardiac death', *Circulation Research*, 116: 1956-70.

Wan, S. H., M. W. Vogel, and H. H. Chen. 2014. 'Pre-clinical diastolic dysfunction', *Journal of American College Cardiology*, 63: 407-16.

Wang, J., D. S. Khoury, Y. Yue, G. Torre-Amione, and S. F. Nagueh. 2007. 'Left ventricular untwisting rate by Speckle Tracking Echocardiography', *Circulation*, 116: 2580-86.

Wang, Y., G. Z. Wang, P. S. Rabinovitch, and I. Tabas. 2014. 'Macrophage mitochondrial oxidative stress promotes atherosclerosis and nuclear factor-κB–mediated inflammation in macrophages', *Circulation Research*, 114: 421-33.

Warren, C.M., M.C. Jordan, K.P. Roos, P.R. Krzesinski, and M.L. Grease. 2003. 'Titin isoform expression in normal and hypertensive myocardium', *Cardiovascular Research*, 59: 86-94.

Weber, S., S. Meyer-Roxlau, M. Wagner, D. Dobrev, and A. El-Armouche. 2015. 'Counteracting protein kinase activity in the heart: The multiple roles of Protein Phosphatases', *Frontiers in Pharmacology*, 6.

Westermann, D., and S. Heymans. 2014. 'Fibrosis or hypertrophy: let TIMPs decide', *Cardiovascular Research*, 103: 196-7.

Westermann, D., M. Kasner, P. Steendijk, F. Spillmann, A. Riad, K. Weitmann, W. Hoffmann, W. Poller, M. Pauschinger, H. P. Schultheiss, and C. Tschöpe. 2008. 'Role of left ventricular stiffness in heart failure with normal ejection fraction', *Circulation*, 117: 2051-60.

Westermann, D., K. Savvatis, D. Lindner, C. Zietsch, P. M. Becher, E. Hammer, M. M. Heimesaat, S. Bereswill, U. Völker, F. Escher, A. Riad, J. Plendl, K. Klingel, W. Poller, H. P. Schultheiss, and C. Tschöpe. 2011. 'Reduced degradation of the chemokine MCP-3 by matrix metalloproteinase-2 exacerbates myocardial inflammation in experimental viral cardiomyopathy', *Circulation*, 124: 2082-93.

Weytjens, C., B. Cosyns, J. Dhooge, C. Gallez, S. Droogmans, T. Lahoute, P. Franken, and G. Vancamp. 2006. 'Doppler myocardial imaging in adult male rats: Reference values and reproducibility of velocity and deformation parameters', *European Journal of Echocardiography*, 7: 411-17.

WHO. 2021. 'Cardiovascular diseases (CVDs)', https://www.who.int/news-room/fact-sheets/detail/cardiovascular-diseases-(cvds)

Winter, C. A., E. A. Risley, and G. W. Nuss. 1962. 'Carrageenin-induced edema in hind paw of the rat as an assay for antiiflammatory drugs', *Proceedings of the Society for Experimental Biology and Medicine*, 111: 544-7.

Witasp, A., M. Rydén, J. Jesús Carrero, A. R. Qureshi, L. Nordfors, E. Näslund, F. Hammarqvist, S. Arefin, K. Kublickiene, and P. Stenvinkel. 2013. 'Elevated circulating levels and tissue expression of Pentraxin 3 in uremia: A reflection of endothelial dysfunction', *PLoS ONE*, 8: e63493.

Wright, N. T., B. R. Cannon, D. B. Zimmer, and D. J. Weber. 2009. 'S100A1: Structure, function, and therapeutic potential', *Current Chemical Biology*, 3: 138-45.

Wu, C., J.g Lee, F. Chiang, C. Yang, S. Huang, J. Hwang, Jiunn-Lee Lin, C. Tseng, J. Chen, and C. Tsai. 2011. 'Plasma levels of tumor necrosis factor-α and interleukin-6 are associated with diastolic heart failure through downregulation of sarcoplasmic reticulum Ca^{2+} ATPase', *Critical Care Medicine*, 39: 984-92.

Yip, G. 2002. 'Left ventricular long axis function in diastolic heart failure is reduced in both diastole and systole: time for a redefinition?', *Heart*, 87: 121-25.

Yokoe, I, H Kobayashi, Y Kobayashi, JT Giles, K Yoneyama, N Kitamura, and M Takei. 2018. 'Impact of tocilizumab on N-terminal pro-brain natriuretic peptide levels in patients with active rheumatoid arthritis without cardiac symptoms', *Scandinavian Journal of Rheumatology*, 47: 364-70.

Yu, C., H. Lin, H. Yang, S. Kong, Q. Zhang, and S. Wai-Luen Lee. 2002. 'Progression of systolic abnormalities in patients with "isolated" diastolic heart failure and diastolic dysfunction', *Circulation*, 105: 1195-201.

Yu, Y., G. Yin, S. Bao, and Z. Guo. 2017. 'Kinetic alterations of collagen and elastic fibres and their association with cardiac function in acute myocardial infarction', *Molecular Medicine Reports*.

Yuyun, M. F., K. Sliwa, A. P. Kengne, A. O. Mocumbi, and G. Bukhman. 2020. 'Cardiovascular diseases in Sub-Saharan Africa compared to highIincome countries: An epidemiological perspective', *Global Heart*, 15: 15.

Zerbib, Y., J. Maizel, and M. Slama. 2019. 'Echocardiographic assessment of left ventricular function', *Journal of Emergency and Critical Care Medicine*, 3: 33-33.

Zhang, S., L. Li, A. Shen, Y. Chen, and Z. Qi. 2020. 'Rational use of tocilizumab in the treatment of novel coronavirus pneumonia', *Clinical Drug Investigation*, 40: 511-18.

Zhao, L., G. Cheng, R. Jin, M. R. Afzal, A. Samanta, Y. Xuan, M. Girgis, H. K. Elias, Y. Zhu, A. Davani, Y. Yang, X. Chen, S. Ye, O. Wang, L. Chen, J. Hauptman, R. J. Vincent, and B. Dawn. 2016. 'Deletion of Interleukin-6 attenuates pressure overload-induced left ventricular hypertrophy and dysfunction', *Circulation Research*, 118: 1918-29.

Ziaeian, B., and G. C. Fonarow. 2016. 'Epidemiology and aetiology of heart failure', *Nature Reviews Cardiology*, 13: 368-78.

Zile, M. R., C. F. Baicu, J. S. Ikonomidis, R. E. Stroud, P. J. Nietert, A. D. Bradshaw, R. Slater, B. M. Palmer, P. Van Buren, M. Meyer, M. M. Redfield, D. A. Bull, H. L. Granzier, and M. M. Lewinter. 2015. 'Myocardial stiffness in patients with heart failure and a preserved ejection fraction', *Circulation*, 131: 1247-59.

CHAPTER 9: APPENDICES

9.1 Appendix A: Animal ethical clearance certificate

STRICTLY CONFIDENTIAL

ANIMAL ETHICS SCREENING COMMITTEE (AESC)

CLEARANCE CERTIFICATE NO. 2017/03/21/C

APPLICANT: Ms L Mokotedi

SCHOOL: Physiology
DEPARTMENT:
LOCATION:

PROJECT TITLE: Cardiovascular morphology and function in a rat model of rheumatoid arthritis

Number and Species

30 X 3 month old male Sprague-Dawley rats

Approval was given for the use of animals for the project described above at an AESC meeting held on 2017/03/28. This approval remains valid until 2019/04/12.
Unreported changes to the application may invalidate the clearance given by the AESC
An annual progress report must be provided

The use of these animals is subject to AESC guidelines for the use and care of animals, is limited to the procedures described in the application form and is subject to any additional conditions listed below:

None

Signed: _____ (Chairperson, AESC) Date: 13/04/2017

I am satisfied that the persons listed in this application are competent to perform the procedures therein, in terms of Section 23 (1) (c) of the Veterinary and Para-Veterinary Professions Act (19 of 1982)

Signed: _____ (Registered Veterinarian) Date: 18/4/17

cc: Supervisor: Drs A Millen and F Michel
Director: CAS

Works 2000/lain0015/AESCCert.wps

9.2 Appendix B: Modification/Extension clearance for animal study

AESC 2012 M&E

Please note that only type written applications will be accepted.

UNIVERSITY OF THE WITWATERSRAND

ANIMAL ETHICS SCREENING COMMITTEE

MODIFICATIONS AND EXTENSIONS TO EXPERIMENTS

a. Name: Lebogang Mokotedi

b. Department: School of Physiology

c. Experiment to be modified / extended

		AESC NO	
Original AESC number:	2017	03	21C
Other M&Es			1

d. Project Title: Cardiovascular morphology and function in a rat model of rheumatoid arthritis

		No.	Species
e.	Number and species of animals originally approved:	30	SD
f.	Number of additional animals previously allocated on M&Es:	5	SD
g.	Total number of animals allocated to the experiment to date:	35	SD
h.	Number of animals used to date:	35	SD

i. Specific modification / extension requested:

- Addition of co-workers:

1. Ashmeetha Manilal (technical staff and PhD student) Staff number: A0029214, Tel: 0824617340, email: Ashmeetha.Manilal@wits.ac.za
2. Sulé Gunter (post-doctoral fellow). Staff number: A0045488, Tel: 0828141066, email: suledreyer@gmail.com
3. Serena Fourie, (MSc student) student number: 804802; Tel: 0741548402, email: fourie.serena@gmail.com
4. Regina le Roux, (MSc student) student number: 1588322; Tel: 0718719596, email: reginalecroux4@gmail.com

- Additional rats required

As per the original application, arthritis will be induced with Bovine Collagen and incomplete Freund's Adjuvent and compared to a control group. In addition we would like to add two groups where the groups will also have collagen induced arthritis but they are given treatment to reduce inflammation. A flow diagram of the groups is presented below.]

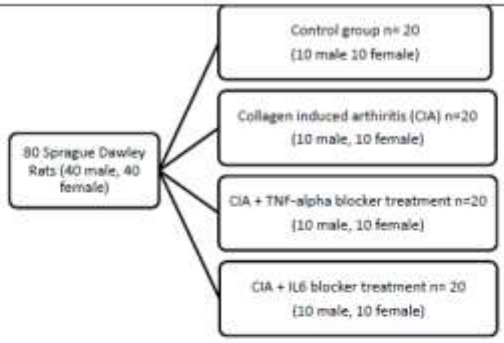

- **Addition of drug treatment regimen to reduce inflammation**
- **Use of pulse-pen to measure pulse wave velocity at termination.**

j. **Motivation for modification / extension:**

The addition of co-workers:

These added students and co-workers will contribute to all aspects of the projects. Two masters and one PhD students will also obtain higher degrees from work performed as a part of the modification of this project.

Additional rats required:

The original project was largely a pilot study in order to determine whether the inflammatory model will be successful. All the rats were used for this first part of the study and we have successfully established that the collagen induced inflammatory model is indeed successful. None of the animals died during the experiment due to adverse effects. In the first part of this study we have shown substantial differences in those rats that were exposed to inflammation. We would like to request an additional 80 rats for further study. The 80 (40 male and 40 female) rats will be divided into 4 groups (control group, inflammation group, inflammation + TNFα inhibitor group, and inflammation + IL6 inhibitor group) as indicated in the flow diagram. In essence the intervention to the animals and measures obtained will not change as per the original application, hence the rationale for applying for a modification to the original application. The addition of extra groups will not change the intervention to the animals, except for the addition of drugs to reduced inflammation and therefore it will not be harmful to the animal, but rather beneficial.

Addition of drug treatment regimen to reduce inflammation:

In order to reduce inflammation in persons with rheumatoid arthritis drugs that have shown good outcomes in these patients are biological disease modifying agents (DMARDS) (1). Two of these biological DMARDS that have shown to be effective for reducing inflammation as well as decreasing cardiovascular disease risk markers in persons with rheumatoid arthritis are TNFα

inhibitors and Interleukin-6 inhibitors (1). However the mechanisms whereby these drugs improve cardiac function is currently unknown. These drugs have also shown benefits in previous animal models of rheumatoid (2) and osteoarthritis (3), with no reported side-effects. The drugs will be administered intraperitoneally upon the first sign of arthritis (roughly 12 days after immunization) and given as indicated (below) until the termination of the study. The other two groups will receive intraperitoneal injections of phosphate buffered saline solution. The TNFα inhibitor (Enbrel) will be given at a dosage of 10 mg/kg (2) three time a week and the IL-6 inhibitor (Actemra (tocilizumab)) will be given at a dosage of 8 mg/kg once a week as previously described (4,5). The use of these drugs will provide us with a further understanding of the effect of inflammation on vascular and cardiac function and possibly identify novel targets for the treatment of diastolic dysfunction in inflammation induced heart disease. The protocol of inducing inflammation in the rats will not change from the previous application. The addition of these drugs will in all likelihood reduce inflammation and hence limit the discomfort of the animals.

Use of pulse-pen to measure pulse wave velocity at termination:

At termination we would like to measure aortic pulse wave velocity (PWV) by applanation tonometry (PulsePen device, DiaTecne, Milan, Italy). The measurement of PWV is non-invasive and will provide a further understanding to the arterial function of the animals and the effect of inflammation on aortic stiffness. This procedure will happen during the period when the rats are anesthetized for echocardiography (as per the initial application). In order to obtain the measurement the neck and inner right thigh will be shaved and animals will be placed on a heating pad in the supine position. Briefly, the carotid and femoral pulse wave velocities will be recorded simultaneously by placing one probe on the common carotid artery and one probe on the femoral artery. The two probes will be positioned and fixed on the arteries by means of mechanical arms, equipped with micro-regulators. After that, pressure signals will be transmitted to a computer by means of an optical fiber that ensures the electromagnetic isolation for the rat undergoing the test. After the tonometric pulse wave acquisition, the sites where probes will be placed will be marked on the skin and the distance from the carotid to the femoral will be measured. PWV will be calculated as the distance between the two recording sites divided by the time delay between the two arterial waveforms at each site (6).

References

1. Beniaamam M, Paulus WJ, Blanken AB, Nurmohamed MT (2018): The effect of biological DMARDs on the risk of congestive heart failure in rheumatoid arthritis: a systematic review. Exp Opin Biol Ther 2018; DOI:10.1080/14712598.2018.1462794.

2. Totoson P, Maguin-Gate K, Prigent-Tessier A et al. Etanercept improves endothelial function via pleiotropic effects in rat adjuvant-induced arthritis. Rheumatol 2016;55:1308-17.

3. Lin Y, Liu L, Jiang H, Zhou J, Tang Y. Inhibition of interleukin-6 function attenuates the central sensitization and pain behavior induced by osteoarthritis. Eur J Pharmacol. 2017;811:260-7.

4. Kobayashi Y, Takei M, Giles JT et al. Association of tocilizumab treatment with changes in measures of regional left ventricular function in rheumatoid arthritis, as assessed by cardiac magnetic resonance imaging. Int J Rheum Dis 2016;19:1169–1174.

5. Hançerli Y, Kaplan M, Tanoğlu A et al. Efficacy of tocilizumab treatment in cerulein-induced experimental acute pancreatitis model in rats. Turk J Gastroenterol. 2017;28:485-91.

6. Salvi P, Lio G, Labat C, Ricci E, Pannier B, Benetos A. Validation of a new non-invasive portable

9.3 Appendix C: Ethical waiver

UNIVERSITY OF THE WITWATERSRAND, JOHANNESBURG

HUMAN RESEARCH ETHICS COMMITTEE (MEDICAL)

Human Research Ethics Committee (Medical)

Research Office Secretariat:
Faculty of Health Sciences, Phillip Tobias Health Sciences Building, 3rd Floor, Office 301/2/4, 29 Princess of Wales Terrace, Parktown, 2193
Private Bag 3, Wits 2050
Office email: HREC-Medical.ResearchOffice@wits.ac.za
Website: www.wits.ac.za/research/about-our-research/ethics-and-research-integrity/

Ref: W-CBP-200627-06 27/06/2020

TO WHOM IT MAY CONCERN:

Waiver:	This certifies that the following research does not require clearance from the Human Research Ethics Committee (Medical)
Investigator: **Supervisor:**	Professor Aletta Millen *et al.*
Department:	School of Physiology, Faculty of Health Sciences, University of the Witwatersrand
Project title:	The molecular effects of inflammation on mechanisms of diastolic dysfunction in a human cardiomyocyte cell line.
Reason:	An *in vitro* cell culture study with the commercially acquired human adult ventricular cardiomyocyte AC16 cell line. No human participants, human data or human tissues will be involved in the study.

Dr CB Penny

Chairperson: Human Research Ethics Committee (Medical) Copy – HREC (Medical) Secretariat: Ms Zanele Ndlovu, Ms Mapula Ramaila and Mr Rhulani Mkansi

9.4 Appendix D: Copy of publication of data in larger animal study

TNF-α inhibitors reduce inflammation-induced concentric remodelling, but not diastolic dysfunction in collagen-induced arthritis

R. Le Roux, L. Mokotedi, S. Fourie, A. Manilall, S. Gunter, A.M.E. Millen

Cardiovascular Pathophysiology and Genomics Research Unit, School of Physiology, Faculty of Health Sciences, University of the Witwatersrand, Johannesburg, South Africa.

Abstract

Objective

To determine biologic disease-modifying anti-rheumatic drug effects on inflammation-induced cardiac geometry and function changes.

Methods

Male and female Sprague-Dawley rats (n=92) were divided into four groups: control group, collagen-induced arthritis (CIA) group, anti-TNF-α group and anti-IL-6 group. Inflammation was induced by injecting bovine type-II collagen emulsified in incomplete Freund's adjuvant at the base of the tail, in all groups except the control group. Following the onset of arthritis, the anti-TNF-α group received etanercept, and the anti-IL-6 group received tocilizumab, for six weeks. Left ventricular (LV) geometry and function were assessed with echocardiography and circulating inflammatory markers were measured with ELISA.

Results

Relative wall thickness in the CIA and anti-IL-6 groups were increased compared to controls ($p<0.001$ and $p=0.02$, respectively). TNF-α inhibition protected against inflammation-induced LV concentric remodelling, as relative wall thickness in the anti-TNF-α group was similar to controls ($p=0.55$). Systolic function variables were not different between the groups. In all groups inoculated with collagen, myocardial relaxation (lateral e') were impaired compared to controls (all $p<0.001$). LV filling pressures (E/e') were increased in the CIA, anti-TNF-α and anti-IL-6 groups compared to controls ($p<0.001$, $p<0.001$ and $p=0.05$, respectively). Independent of concentric remodelling, circulating CRP concentrations were associated with decreased e' and increased E/e', while TNF-α concentrations were associated with E/A.

Conclusion

TNF-α inhibition protected against inflammation-induced adverse cardiac remodelling, but not diastolic dysfunction. IL-6 receptors blocker effects on inflammation-induced cardiac changes were inconclusive. Systemic inflammation likely impacts LV concentric remodelling and diastolic dysfunction through distinct pathways.

Key words

diastolic function, inflammation, tumour necrosis factor-alpha inhibitor, interleukin-6 receptor blocker.

Clinical and Experimental Rheumatology 2021

Regina Le Roux, MSc
Lebogang Mokotedi, PhD
Serena Fourie, MSc
Ashmeetha Manilall, MSc
*Sulè Gunter, PhD**
*Aletta M.E. Millen, PhD**

**These authors share senior authorship.*

Please address correspondence to:
Aletta Millen,
Cardiovascular Pathophysiology and Genomics Research Unit,
School of Physiology,
University of the Witwatersrand Medical School,
7 York Road,
Parktown 2193,
Johannesburg, South Africa.
E-mail: aletta.millen@wits.ac.za

Received on September 1, 2020; accepted in revised form on December 14, 2020.

© Copyright CLINICAL AND EXPERIMENTAL RHEUMATOLOGY 2021.

Funding: this work was supported by the National Research Foundation (Thuthuka programme) and the Faculty of Health Sciences Research Committee at the University of the Witwatersrand.

Competing interests: none declared.

Introduction

Patients with rheumatoid arthritis (RA) have an increased risk of developing heart failure that contributes to the increased cardiovascular disease mortality in RA (1). RA patients with heart failure are more likely to have a preserved ejection fraction (2). Left ventricular (LV) diastolic dysfunction is a pre-clinical disorder that often precedes heart failure with a preserved ejection fraction (HFpEF) (3). Independent of traditional risk factors, LV diastolic dysfunction predicts cardiovascular events in the general population and RA (4, 5).

Several traditional risk factors and comorbid conditions are associated with LV diastolic dysfunction (3,6). Although comorbidities are implicated in LV diastolic dysfunction development, systemic inflammation mediates the causal molecular mechanisms of LV diastolic dysfunction (6). Biomarkers of systemic inflammation, including tumour necrosis factor alpha (TNF-α) and interleukin 6 (IL-6) have been associated with LV diastolic dysfunction and HFpEF (7). These cytokines have been linked to the initiation and progression of cardiac structural and functional changes (8-10) and the mechanisms of LV diastolic dysfunction and its progression to HFpEF (11).

The development of LV diastolic dysfunction and the phenotypes of HFpEF are complex and multifactorial (12, 13). Factors affecting extracellular matrix remodelling, calcium reuptake or titin phosphorylation have shown to contribute to the development of diastolic dysfunction (3, 12, 13). This heterogeneity in signalling pathways contributes to the lack of successful therapeutic interventions to manage HFpEF (14). Considering the role of inflammation in LV diastolic dysfunction pathogenesis, managing systemic inflammation has been proposed as a potential treatment target (15).

In RA, although biologic disease-modifying anti-rheumatic drug (DMARD) treatment effectively controls disease progression and joint damage, its effects on cardiovascular disease risk and specifically cardiac function have been contradictory (16). Taken together, inflammation plays a central role in diastolic dysfunction pathogenesis. Inflammatory cytokines and disease profiles contribute to the increased incidence of diastolic dysfunction in RA (17). However, the role of biologic DMARD treatment in LV diastolic dysfunction warrant further investigation. An improved understanding of anti-inflammatory treatments on cardiac geometry and function will elucidate the possibility of novel treatment strategies for the management of diastolic dysfunction and HFpEF. Therefore, this study aims to determine whether biologic DMARDs alter the outcomes of inflammation-induced changes in cardiac structure and function.

Methods

Animals

Ninety-two three-month-old, male (n=53) and female (n=39) Sprague-Dawley rats were housed individually, in temperature-controlled rooms. Experimental procedures were approved by the Animal Ethics Screening Committee of the University of the Witwatersrand (AESC approval: 2017/03/21C). Rats underwent a two-week familiarisation period during which body weight, food intake, paw arthritis scores and blood pressures were measured. Following the familiarisation period, rats were randomly divided into four groups: the control group (n=28, males: n=17; females: n=11), the collagen-induced arthritis (CIA) group (n=33, males: n=20; females: n=11), the anti-TNF-α group (n=15, males: n=8; females: n=7) and the anti-IL-6 group (n=16, males: n=8; females: n=8). Rats had *ad libitum* access to standard rat chow and water during the study.

Experimental protocol

The control group was injected with a phosphate-buffered saline solution at the base of the tail. The CIA, anti-TNF-α and anti-IL-6 groups were injected with an arthritis-inducing emulsion (18). For the arthritis-inducing emulsion, type II collagen (Chondrex cat. #20021, Redmond, WA, USA) was dissolved in 0.05M acetic acid by stirring it overnight at 4°C. The dissolved bovine collagen (2mg/ml) was

mixed with an equal amount of incomplete Freund's adjuvant (Chondrex cat. #7002, Redmond, WA, USA). Immediately after preparation, rats were immunised by administrating 0.2ml (200μg) of the arthritis-inducing emulsion, subcutaneously at the base of the tail, under general anesthesia (isoflurane). To ensure a high incidence of arthritis, the rats in the CIA, anti-TNF-α and anti-IL-6 groups received 0.1ml (100μg) booster injections of the emulsion seven and 21 days after the primary immunisation.

Following the onset of arthritis, the anti-TNF-α group received a TNF-α inhibitor, etanercept (Enbrel) intraperitoneally, at a dosage of 10mg/kg every three days for six weeks. The anti-IL-6 group received an IL-6 receptor blocker, tocilizumab (Actemra) intraperitoneally, at a dosage of 8mg/kg once a week for six weeks. All rats exposed to the arthritis inducing protocol received 1-4mg/kg Tramazec daily, for pain relief. The severity of arthritis was quantified every two weeks using an arthritis scoring system and measuring the hind paw thickness at the tarsometatarsal and ankle joints with a digital caliper, as previously reported (19).

Tail cuff blood pressures

Non-invasive blood pressure was measured using the tail cuff technique (Biopac Systems, Santa Barbara, CA, USA) as previously described (19).

Echocardiography

The rats were anaesthetised by intramuscular injections of ketamine (100 mg/kg) and xylazine (5 mg/kg) to measure cardiac function using an echocardiogram (Acuson SC2000, Siemens Medical Solutions, USA, Inc.) coupled with a high-resolution ultrasound probe (10MHz). Echocardiography was performed according to the American Society of Echocardiography conventions (20). In the long axis parasternal view, using 2-dimensional directed M-mode imaging left ventricular internal diameter (LVID), interventricular septal thickness (IVST) and posterior wall thickness (PWT) were measured in diastole and systole. LV stroke volume and ejection fraction were determined using the Teichholz formula (21). Endocardial and midwall fractional shortening was calculated as previously described (19, 20). Relative wall thickness (RWT) was calculated as the IVST + PWT in diastole divided by LVID in diastole (20).

LV diastolic function was assessed using pulsed wave and Tissue Doppler Imaging. Mitral inflow velocity was determined during the early (E) and late (atrial, A) periods of diastole in the apical four-chamber view, with the sample volume placed at the tip of the mitral valve. Trans-mitral flow velocity was expressed as E/A, an index of LV relaxation. Tissue Doppler Imaging (TDI) was used to measure the motion of the mitral annulus in the apical four-chamber view. The peak relaxation velocities during early (e') and late (a') diastole were obtained at the lateral mitral annulus. Lateral wall e' was considered an index of myocardial relaxation. Because early mitral inflow velocity (E) is influenced by ventricular relaxation and left atrial pressures, while e' is influenced by ventricular relaxation, E/e' was calculated by dividing mitral inflow velocity (E) by the peak relaxation velocity during early diastole (e') and was considered an index of LV filling pressures. The ratio of early to late peak tissue relaxation velocities (e'/a'), was calculated and considered an index of LV stiffness.

Heart weight and circulating inflammatory markers

After echocardiography, the rats were terminated by thoracotomy. The hearts were removed and weighed. Blood samples were collected and stored at -80°C. Serum concentrations of IL-6, TNF-α and C-reactive protein (CRP) were measured by solid phase sandwich enzyme-linked immunosorbent assay (ELISA) (Elabscience Biotechnology Co. Ltd, China). The lower detection limits for TNF-α, IL-6 and CRP were 78.13pg/ml, 62.50pg/ml and 0.31ng/ml respectively, all with coefficients of variation <10%.

Statistical analysis

Statistical analysis was performed using SAS software, v. 9.4 (SAS Institute Inc., USA). Continuous data are expressed as mean ± standard error of the mean (SEM). Differences in food intake, body weight, blood pressure and arthritis scores and paw thickness measurements between the groups were determined by repeated-measures analysis of variance (ANOVA) and Tukey *post-hoc* tests. Differences in cardiac geometry and function between the groups were determined using a two-way ANOVA with Tukey *post-hoc* tests. There were no differences in echocardiographic variables between males and females, hence variables were pooled for statistical analysis. Associations between inflammatory markers and echocardiographic measures were determined using Pearson's correlations in all groups and in control and inflammation groups in unadjusted and multivariate adjusted models. Potential confounders included in the multivariate adjusted models were sex, body weight and blood pressure. As concentric remodelling is one of the main risk factors for the development of LV diastolic dysfunction, relative wall thickness was included in the multivariate adjusted correlation analysis for LV diastolic function variables. Differences were considered statistically significant when $p \leq 0.05$.

Results

Experimental model characterisation

There were no differences in body weight, systolic or diastolic blood pressure at baseline or termination between the groups (Table I). The circulating inflammatory marker concentrations were significantly higher in all groups immunised with collagen compared to the control group. Serum CRP concentrations were higher in the CIA and anti-IL-6 groups compared to the anti-TNF-α group (Table I).

All groups immunised with collagen showed signs of arthritis, as evidenced by the presence of erythema, oedema and joint rigidity (Fig. 1A). The arthritis scores (Fig. 1B) in the CIA group were increased compared to baseline (week 0) and compared to the control group from four weeks onwards and from six weeks onwards in the anti-TNF-α and anti-IL-6 groups. There were no differences in the arthritis scores between

Table I. Body weight, food intake, blood pressure and circulating inflammatory markers in the control, CIA, anti-TNF-α and anti-IL-6 groups.

	Control	CIA	anti-TNF-α	anti-IL-6
n	28	33	15	16
Male (%)	17 (61)	20 (61)	8 (53)	8 (50)
Baseline				
Body weight (g)	426.3 ± 22.2	402.2 ± 20.5	379.3 ± 32.6	399.7 ± 29.3
Food intake (g/week)	210.6 ± 11.3	200.3 ± 10.4	212.1 ± 16.6	220.6 ± 14.9
Systolic BP (mm Hg)	129 ± 2	129 ± 1	129 ± 2	130 ± 2
Diastolic BP (mm Hg)	90 ± 1	88 ± 1	88 ± 2	87 ± 2
Termination				
Body weight (g)	491.0 ± 22.2	442.6.1 ± 20.5	394.1 ± 32.6	384.1 ± 29.3
Food intake (g/week)	176.7 ± 11.3	186.2 ± 10.4	156.6 ± 16.6	142.6 ± 14.9*
Systolic BP (mm Hg)	127 ± 2	129 ± 1	130 ± 2	129 ± 2
Diastolic BP (mm Hg)	87 ± 1	89 ± 1	86 ± 2	90 ± 2
Inflammatory markers				
TNF-α (pg/ml)	95.5 ± 8.5	177.1 ± 7.7*	145.6 ± 10.7*	164.1 ± 11.1*
IL-6 (pg/ml)	17.3 ± 2.0	30.5 ± 1.8*	27.9 ± 2.5*	30.8 ± 2.6*
CRP (ng/ml)	0.12 ± 0.04	0.61 ± 0.03*#	0.44 ± 0.05*	0.65 ± 0.05*#

Data expressed as means ± SEM.
CIA: collagen-induced arthritis; TNF-α: tumour necrosis factor-alpha; IL-6: interleukin 6; BP: blood pressure; CRP: C-reactive protein.
*$p<0.05$ compared to controls; #$p<0.05$ compared to anti-TNF-α.

the CIA, anti-TNF-α and anti-IL-6 groups at any time point (Fig. 1B). Paw thickness at the tarsometatarsal joint (Fig. 1C) did not change compared to baseline (week 0) in the control or anti-TNF-α groups at any time point. The paw thickness at the tarsometatarsal joint of the rats in the CIA group was increased compared to the control ($p=0.002$) and anti-TNF-α ($p=0.01$) groups at week 10 (Fig. 1C). Paw thickness at the ankle joint (Fig. 1D) did not change compared to baseline (week 0) in the control or the anti-TNF-α group at any time point. The paw thickness at the ankle joint in the CIA group ($p<0.001$) and the anti-IL-6 ($p=0.02$) groups were increased at week 10 compared to baseline (week 0; Fig. 1D). The paw thickness at the ankle joint in the CIA group was increased compared to the control group at week 10 ($p=0.04$).

Inflammation induced changes in cardiac weight and geometry

The mean heart weight in the anti-TNF-α group was lower than the control group (Table II). When indexed to body weight, the heart weight in the CIA and anti-IL-6 groups were increased compared to the control group. There were no differences in the heart weight indexed to body weight between the control and anti-TNF-α groups. The interventricular septal thickness and posterior wall thickness in diastole of the CIA group were increased compared to the control and anti-TNF-α groups. The anti-IL-6 group had significantly greater interventricular septal wall thickness in diastole compared to the control group. The relative wall thickness of the CIA and the anti-IL-6 groups, but not the anti-TNF-α group, were significantly higher than the control group.

Inflammation induced changes in cardiac function

There were no differences in any of

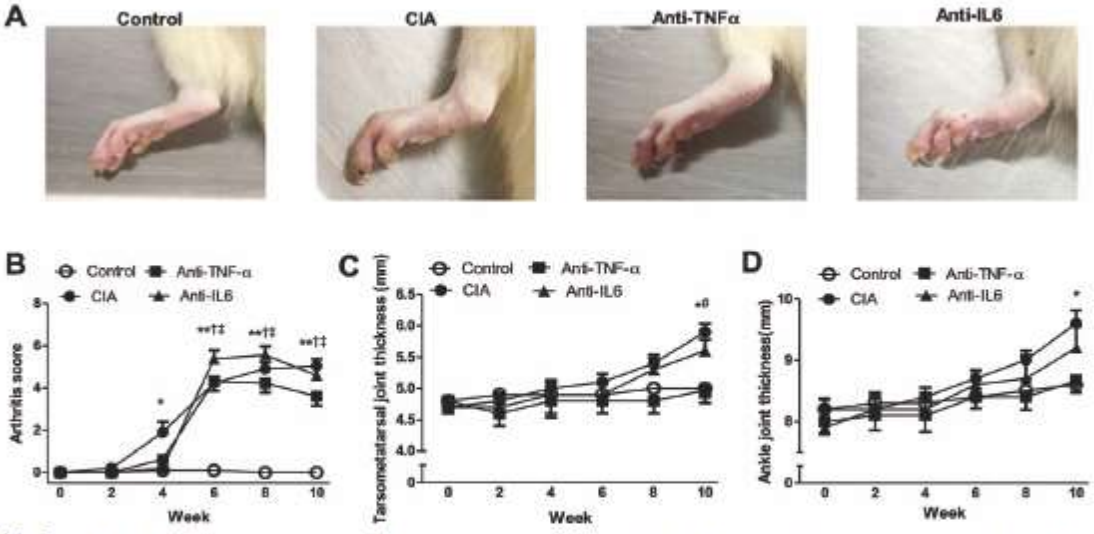

Fig. 1. Change in the hind limbs (A), arthritis scores (B), paw thickness at the tarsometatarsal joint (C) and paw thickness at the ankle joint (D) in the control (n=28), CIA (n=33), anti-TNF-α (n=15) and anti-IL6 (n=16) groups. Data expressed as mean ± SEM.
CIA: collagen-induced arthritis; TNF-α: tumour necrosis factor alpha; IL-6: interleukin 6.
*$p<0.05$ CIA *vs.* control; **$p<0.001$ CIA *vs.* control; †$p<0.001$ anti-TNF-α *vs.* control; ‡$p<0.001$ anti-IL6 *vs.* control; #$p<0.05$ CIA *vs.* anti-TNF-α.

Table II. Heart-weight, left ventricular geometry and function in the control, inflammation and TNF-α inhibitor and IL-6 receptor blocker groups.

	Control (n=28)	CIA (n=33)	Anti-TNF-α (n=15)	Anti-IL-6 (n=16)
Cardiac geometry				
Heart weight (g)	1.21 ± 0.02	1.18 ± 0.02	1.12 ± 0.03*	1.14 ± 0.03
Heart weight/BW x10³	2.71 ± 0.06	2.90 ± 0.05*	2.88 ± 0.07	2.99 ± 0.07*
End diastolic IVST (mm)	2.1 ± 0.04	2.4 ± 0.04*†	2.2 ± 0.06	2.4 ± 0.06*
LV end diastolic diameter (mm)	6.7 ± 0.13	6.4 ± 0.12	6.7 ± 0.18	6.6 ± 0.17
End diastolic LV PWT (mm)	2.1 ± 0.05	2.4 ± 0.06*†	2.2 ± 0.07	2.3 ± 0.07
End systolic IVST (mm)	3.4 ± 0.06	3.5 ± 0.06	3.3 ± 0.09	3.5 ± 0.08
LV end systolic diameter (mm)	3.6 ± 0.12	3.5 ± 0.11	3.7 ± 0.16	3.6 ± 0.15
End systolic LV PWT (mm)	3.1 ± 0.06	3.1 ± 0.05	3.1 ± 0.08	3.0 ± 0.08
Relative wall thickness	0.63 ± 0.02	0.75 ± 0.02*†	0.65 ± 0.03	0.71 ± 0.03*
Systolic function measures				
Ejection fraction (%)	83.0 ± 1.2	81.2 ± 1.1	80.9 ± 1.7	81.0 ± 1.6
Endocardial fractional shortening (%)	47.4 ± 1.2	44.7 ± 1.1	44.9 ± 1.7	44.9 ± 1.6
Midwall fractional shortening (%)	22.9 ± 0.7	21.8 ± 0.6	21.2 ± 0.9	21.9 ± 0.8
Diastolic function measures				
E/A	1.78 ± 0.06	1.69 ± 0.05	1.94 ± 0.08†	1.81 ± 0.08
e' (cm/s)	4.51 ± 0.10	3.67 ± 0.10*	3.48 ± 0.14*	3.62 ± 0.13*
a' (cm/s)	3.05 ± 0.11	3.15 ± 0.10	3.23 ± 0.15	2.97 ± 0.15
e'/a'	1.45 ± 0.06	1.23 ± 0.05*	1.03 ± 0.08*	1.28 ± 0.08
E/e'	25.1 ± 1.1	31.6 ± 1.0*	32.7 ± 1.5*	29.9 ± 1.4*

Data expressed as means ± SEM.
CIA: collagen-induced arthritis; TNF-α: tumour necrosis factor alpha; IL-6: interleukin 6; BW: body weight; IVST: interventricular septal thickness; LV: left ventricular; PWT: posterior wall thickness.
*$p<0.05$ *vs.* control; †$p<0.05$ *vs.* CIA.

the systolic function measures between any of the groups (Table II). The ratio of early to late mitral inflow velocity (E/A), a marker of LV relaxation, was higher in the anti-TNF-α group compared to the CIA group (Table II). There were no differences in the E/A between the control, CIA and anti-IL-6 groups. The lateral wall early mitral annular velocity (e'), a measure of LV relaxation, of the CIA, anti-TNF-α and anti-IL-6 groups were significantly lower than the control group (all $p<0.0001$). The e'/a' ratio, a measure of myocardial stiffness, in the CIA and anti-TNF-α groups were significantly lower compared to the control group. The e'/a' was lower in the anti-IL-6 group compared to controls but did not reach statistical significance ($p=0.25$). The E/e' ratio, a measure of LV filling pressures, were increased in the CIA, anti-TNF-α and anti-IL-6 groups compared to controls.

Associations between circulating inflammatory markers and concentric remodelling

All circulating inflammatory markers were associated with relative wall thickness in bivariate and multivariate analysis in all groups (Fig. 2). In the control and inflammation groups, all inflammatory markers were associated with relative wall thickness. When including potential confounders in the analysis, circulating CRP (r=0.38,

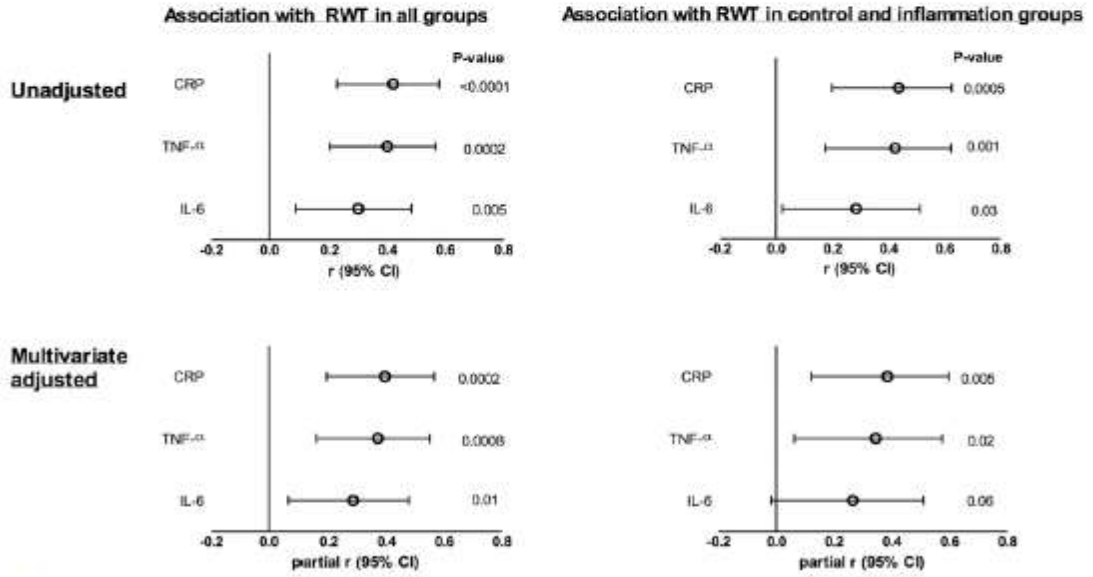

Fig. 2. Associations of inflammatory markers and relative wall thickness (RWT) in all groups (n=86) and in the control and CIA groups (n=57).
CRP: C-reactive protein; TNF-α: tumour necrosis factor alpha; IL-6: interleukin 6.
Multivariate adjusted model included body weight, sex and systolic and diastolic blood pressure as potential confounders.

p=0.005) and TNF-α (r=0.34, p=0.02), but not IL-6 concentrations (r=0.27, p=0.06) remained associated with relative wall thickness.

Independent contribution of inflammation to diastolic dysfunction

Serum CRP concentrations were related to lower lateral e' and increased filling pressures (E/e') in all groups and in the control and inflammation groups (Table III). When including potential confounders in the analysis, these associations were materially unaltered. When further including relative wall thickness as a potential confounder, CRP concentrations remained associated with lateral e' and E/e' in all groups and in the control and inflammation groups.

Serum TNF-α concentrations were significantly associated with the E/A ratio in all groups in bivariate and multivariate analysis (Table III). In the control and inflammation groups, serum TNF-α concentrations were associated with the E/A ratio and with E/e' in bivariate and multivariate analysis. In all groups, serum IL-6 concentrations were not associated with any measure of diastolic function in unadjusted or multivariate adjusted analysis. Serum inflammatory marker concentrations were not related to e'/a' in all groups.

Discussion

The main findings of this study are that TNF-α inhibitors protected against adverse LV concentric remodelling, but not diastolic dysfunction. IL-6 receptor blocker treatment did not ameliorate inflammation-induced LV structural or functional changes. Exposure to inflammation induced LV concentric remodelling independent of pressure load, and diastolic dysfunction independent of concentric remodelling. Our findings suggest that TNF-α is implicated in the pathways of extracellular matrix remodelling, but less important in other cellular signalling pathways involved in diastolic dysfunction.

The selective inhibition of TNF-α ameliorated inflammation-induced LV concentric remodelling. Previous preclinical studies in heart failure also reported improvements in LV remodelling following TNF-α treatment (22, 23). Circulating cytokines are reported to induce LV hypertrophy and adverse cardiac remodelling through activation of fibroblasts to secrete transforming growth factor (TGF)-β that stimulate collagen production (9, 19, 24). Anti-TNF-α treatment has previously shown to reduce inflammation-induced up-regulation of TGF-β (25) and collagen production (26). Others have shown no effects of etanercept on TGF-β (27). In the present study, inhibiting TNF-α may have prevented collagen production, evidenced by the lower LV wall thickness compared to the CIA group. However, the molecular pathways whereby anti-TNF-α treatment affect myocardial fibrosis require further investigation.

TNF-α inhibition failed to protect against inflammation-induced diastolic function impairments. Previous preclinical heart failure models showed TNF-α treatment protected against LV remodelling but not LV functional changes (22, 23). In clinical studies, TNF-α inhibitor effects on the different diastolic function variables have been contradictory (16, 28). These contrasting findings of TNF-α inhibition on cardiac geometry and function may be explained by the disparate effects of TNF-α in the different cellular pathways involved in diastolic dysfunction (13, 28).

It is well accepted that concentric remodelling is one of the main risk factors for diastolic dysfunction (29). However, the current study showed associations between inflammatory markers and LV diastolic dysfunction, independent of relative wall thickness. Moreover, adequate LV relaxation during diastole is dependent on both active processes and passive LV stiffness (30). Active myocardial relaxation requires rapid removal of cytosolic calcium, by the sarcoplasmic endoplasmic reticulum Ca^{2+} transport ATPase (SERCA) pump (31). Inflammation impairs active LV relaxation by decreasing SERCA activity (32). Indeed, we showed impaired active relaxation (e') in rats exposed to inflammation. Furthermore, TNF-α downregulates SERCA (33). Hence inhibition of TNF-α may have contributed to impaired LV relaxation (reduced e') by decreasing the reuptake of calcium in the sarcoplasmic reticulum. Future studies should confirm the effects of anti-TNF-α treatment on SERCA.

Inhibition of TNF-α did not ameliorate inflammation-induced changes in passive LV stiffness, as evidence by the decreased e'/a'. The passive elastic capacity of the ventricle is mediated by the stiffness of the extracellular matrix and the cardiomyocyte (30). Inflammation impacts diastolic relaxation through changes in the extracellular matrix and cardiomyocytes (16). Besides collagen production, inflammation impacts extracellular matrix remodelling by activating matrix metalloproteinases (MMPs) that are responsible for collagen turnover (34, 35). Increased TNF-α expression in the heart increases local production of MMPs (22) and inhibiting TNF-α impacts collagen turnover via altered MMP expression (36). Furthermore, collagen cross-linking has also been implicated in LV stiffness (37). TNF-α affects collagen cross-linking through lysyl oxidase activation (38). Hence, inhibiting TNF-α in the current study possibly altered extracellular matrix composition and compliance.

With regards to cardiomyocyte stiffness, a stiff isoform of titin impairs distensibility of the ventricle (30). Inflammation has been implicated in the hypophosphorylation of titin, which enhances cardiomyocyte stiffness and contribute to LV diastolic dysfunction (6, 39). Although TNF-α inhibition affects several molecular markers implicated in the cellular pathways involved in microvascular endothelial inflammation and nitric oxide bio-availability (6, 40), whether these effects translate into changes in titin phosphorylation is currently unknown and requires further investigation.

Besides increases in stiffness, inhibition of TNF-α did not prevent increases in LV filling pressures (E/e'). Both the impairment in active and passive relaxation in the rats exposed to inflammation may have contributed to the increased filling pressure. The increase in filling pressures may further explain the increased E/A in the anti-TNF-α group. When filling pressure in the LV increases, left atrial pressure is increased and acts as a driving force for early diastolic

Table III. Association between systemic inflammatory markers and diastolic function variables in all groups and in the control and CIA groups.

	In all groups						In control and inflammation groups					
	CRP (n=86) r (95%CI)	p	TNF-α (n=82) r (95%CI)	p	IL-6 (n=84) r (95%CI)	p	CRP (n=57) r (95%CI)	p	TNF-α (n=56) r (95%CI)	p	IL-6 (n=55) r (95%CI)	p
Unadjusted												
E/A	-0.12(-0.33-0.09)	0.25	**-0.29(-0.48--0.08)**	**0.01**	-0.16(-0.36-0.06)	0.15	-0.22(-0.46-0.04)	0.09	**-0.39(-0.60--0.13)**	**0.003**	-0.24(-0.48-0.02)	0.07
e'	**-0.33(-0.51--0.13)**	**0.002**	-0.16(-036-0.06)	0.15	-0.16(-0.36-0.06)	0.15	**-0.34(-0.55-0.09)**	**0.008**	-0.20(-0.45-0.07)	0.15	-0.15(-0.40-0.12)	0.26
e'/a'	-0.15(-0.35-0.06)	0.15	-0.16(-0.36-0.06)	0.15	-0.11(-0.32-0.11)	0.31	0.21(-0.45-0.05)	0.11	-0.21(-0.46-0.06)	0.12	-0.11(-0.36-0.16)	0.44
E/e'	**0.25(0.04-0.44)**	**0.02**	0.20(-0.02-0.40)	0.07	0.10(-0.11-0.31)	0.34	**0.37(0.12-0.57)**	**0.005**	**0.27(0.01-0.50)**	**0.05**	0.14(-0.13-0.39)	0.30
Adjusted Model 1*												
E/A	-0.21(-0.41-0.01)	0.06	**-0.44(-0.06--0.23)**	**<0.001**	-0.22(-0.42--0.01)	0.05	-0.26(-0.50-0.01)	0.06	**-0.50(-0.69--0.25)**	**0.001**	**-0.32(-0.55--0.04)**	**0.03**
e'	**-0.36(-0.54--0.15)**	**0.001**	-0.13(-0.35-0.10)	0.25	-0.14(-0.35-0.09)	0.22	**-0.42(-0.62--0.16)**	**0.002**	-0.24(-0.50-0.05)	0.1	-0.08(-0.35-0.21)	0.60
e'/a'	-0.14(-0.35-0.08)	0.22	-0.14(-0.35-0.09)	0.24	-0.07(-0.29-0.15)	0.51	**-0.30(-0.52--0.03)**	**0.03**	**-0.34(-0.57--0.06)**	**0.02**	-0.04(-0.32-0.24)	0.79
E/e'	**0.29(0.07-0.48)**	**0.01**	0.20(-0.03-0.41)	0.08	0.07(-0.16-0.29)	0.56	**0.44(0.19-0.64)**	**0.001**	**0.32(0.03-0.55)**	**0.03**	0.13(-0.16-0.40)	0.37
Adjusted Model 2**												
E/A	-0.18(-0.38-0.04)	0.11	**-0.33(-0.52--0.12)**	**0.002**	-0.18(-0.39-0.05)	0.12	-0.23(-0.47-0.05)	0.1	**-0.46(-0.66--0.20)**	**0.001**	-0.27(-0.51-0.01)	0.06
e'	**-0.32(-0.50--0.11)**	**0.004**	-0.15(-0.35-0.08)	0.50	-0.09(-0.30-0.14)	0.45	**-0.36(-0.58--0.09)**	**0.01**	-0.18(-0.45-0.11)	0.22	-0.08(-0.35-0.21)	0.60
e'/a'	-0.12(-0.33-0.10)	0.27	-0.18(-0.39-0.04)	0.10	-0.05(-0.27-0.17)	0.66	-0.24(-0.48-0.04)	0.09	-0.28(-0.52-0.01)	0.06	-0.04(-0.32-0.24)	0.79
E/e'	**0.26(0.04-0.45)**	**0.02**	0.21(-0.01-0.41)	0.06	0.02(-0.20-0.25)	0.83	**0.41(0.15-0.62)**	**0.002**	0.26(-0.03-0.51)	0.07	0.08(-0.21-0.35)	0.58

Significant associations are shown in bold. *Model 1: adjusted for sex, body weight and systolic and diastolic blood pressure; **Model 2: adjusted for model 1 + relative wall thickness. CRP: C-reactive protein; TNF-α: tumour necrosis factor alpha; IL-6: interleukin 6.

filling (41, 42). The increased early filling in a non-distensible ventricle causes a higher transmitral pressure gradient resulting in a pseudonormal filling pattern (41, 42). Taken together, despite protective effects of TNF-α inhibitors on cardiac geometry, it failed to protect against inflammation-induced diastolic functional impairments. Importantly, etanercept was considered the most appropriate anti-TNF-α treatment for this study, as it reportedly has the least adverse cardiovascular effects (16). However, using alternative anti-TNF-α treatments may have distinct effects on LV diastolic dysfunction (43, 44). Future studies should determine the impact of different anti-TNF-α therapies on specific mechanisms in the various cellular pathways involved in diastolic function.

The role of IL-6 in cardiac remodelling has been controversial. In models of LV pressure overload, some suggest IL-6 is central (45), while others reported no involvement of IL-6 in LV hypertrophy (46). Independent of pressure overload, Melendez *et al*. (9) showed that infusion of IL-6 resulted in concentric hypertrophy and diastolic dysfunction in rats. In clinical RA studies, IL-6 concentrations are associated with impaired diastolic function (17) and tocilizumab improved LV mass index (47). Nevertheless, in the present study anti-IL-6 treatment had no effect on inflammation induced changes in concentric remodelling, LV relaxation (e') or filling pressures (E/e'). However, anti-IL-6 treatment partially impacted inflammation-induced changes in LV stiffness (e'/a'). IL-6 has been implicated in cardiomyocyte stiffness by altering the phosphorylation of titin (39). The lack of conclusive effects of IL-6 receptors blockers in this study may be explained by several mechanisms. First, activation of gp130, a key signal-transducing receptor component of the IL-6 signalling pathways in cardiomyocytes, has been implicated in myocardial remodelling (48). However, gp130 is not specific to IL-6 and may have been upregulated by other members in the IL-6 cytokine family (49). Indeed, activation of gp130 in the absence of IL-6, causes myocardial remodelling (48). Second, if membrane bound interleukin-6 receptor (IL-6R) is absent or blocked, IL-6 can exert it effects on target tissue through the formation of a complex with the agonistic soluble IL-6R (sIL-6R) (50). Hypertrophic responses in cardiomyocytes are dependent on the presence of the sIL-6R (51). As membrane bound IL-6 signalling in heart failure appears to be cardioprotective, it is possible that inhibition thereof may be detrimental (52). Lastly, IL-6 treatment in the current study may have been ineffective. IL-6 drives inflammation in a receptor-mediated manner by exerting effects on different cell types, which in turn produce downstream pro-inflammatory products, including CRP. Blocking the IL-6 receptors decrease downstream signalling and hence reduces CRP (53). The lack of effectiveness of anti-IL-6 treatment may be due to an insufficient frequency of tocilizumab administration in rats, or the use of a humanised monoclonal antibody that resulted in inadequate receptor binding. Nevertheless, a previous rat study using tocilizumab showed significant effects on disease progression. However, the mode of administration and the dosage were different from the current study (54). Further investigation is required to determine specific IL-6 signalling during inflammation driven cardiac remodelling.

This study has further limitations. The inclusion of both male and female rats for the given sample size, may have reduced statistical power. Measuring intracellular expression of cytokines and downstream signalling molecules may have improved our understanding of the cellular pathways implicated in inflammation-induced LV remodelling and dysfunction. In the current study, a

humanised TNF-α dimer and a humanised anti-IL-6 monoclonal antibody were used, which may have limited the effectiveness of the drugs. Future studies should use rat specific anti-inflammatory treatments. In cross-sectional and longitudinal investigations in RA patients, several traditional risk factors including age, blood pressure and obesity are associated with LV diastolic dysfunction (55, 56). Moreover, several cellular components, genetic, epigenetic and environmental factors affect RA pathogenesis, disease progression and structural changes in internal organs (57). Although this study provides new insight into the development of inflammation-induced LV diastolic dysfunction, a broad assessment approach should be encouraged in RA patients to allow for consideration of all predictive factors and enable the development of specific disease-modifying agents.

In conclusion, the results of the current study aid our understanding of the role of biologic DMARDs on cardiac structure and function in high-grade inflammatory disorders. Our results show TNF-α inhibitors may prevent adverse remodelling in the extracellular matrix but does not affect the passive stiffness processes. Anti-IL-6 treatment was not effective in reducing circulating cytokine concentrations, as its administration may have been insufficient to produce clinical effects. The effects of IL-6 receptor blockers on inflammation-induced cardiac function changes remain inconclusive and requires further investigation. Our results support previous reports of disparate signalling pathways in pathogenesis of diastolic dysfunction.

Acknowledgements

The authors thank the staff from the Central Animal Services and Ms Monica Gomes from the School of Physiology for their technical support.

References

1. NICOLA PJ, CROWSON CS, MARADIT-KREMERS H *et al.*: Contribution of congestive heart failure and ischemic heart disease to excess mortality in rheumatoid arthritis. *Arthritis Rheum* 2006; 54: 60-7.
2. ASLAM F, HANDEALI SJ, KHAN NA, ALAM M: Diastolic dysfunction in rheumatoid arthritis: a meta-analysis and systematic review. *Arthritis Care Res* 2013; 65: 53-43.
3. WAN S-H, VOGEL MW, CHEN HH: Preclinical diastolic dysfunction. *J Am Coll Cardiol* 2014; 63: 407-16.
4. MOGELVANG R, BIERING-SØRENSEN T, JENSEN JS: Tissue Doppler echocardiography predicts acute myocardial infarction, heart failure, and cardiovascular death in the general population. *Eur Heart J - Cardiovasc Imaging* 2015; 16: 1331-7.
5. VIZZARDI E, BAZZANI C, CAVAZZANA I *et al.*: Prognostic value of diastolic dysfunction in asymptomatic rheumatoid arthritis patients without cardiovascular risk factors. *Clin Exp Rheumatol* 2016; 34: 352.
6. PAULUS WJ, TSCHÖPE C: A novel paradigm for heart failure with preserved ejection fraction: comorbidities drive myocardial dysfunction and remodeling through coronary microvascular endothelial inflammation. *J Am Coll Cardiol* 2013; 62: 263-71.
7. MOCAN M, MOCAN HOGNOGI LD, ANTON FP *et al.*: Biomarkers of inflammation in left ventricular diastolic dysfunction. *Dis Markers* 2019: 7583690.
8. DUNLAY SM, WESTON SA, REDFIELD MM, KILLIAN JM, ROGER VL: Tumor necrosis factor-alpha and mortality in heart failure: a community study. *Circulation* 2008; 118: 625-31.
9. MELÉNDEZ GC, MCLARTY JL, LEVICK SP, DU Y, JANICKI JS, BROWER GL: Interleukin 6 mediates myocardial fibrosis, concentric hypertrophy, and diastolic dysfunction in rats. *Hypertension* 2010; 56: 225-31.
10. DANESH J, KAPTOGE S, MANN AG *et al.*: Long-term interleukin-6 levels and subsequent risk of coronary heart disease: two new prospective studies and a systematic review. *PLoS Med* 2008; 5: e78.
11. SANTHANAKRISHNAN R, CHONG JPC, NG TP *et al.*: Growth differentiation factor 15, ST2, high-sensitivity troponin T, and N-terminal pro brain natriuretic peptide in heart failure with preserved vs. reduced ejection fraction. *Eur J Heart Fail* 2012; 14: 1338-47.
12. LEWIS GA, SCHELBERT EB, WILLIAMS SG *et al.*: Biological phenotypes of heart failure with preserved ejection fraction. *J Am Coll Cardiol* 2017; 70: 2186-200.
13. DUNLAY SM, ROGER VL, REDFIELD MM: Epidemiology of heart failure with preserved ejection fraction. *Nat Rev Cardiol* 2017; 14: 591-602.
14. SHAH SJ, KITZMAN DW, BORLAUG BA *et al.*: Phenotype-specific treatment of heart failure with preserved ejection fraction: a multiorgan roadmap. *Circulation* 2016; 134: 73-90.
15. GLEZEVA N, BAUGH JA: Role of inflammation in the pathogenesis of heart failure with preserved ejection fraction and its potential as a therapeutic target. *Heart Fail Rev* 2014; 19: 681-94.
16. BANIAAMAM M, PAULUS WJ, BLANKEN AB, NURMOHAMED MT: The effect of biological DMARDs on the risk of congestive heart failure in rheumatoid arthritis: a systematic review. *Expert Opin Biol Ther* 2018; 18: 585-94.
17. LIANG KP, MYASOEDOVA E, CROWSON CS *et al.*: Increased prevalence of diastolic dysfunction in rheumatoid arthritis. *Ann Rheum Dis* 2010; 69: 1665-70.
18. JASEMIAN Y, SVENDSEN P, DELEURAN B, DAGNAES-HANSEN F: Refinement of the collagen induced arthritis model in rats by infrared thermography. *J Adv Med Med Res* 2011: 469-77.
19. MOKOTEDI L, MICHEL FS, MOGANE C *et al.*: Associations of inflammatory markers with impaired left ventricular diastolic and systolic function in collagen-induced arthritis. *PLoS One* 2020; 15: e0230657.
20. LANG RM, BADANO LP, MOR-AVI V *et al.*: Recommendations for cardiac chamber quantification by echocardiography in adults: an update from the American Society of Echocardiography and the European Association of Cardiovascular Imaging. *J Am Soc Echocardiogr* 2015; 28: 1-39. e14.
21. TEICHHOLZ LE, KREULEN T, HERMAN M V, GORLIN R: Problems in echocardiographic volume determinations: echocardiographic-angiographic correlations in the presence of absence of asynergy. *Am J Cardiol* 1976; 37: 7-11.
22. BRADHAM WS, MOE G, WENDT KA *et al.*: TNF-alpha and myocardial matrix metalloproteinases in heart failure: relationship to LV remodeling. *Am J Physiol Heart Circ Physiol* 2002; 282: H1288-95.
23. MOE GW, MARIN-GARCIA J, KONIG A, GOLDENTHAL M, LU X, FENG Q: *In vivo* TNF-alpha inhibition ameliorates cardiac mitochondrial dysfunction, oxidative stress, and apoptosis in experimental heart failure. *Am J Physiol Heart Circ Physiol* 2004; 287: H1813-20.
24. WESTERMANN D, LINDNER D, KASNER M *et al.*: Cardiac inflammation contributes to changes in the extracellular matrix in patients with heart failure and normal ejection fraction. *Circ Heart Fail* 2011; 4: 44-52.
25. SRIRAMULA S, FRANCIS J: Tumor necrosis factor-alpha is essential for angiotensin II-induced ventricular remodeling: role for oxidative stress. *PLoS One* 2015; 10: e0138372.
26. WESTERMANN D, VAN LINTHOUT S, DHAYAT S *et al.*: Tumor necrosis factor-alpha antagonism protects from myocardial inflammation and fibrosis in experimental diabetic cardiomyopathy. *Basic Res Cardiol* 2007; 102: 500-7.
27. LI Q, YU Q, NA R, LIU B: Etanercept protects rat cardiomyocytes against hypertrophy by regulating inflammatory cytokines secretion and cell apoptosis. *Braz J Med Biol Res* 2017; 50: e5868.
28. KOTYLA PJ: Bimodal function of anti-TNF treatment: shall we be concerned about anti-TNF treatment in patients with rheumatoid arthritis and heart failure? *Int J Mol Sci* 2018; 19: 1739.
29. GAASCH WH, ZILE MR: Left ventricular structural remodeling in health and disease: with special emphasis on volume, mass, and geometry. *J Am Coll Cardiol* 2011; 58: 1733-40.
30. ZILE MR, BAICU CF, IKONOMIDIS JS *et al.*: Myocardial stiffness in patients with heart failure and a preserved ejection fraction: contributions of collagen and titin. *Circulation* 2015;131: 1247–59.
31. BIESIADECKI BJ, DAVIS JP, ZIOLO MT, JANSSEN PML: Tri-modal regulation of cardiac

muscle relaxation; intracellular calcium decline, thin filament deactivation, and cross-bridge cycling kinetics. *Biophys Rev* 2014; 6: 273-89.

32. WU C-K, LEE J-K, CHIANG F-T *et al.*: Plasma levels of tumor necrosis factor-α and interleukin-6 are associated with diastolic heart failure through downregulation of sarcoplasmic reticulum Ca2+ ATPase. *Crit Care Med* 2011; 39: 984-92.
33. FELDMAN AM, COMBES A, WAGNER D *et al.*: The role of tumor necrosis factor in the pathophysiology of heart failure. *J Am Coll Cardiol* 2000; 35: 537-44.
34. SIWIK DA, COLUCCI WS: Regulation of matrix metalloproteinases by cytokines and reactive oxygen/nitrogen species in the myocardium. *Heart Fail Rev* 2004; 9: 43-51.
35. LIU P, SUN M, SADER S: Matrix metalloproteinases in cardiovascular disease. *Can J Cardiol* 2006; 22: 25B-30B.
36. JOBE LJ, MELÉNDEZ GC, LEVICK SP, DU Y, BROWER GL, JANICKI JS: TNF-alpha inhibition attenuates adverse myocardial remodeling in a rat model of volume overload. *Am J Physiol Heart Circ Physiol* 2009; 297: H1462-68.
37. BADENHORST D, MASEKO M, TSOTETSI OJ *et al.*: Cross-linking influences the impact of quantitative changes in myocardial collagen on cardiac stiffness and remodelling in hypertension in rats. *Cardiovasc Res* 2003; 57: 632-41.
38. VOLOSHENYUK TG, HART AD, KHOUTOROVA E, GARDNER JD: TNF-α increases cardiac fibroblast lysyl oxidase expression through TGF-β and PI3Kinase signaling pathways. *Biochem Biophys Res Commun* 2011; 413: 370-5.
39. SAVVATIS K, MÜLLER I, FRÖHLICH M *et al.*: Interleukin-6 receptor inhibition modulates the immune reaction and restores titin phosphorylation in experimental myocarditis. *Basic Res Cardiol* 2014; 109: 449.
40. MURDACA G, SPANÒ F, CAGNATI P, PUPPO F: Free radicals and endothelial dysfunction: potential positive effects of TNF-α inhibitors. *Redox Rep* 2013; 18: 95-99.
41. NISHIMURA RA, TAJIK AJ: Evaluation of diastolic filling of left ventricle in health and disease: Doppler echocardiography is the clinician's Rosetta Stone. *J Am Coll Cardiol* 1997; 30: 8-18.
42. MOTTRAM PM, MARWICK TH: Assessment of diastolic function: what the general cardiologist needs to know. *Heart Br Card Soc* 2005; 91: 681-95.
43. MPOFU S, FATIMA F, MOOTS RJ: Anti-TNF-α therapies: they are all the same (aren't they?). *Rheumatology* 2005; 44: 271-3.
44. SZONDY Z, PALLAI A: Transmembrane TNF-alpha reverse signaling leading to TGF-beta production is selectively activated by TNF targeting molecules: Therapeutic implications. *Pharmacol Res* 2017; 115: 124-32.
45. ZHAO L, CHENG G, JIN R *et al.*: Deletion of interleukin-6 attenuates pressure overload-induced left ventricular hypertrophy and dysfunction. *Circ Res* 2016; 118: 1918-29.
46. LAI NC, GAO MH, TANG E *et al.*: Pressure overload-induced cardiac remodeling and dysfunction in the absence of interleukin 6 in mice. *Lab Investig J Tech Methods Pathol* 2012; 92: 1518-26.
47. KOBAYASHI H, KOBAYASHI Y, GILES JT, YONEYAMA K, NAKAJIMA Y, TAKEI M: Tocilizumab treatment increases left ventricular ejection fraction and decreases left ventricular mass index in patients with rheumatoid arthritis without cardiac symptoms: assessed using 3.0 tesla cardiac magnetic resonance imaging. *J Rheumatol* 2014; 41: 1916-21.
48. HIROTA H, YOSHIDA K, KISHIMOTO T, TAGA T: Continuous activation of gp130, a signal-transducing receptor component for interleukin 6-related cytokines, causes myocardial hypertrophy in mice. *Proc Natl Acad Sci* 1995; 92: 4862-6.
49. FREDJ S, BESCOND J, LOUAULT C, DELWAIL A, LECRON J-C, POTREAU D: Role of interleukin-6 in cardiomyocyte/cardiac fibroblast interactions during myocyte hypertrophy and fibroblast proliferation. *J Cell Physiol* 2005; 204: 428-36.
50. PETERS M, JACOBS S, EHLERS M *et al.*: The function of the soluble interleukin 6 (IL-6) receptor in vivo: sensitization of human soluble IL-6 receptor transgenic mice towards IL-6 and prolongation of the plasma half-life of IL-6. *J Exp Med* 1996; 183: 1399-406.
51. WOLLERT KC, DREXLER H: The role of interleukin-6 in the failing heart. *Heart Fail Rev* 2001; 6: 95-103.
52. HILFIKER-KLEINER D, LANDMESSER U, DREXLER H: Molecular mechanisms in heart failure: focus on cardiac hypertrophy, inflammation, angiogenesis, and apoptosis. *J Am Coll Cardiol* 2006; 48: A56-66.
53. KIM GW, LEE NR, PI RH *et al.*: IL-6 inhibitors for treatment of rheumatoid arthritis: past, present, and future. *Arch Pharm Res* 2015; 38: 575-84.
54. ABDEL-MAGED AE-S, GAD AM, ABDEL-AZIZ AK, ABOULWAFA MM, AZAB SS: Comparative study of anti-VEGF Ranibizumab and Interleukin-6 receptor antagonist Tocilizumab in Adjuvant-induced Arthritis. *Toxicol Appl Pharmacol* 2018; 356: 65-75.
55. DAL PIAZ EC, CIOFFI G, OGNIBENI F *et al.*: Incidence and predictors of new onset left ventricular diastolic dysfunction in asymptomatic patients with rheumatoid arthritis without overt cardiac disease. *Monaldi Arch Chest Dis* 2019; 89: 1053.
56. MOKOTEDI L, GUNTER S, ROBINSON C *et al.*: The impact of different classification criteria sets on the estimated prevalence and associated risk factors of diastolic dysfunction in rheumatoid arthritis. *Int J Rheumatol* 2017; 2017: 2323410.
57. CROIA C, BURSI R, SUTERA D, PETRELLI F, ALUNNO A, PUXEDDU I: One year in review 2019: pathogenesis of rheumatoid arthritis. *Clin Exp Rheumatol* 2019; 37: 347-57.